Environment Canterbury Regional Council
Kaunihera Taiao ki Waitaha

TECHNICAL REPORT Science Group

Evaluation of potential impacts of the Rangitata South Irrigation Scheme on groundwater

Report No. R16/3

ISBN **978-0-947507-33-6 (print)**
978-0-947507-34-3 (web)

Evaluation of potential impacts of the Rangitata South Irrigation Scheme on groundwater

Report No. R16/3
ISBN 978-0-947507-33-6 (print)
978-0-947507-34-3 (web)

Nicola Kaelin
Patrick Durney
Mark Trewartha

June 2017

	Name	Date
Prepared by :	*Nicola Kaelin* *Patrick Durney* *Mark Trewartha*	*March 2017*
Reviewed by :	*Carl Hanson* *Groundwater Science Manager*	
External review by:	*Stephen Douglass* *GHD*	
Approved by:	*Stefanie Rixecker* *Director Science Group*	

Report No. R16/3
ISBN 978-0-947507-33-6 (print)
978-0-947507-34-3 (web)

200 Tuam Street
PO Box 345
Christchurch 8140
Phone (03) 365 3828
Fax (03) 365 3194

75 Church Street
PO Box 550
Timaru 7940
Phone (03) 687 7800
Fax (03) 687 7808

Website: www.ecan.govt.nz
Customer Services Phone 0800 324 636

Summary

Background:
Construction of the Rangitata South Irrigation Scheme (RSIS) began in 2011. By late 2013, the main ponds were being filled and water was being supplied down the main races. The scheme diverts water from the Rangitata River in times of high flow (greater than 110 cubic metres per second) into seven stepped storage ponds located near Arundel. A network of open races supplies water from the storage ponds to farms. Scheme shareholders must have an on-farm storage pond with a minimum capacity of 250 m^3 per hectare of irrigated land.

The issue:
We received reports of flooding in the RSIS area, including a report about a flooded stock underpass in November 2013. We also received reports on other flooding incidents near old river channels such as the Rangitata River middle channel and Kapunatiki Creek.

What we did:
We undertook a review of groundwater level and quality data collected from wells in the area. We checked for anomalous changes in groundwater quantity and quality and looked at reasons that may have led to the changes we saw. We created a numerical groundwater model to check the viability of our analyses and conclusions. Our assessment considers the RSIS to include the main storage ponds, all races and on-farm storage ponds, and any changes to irrigation practices that have resulted from the scheme.

What we found:
Following the commissioning of the RSIS scheme, groundwater levels rose near the scheme's main storage ponds and races as well as near on-farm storage ponds. Groundwater levels in some wells rose to over a metre above previously recorded high levels in the area immediately downgradient of the main storage ponds, but increases were less farther down the plain. At the same time, groundwater nitrate concentrations have decreased in at least one location.

We calibrated our numerical model using groundwater level data from wells in the area. Then, we used the calibrated model to simulate the long-term effects of the various components of the RSIS on the area's groundwater levels. The model indicates that increased recharge from the RSIS could cause groundwater levels to rise by up to 5 m directly beneath the main storage ponds, up to 3 m in the immediate vicinity of the RSIS ponds and main race, and up to 2 m downstream of the ponds and main race in the middle plain. The results show that the observed changes in groundwater levels can reasonably be attributed to the RSIS and associated infrastructure.

What it means:
We have not identified any other factors that could explain the observed changes in groundwater levels and quality, so we conclude that they were caused by the installation and utilisation of the RSIS. The recently observed flooding and increases in intermittent stream flows are probably also related to the RSIS, though the extent the flooding would have occurred even without the scheme is not known. Groundwater levels may decline somewhat over time as silt settles on the bottom of scheme ponds and races and reducing leakage, but they are unlikely to return to pre-scheme levels.

Table of contents

List of Figures

List of Tables

1 Introduction

1.1 Background

The Rangitata South Irrigation Scheme (RSIS) is a large irrigation water storage and distribution scheme located on the land between the Rangitata and Orari rivers in South Canterbury (Figure 1-1). The scheme takes water from the Rangitata River to seven large storage ponds for later distribution to smaller on-farm ponds for irrigation.

Following the commissioning of the scheme in 2013, Environment Canterbury received reports of flooding incidents in the area, including a stock underpass and normally dry stream channels. The RSIS scheme could cause groundwater levels in the area to rise, leading to such flooding through:

- leakage from scheme infrastructure such as the main storage ponds, distribution races and on-farm storage ponds
- increased infiltration from additional irrigated areas/activities
- reduction in groundwater abstraction due the provision of a more feasible alternative water source.

Increased groundwater recharge and reduced abstraction can lead to increased groundwater availability, dilution of nutrients and higher flows in spring-fed streams, but the resulting rise in the water table can also cause flooding.

1.2 Study objectives

Our specific objectives for this study were to:

- assess changes in groundwater levels and/or quality in the Rangitata South area
- review available information on potential impacts of the RSIS to the groundwater system
- evaluate (via a groundwater flow model) the potential long-term effects on groundwater levels due to changes in the hydrologic system in the study area
- check whether the observed changes are consistent with the model predictions.

In order to evaluate and/or quantify the potential effects of implementation of the RSIS scheme, we have reviewed the available monitoring data and built a simple steady-state groundwater model using MODFLOW 2000 (USGS, 2000).

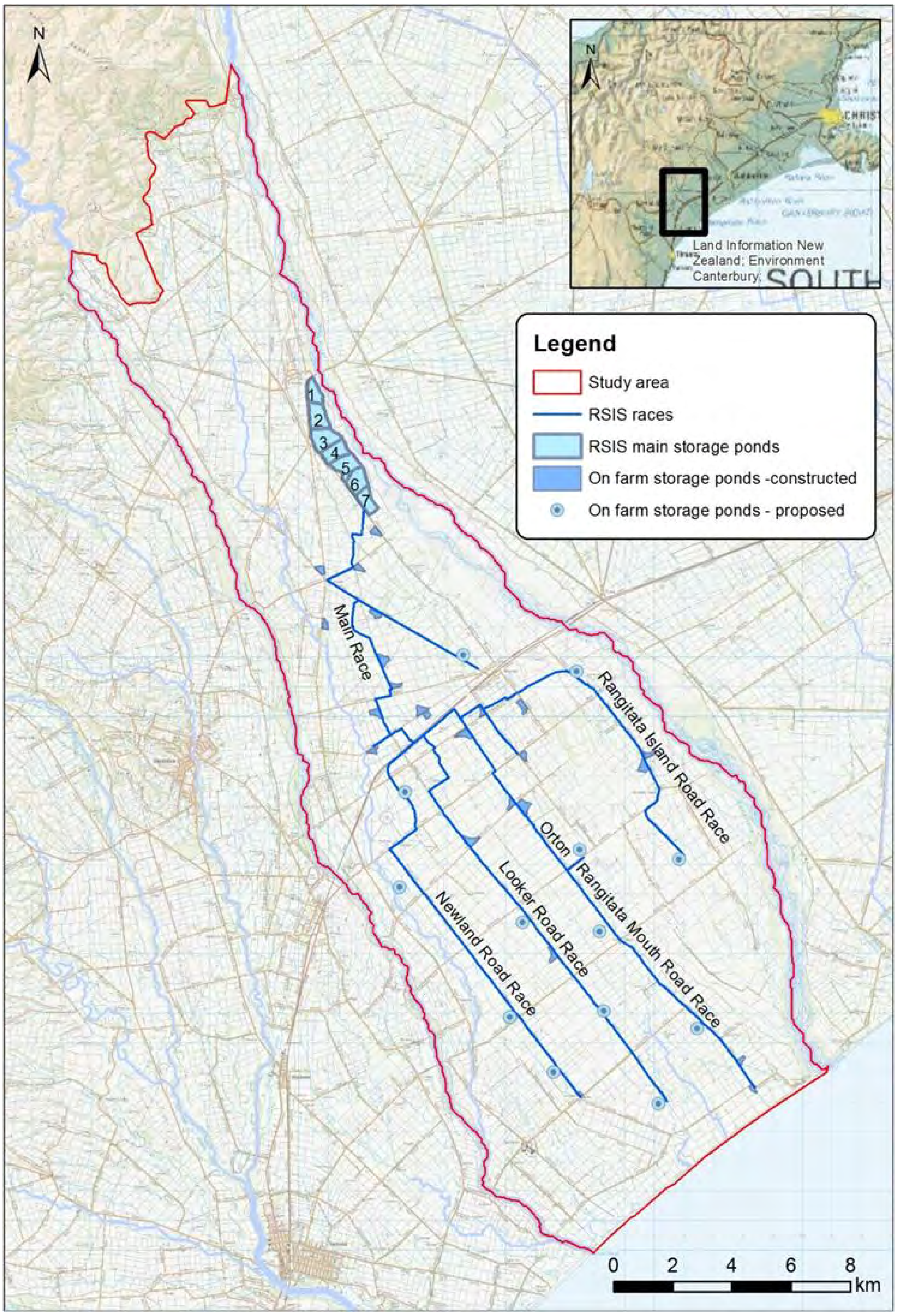

Figure 1-1: Map showing the study area and RSIS scheme layout. Labels 1-7 indicate the main storage pond number[1]

[1] Note: The base map of this figure and later figures in the report is based on 2010 data. It is our understanding at the time of publication that all on-farm storage ponds have now been constructed.

2 Conceptual model

2.1 Topography and climate

The study area is largely flat land, sloping gently from an elevation of around 280 metres above sea level (masl) at the foothills of the Southern Alps down to the coast over a distance of approximately 40 km.

The area has a temperate climate, with temperatures typically in the range of 0ºC to 22ºC. Rainfall is consistent throughout the year on the plains, but the foothills receive more rain in the summer. Total annual rainfall is in the order of 600-1,000 mm (higher towards the foothills). Over the summer, monthly average potential evapotranspiration rates are higher than rainfall (Figure 2-1).

Annual precipitation totals since 2006 have been in the range of approximately 470 to 770 mm, consistent with or a little lower than historical average. Figure 2-2 shows that there have been fewer wet periods in the last thirty years. Monthly rainfalls have been relatively consistent with historical rates, with few anomalies.

Irrigation demand modelling undertaken during the consent hearing for the RSIS predicted a maximum seven day irrigation demand of 30 mm, an annual demand for the irrigation season (1 September to 20 April) of 469 mm, and a one-in-five-year drought demand of 543 mm (Lloyd, 2008).

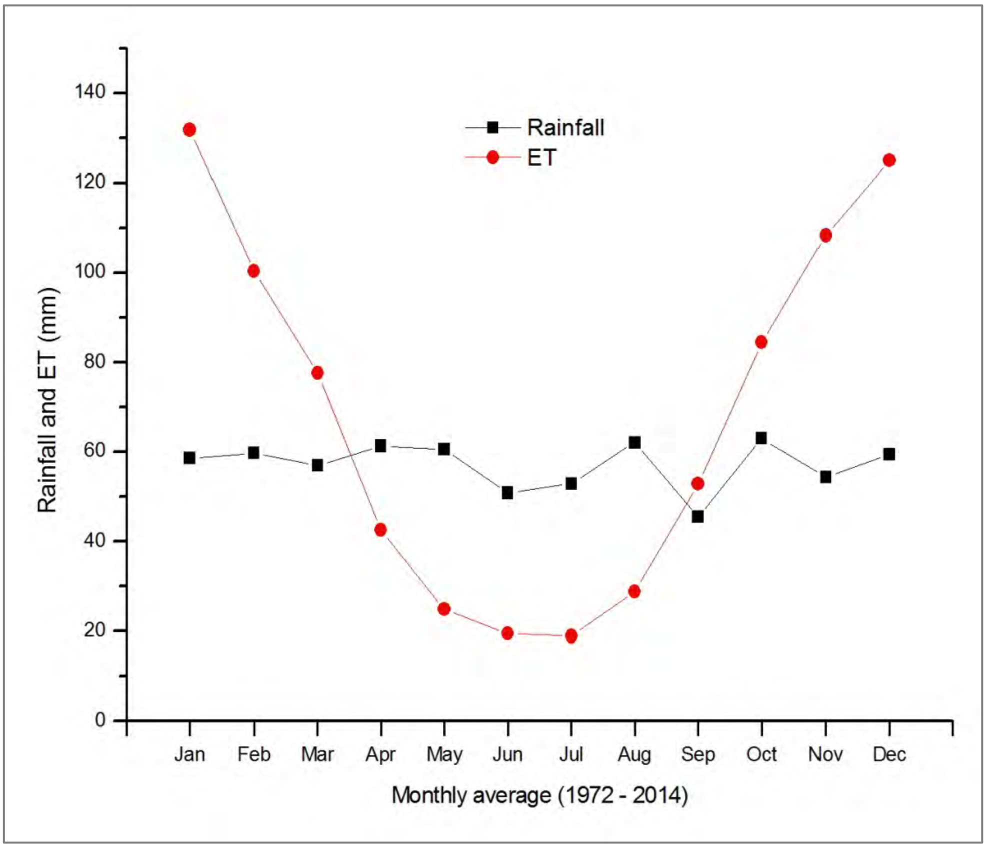

Figure 2-1: Rainfall and potential evapotranspiration records for our study area (obtained from NIWA virtual climate station P108071)

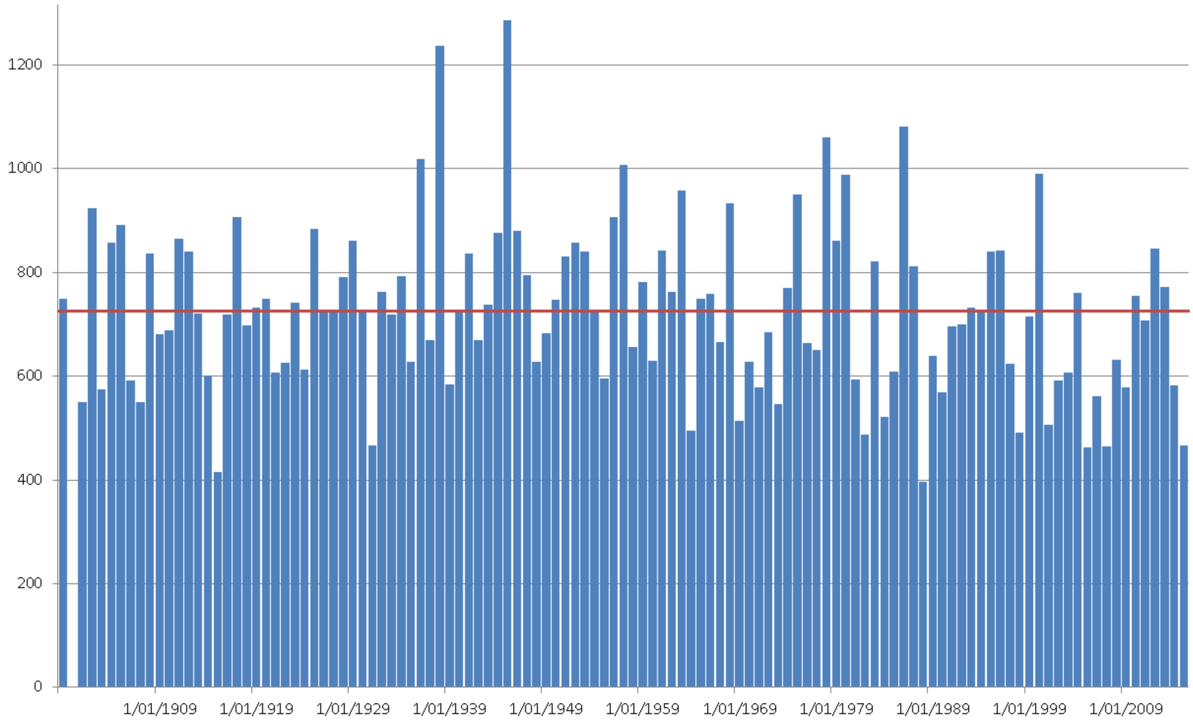

Figure 2-2: Annual rainfall 1900-2016, mean given by the red line

2.2 Hydrology

Two rivers bound our study area: the Rangitata River to the north and the Orari River to the south (Figure 2-3). The Rangitata River is the larger of the two, with a mean flow of approximately 100 m^3/s and a median flow of approximately 70 m^3/s. Flows are generally highest in the spring due to snowmelt in the Southern Alps. The river splits into two branches between Arundel and State Highway 1 (SH1). The North Branch flows continuously, whereas stop banks keep the South Branch dry except in flood conditions. The South Branch flows when flow in the North Branch reaches roughly 1,500 m^3/s.

Flow measurements from simultaneous gaugings along the length of the Rangitata River tend to lie within the standard error associated with river gauging (±8%), so they do not provide clear evidence of gains or losses to/from groundwater (Wilson, 2013). However, there could still be substantial exchange with groundwater hidden within that error margin, which equates to a flow of approximately ±8 m^3/s. In fact, there must be some exchange because water levels in shallow wells close to the river (e.g. well K37/0501) rise in response to high flow events (Burbery, 2012). Dodson (*pers comm.* 2015) also reports that summer gaugings suggest a loss to groundwater.

The mean flow in the Orari River is approximately 10 m^3/s, measured in the gorge at the top of the plain. Flow at the coast is roughly one third of this[2] as a result of surface water abstractions and losses to groundwater. The river loses water in its upper reaches, and it is often dry in its middle reaches during the summer. It then gains flow between SH1 and the coast due to an influx of groundwater. Much of the flow lost from the river is understood to flow through paleo-channels created by an old river course (the Umukaha River) and discharge into the Waihi River to the south of our study area (Burbery and Ritson, 2010).

Coopers Creek is a spring-fed tributary of the Orari River. The springs emerge in the upper plain at Spring Farm, approximately 500 m east of the Orari River and 27 km from the coast. Burbery (2011)

[2] If flow at the Orari Gorge (Gorge Q) is less than 9,700 l/s, then loss = 0.685*(Gorge Q) – 632 l/s. If Gorge Q > 9,700 l/s then loss = 6,000 l/s (Ritson and Stapleton, 2013).

suggests the majority of flow to the springs is supported by losses from the Orari River. Like the Orari River, Coopers Creek loses water in its upper reaches, is dry in its middle reaches during the summer, and gains flow in its lower reaches towards the coast. It joins the Orari River 5 km from the coast.

Scotsburn Stream joins Coopers Creek just south of the springheads. It is normally dry and channels water off the foothills in flood events.

Kapunatiki Creek is marked on topographic maps on the lower plain between the Rangitata and Orari rivers. Area residents report that it is usually dry in the summer and typically only flows during flood events and over a short period in the winter (mid-June to September/October).

A review of recent surface water flows in the study area indicates that pre- and post- scheme surface water flows are relatively consistent with historical observations and trends.

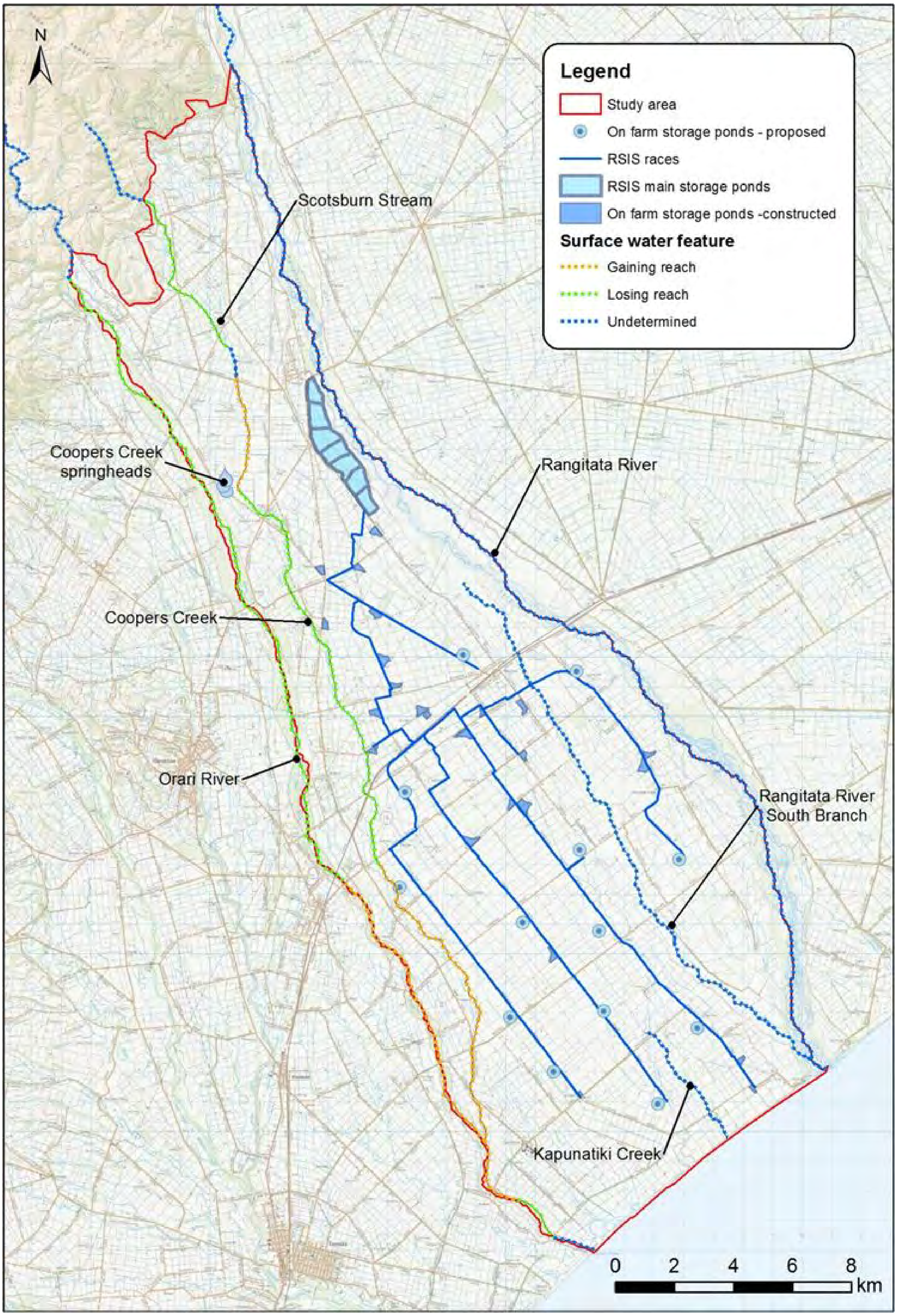

Figure 2-3: Surface water features in the study area

2.3 Geology

The surficial geology of the study area comprises alluvial sediments deposited in the Quaternary period (2.6 million to present), most of which were deposited by the Rangitata River (Figure 2-4). The modern Orari River has incised into this Rangitata fan material, reworked the Rangitata River gravel deposits, and deposited its own gravel. The more recent gravels associated with the Orari River are more permeable than older gravels associated with the Rangitata River. Quaternary gravels are thinner towards the southeast and towards the foothills (Aitchison-Earl, 2005).

The Quaternary deposits overlie older gravel of the Kowai Formation (known in South Canterbury as the Cannington Gravels). It is difficult to distinguish the older Kowai gravels from younger Quaternary gravels deposited by Rangitata and Orari Rivers. The total thickness of gravels (Quaternary and Kowai Formation gravels) in the study area is thought to be in the order of 160 m (Woodward, 1989).

The basement rocks underlying the gravels include sandstone, siltstone and greywacke. Some of these basement rocks crop out in the hills of the upper catchments. A localised occurrence of Pliocene (5.3 to 2.6 million years old) volcanic rocks is present outside of our study area behind the settlement of Geraldine.

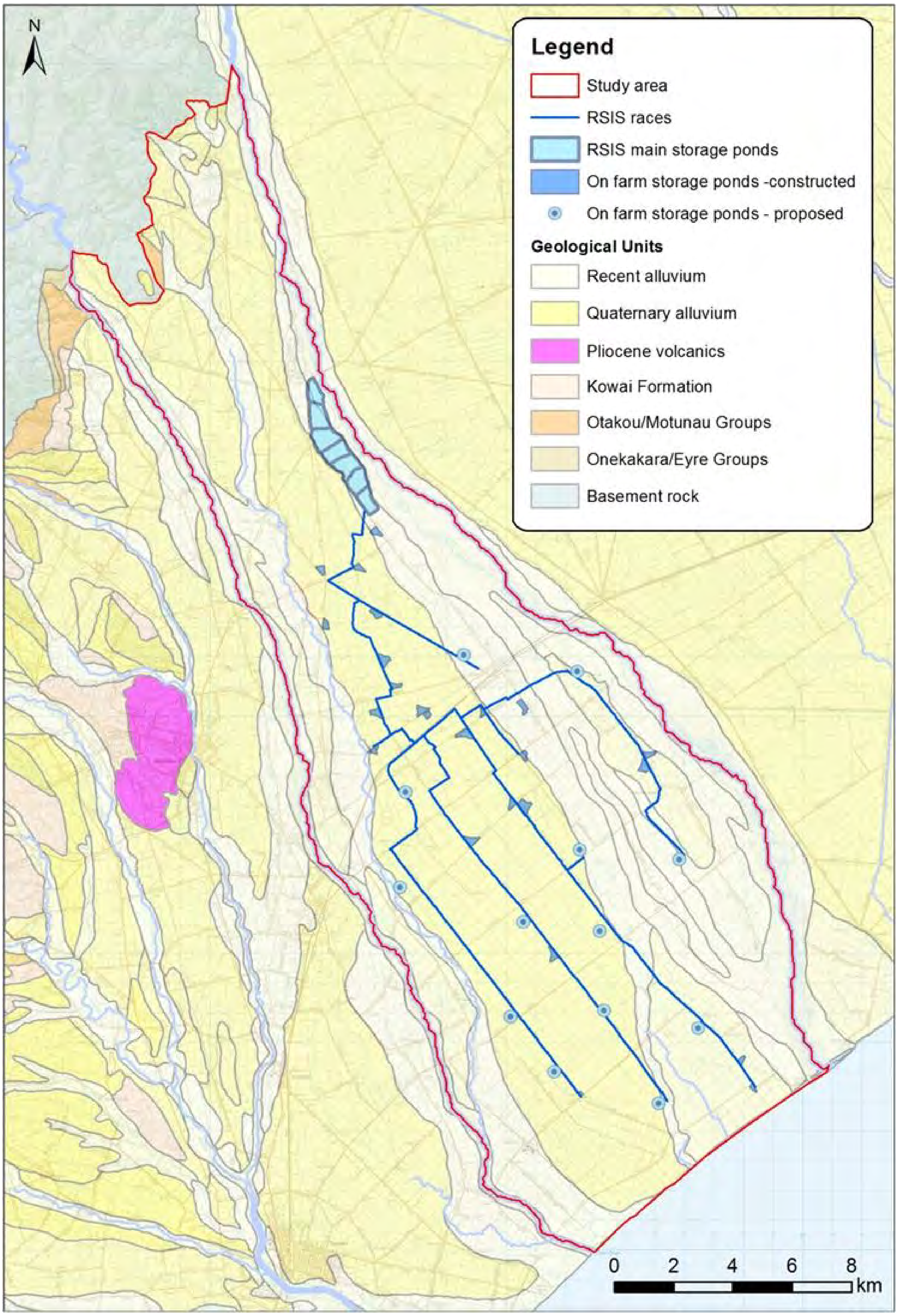

Figure 2-4: Simplified geological map of the study area (from Cox and Barrel, 2007)

2.4 Hydrogeology

Most of the wells in the study area are less than 150 m deep; targeting water in the Quaternary gravels. In general, shallower groundwater abstractions are concentrated near the Orari River. Shallow (<20 m deep) groundwater near the Orari River is highly connected to the river. Transmissivity and specific capacity values measured in pumping tests are highest near the Orari River and lowest in the central part of the plain (Figure 2-5).

2.4.1 Groundwater flow

Groundwater flows in a south-easterly direction, from the foothills to the sea. Piezometric contours suggest that the Rangitata River loses flow to groundwater near where it splits into the North and South branches (Wilson, 2013). The water table is shallowest alongside the Orari River and deepens towards the Rangitata River. It is deepest in the upper plains alongside the Rangitata River near Arundel.

A downward hydraulic gradient exists through the majority of our study area, indicating groundwater recharge settings. However, this reverses near the coast. Deeper wells near Clandeboye show artesian conditions and this coincides with a groundwater discharge zone and an area of former swamp deposits (Wilson, 2013).

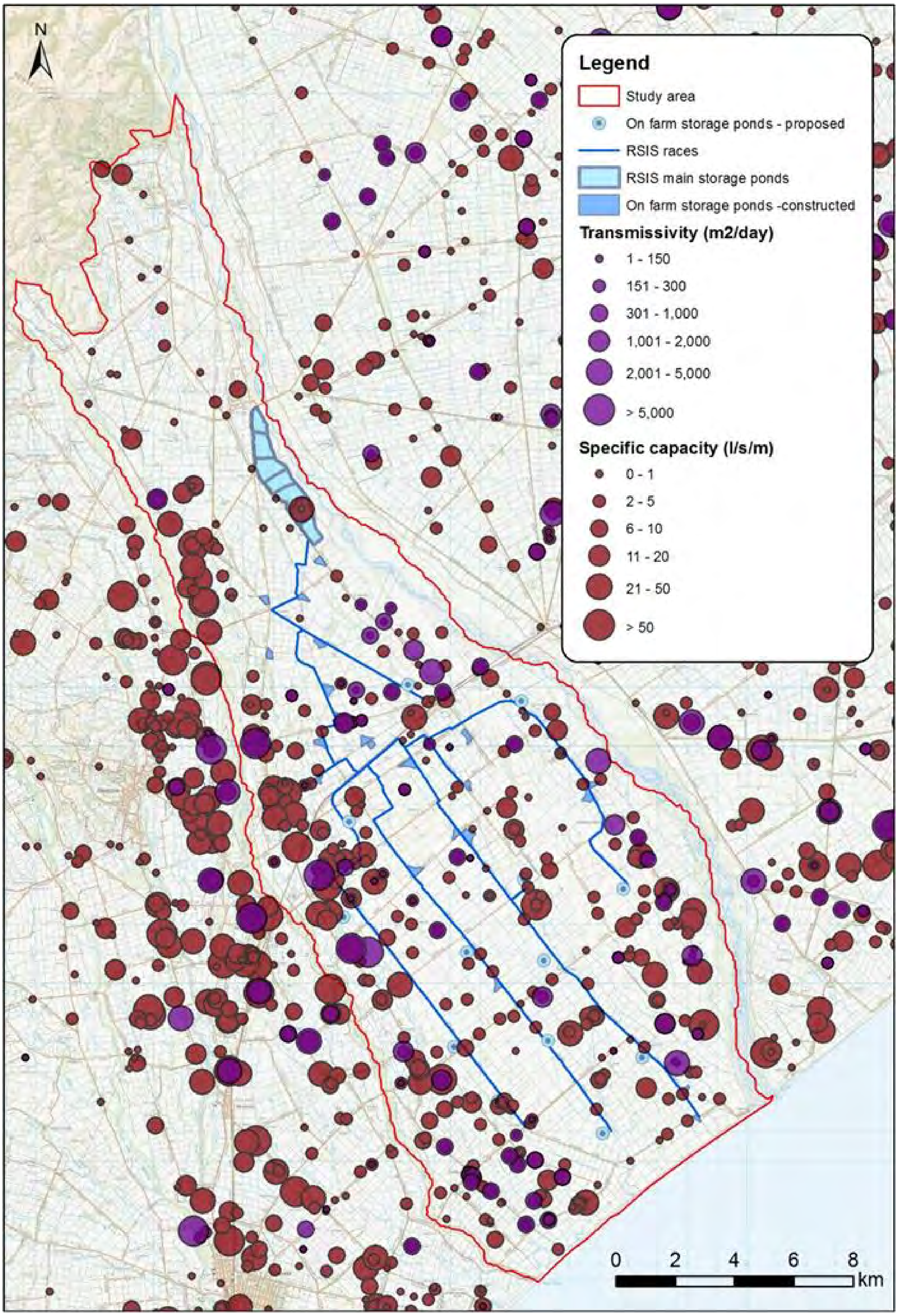

Figure 2-5: Transmissivity and specific capacity values from well and aquifer tests

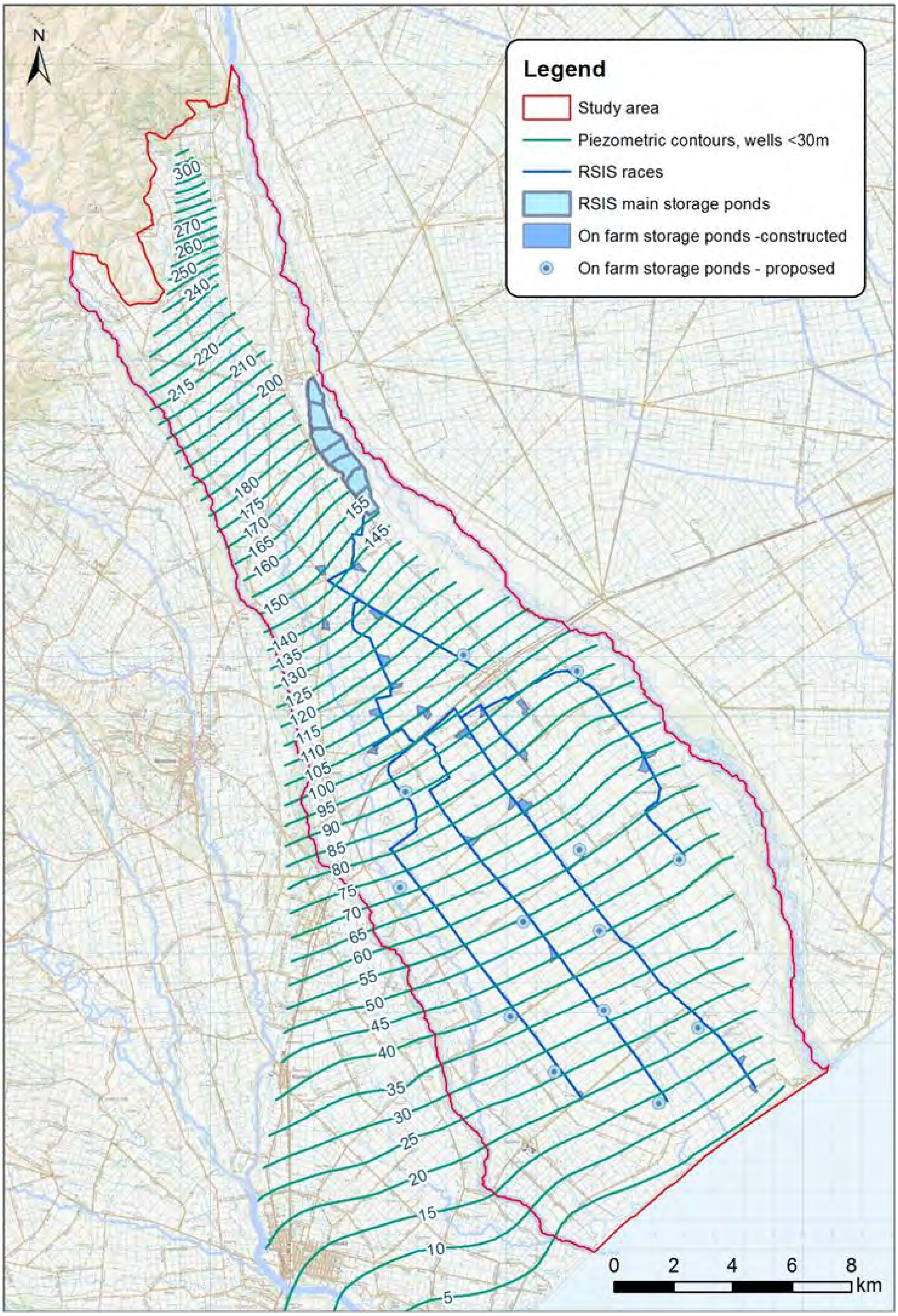

Figure 2-6: Piezometric contours (from Wilson, 2013)

2.4.2 Groundwater recharge

Groundwater recharge sources in our study area include rainfall, irrigation, river/stream flow losses and losses from agricultural water infrastructure (irrigation storage ponds, delivery races and stock water races). Rainfall and river/stream flows are discussed in Sections 2.1 and 2.2.

The Timaru District Council (TDC) operates a system of stock water races within the study area consisting of approximately 230 km of open races. Losses from this race system have been estimated to be approximately 350 L/s or 73% of the water abstracted (de Joux, 2013). The intake for this system is from the upper Orari River near Leamington, approximately 4 km downstream of the gorge. The race network extends to the coast on the northern side of the Orari, and to Geraldine on the southern side.

The Rangitata South Irrigation Scheme was consented in 2009 and scheme commissioning commenced in 2013. The scheme takes water from the Rangitata River at high flows, storing the water in seven large ponds (16.5 million m^3) and distributed through scheme command area via open channel races and into farm storage ponds (3.5 million m^3). Details of the Rangitata South Irrigation Scheme are discussed in Section 3.

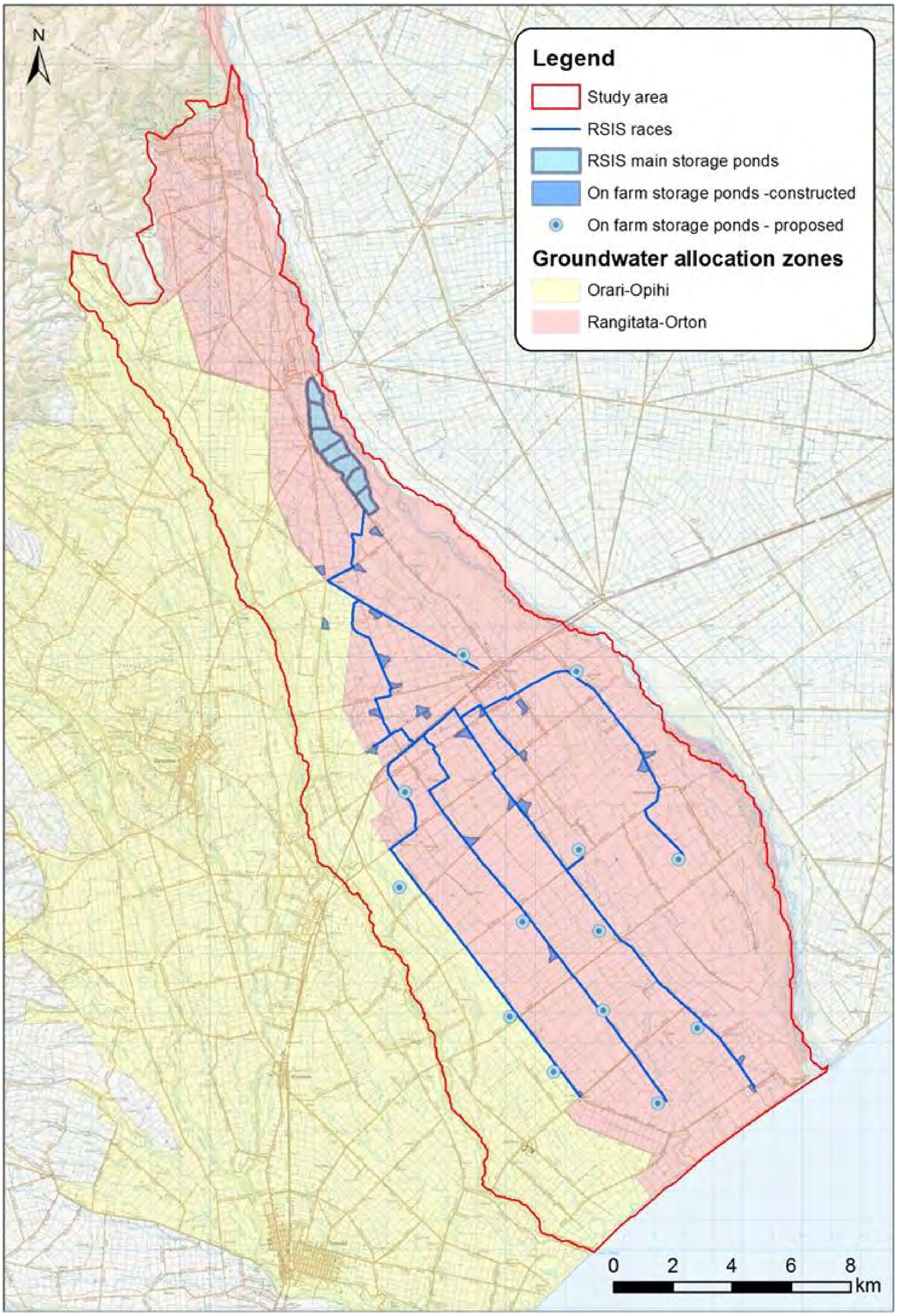

Figure 2-7: Groundwater allocation zones in our study area

2.4.3 Land use and irrigation

Most of the land in the study area is used for dairy farming (Figure 2-8). Sheep and beef farming is scattered throughout the area and deer farming dominates in the northern part of the area. Arable land uses are located along the southwest boundary and in coastal areas.

The vast majority of the land within the command area of the RSIS is irrigated (Figure 2-9). The introduction of the scheme has facilitated a more reliable water supply for land owners rather than enabling large areas of additional irrigation, but this increased reliability may lead to some land use change in the future.

2.4.4 Groundwater use

The majority of groundwater use in our study area is for irrigation (Table 2-1). Other uses include a salmon farm hatchery at McKinnon’s Creek (aquaculture), a dairy factory at Clandeboye (industrial), water supply at the Peel Forest camp ground (recreation), dairy shed wash-down (other), and public water supply.

Most of the active groundwater take consents are located in the coastal half of our study area and are associated with dairy farming (Figure 2-8). There is less groundwater abstraction north of the RSIS main storage ponds, where deer farming is common, and towards the coast, where grazing, beef cattle and arable land uses dominate (Figure 2-8).

Table 2-1: Groundwater use as recorded in Environment Canterbury’s database (July 2015)

Recorded use	Number of active groundwater take consents	Proportion of total annual volume for study area
Aquaculture	1	0.91%
Augment River	1	0.00%
Industrial	2	9.51%
Intensive farming (irrigation)	2	5.30%
Irrigation	121	84.19%
Other	1	0.04%
Public water supply	1	0.03%
Recreation	1	0.01%

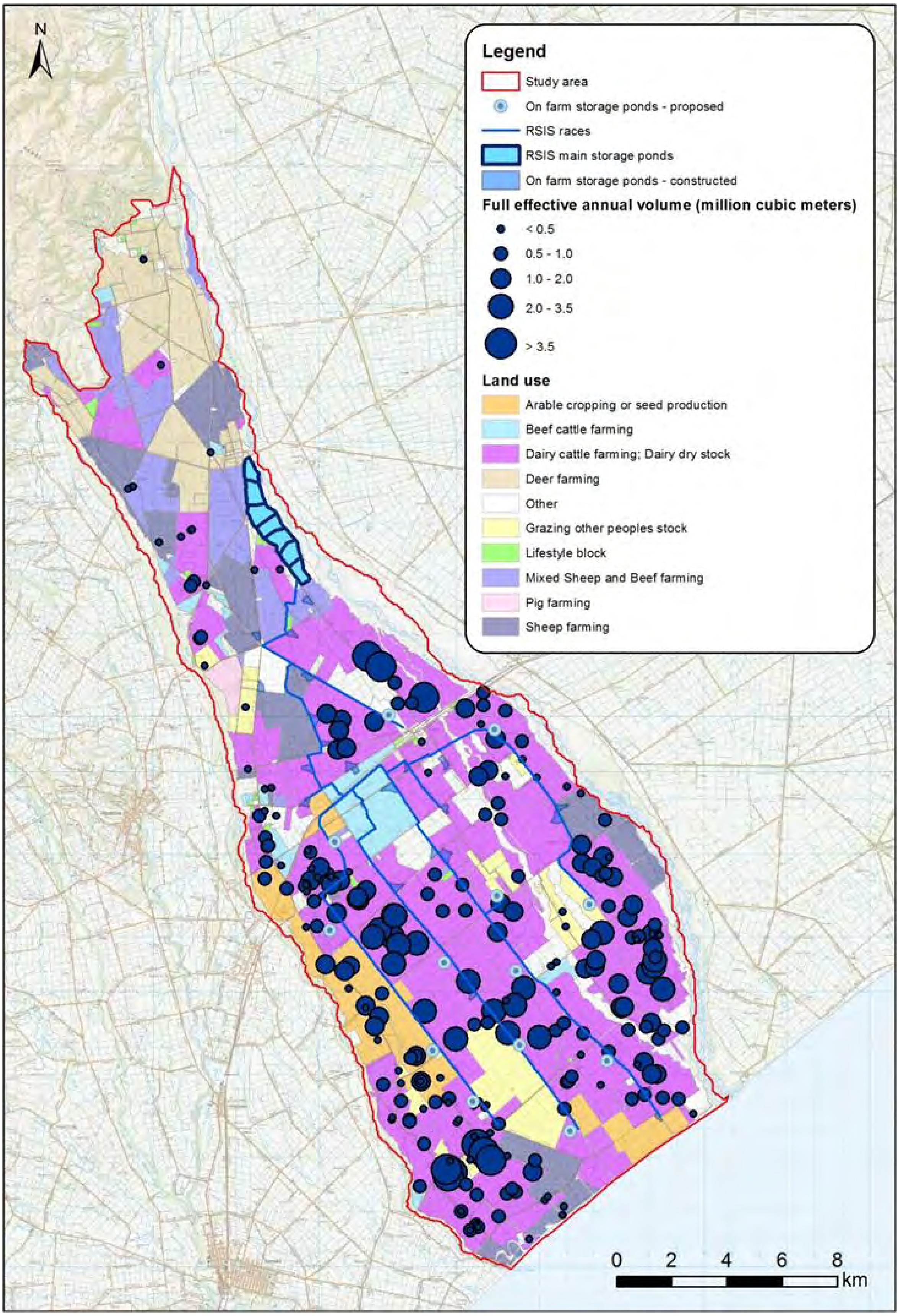

Figure 2-8: Location and annual volumes of current groundwater take consents showing relationship with land use (land use sourced from Agribase, provided by AsureQuality)

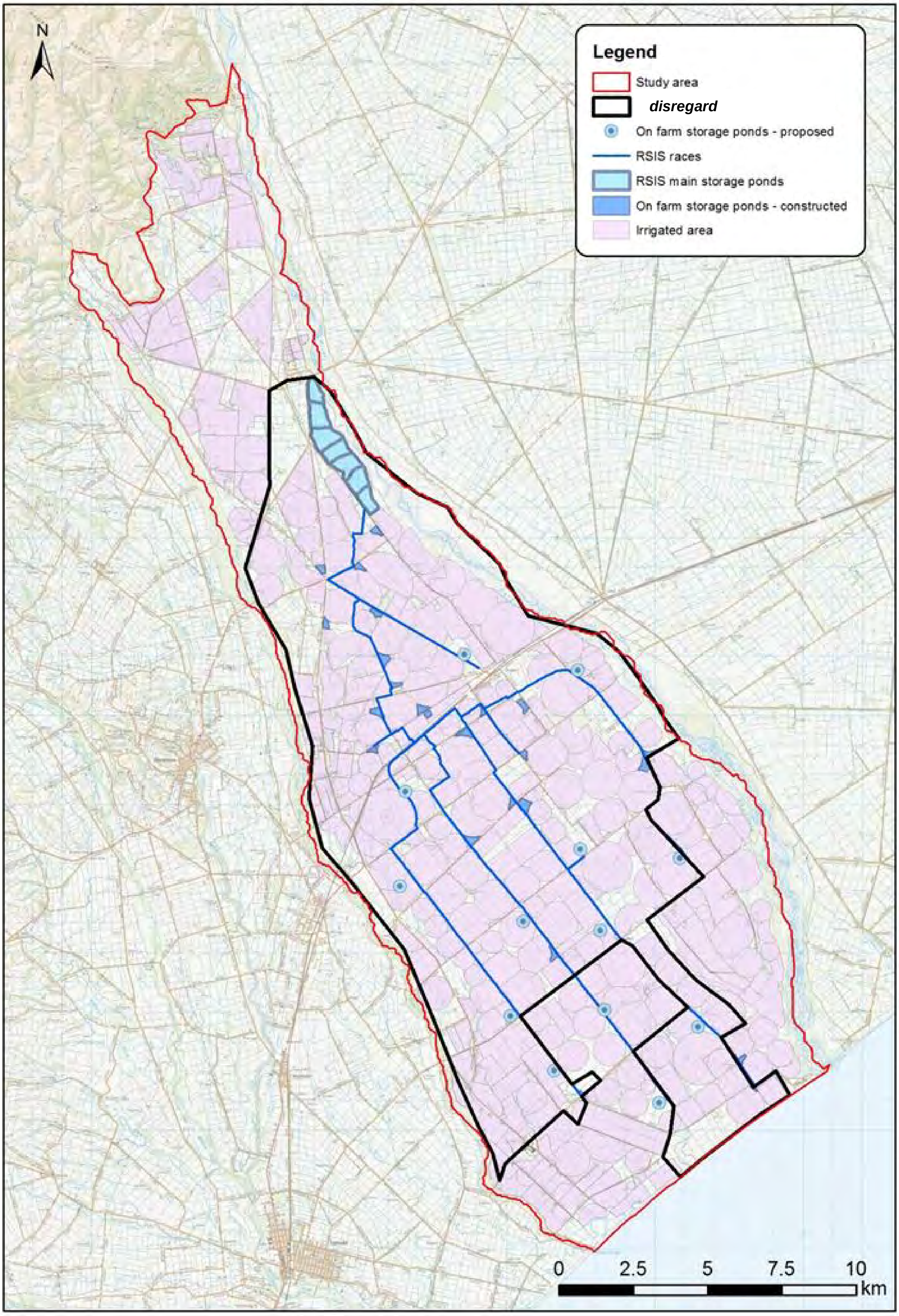

Figure 2-9: Existing irrigated areas - 2014 (from Aqualinc, 2015)

3 RSIS construction

The main storage ponds and races of the RSIS were constructed by Rooney Earthmoving Ltd (REL). REL staff have provided the following details of the construction. The scheme takes water from the Rangitata River upstream of Arundel Bridge in times of high flow (greater than 110 m^3/sec) and channels it into a series of seven stepped storage ponds adjacent and south of the Arundel Bridge. A network of unlined, open races conveys water from the main storage ponds to on-farm ponds. The scheme is designed to provide irrigation water to approximately 16,000 hectares of farmland. Scheme shareholders must have an on-farm storage pond with a minimum capacity of 250 m^3/ha. When full, the main storage ponds at Arundel hold four weeks' supply and the on-farm ponds at least one week's supply.

Consent was granted for the RSIS in 2009 (Environment Canterbury, 2009) and construction began in 2011 (Figure 3-1). The earthworks on the main ponds were completed in 2012, and lining of the sides of the main ponds commenced. High-density polyethylene (HDPE) geo-membrane lines the sides of the main ponds and a 30 m skirt around the base of each pond (Figure 3-2). This HDPE was laid on top of a 20-200 mm layer of silt.

The design of the RSIS is based on the assumption that the bases of the ponds will be sealed naturally over time as silt settles out of the turbid floodwater used to fill the ponds.

Figure 3-1: Construction of Main Pond 1 looking south (photo taken 2011, John Bisset/Fairfax NZ)

Figure 3-2: High-density polyethylene geo-membrane lining on the sides and a 30 m skirt of the main ponds (photo taken 2013, John Bisset/Fairfax NZ)

In October 2013, the first water was run through the intake structure into Pond 7 (Figure 3-3). By November 2013, Pond 7 was 90% full and water was being released into the irrigation races for race commissioning and supply. Filling of the remaining ponds and continued releases of water down the races followed.

During commissioning, the irrigation races were filled with water progressively. If losses were observed, REL “puddled” the race in 100 metre stages. “Puddling” is when 100 metres of race is filled slowly with water, and silt is mixed into the water and allowed to settle out into the race lining, After initial testing phases, the seven ponds were filled at the same time from a ring race that runs around the outside of the ponds (Figure 3-4), allowing the even spread of suspended silt throughout the seven ponds.

Figure 3-3: Main ponds of the Rangitata South Irrigation Scheme mid-way through filling (looking north-west). Pond 7 is full in the foreground with Pond 6 semi-full behind it (photo taken 2013, John Bisset/Fairfax NZ)

Figure 3-4: Photograph showing the completed, full ponds 5 (foreground), 6 and 7 (photo taken 2014, John Bisset/Fairfax NZ)

We visited the study area on 26 June 2015 to visually inspect the main ponds, on-farm ponds and irrigation races. We found that all of the main ponds were holding some water, as were the majority of completed on-farm ponds. Water was flowing down the main race, the Looker Road race and the Newlands Road race. The Rangitata Island Road race and the Orton Rangitata Mouth Road race had no flow; their bases were gravelly and there was no indication of a silt sealing layer (Figure 3-5, Figure 3-6). According to REL, all seven ponds were full together for the first time in September 2015. REL reports that losses from the ponds has reduced over time as the bases have sealed with silt. However, the upper main race, roughly 3.3 kilometres long between the main ponds and Rangitata Orari Bridge Road, did not seal well. To stop the continued losses, this portion of the race was artificially lined in October-November 2016.

Figure 3-5: The Orton Rangitata Mouth Road delivery race near George Road, showing gravelly base (photograph taken by Environment Canterbury on 26/05/2015, looking north west)

Figure 3-6: The Orton Rangitata Mouth Road delivery race at the Burnham Road siphon, showing gravelly base (photograph taken by Environment Canterbury on 26/05/2015, looking north west)

Figure 3-7: The Rangitata Island Road delivery race between Old Main South Road and Brodie Road (photograph taken by Environment Canterbury on 26/05/2015, looking north west)

4 Recent observed groundwater trends in the Rangitata South groundwater system

4.1 Groundwater levels

Based on analyses of groundwater level data collected from our long-term monitoring well network, groundwater levels have risen in some parts of the study area following the implementation of the RSIS. Most of the wells showing increasing water levels are located in the central part of the RSIS (Figure 4-1). At the same time, groundwater levels recorded in wells located upgradient or further from the ponds and distribution races did not exhibit clear increases and in some cases showed or continued to show decreasing trends. We have attached groundwater level records and graphs for long-term monitoring wells in the study area in Appendix A.

In some cases, the increasing groundwater levels are very clear. For example, groundwater levels in well K37/2170 (Figure 4-2), 10.0 metres deep and located 2 km downstream of the main ponds, rose to over a metre higher than previously recorded highs in May 2014.

In other cases, the increases are more subtle. Groundwater levels in well K38/2111, for example, show no overall increase, but the summer low levels have not been as low recently as they were before the commissioning of the RSIS (Figure 4-3).

Some wells do not show any obvious signs of a groundwater level increase, such as well K38/1381 (Figure 4-4). Additionally, we see continued decreasing trends in groundwater levels for wells upgradient and cross gradient of the RSIS storage ponds and main race just below the storage ponds.

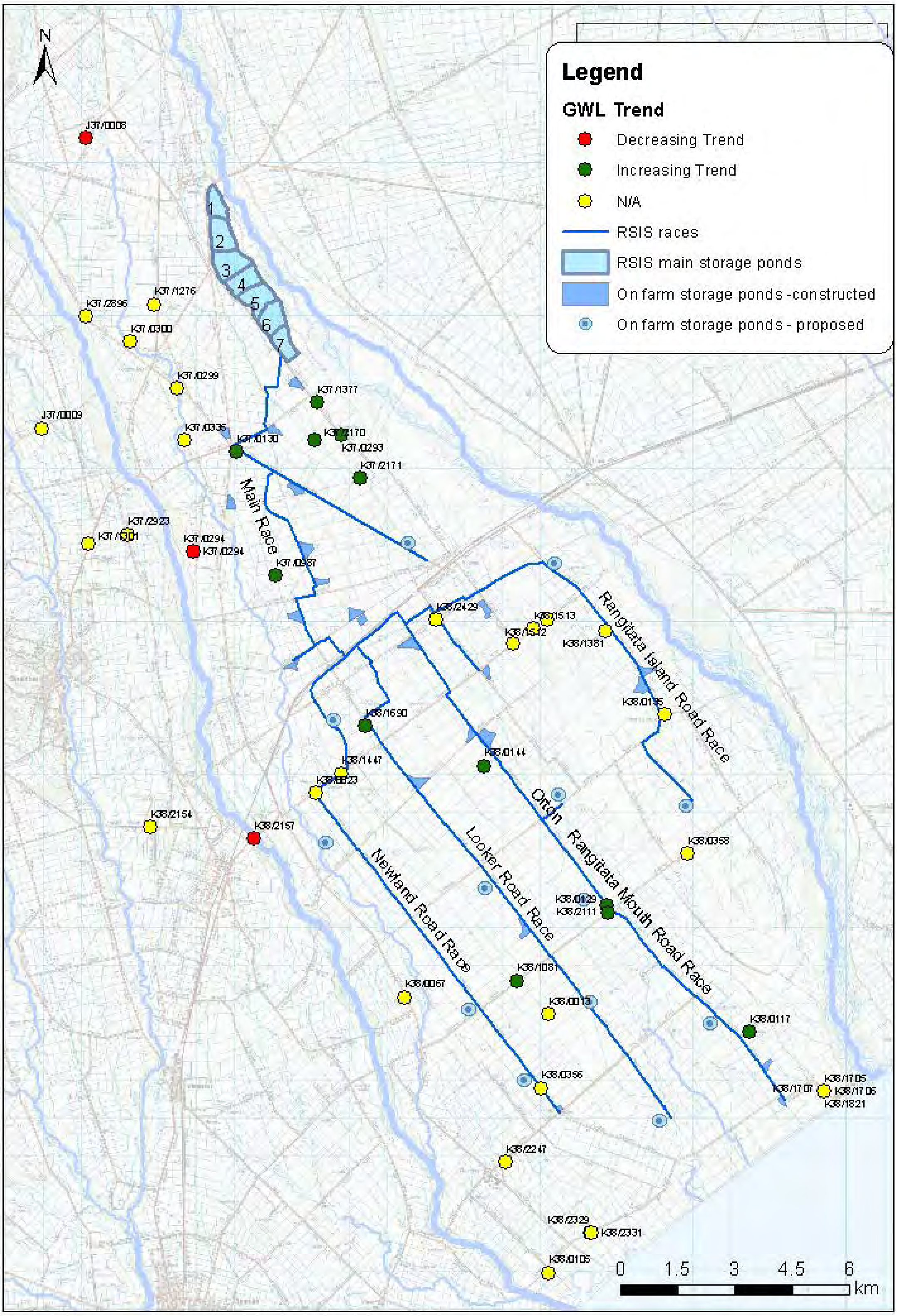

Figure 4-1: Map of wells with water level records showing observed groundwater level trends

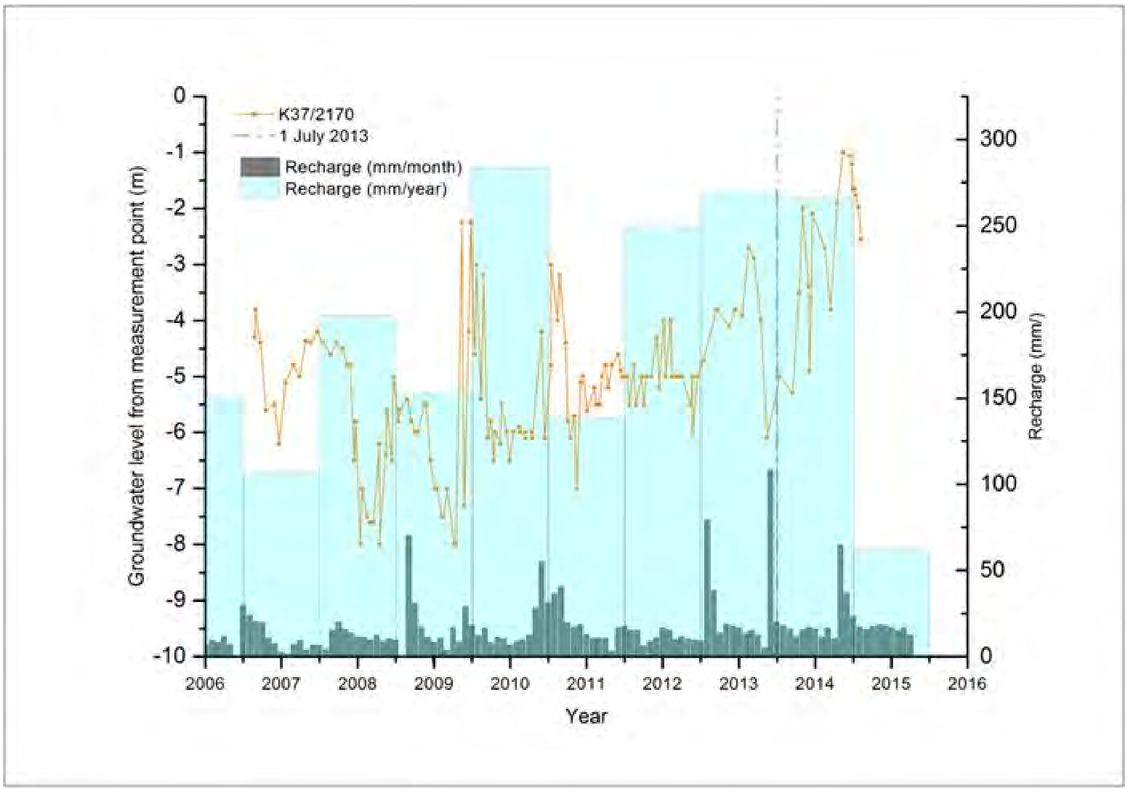

Figure 4-2: **Groundwater level record for well K37/2170 and recharge calculated in this location from our model. The groundwater level showing obvious signs of increasing water levels**

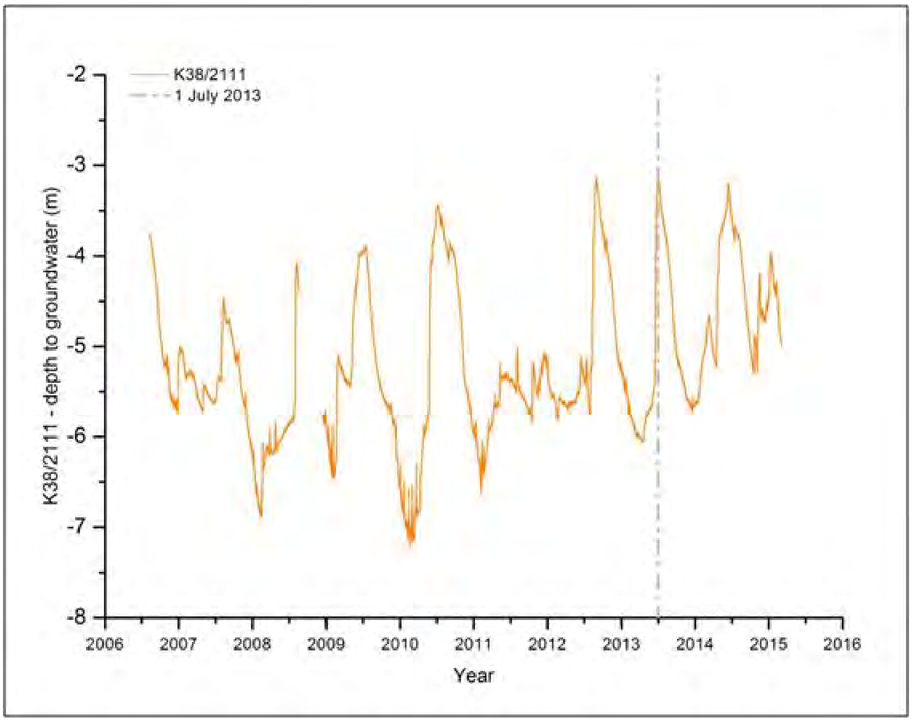

Figure 4-3: **Groundwater level record for well K38/2111 showing subtle signs of increasing water levels coinciding with the commissioning of the RSIS (rising summer lows)**

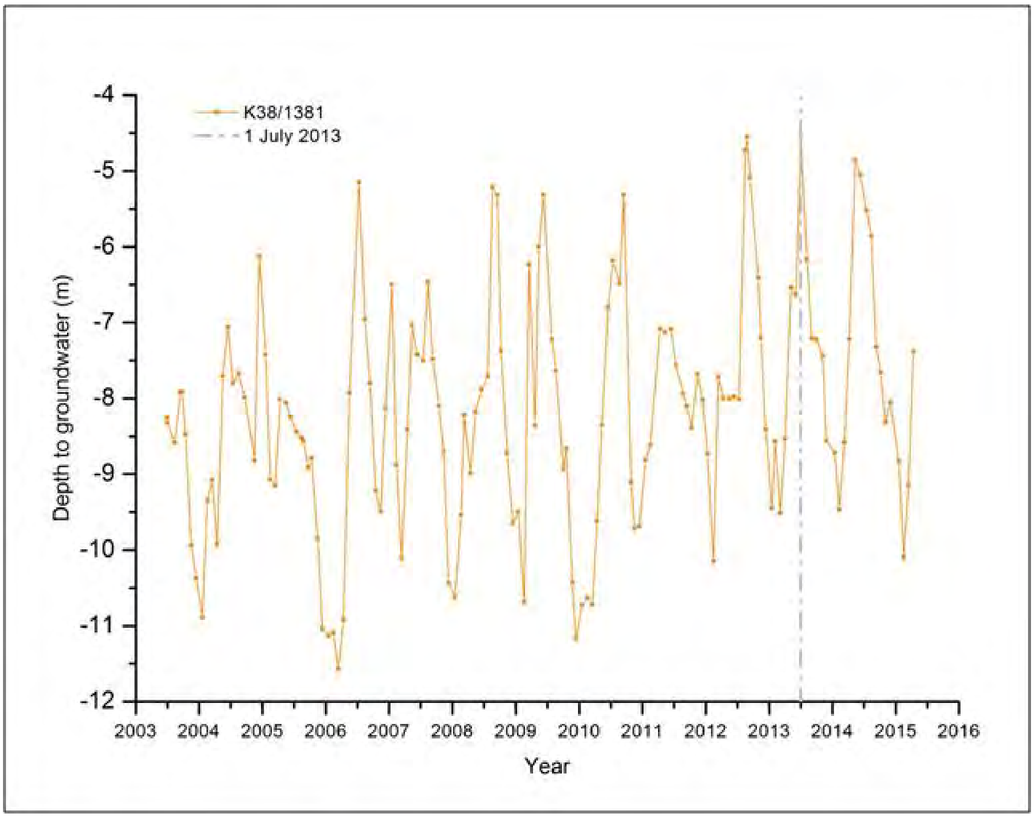

Figure 4-4: Groundwater level record for well K38/1381 showing no obvious changes in water levels coinciding with the commissioning of the RSIS

4.2 Flooding

In November 2013, Environment Canterbury received a report that a stock underpass on Arundel Rangitata Road had had flooded (Figure 4-5, Figure 4-6). The underpass is located 2.6 km downstream of the main RSIS ponds (site 0 on Figure 4-5). It was constructed in 2006 (Irricon, 2013). The owner reported that groundwater levels had previously been in the range of 4 to 6 metres below ground surface, but that the level had risen to 1.5 metres below ground surface since the RSIS canals had started to be used.

The closest shallow water level monitoring wells to the underpass are K37/0293 (5.97 metres deep, located about 250 m up the road from the underpass) and K37/1377 (9.96 metres deep, located about 1.3 km up the road (Figure 4-1). Data from these wells indicate that the water table in the vicinity of the underpass was generally deeper than 3 metres below groundwater surface (mbgs) prior to 2013, and that it has risen to within roughly 1.5 to 2 metres of the ground surface in recent years. However, data from K37/0293 (Figure 4-7) also shows that levels did come within 1.5 metres of the ground surface at times in the past, including 1990 and 2000.

Staff at Rooney Earthmoving Ltd (REL) have suggested that the underpass flooded not as a result of high water table, but because of leakage from an adjacent stock water race (Gary Rooney, personal communication). They report that the when the stock water race is turned off, the underpass drains within 10 days, and when the race is turned back on, the underpass re-fills. They have also used a dye to trace water from the race entering the underpass.

We agree that leakage from the stock water race is contributing to the flooding. However, the data from wells K37/0293 and K37/1377 suggest that the water table is frequently higher than the base of the underpass and that there would be flooding even without the stock water. The frequency of the higher water table occurrence appears to have increased since the RSIS was put in place.

REL staff also measured the water level in well K37/2502, immediately adjacent to the underpass, at 22 metres below ground surface. However that well is relatively deep, screened from 71 to 77 metres below ground surface, so the water level does not necessarily reflect the water table. Data from other wells in the area show a similar pattern with lower water levels in deeper wells, suggesting a strong downward hydraulic gradient. Therefore, only shallow wells provide a reliable estimate of the level of the water table.

During September 2015, Environment Canterbury received complaints from land owners in the vicinity of the Rangitata River middle channel (site 1 in Figure 4-5) and Kapunatiki Creek (sites 2, 3 and 4 in Figure 4-5) in regard to flooding on their properties. Durney (2015) visited the sites on 21 September 2015 (Figure 4-8 and Figure 4-9) and concluded that the flows were caused by groundwater discharging to old river channels. He thought it was likely that the groundwater levels were high as a result of the RSIS, but he could not link the effect to any individual distribution race or on-farm pond.

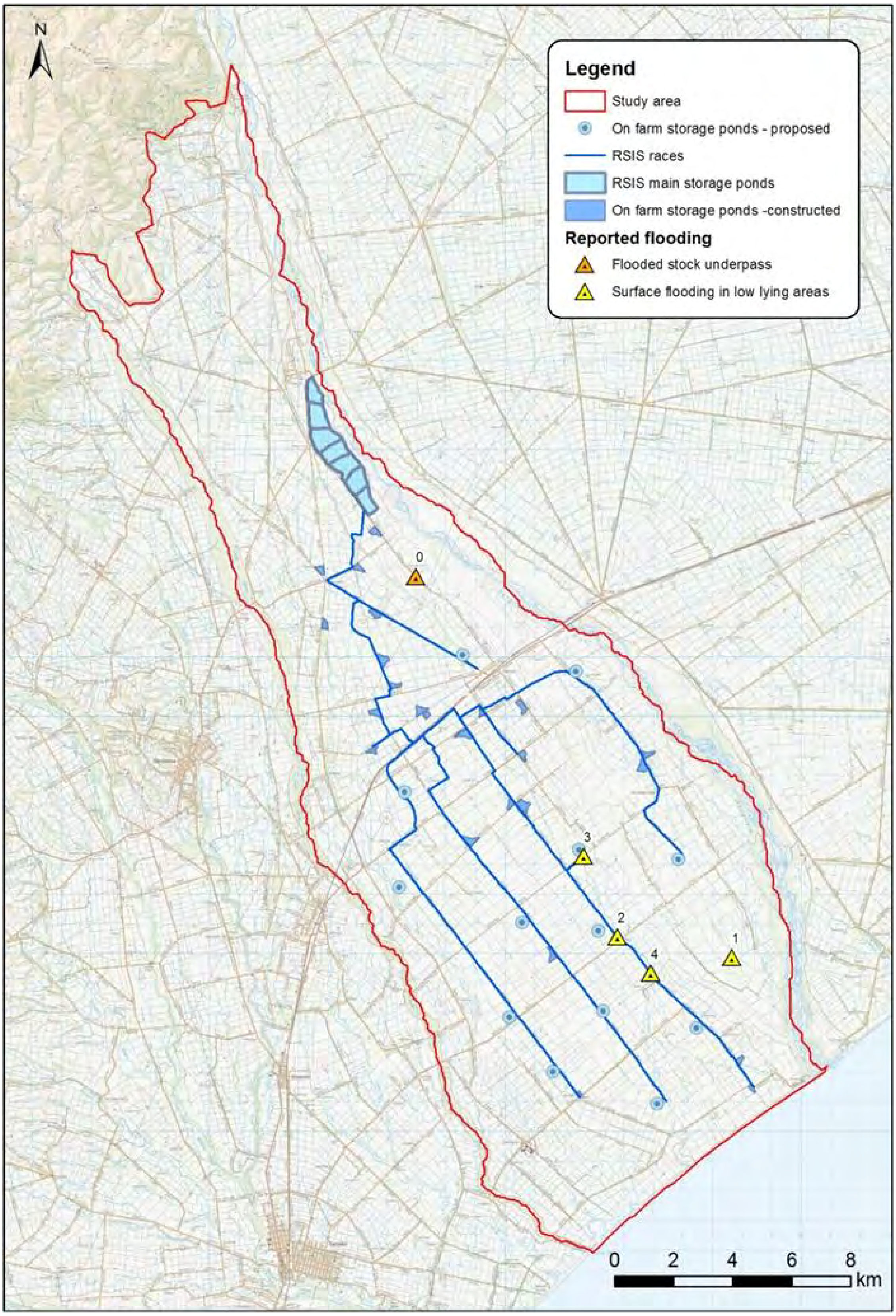

Figure 4-5: Location of reported flooding incidents thought to be associated with the RSIS

Figure 4-6: Photograph of flooded stock underpass on Arundel Rangitata Road, immediately downstream on the header ponds (Site 0 in Figure 4-5). Photograph taken by Environment Canterbury on 13/11/2013

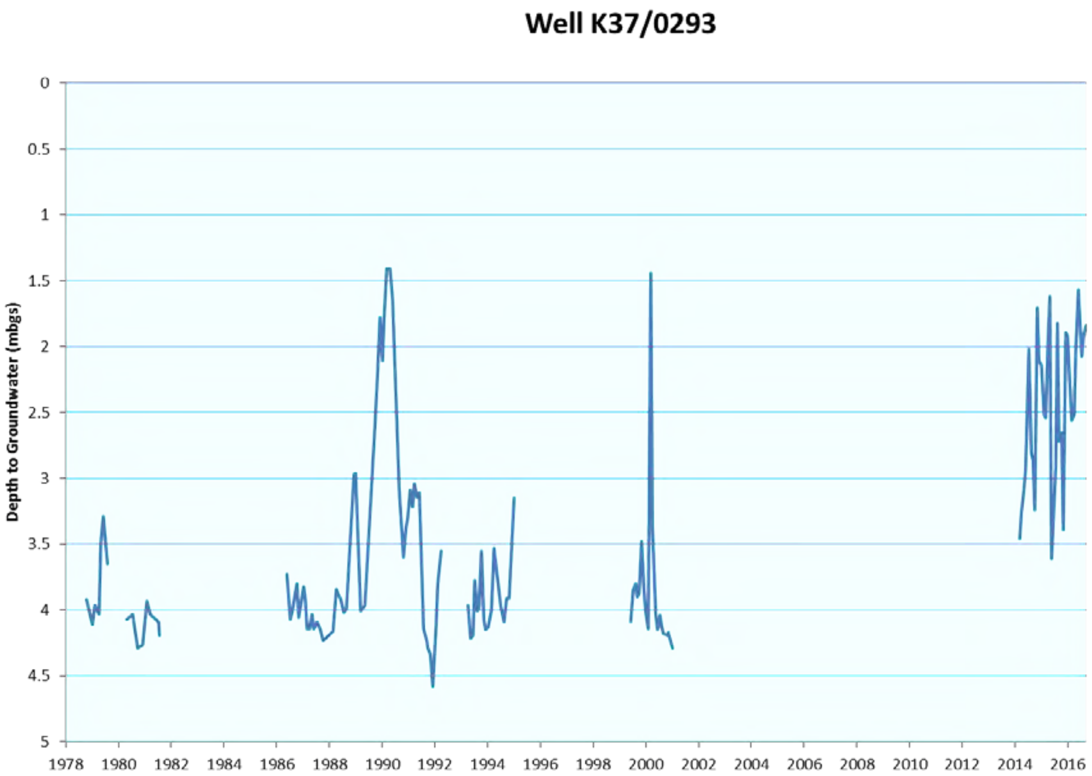

Figure 4-7: Time series graph of depth to groundwater levels at Well K37/0293

Figure 4-8: Photograph of surface flooding believed to be the result of groundwater discharge in the vicinity of the Rangitata River middle channel (Site 1 in Figure 4-5). Photograph taken by Environment Canterbury on 21/09/2015

Figure 4-9: Photograph of surface flooding believed to be the result of groundwater discharge in the vicinity of Kapunatiki Creek (Site 3 in Figure 4-5). Photograph taken by Environment Canterbury on 21/09/2015

4.3 Groundwater quality

Intensive farming has the potential to increase nutrient concentrations in the groundwater. Higher dilution due to leakage from the ponds and races may or may not offset nutrient concentrations. PDP (2006) and Brough (2008) undertook modelling of potential effects of the RSIS on groundwater quality to support the RSIS consent application. Evidence presented on groundwater quality impacts in the resource consent hearing for the RSIS was contradictory and the conclusion of hearing commissioners was that the effects could not be predicted with any certainty (Cowie and Nixon, 2009). More recent modelling undertaken by URS (2014) has indicated that nitrate nitrogen concentrations in groundwater would improve if distribution losses (i.e. race losses) from the RSIS were more than 10% of flow and remained at this level over time. Nitrate concentrations in groundwater would increase if race losses were in the order of 5% of flow. Further predictions to changes to groundwater quality resulting from the RSIS are outside the scope of this investigation, but we have looked at actual groundwater quality data collected to assess observable changes to groundwater quality.

4.3.1 Groundwater quality trends

There are seven wells in our study area that are part of our long-term groundwater quality monitoring network (Figure 4-10). One of these wells (K38/0144) is sampled monthly, four are sampled quarterly (J37/0012, K38/0148, K38/0404 and K38/1017) and two are sampled annually (K37/0465 and K38/0105).

Results of recent monitoring indicate that two wells (K38/0144 and K38/0404) show clear groundwater quality changes, including decreases in concentrations of calcium, chloride, conductivity, magnesium, nitrate, potassium, sodium, sulphate and hardness (Figure 4-11, Figure 4-12). Another monitoring well hydraulically down gradient of the RSIS (K38/1017) also show indications of improved groundwater quality. However a well up-gradient (J37/0012) shows no indications of changes in groundwater quality. We have attached water quality time series plots of nitrate and conductivity of groundwater for all our monitoring wells in Appendix B.

Our review of the data shows that changes in groundwater quality coincide with the commissioning of the RSIS. Interestingly, modelling of the potential effects of the RSIS on groundwater quality by PDP (2006) for the original consent application predicted increases in nitrate concentration by approximately 4.5 g/m^3 nitrate-nitrogen below the command area. Further modelling (also undertaken by PDP) for the hearing predicted a 20% increase in mass nitrate loading. However, when accounting for dilution from scheme infrastructure and the removal of cattle over the winter, Brough (2008) predicted nitrate-nitrogen concentrations would stay the same or slightly decrease. More recent modelling undertaken by URS (2014) has indicated that nitrate concentrations in groundwater would improve if distribution losses from the RSIS were more than 10% of flow and remained at this level over time.

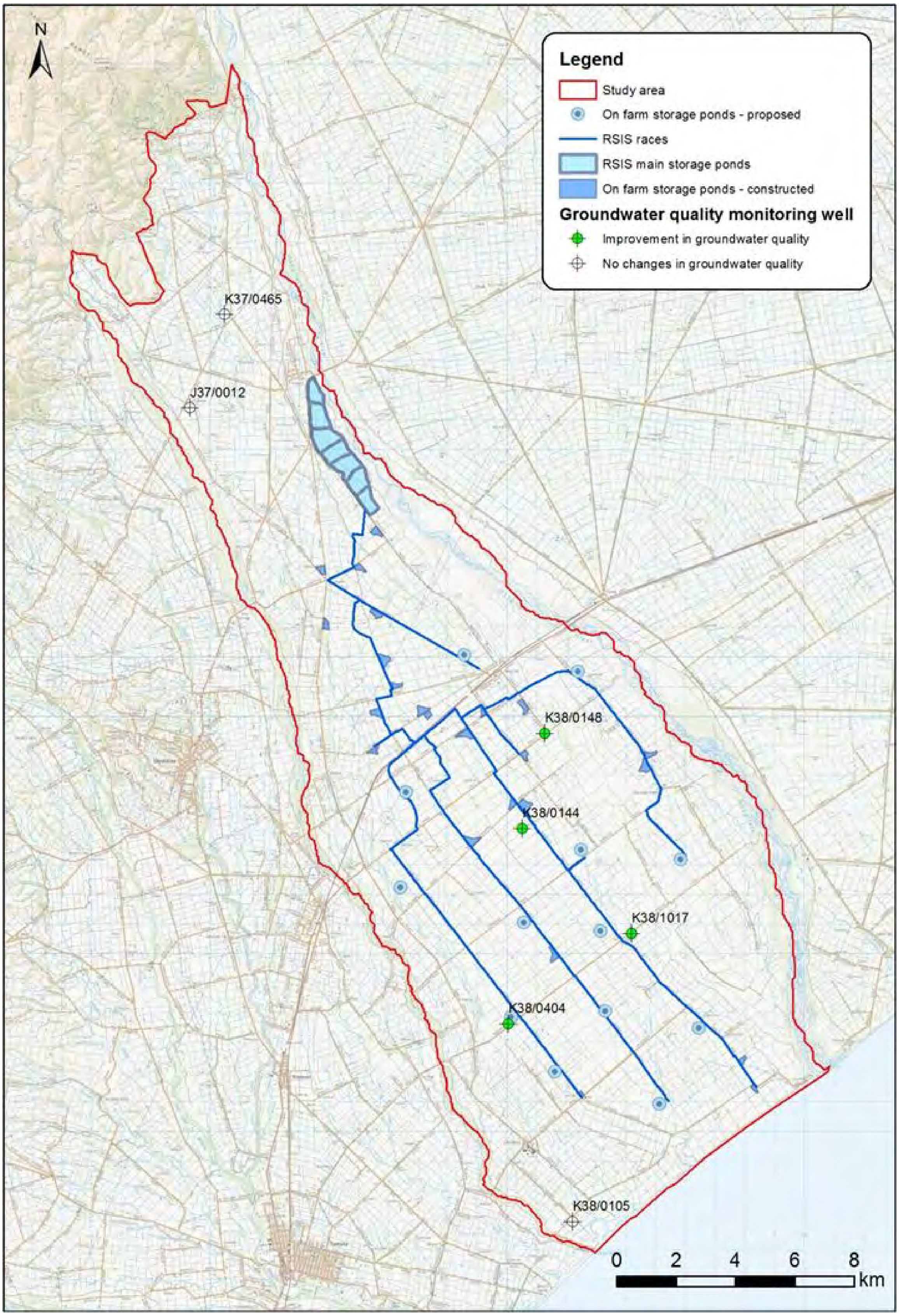

Figure 4-10: Map showing location of Environment Canterbury groundwater quality monitoring wells in our study area

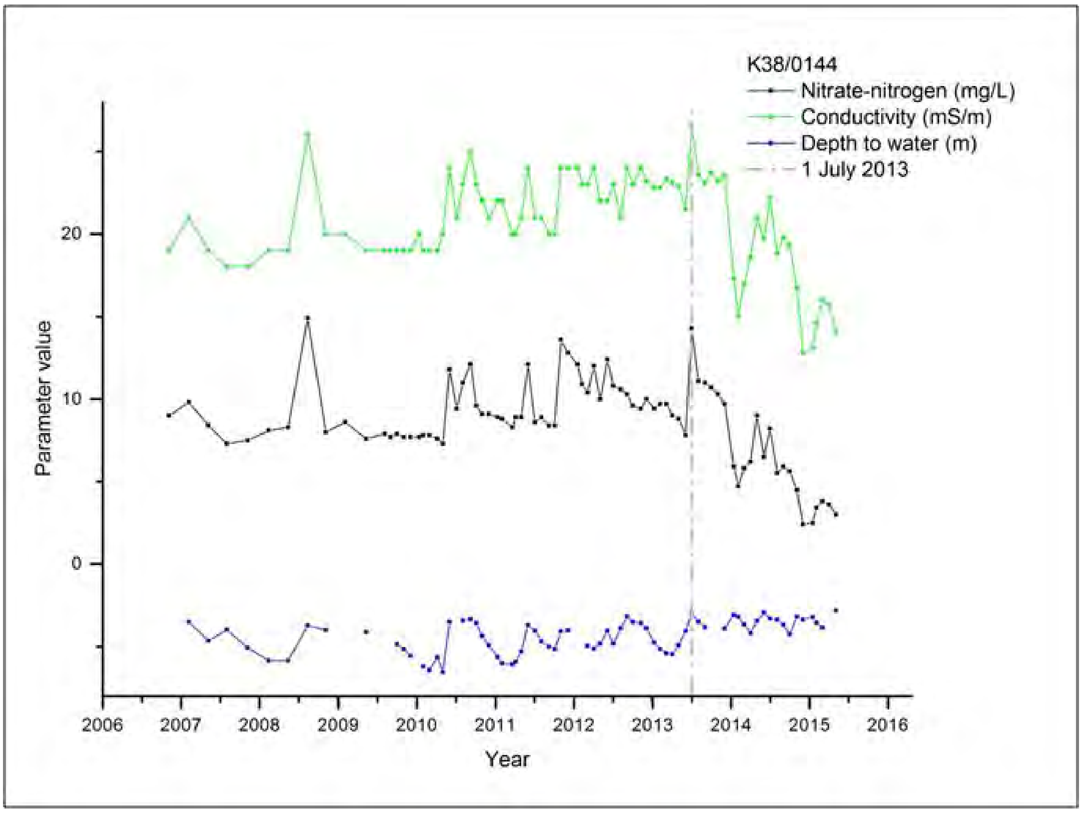

Figure 4-11: Nitrate-nitrogen, conductivity and depth to water trends in well K38/0144

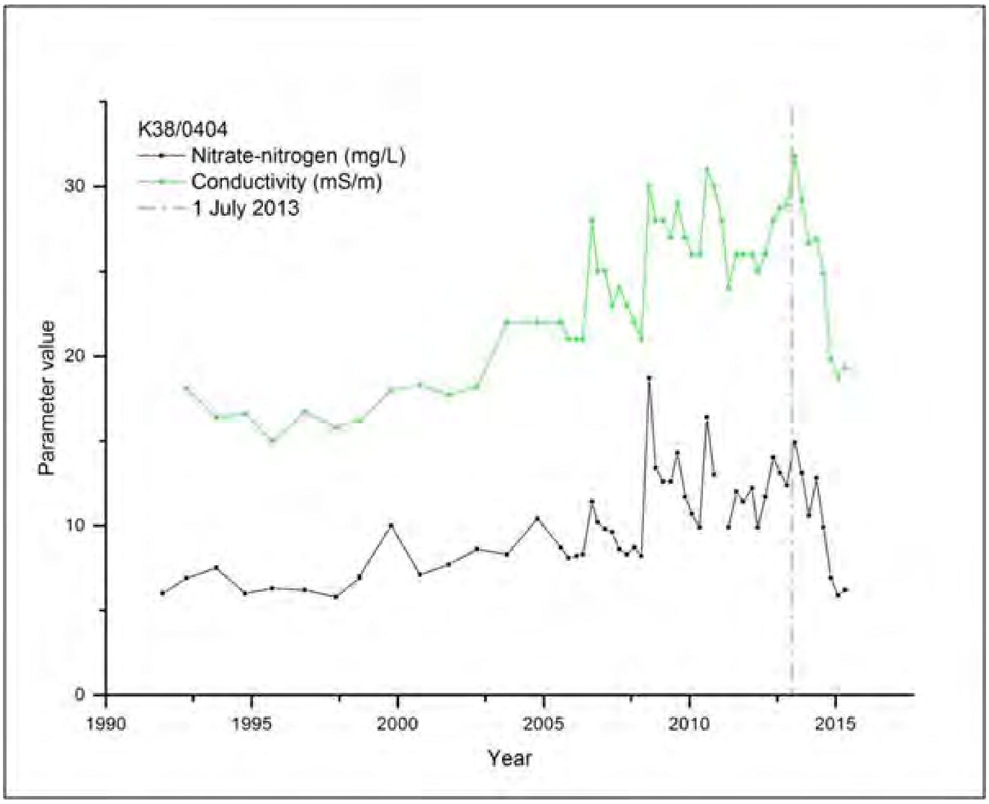

Figure 4-12: Nitrate-nitrogen and conductivity trends in well K38/0404. Pre-scheme the concentrations are observed to be rising (note there is no depth to water data available for K38/0404)

5 Numerical modelling

5.1 Introduction

Groundwater modelling provides a methodology to simulate system behaviours under various natural and manmade conditions. We built a steady-state numerical model of the groundwater system in the area and used it to simulate potential impacts of the RSIS on groundwater levels. The modelling exercise helped us to test whether the observed changes to the groundwater system that we discussed in Section 4 could reasonably be attributed to the RSIS, and it enabled us to evaluate the potential long-term effects of the scheme on the area's groundwater system.

We first built the model and calibrated it to match data collected before the commissioning of the RSIS. This gave us a model representative of the groundwater system and its behaviour before the introduction of the RSIS. Then, we added extra recharge to the model to represent leakage from the RSIS and associated infrastructure. As we were not certain how much leakage there might be, we used a 'stochastic' process, which means we ran the model many times, each time using different leakage values taken at random from probability distributions that we defined. This gave us an array of results that represent what we think is the range of possible effects that the scheme might have on the groundwater system. Specifically, changes in groundwater levels that may result from the introduction of RSIS ponds and races.

We built our model using MODFLOW [USGS, 2000] in the GMS graphical user interface software. Recharge to the groundwater system was estimated using MIKE SHE software [DHI, 2014], and the pre-scheme model was calibrated using PEST [Doherty, 2002]. Details of the model are presented in Appendices C through F.

In our modelling, we did not consider irrigation returns from any additional irrigated areas resulting from the RSIS. With respect to this question, therefore, our model slightly under-predicted the rise in groundwater levels.

In order to achieve our modelling aim we first set up a calibrated, steady-state model representing hydrogeological conditions before the commissioning of the RSIS using. We used the calibrated model to run a series of probabilistic (stochastic) simulations to represent a range of possible impacts on groundwater levels from the storage and distribution network of RSIS.

5.2 Pre-scheme model

5.2.1 Model configuration

Our model domain covers the area from the coast to the foothills and extends outside our study area to capture the effects of the Rangitata and Orari Rivers (Figure 5-1). We used a specified head boundary to represent the coastline. We extended the north-eastern and south-western boundaries beyond the study area to capture the effects of the Rangitata and Orari rivers. Because we set the boundaries along groundwater divides, these boundaries are no-flow. Additionally, because of minimal input from the groundwater system from the basement rocks underlying the foothills, we defined the inland boundary along the base of the foothills as a no-flow boundary.

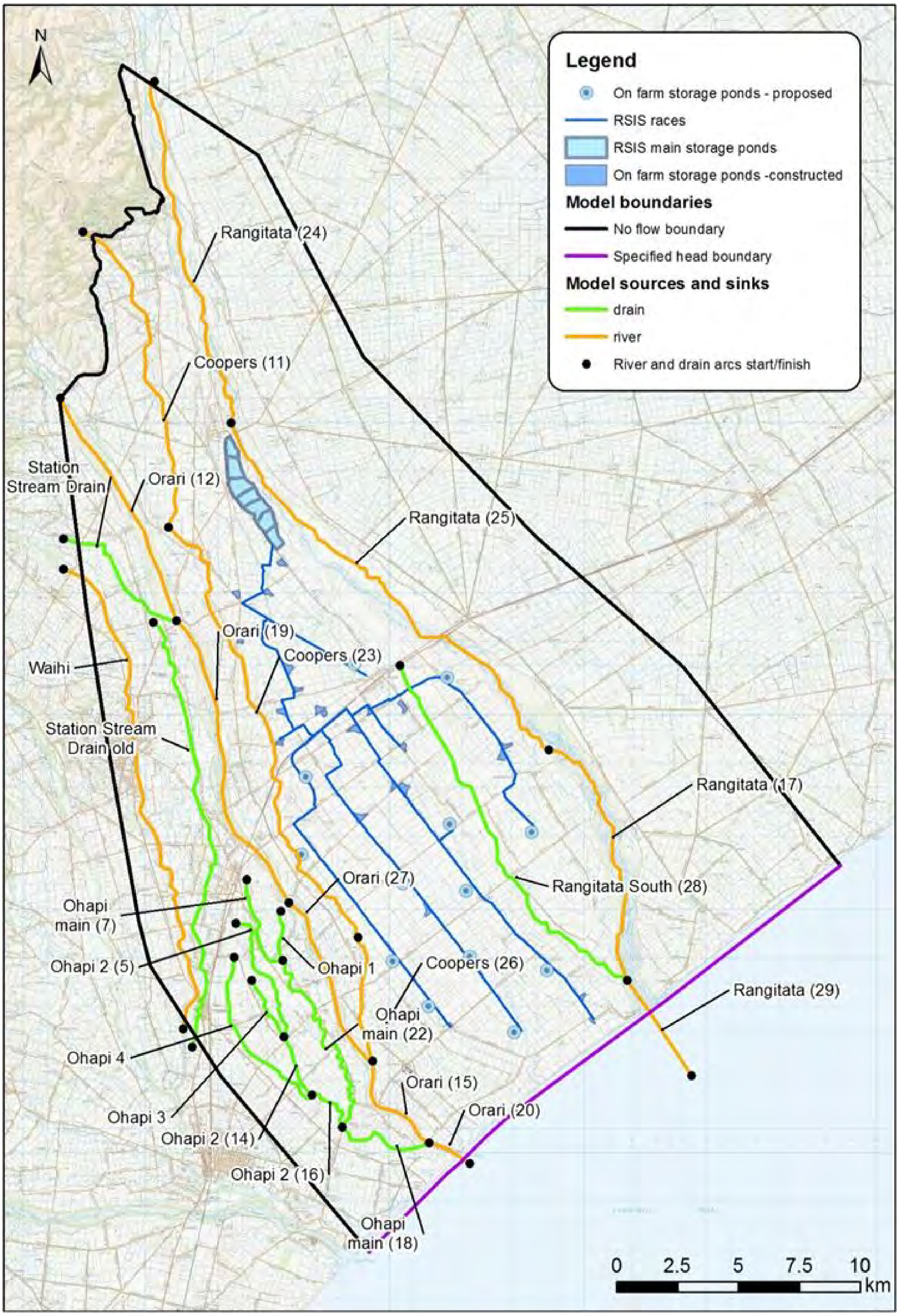

Figure 5-1: Model boundary conditions, sources and sinks (including labelled sections of rivers/drains)

Vertically, we used four layers to represent the aquifer. We defined the top of the model (ground surface) using a 250 m mean aggregated 2 m LiDAR digital elevation model (DEM). We set the base of model at 150 m below the ground surface. The model layers do not correspond to any actual hydrogeological settings. We simply defined them to allow for the consideration of vertical flow within the aquifer system. The model had a grid cell size is 250 x 250 m.

5.2.2 Groundwater recharge and abstraction

We calculated recharge to the groundwater system using a MIKE SHE model (Appendix C) with grid configuration similar to what we used in our MODFLOW model. The MIKE SHE model was a transient, fully coupled groundwater/surface water model that calculated daily recharge based on 30 years of weather data. From the MIKE SHE results, we derived a long-term average annual recharge value for each cell of our model.

In the MIKE SHE model, we based the irrigable area on 2014 land use data obtained from Aqualinc (2015). MIKE SHE incorporates an evapotranspiration and rainfall model and uses the Richards equation (1931) to calculate the infiltration.

For simplicity, we accounted for groundwater abstraction in the recharge inputs. MIKE SHE calculates irrigation demand on a daily time step over the irrigation season. We aggregated this into annual average irrigation demand and deducted this from the modelled recharge to estimate groundwater abstractions.

5.2.3 Surface water sources and sinks

We modelled the Rangitata River, the Orari River, Coopers Creek and the Waihi River (Figure 5-1) using the Rivers Package in MODFLOW. The Rivers Package allows for the exchange of water between surface water and groundwater (in both directions) based on the hydraulic head in the aquifer, the stage and bottom elevation of the river, and the conductance of the riverbed material. The bases (bottoms) of the rivers were set at 1 m below the topographic surface (derived from the DEM). The water depth in the rivers were set at 0.5 m. Streambed conductance values (Appendix F, Table 3) were automatically adjusted during model calibration using PEST to calculate river losses (through varying streambed conductance) to achieve a match to the observed hydraulic heads in groundwater wells.

We modelled Station Stream, Dobies Stream and Ohapi Creek (and tributaries) using the Drains Package in MODFLOW (Figure 5-1) as all these surface water features only gain flow in the area of our model (i.e. they drain the groundwater).

5.2.4 Model calibration

We calibrated our model by varying the input values for hydraulic conductivity and riverbed conductance until the model calculated groundwater levels matched the levels that we have observed in the field measurements. To calibrate the model, we used PEST software, which automatically runs the model repeatedly, varying the input values within specified ranges until it achieves a reasonable fit to the observation data.

The observation data included average groundwater levels from our monitoring network wells and interpolations from piezometric survey data. We assigned monitoring network wells to model layers that corresponded to well screen placement/elevations.

We applied the same average hydraulic conductivity values to all numerical layers in our model and assumed an isotropic system, i.e. permeability is the same in all directions at any specific point within the model. Hydraulic conductivity was restricted to vary between 0.001 and 100 m/d.

Figure 5-2 shows the resulting hydraulic conductivity after calibration. This hydraulic conductivity range compares favourably with hydraulic conductivities (Table 5-1, using an average aquifer thickness of 50 m).

Riverbed conductance values are tabulated in Appendix F.

Table 5-1: Hydraulic conductivity

Hydraulic conductivity (m/day) based on aquifer test transmissivities'	**<10**	**20**	**30**	**40**	**50**	**60**	**70**	**80**	**90**	**100**	**110**	**120**	**>120**
Frequency	77	30	6	6	5	5	2	1	2	2	3	0	4

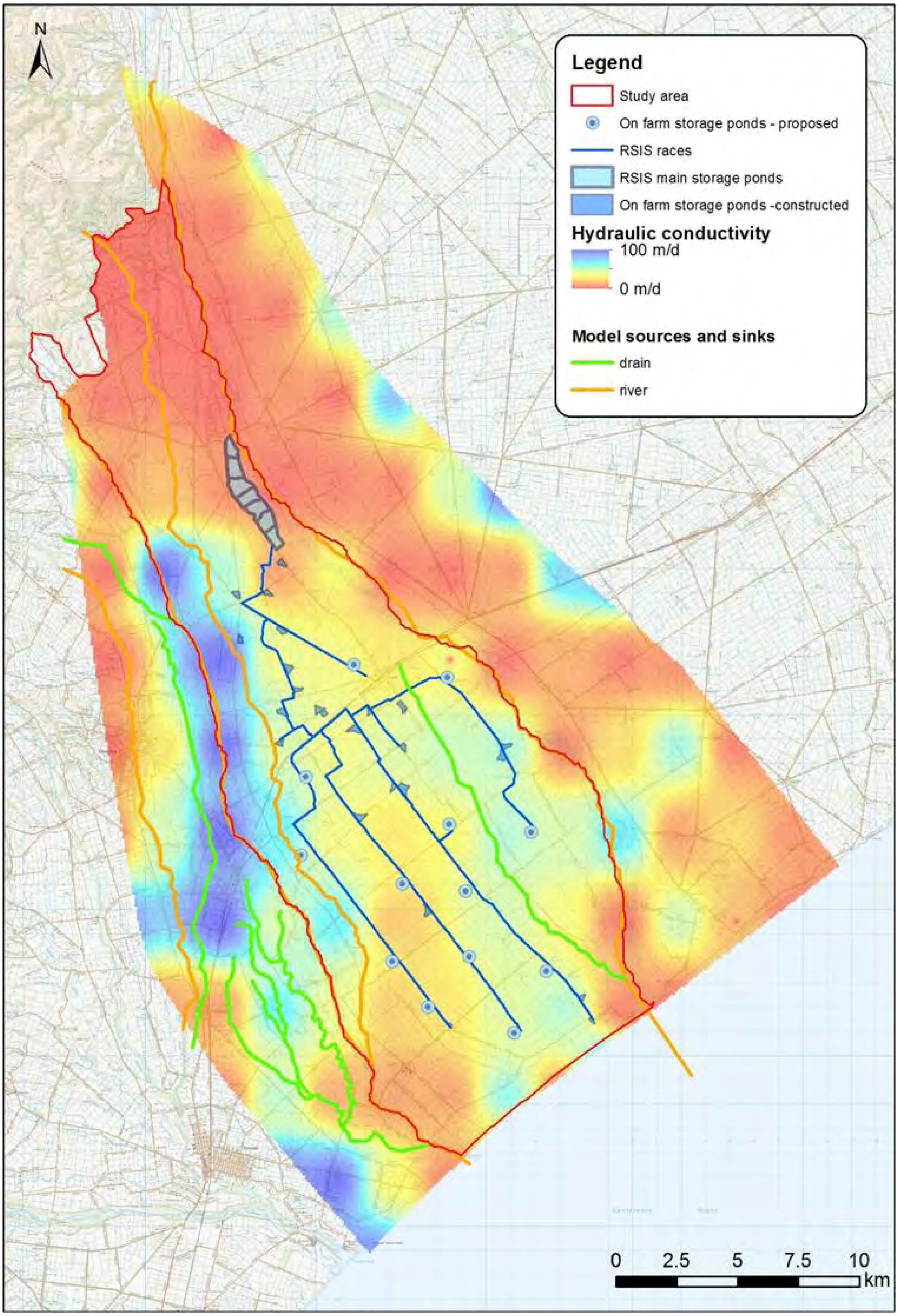

Figure 5-2: Calibrated model hydraulic conductivities (conductivities applied for all layers)

5.2.5 Calibration results

We achieved a good fit of our model to the calibration targets. 92% of the head elevation calibration targets were within the target range of less than two metres variance (detailed in Appendix F). In terms of calibration statistics, the root mean square error (RMSE) for the adopted solution was 1.378 m. For a model with 574 calibration points, we deemed this to be reasonable given the inherent accuracy of our observation points[3] and the simplifications used in the model design.

The model's water balance error was less than 1%, also indicating the model was performing appropriately.

5.3 Post-scheme model

Once we had a calibrated model of the groundwater system, we added recharge to simulate leakage from the RSIS infrastructure to assess the potential long-term effects of the scheme. Because we were interested in long-term effects, we assumed all infrastructure and ponds related to the RSIS were operational, including on-farm ponds. We ran the model 1,000 times using a stochastic simulation that randomly varied pond and race losses within specified realistic ranges. From those results, we calculated the mean, maximum and minimum groundwater level changes.

For simplicity, we assumed that groundwater abstraction will remain the same following the commissioning of the RSIS (i.e. that no surrender of groundwater abstraction will occur).

We have not been able to find any studies specifically estimating seepage from irrigation ponds. Ray *et al.* (1997) estimated losses from dairy farm effluent treatment ponds in the Waikato (which will be clay/silt lined) to be between 0.0009 and 0.0044 m/d. Poulsen (2013) estimated infiltration rates through loess soils (with a fragipan) in Canterbury to be between 0.00001 and 0.001 m/d. Since coarser grained materials typically have higher infiltration rates, these values are likely to underestimate the losses through the gravelly bottoms of the RSIS ponds.

Yoo and Boyd (2012) classified pond seepage rates for aquacultural ponds (Table 5-2). They suggested that properly constructed ponds have seepage rates below 0.00254 m/d and that few lose more than 0.00635 m/d.

Table 5-2: Pond seepage classification for aquacultural ponds (from Yoo and Boyd, 2012)

Classification	Seepage rate (m/d)
Low	0 – 0.00482
Moderate	0.00483 – 0.00991
High	0.00992 – 0.01499
Extreme	>0.015

We set the mean value for seepage from the main ponds and on-farm ponds to be 0.01 m/d, which equates to the permeability of a silt and represents a moderate to high seepage rate using the classification of Yoo and Boyd (2012). We set the minimum and maximum rates to an order of magnitude either side of this (i.e. 0.001 to 0.1 m/d). We assumed the on-farm ponds are not lined with synthetic liners.

[3] The general accuracy of manual measurements is likely no better than 0.1 m and interpolated points from piezometric contours no better than 2.5 m. Further, if we assume that the general accuracy of the observation point mean representing the true mean is 0.1 m (large sample size) and the interpolated point is 2 m (single sample) then the standard deviation of the prediction points is 0.972 m using n-1. Whilst the computed RMSE is larger than the predictor accuracy standard deviation, they are very close.

Lloyd (2008) estimated race losses from the RSIS irrigation scheme to be in the order of 20% at the start of the season, reducing to 10-15% as the season progresses. He assumed losses would be greater at the start of the season because silt sealing the bottom of the races would be blown away during the off-season when the races are dry. Losses from the TDC stock water race system in our study area are estimated to be approximately 350 L/s or 73% of the water abstracted (de Joux, 2013).

We estimated race losses to the groundwater system to be 20% ±10% for our modelling. Flow in the main race of the RSIS is 6 m^3/sec; this reduces to 0.25 m^3/sec in smaller races approaching the coast (Irrigation New Zealand, 2015). We have assumed the races to be flowing only during the irrigation season, September to April (eight months). Based on a 250 m x 250 m model grid size, this equates to 0.03 m/d and 0.0002 m/d of recharge to the groundwater system for the main race and smaller races, respectively, for each model grid cell which contains a race (Table 5-3).

Table 5-3: Calculation details for race losses

	Main race	**Smaller races**
Flow (m^3/sec)	6	0.25
Average flow assuming flowing 8 out of 12 months (m^3/sec)	4	0.167
Flow to groundwater assuming 20% loss (m^3/sec)	0.8	0.033
Daily loss (m^3/day)	69,120	2,880
Number of 250 m by 250 m grid cells in model representing race	35	217
Area of race representation (m^2)	2,187,500	13,562,500
Daily loss assuming 20% loss rate (m/d)	0.03	0.0002

Table 5-4 shows the recharge values we used in our model. Within the ranges shown in the table, we used random statistical sampling of uniform distributions for the model runs. Figure 5-3 shows the locations of the model cells where we applied varying recharge to our model.

Table 5-4: Recharge values used for stochastic simulations

	Recharge (m/day)			**Distribution**
	Minimum	**Maximum**	**Mean**	
Main Ponds	0.001	0.1	0.01	Uniform
On-farm ponds	0.001	0.1	0.01	Uniform
Main race	0.01	0.05	0.03	Uniform
Other races	0.0001	0.00032	0.0002	Uniform

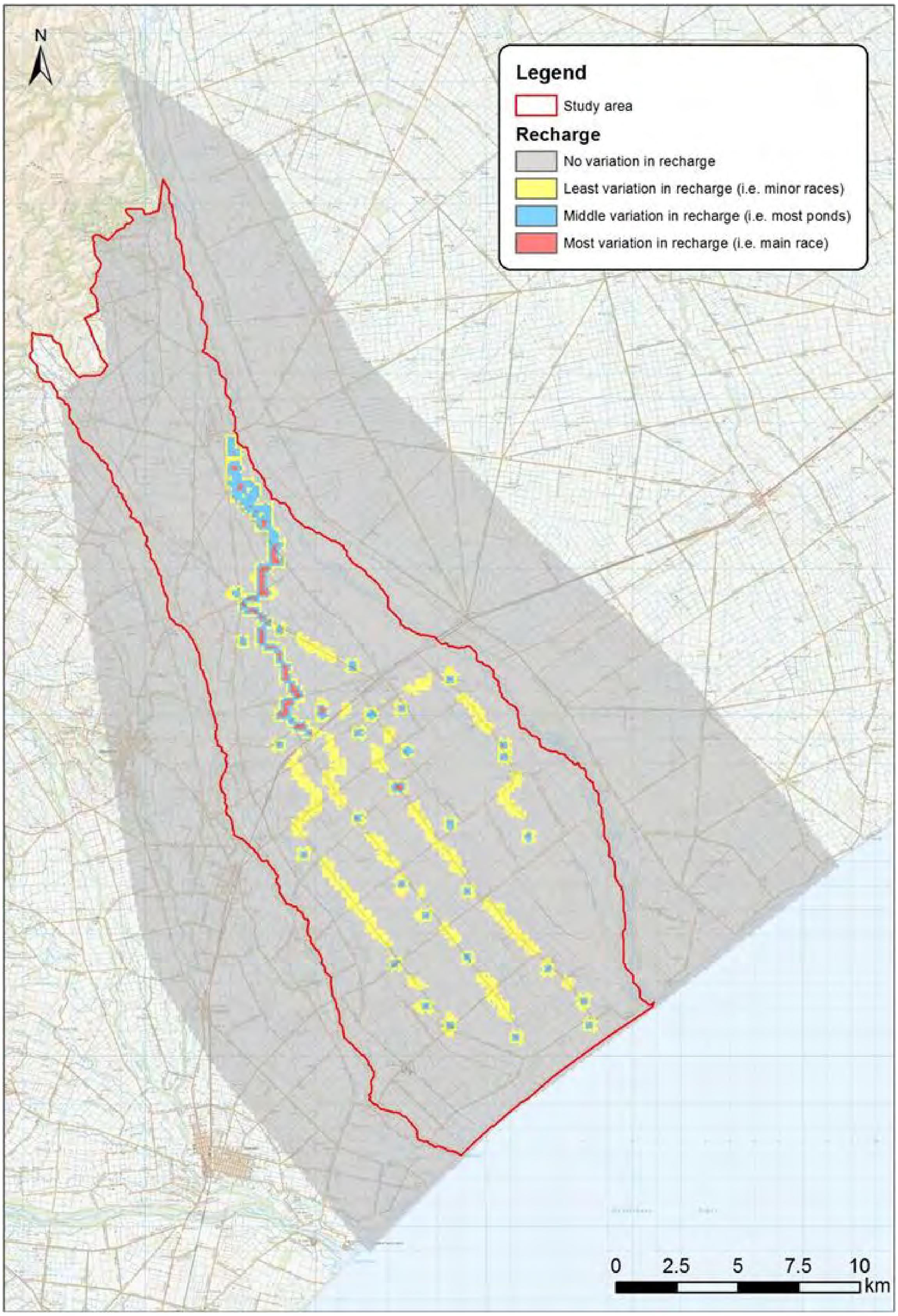

Figure 5-3: Map showing recharge cells stochastically varied in the model (yellow, blue and red cells), and those cells with constant recharge values (grey)

5.4 Results of modelled scenarios

The model results suggest that the water table beneath the study area will rise as a result of leakage from the RSIS infrastructure and on-farm ponds. Our stochastic modelling process produced a range of results (Table 5-5. Also see Appendices E and F). Most of the model runs predicted increases in groundwater levels, with the largest increases under the main storage ponds and near the main distribution race (Figure 5-4). The maximum predicted rise was about 5 metres beneath Pond 4.

The observed groundwater trends to date are generally within the range of the modelled groundwater level increases (Table 5-6).

Table 5-5: Summary of model calculated groundwater level changes

Study area locale	Modelled groundwater level change (m)		
	Minimum	Maximum	Mean
Upper plain	0.003	0.005	0.004
Pond 4	0.165	5.007	3.151
Downstream ponds	0.144	1.740	0.545
Middle plain	0.007	0.707	0.319
Lower plain	-0.009	0.215	0.123

Table 5-6: Comparison of observed groundwater level changes to modelling results (see Figures 4-1 and 4-13 for locations of the wells and underpass referenced)

Well/site	Observed increase (m)	Min modelled increase (m)	Max modelled increase (m)	Mean modelled increase (m)
K37/2170	>1.0	0.214	2.465	0.768
K38/2111	1.0	-0.001	0.411	0.225
K38/1381	None	0.014	0.345	0.161
Flooded underpass	1.0 – 1.5	0.144	1.740	0.545

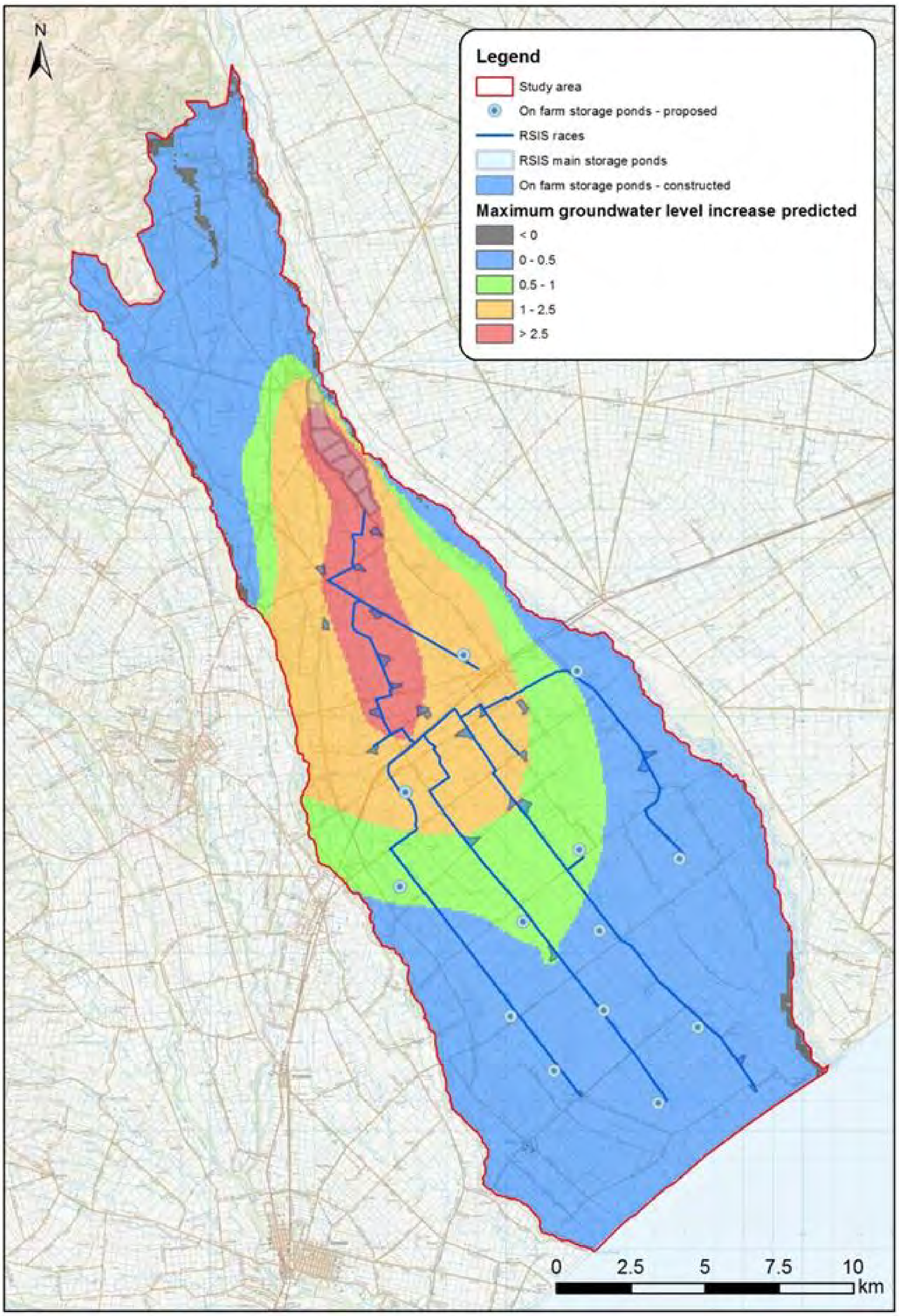

Figure 5-4: **Maximum predicted groundwater level increase resulting from losses from RSIS infrastructure**

Our model suggests no change in general groundwater flow directions. In addition, the water balance from the calibrated model (Table 5-7) shows an error of approximately 0.0004%. More detail on individual river and drain gains/losses is given in Appendix D.

Table 5-7: Model water balance summary

Sources/sinks	Inflow	Outflow
Constant head (coastline)	52,096	496,632
Drains	0	138,848
Rivers	1,116,203	866,623
Recharge (rainfall and irrigation returns)	343,491	9,683
Balance (total in/out)	1,511,790	1,511,785

6 Discussion

The potential drivers for the observed increase in groundwater levels in the study area may include: increase in natural recharge (increase in rainfall), reduction in groundwater abstraction, and/or implementation and utilisation of the RSIS. The following sections discuss the potential of each of these possible drivers.

6.1 Increase in natural recharge

Increased rainfall could raise groundwater levels and dilute nitrate concentrations in the groundwater. We have considered the possibility of increased rainfall recharge by reviewing annual rainfall data from the NIWA-operated climate stations at Orari Estate and Coldstream.

Figure 6-1 shows that there have been fewer wet periods in the last thirty years than there had been earlier in the 1900s. When we zoom in on the 2000-2016 period (Figure 6-2), we see that there was a wetter period between 2010 and 2013, but since then the weather has been significantly drier. Comparison of the recorded rainfall to groundwater levels in well K38/2111 (Figure 6-3) shows a divergence in the relationship between groundwater levels and rainfall after about 2013. This indicates that another driver of groundwater levels has come into play. Rainfall, therefore, cannot explain the increases in groundwater levels since the commissioning of the RSIS.

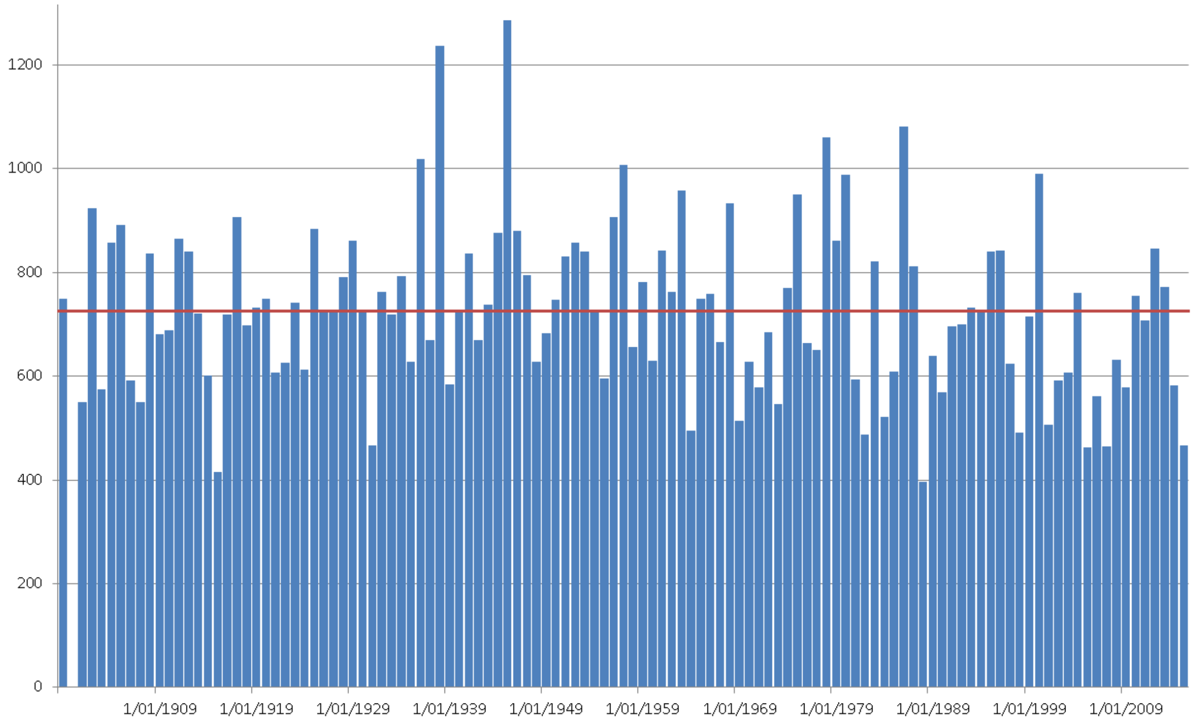

Figure 6-1: Annual rainfall 1900-2016, mean given by the red line

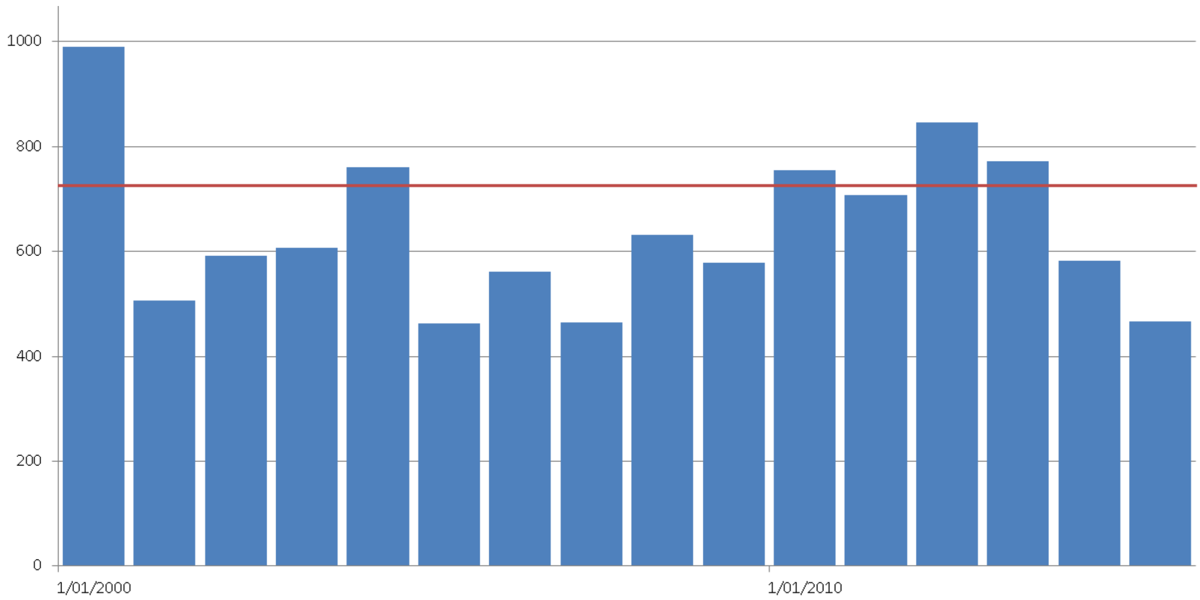

Figure 6-2: Rainfall 2000-2016 (red line = mean rainfall)

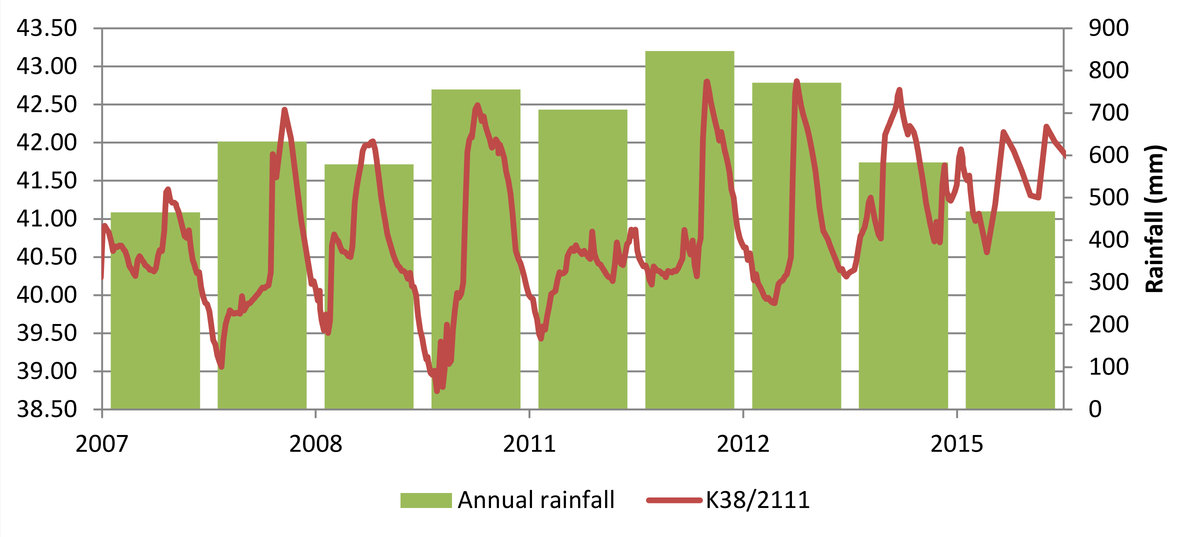

Figure 6-3: Comparison of water levels in K38/2111 and rainfall. Despite a decline rainfall since 2012 groundwater levels have increased

6.2 Groundwater abstraction

If groundwater abstraction had been significantly reduced after the RSIS became operational, this may have resulted in higher groundwater levels during summer. To assess this possibility, we have reviewed the available groundwater abstraction data collected as part of Environment Canterbury's water metering programme.

There are 13 wells for which we have metering data dating back to before the RSIS went into operation. Table 6-1 shows the annual usage at each well, calculated as a percentage of the mean annual volume. Overall, there is no clear pattern of usage in the data. Some sites have used more than average since the RSIS became operational, and some have used less.

Further, decreased groundwater abstraction would not explain the observed improvements in water quality. Given this, combined with the random changes in usage with irrigation year, we do not believe that the increases in observed groundwater levels can be attributed to decreased groundwater abstraction.

Table 6-1: Yearly abstraction as a percentage of annual mean usage

Row Labels	K37/ 0419	K37/ 0494	K37/ 2170	K37/ 2171	K37/ 2391	K37/ 2502	K37/ 2706	K37/ 2707	K37/ 3205	K37/ 3206	K37/ 3207	K38/ 1512	K38/ 1513
30/06/ 2008			164	215	0	0	174					68	74
30/06/ 2009		48	128	93	116	0	167		59	54	107	128	148
30/06/ 2010	85	148	113	104	218	71	199	44	200	144	253	148	164
30/06/ 2011	97	98	44	31	93	85	43	73	89	101	69	107	113
30/06/ 2012	89	111	45	4	138	152	6	154	43	111	42	59	14
30/06/ 2013	101	146	109	122	70	179	45	153	134	164	72	54	32
30/06/ 2014	128	149	96	131	66	212	67	76	76	26	58	136	155

6.3 Implementation and utilisation of the RSIS

We have noticed groundwater level increases in wells in our study area of up to a metre above previously recorded high levels. The timing of the increases coincided with the implementation and utilisation of the RSIS and the locations of the increases coincide with infrastructure installed as part of the RSIS (main ponds, races) or for utilisation of the RSIS (on-farm ponds).

Additionally, the magnitude of the increases is generally similar to the predictions from our groundwater model. Based on our modelling we predict that the long-term (stabilised, or steady-state) effect of the RSIS will be an increase in groundwater levels of up to 5 m directly underneath the main ponds. A rise in groundwater levels up to 3 m in the immediate vicinity of the main race may occur, up to 2 m downstream of the ponds and main race in the middle plains, and up to 0.5 m closer to the coast. Our model predicts little change to general groundwater flow directions resulting from the RSIS.

7 Conclusions

We conclude that implementation and utilisation of the RSIS is the primary cause of the observed increases in groundwater levels and decreases in groundwater nitrate concentrations. The changes are related to leakage from the main ponds, races, changes in irrigation practices, leakage from newly installed on-farm ponds and races, and/or a combination of these factors.

The water table has risen by over a metre above previous high levels in the area immediately downstream of the main storage ponds, but by lesser amounts farther down the plain. The higher water table has contributed to flooding of a stock underpass near the main ponds, and to increased flows in intermittent streams in the lower part of the plain. Our data indicate that both the flooding and the stream flows would have occurred at times even without the RSIS, but they now occur more frequently.

In the future, silt may seal the ponds and races to some extent, and this may in turn reduce losses to groundwater and allow the water table to decline somewhat. However, it is unlikely to return completely to pre-scheme levels.

8 Recommendations

We make the following recommendations:

1. Continued water level and quality monitoring in all of Environment Canterbury's monitoring wells in the study area and another assessment of groundwater level and quality trends in a few years. Stable isotope analysis may be useful to show the source of groundwater if required.
2. Wells K37/2171 and K38/1447 are added to the groundwater level monitoring network to confirm observed suspected increasing trends in groundwater levels.
3. Kapunatiki Creek should be visually monitored monthly to assess its state (e.g. dry, flowing or ponded) or a transducer placed in a shallow well near to the creek.
4. The piezometric survey of Wilson (2013) be repeated circa 2020 to determine any observable changes in groundwater flow.
5. One well has improvement in groundwater quality within the area. We attribute the decreasing concentrations of nutrients and dissolved solids because of dilution/additional recharge from the RSIS infrastructure. The observed improvement in groundwater quality may not continue if losses from scheme infrastructure reduce through self-sealing, lining or piping. It is our opinion that losses from scheme infrastructure are not included when assessing dilution of nutrients due to uncertainty in their future efficiencies.
6. Groundwater recharge is occurring due to losses from storage ponds and races, but these inefficiencies may change over time (e.g. reduced as races may become piped and ponds lined with silt, etc.), so we recommend that the losses be disregarded when assessing long-term recharge rates for allocation purposes.

9 Acknowledgements

We would like to thank Carl Hanson, Hisham Zarour, Gary Rooney and Stephen Douglass who provided review, comment and suggestions on our draft report and John Bisset for supplying aerial photographs of the RSIS construction.

10 References

Aitchison-Earl, P., 2005. Evidence of Philippa Lauren Aitchison-Earl. Report prepared under Section 42A of the Resource Management Act 1991 in the matter of applications by groundwater users for Water Permits to take and use water in the Rangitata-Orton groundwater allocation zone.

Aqualinc, 2011. Calculation of a revised allocation limit for the Rangitata-Orton Groundwater Allocation Zone. Letter report written by Julian Weir to Keri Johnston, Aqualinc reference C12023, Environment Canterbury reference C13C/43954.

Aqualinc, 2015. Irrigated area mapping: Waimakariri and Orari-Opihi-Pareora. Report C15043/1 prepared for Environment Canterbury. Environment Canterbury reference C15C/190370.

Barringer, J., Pairman, D. and McNeill, S.,2002. *Development of a high resolution Digital Elevation Model for New Zealand*, Landcare Research Technical Report.

Brough, A., 2008. Statement of evidence of Andrew Brough on behalf of Rangitata South Irrigation Limited. Evidence prepared in the matter of applications for resource consent by Rangitata South Irrigation Limited associated with the construction and operation of Rangitata South Irrigation Scheme, 26 November 2008.

Burbery, L. and Ritson, J., 2010. Integrated study of surface water and shallow groundwater resources of the Orari catchment. Environment Canterbury technical report No. R10/36.

Burbery, 2011. Review of the Spring-fed Coopers Creek, South Canterbury. Lincoln Ventures report No. 1050-8-R1 prepared for Environment Canterbury.

Burbery, L. 2012. Delineation of the Rangitata riparian zone. Environment Canterbury Report R12/65, ISBN 978-1-927210-92-5. Report prepared for Environment Canterbury by Lincoln Ventures Limited. Lincoln Ventures report number 1050-9-R1, June 2012.

Chow, V.T., 1959. Open-channel hydraulics. New York, McGraw-Hill, 680p.

Christmas, E., 2012. Decision of Hearing Commissioner Emma Christmas on application CRC090713 by Island Glen Diaries Limited to take and use groundwater for the irrigation purposes from the Rangitata-Orton Groundwater Allocation Zone.

Cichota, R., Vogeler, I., Snow, V.O., Webb, T.H., 2013a. Ensemble pedotransfer functions to derive hydraulic properties for New Zealand soils. Soil Research 51: 94-111.

Cichota, R., Snow, V.O., Vogeler, I., 2013b. Modelling nitrogen leaching from overlapping urine patches. Environmental Modelling & Software 41: 15-26.

Cowie, B. and Nixon, N.C., 2009. Decisions of the Hearing Commissioners on applications to the Canterbury Regional Council and Timaru District Council for resource consents for a proposed irrigation scheme taking water from the Rangitata River.

Cox, S.C. and Barrell, D.J.A., 2007. Geology of the Aoraki area. Institute of Geological and Nuclear Sciences 1:250 000 geological map 15. Institute of Geological and Nuclear Sciences. Lower Hutt.

de Joux, R.T., 2013. Summary provided to Environment Canterbury from a consent application prepared for the Timaru District Council in 2001 (consent number CRC011991). Environment Canterbury reference C13C/70761.

DHI, 2012. *MIKE SHE User Manual, Volume 1: User Guide*. DHI.

DHI, 2012. *MIKE SHE User Manual, Volume 2: Reference Guide*. DHI

Dodson, J., 2015. Senior Hydrology Scientist, Environment Canterbury. Personal communication with the authors. Environment Canterbury reference C15C/147027.

Durney, P., 2015. Rangitata South farm site visit – 21 September 2015. Internal Environment Canterbury email from Patrick Durney, Senior Hydrogeologist to Valyn Barrett, Regional Leader - Investigations & Incident Response Monitoring and Compliance. Environment Canterbury reference C15C/147637.

Environment Canterbury, 2009. Rangitata South Irrigation Scheme consents granted. Media release by Environment Canterbury 3/02/2009.

Environment Canterbury, 2013. Site visit to Rangitata Dairies Ltd on Arundel Rangitata Road. Environment Canterbury file note 13/11/2013, reference C13C/177755.

Fairfax, 2014. Farmers prepare to pay for $90m irrigation scheme. Online newspaper article by Tony Benny, 28/05/2014. http://www.stuff.co.nz/business/farming/agribusiness/10087296/Farmers-prepare-to-pay-for-90m-irrigation-scheme

Irricon, 2013. Application for resource consent to take and use groundwater for the purposes of de-watering a stock underpass. Prepared for RDGP Limited. Environment Canterbury reference C13C/171455.

Irrigation New Zealand, 2015. Scheme details – Rangitata South. http://irrigationnz.co.nz/irrigation_scheme/rangitata-south/

Lilburne, L.R., Webb, T.W., Ford, R., Bidwell, V., 2010. Estimating nitrate-nitrogen leaching rates under rural land uses in Canterbury. Environment Canterbury Technical Report R10/127.

Lilburne, L.R., Hewitt, A.E., Webb, T.W., 2012. *Soil and informatics science combine to develop S-map: A new generation soil information system for New Zealand*. Geoderma 170(0): 232-238.

Lilburne, L.R., Webb, T.W., Robson, M., Watkins, N., 2014. Estimating nitrate-nitrogen leaching rates under rural land uses in Canterbury. Environment Canterbury Technical Report R14/19.

Lloyd, I., 2008. Brief evidence of Ian Daniel Lloyd in the matter of multiple applications from Rangitata South Irrigation Limited to Canterbury Regional Council to take and use water from the Rangitata River for irrigation. Hearing evidence.

NIWA, 2012. *Virtual Climate Station Data and Products*. http://www.niwa.co.nz/our-science/climate/our-services/virtual-climate-stations. Accessed 11/2012.

Pattle Delamore Partners Limited (PDP), 2006. Assessment of Environmental Effects of the Proposed Rangitata South Irrigation Scheme. Prepared for Rangitata South Irrigation Limited, September 2006.

Poulsen, D., 2013. The hydrogeological significance of loess in Canterbury. Environment Canterbury technical report No. R13/60.

Ray, D.E.; Balks, N.R.; Barkle, G.F. and Selvarajah, N., 1997. Why do dairy farm effluent ponds leak? In Proceedings of the New Zealand Water and Wastes Association Conference, Rotorua, New Zealand, 26 – 29 August 1997. pp 27.-278.

Richards, L., (1931). Capillary conduction of liquids through porous mediums. Physics 1 (5): 318–333. Bibcode: 1931Physi...1..318R. doi:10.1063/1.1745010.

Ritson, J. and Stapleton, J., 2013. Environment Canterbury Land and Water Regional Plan S42a Report Group 3, Appendix 3, Orari Hydrology Memo Page 38.

Rooney Earthmoving, 2011 – 2014. Rooney Earthmoving newsletters – October 2011, March 2012, September 2012, March 2013, October 2013, April 2014, October 2014.

Rooney Earthmoving, 2014. RWL Rangitata South Irrigation Scheme Newsletter, March 2014.

Scott D., 2004. Groundwater allocation limits: Land-based recharge estimates. Environment Canterbury technical report No. U04/97.

The Press, 2013. First water released in irrigation scheme. Newspaper clipping by Tony Benny 09/11/2013.

The Timaru Herald, 2011. Moving earth for water. Newspaper clipping by John Bisset 04/04/2011.

The Timaru Herald, 2012. Milestone at Rangitata. Newspaper clipping by Stu Piddington 02/06/2012.

The Timaru Herald, 2013. $90M scheme filling ponds with liquid gold. Newspaper clipping by Stu Piddington 22/10/2013.

The Timaru Herald, 2014. Rangitata irrigation scheme at capacity. Newspaper clipping by John Bisset 14/09/2014.

URS New Zealand Limited, 2014. Orari Opihi Pareora Zone pre-feasibility studies, water quality assessment volume 1 of 2. Report prepared for Environment Canterbury 42192460/R001/F.

Webb, T.H., 2003. Identification of functional horizons to predict physical properties for soils from alluvium in Canterbury, New Zealand. Soil Research 41: 1005–1019.

Webb, T.H., Claydon, J.J., Harris, S.R., 2000. Quantifying variability of soil physical properties within soil series to address modern land-use issues on the Canterbury Plains, New Zealand. Australian Journal of Soil Research 38: 1115–1129.

Webb, T.H., Lilburne, L.R., 2011. *Criteria for defining the soil family and soil sibling : the fourth and fifth categories of the New Zealand Soil Classification.* Lincoln, N.Z. Manaaki Whenua Press, Landcare Research.

Wilson, N., 2013. Survey of groundwater levels and river flows between the Rangitata River and the Opihi River. Environment Canterbury technical report No. R13/37.

Woodward, D.J., 1989., Seismic Survey at Orton, South Canterbury, February 1987. Research Report No. 225. Department of Scientific and Industrial Research, New Zealand.

Yoo, K.H. and Boyd, C.E., 2012. Hydrology and water supply for pond aquaculture. Springer Science & Business Media, 2012.

Appendix A: Groundwater level records for wells in the study area showing signs of increasing groundwater levels

Acronyms:

m	=	metres
mbgs	=	metres below ground surface
mm	=	millimetres
tu	=	time unit month or year)

Well J37/0008

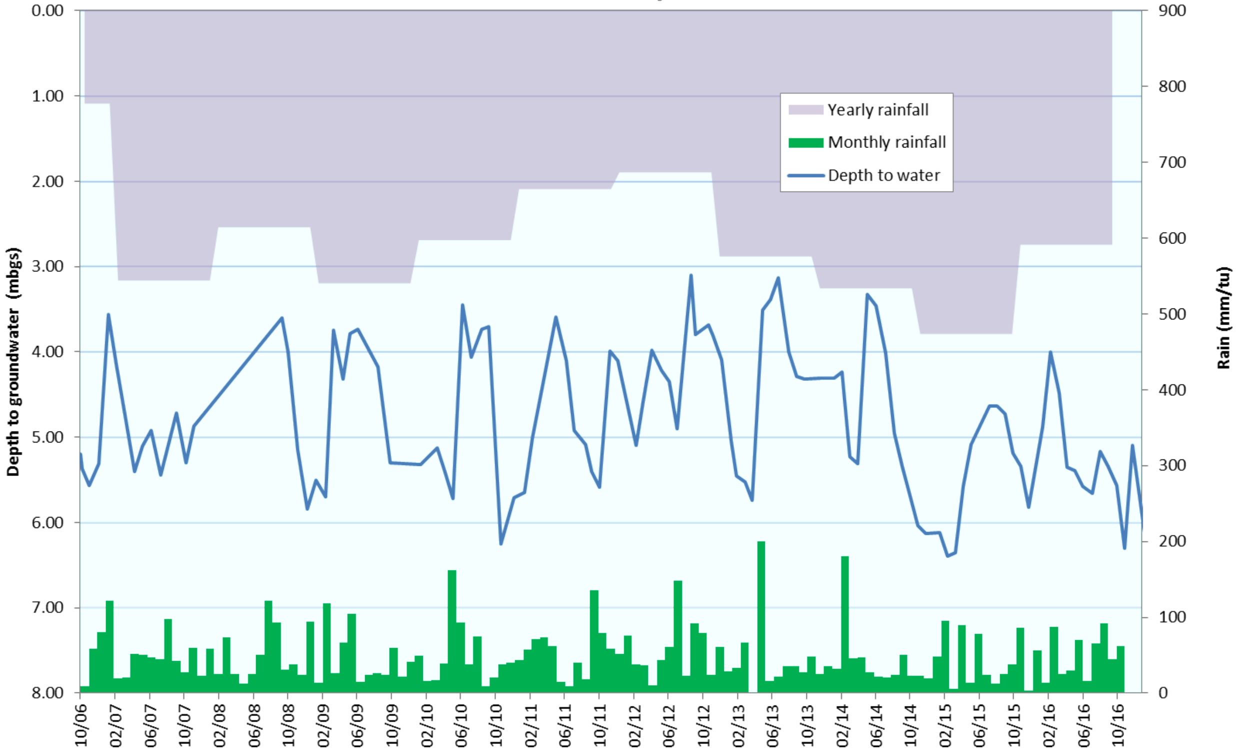

Well J37/0009

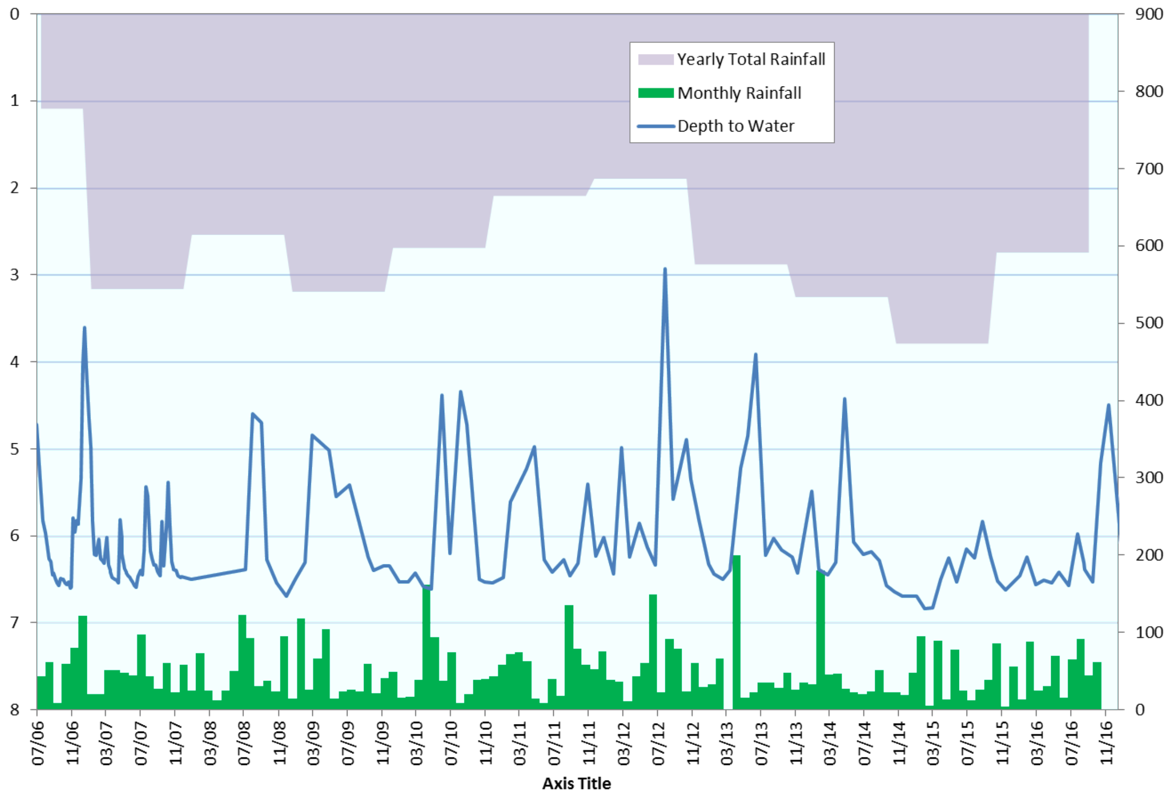

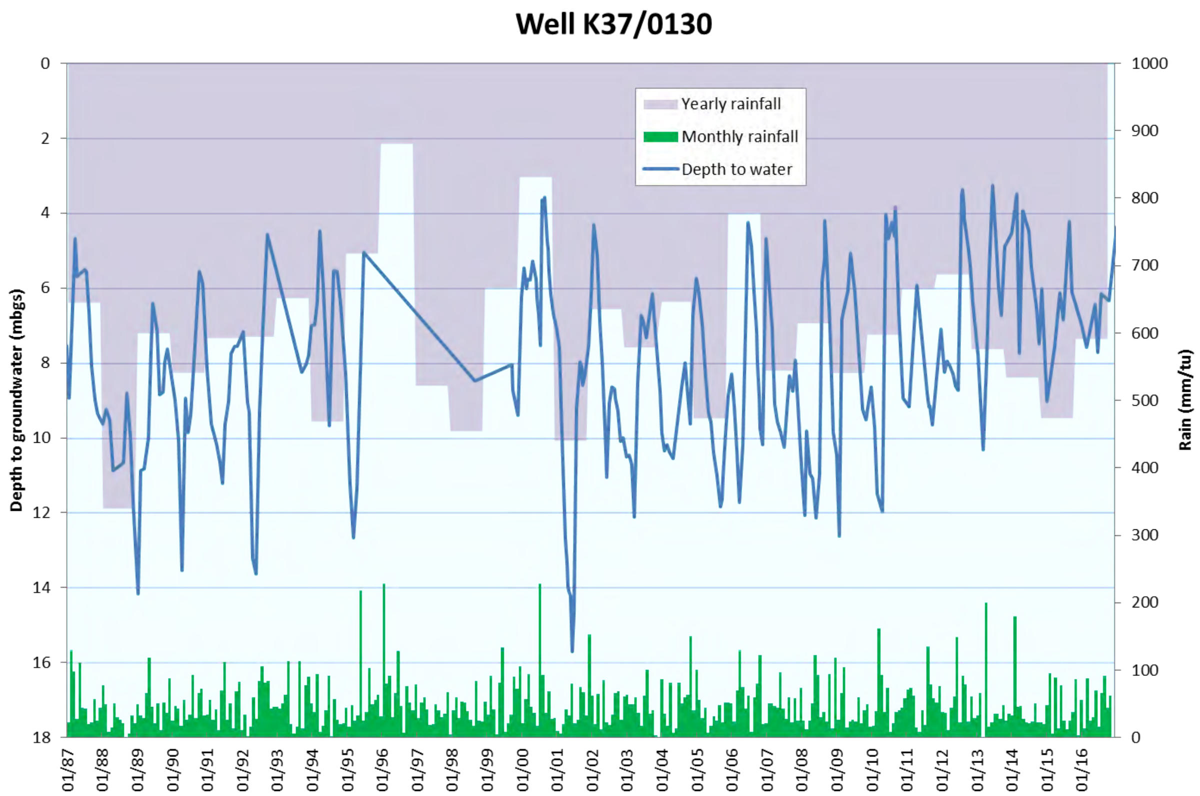
Well K37/0130
Yearly rainfall
Monthly rainfall
Depth to water
Depth to groundwater (mbgs)
Rain (mm/tu)
0
2
4
6
8
10
12
14
16
18
1000
900
800
700
600
500
400
300
200
100
0
01/87
01/88
01/89
01/90
01/91
01/92
01/93
01/94
01/95
01/96
01/97
01/98
01/99
01/00
01/01
01/02
01/03
01/04
01/05
01/06
01/07
01/08
01/09
01/10
01/11
01/12
01/13
01/14
01/15
01/16

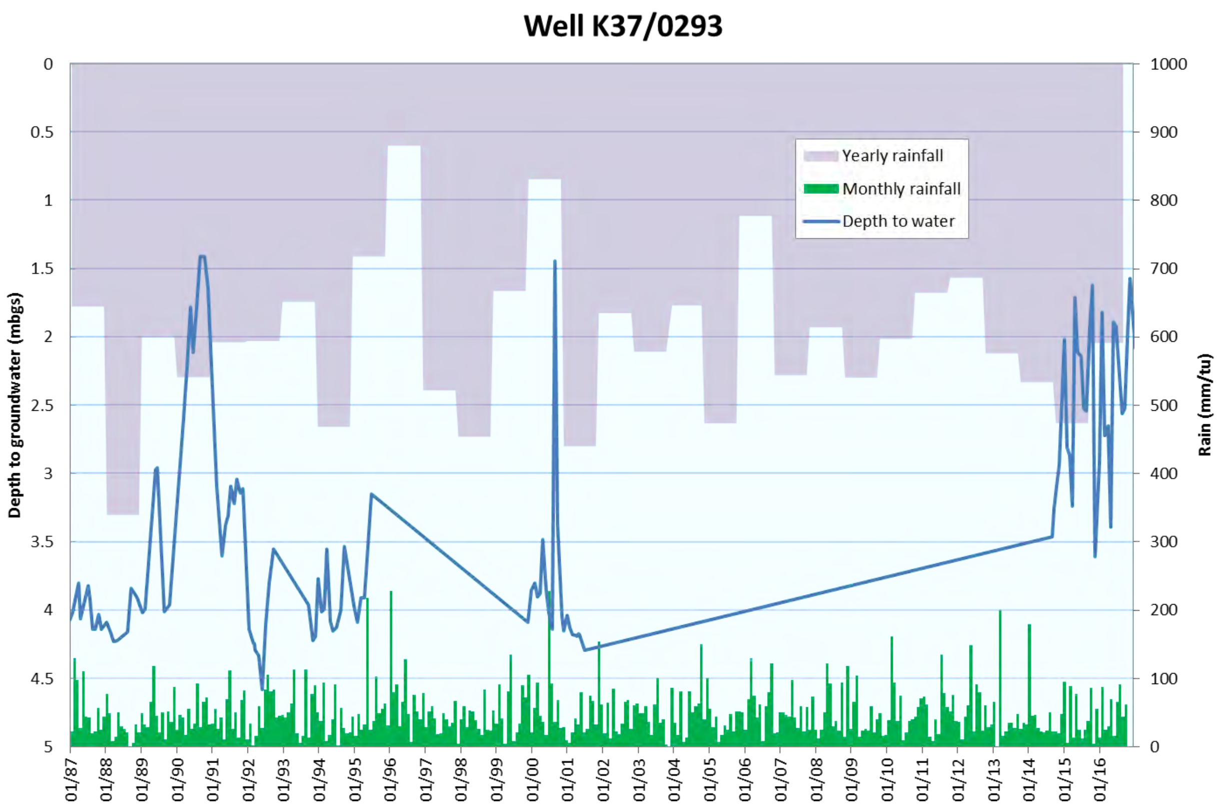
Well K37/0293
Yearly rainfall
Monthly rainfall
Depth to water
Depth to groundwater (mbgs)
Rain (mm/tu)
0
0.5
1
1.5
2
2.5
3
3.5
4
4.5
5
1000
900
800
700
600
500
400
300
200
100
0
01/87
01/88
01/89
01/90
01/91
01/92
01/93
01/94
01/95
01/96
01/97
01/98
01/99
01/00
01/01
01/02
01/03
01/04
01/05
01/06
01/07
01/08
01/09
01/10
01/11
01/12
01/13
01/14
01/15
01/16

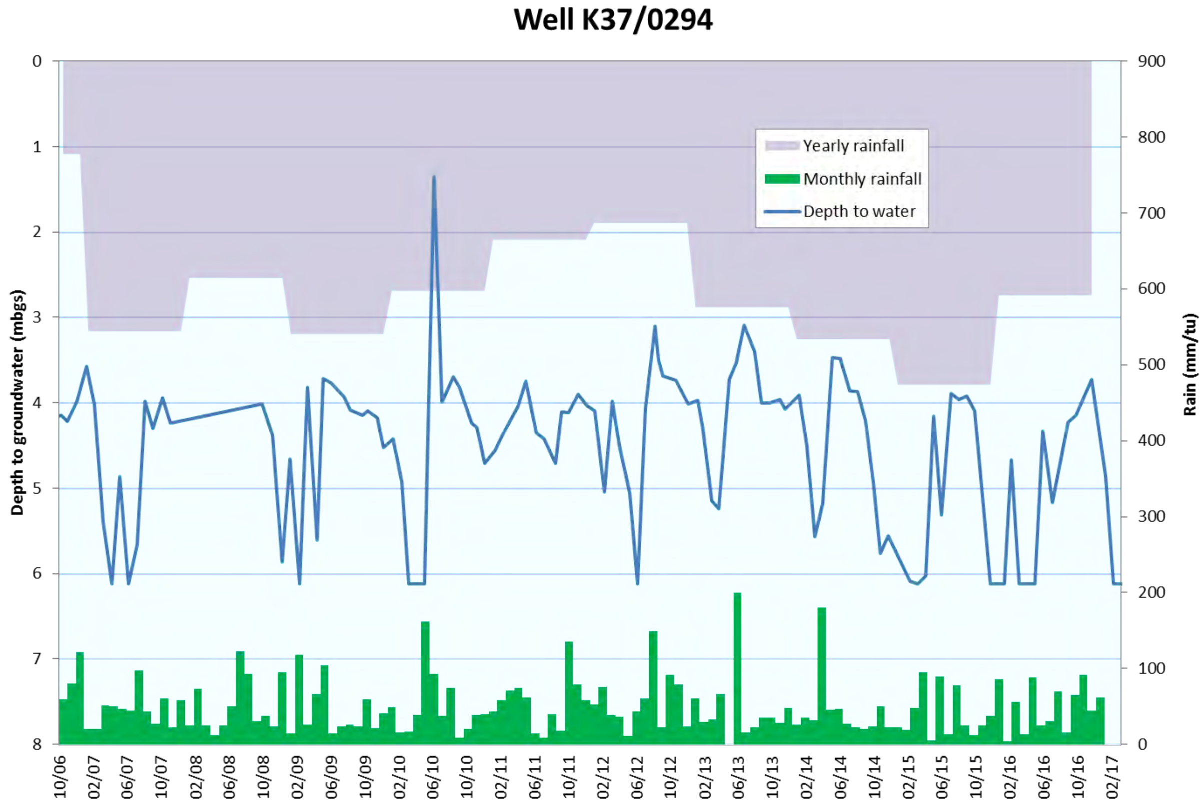

Well K37/0294
Yearly rainfall
Monthly rainfall
Depth to water
Depth to groundwater (mbgs)
Rain (mm/tu)
0
1
2
3
4
5
6
7
8
900
800
700
600
500
400
300
200
100
0
10/06
02/07
06/07
10/07
02/08
06/08
10/08
02/09
06/09
10/09
02/10
06/10
10/10
02/11
06/11
10/11
02/12
06/12
10/12
02/13
06/13
10/13
02/14
06/14
10/14
02/15
06/15
10/15
02/16
06/16
10/16
02/17

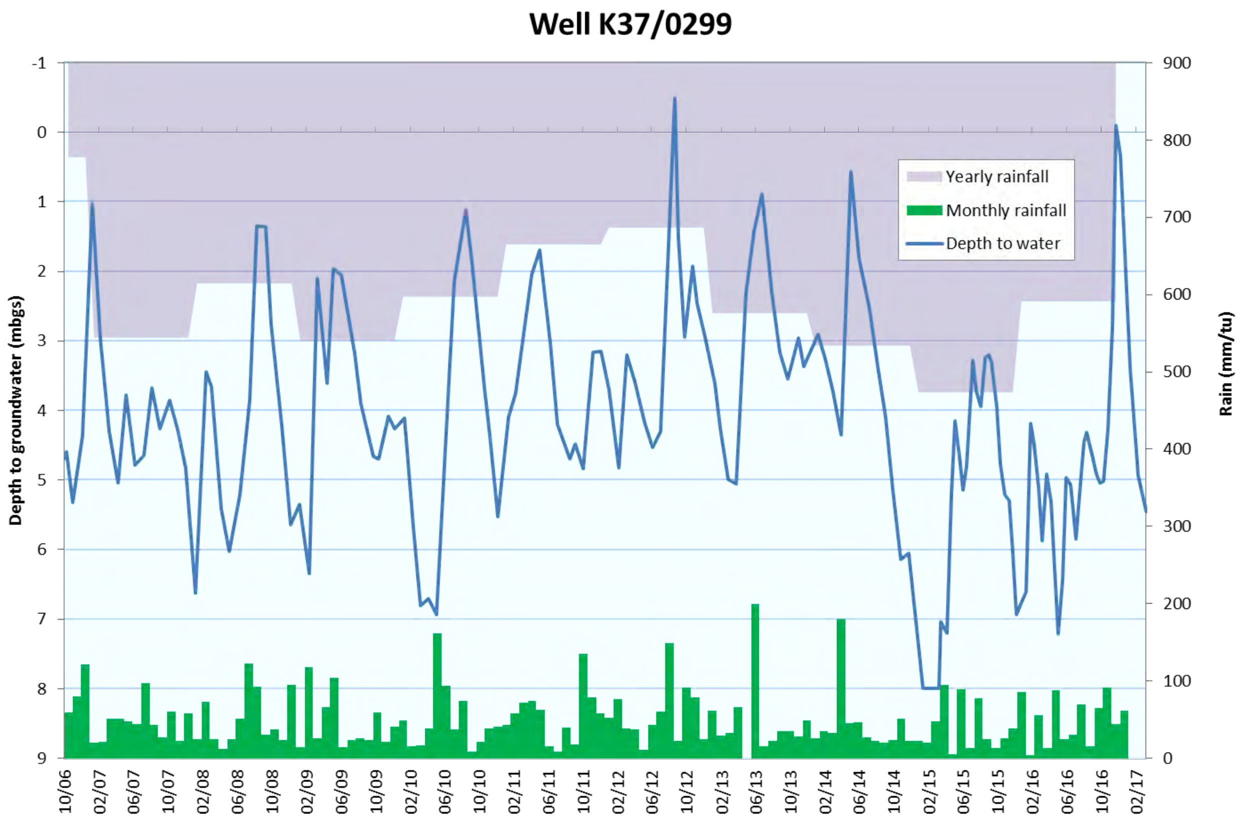

Well K37/0299
Yearly rainfall
Monthly rainfall
Depth to water
Depth to groundwater (mbgs)
Rain (mm/tu)
-1
0
1
2
3
4
5
6
7
8
9
900
800
700
600
500
400
300
200
100
0
10/06
02/07
06/07
10/07
02/08
06/08
10/08
02/09
06/09
10/09
02/10
06/10
10/10
02/11
06/11
10/11
02/12
06/12
10/12
02/13
06/13
10/13
02/14
06/14
10/14
02/15
06/15
10/15
02/16
06/16
10/16
02/17

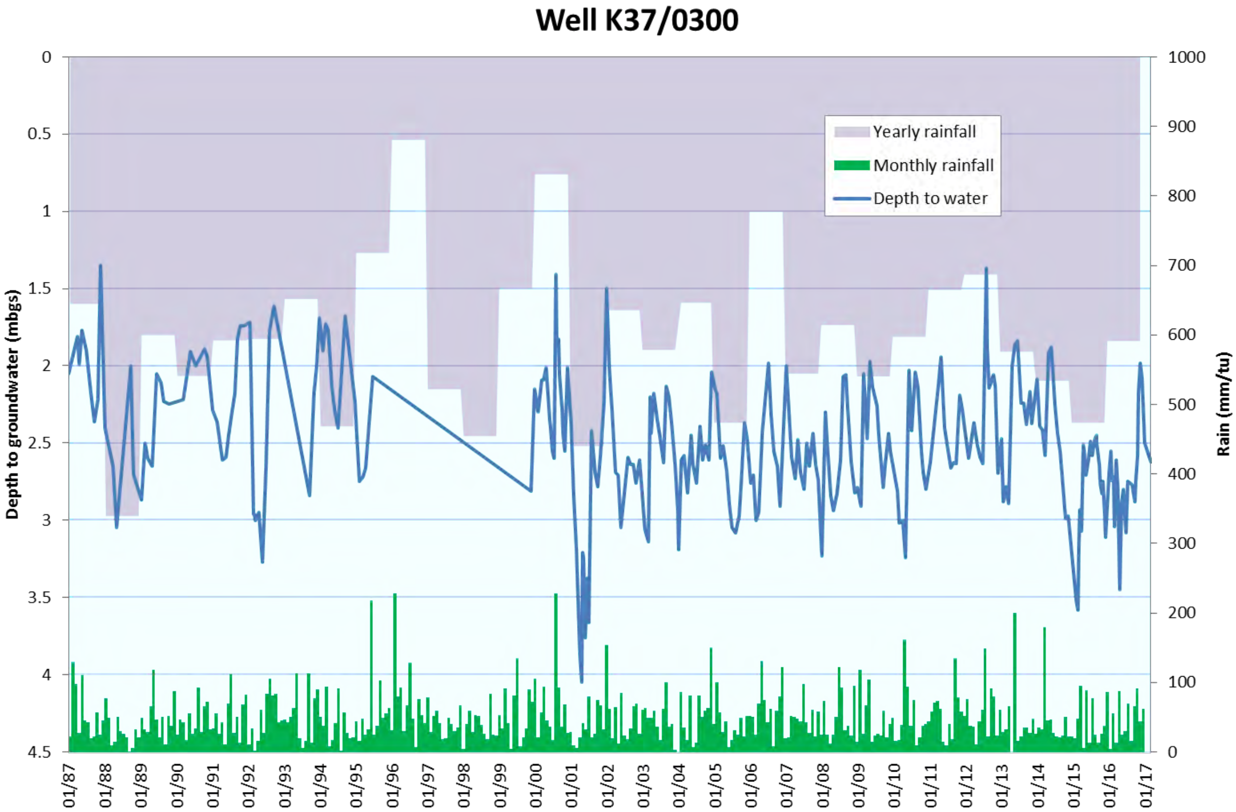
Well K37/0300
Yearly rainfall
Monthly rainfall
Depth to water
Depth to groundwater (mbgs)
Rain (mm/tu)
0
0.5
1
1.5
2
2.5
3
3.5
4
4.5
1000
900
800
700
600
500
400
300
200
100
0
01/87
01/88
01/89
01/90
01/91
01/92
01/93
01/94
01/95
01/96
01/97
01/98
01/99
01/00
01/01
01/02
01/03
01/04
01/05
01/06
01/07
01/08
01/09
01/10
01/11
01/12
01/13
01/14
01/15
01/16
01/17

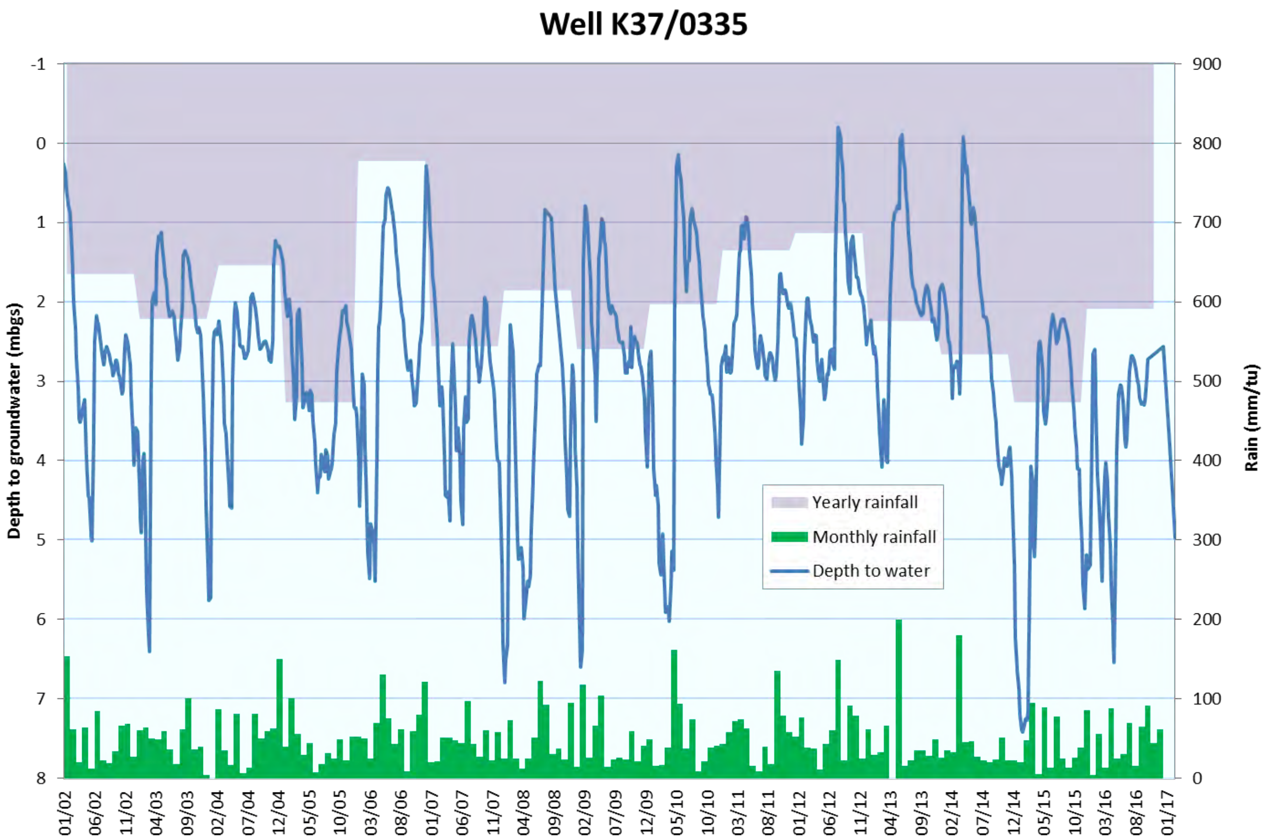
Well K37/0335
Yearly rainfall
Monthly rainfall
Depth to water
Depth to groundwater (mbgs)
Rain (mm/tu)
-1
0
1
2
3
4
5
6
7
8
900
800
700
600
500
400
300
200
100
0
01/02
06/02
11/02
04/03
09/03
02/04
07/04
12/04
05/05
10/05
03/06
08/06
01/07
06/07
11/07
04/08
09/08
02/09
07/09
12/09
05/10
10/10
03/11
08/11
01/12
06/12
11/12
04/13
09/13
02/14
07/14
12/14
05/15
10/15
03/16
08/16
01/17

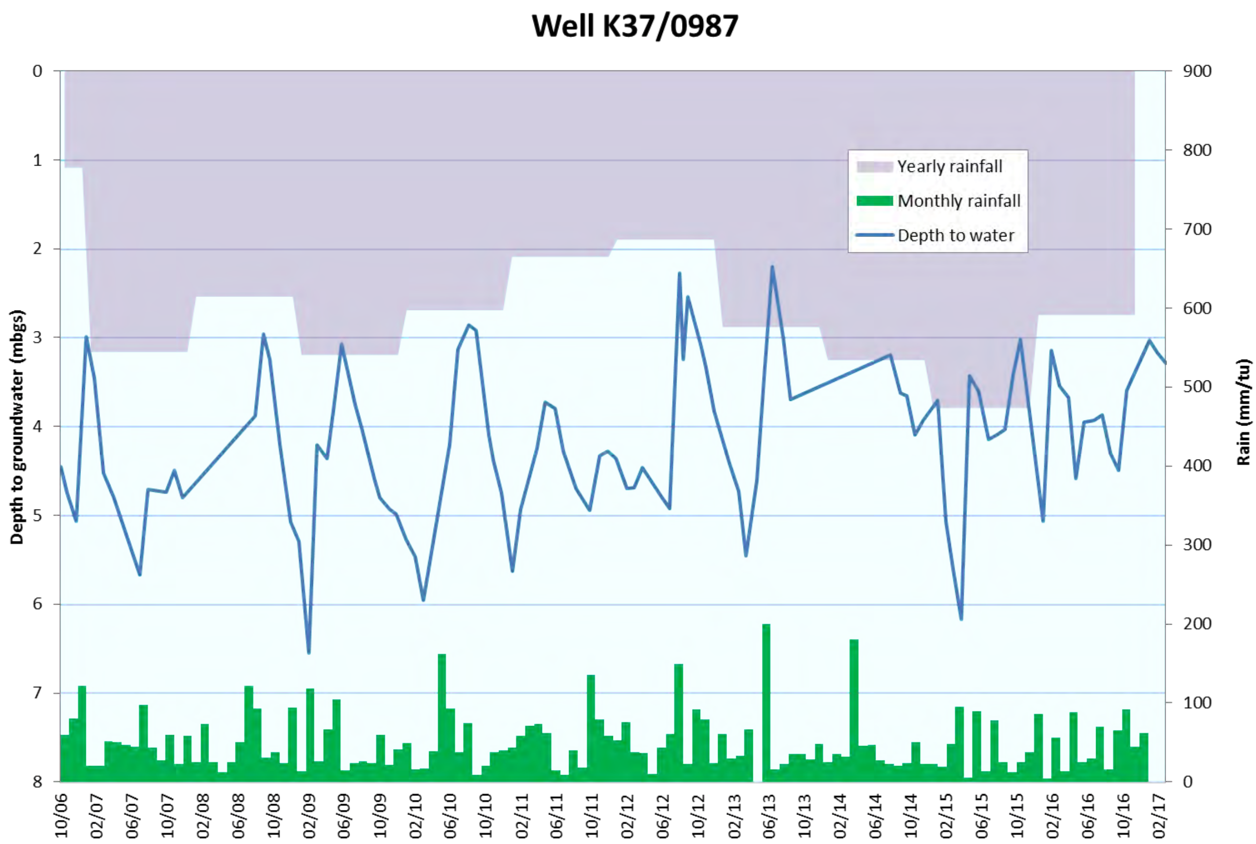
Well K37/0987
Yearly rainfall
Monthly rainfall
Depth to water
Depth to groundwater (mbgs)
Rain (mm/tu)
0
1
2
3
4
5
6
7
8
900
800
700
600
500
400
300
200
100
0
10/06
02/07
06/07
10/07
02/08
06/08
10/08
02/09
06/09
10/09
02/10
06/10
10/10
02/11
06/11
10/11
02/12
06/12
10/12
02/13
06/13
10/13
02/14
06/14
10/14
02/15
06/15
10/15
02/16
06/16
10/16
02/17

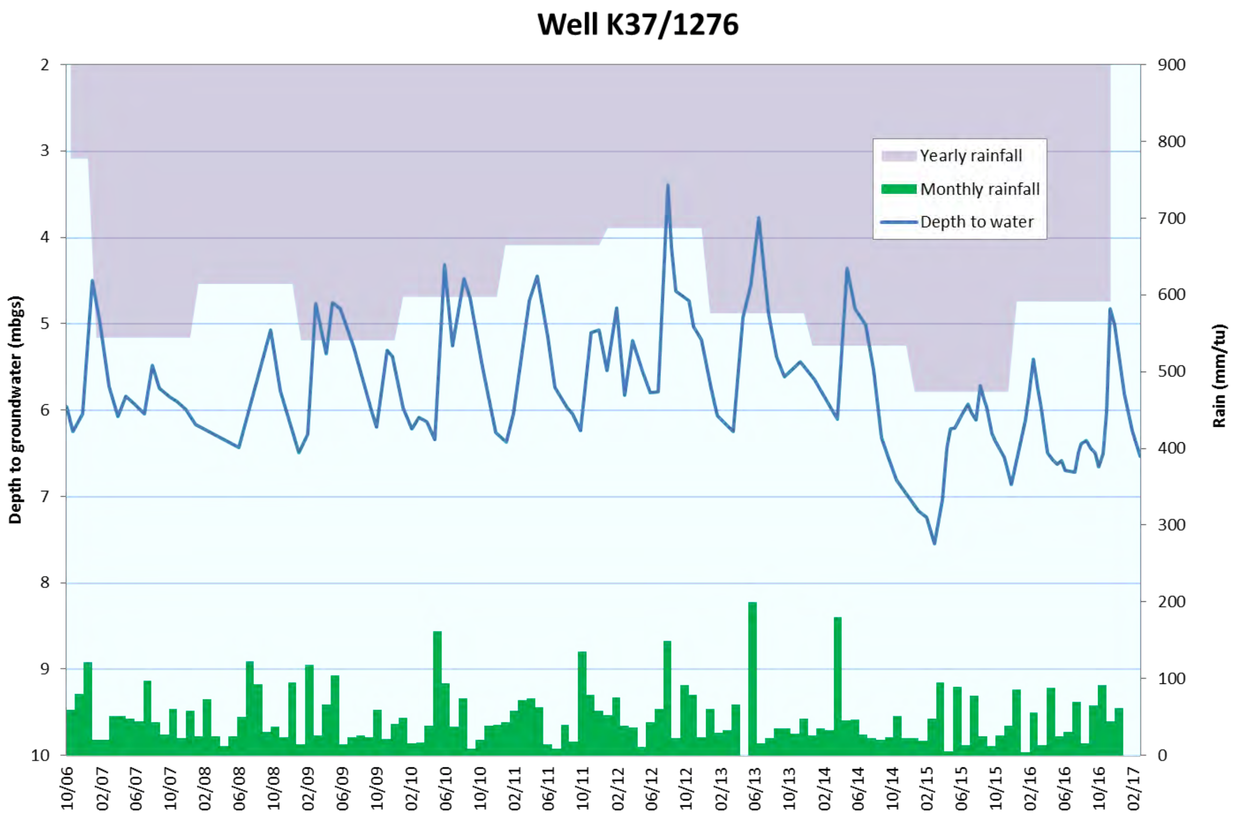
Well K37/1276
Yearly rainfall
Monthly rainfall
Depth to water
Depth to groundwater (mbgs)
Rain (mm/tu)
2
3
4
5
6
7
8
9
10
900
800
700
600
500
400
300
200
100
0
10/06
02/07
06/07
10/07
02/08
06/08
10/08
02/09
06/09
10/09
02/10
06/10
10/10
02/11
06/11
10/11
02/12
06/12
10/12
02/13
06/13
10/13
02/14
06/14
10/14
02/15
06/15
10/15
02/16
06/16
10/16
02/17

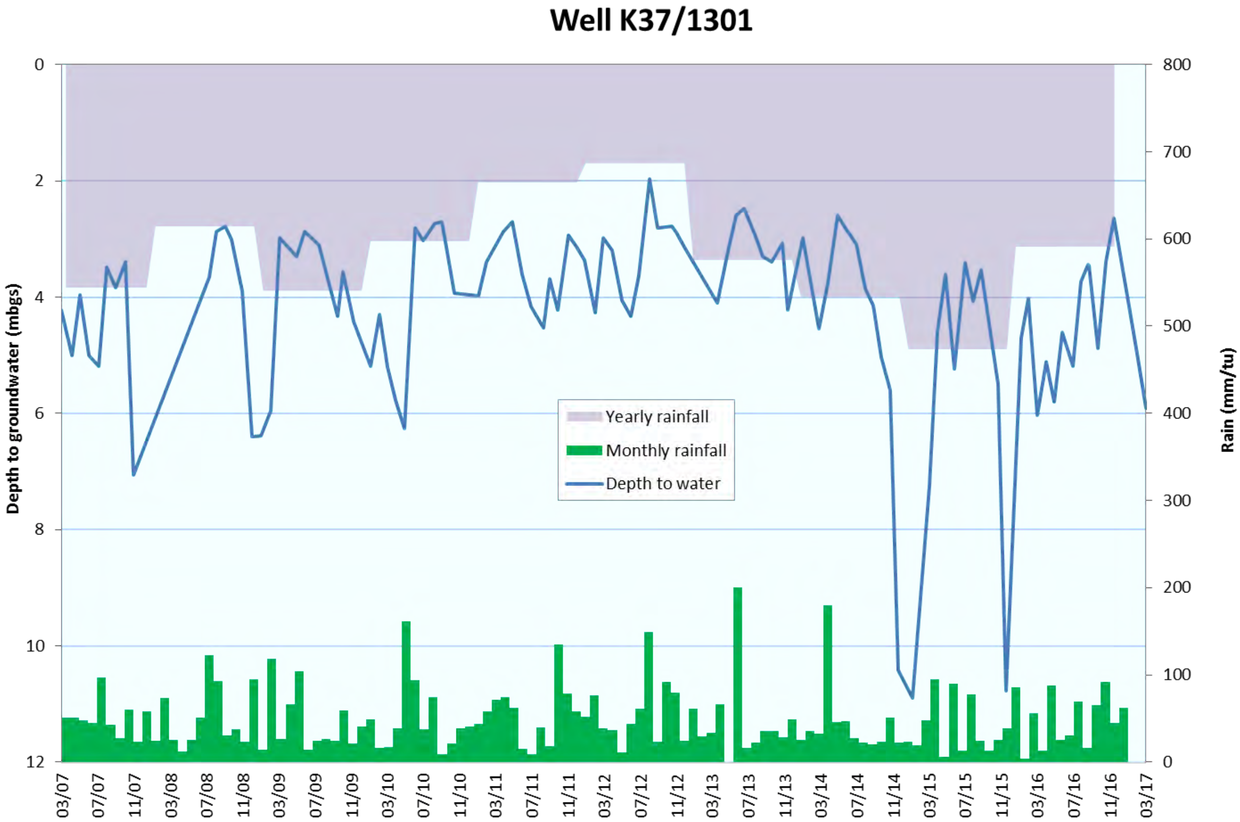
Well K37/1301
Depth to groundwater (mbgs)
Rain (mm/tu)
Yearly rainfall
Monthly rainfall
Depth to water
0
2
4
6
8
10
12
800
700
600
500
400
300
200
100
0
03/07
07/07
11/07
03/08
07/08
11/08
03/09
07/09
11/09
03/10
07/10
11/10
03/11
07/11
11/11
03/12
07/12
11/12
03/13
07/13
11/13
03/14
07/14
11/14
03/15
07/15
11/15
03/16
07/16
11/16
03/17

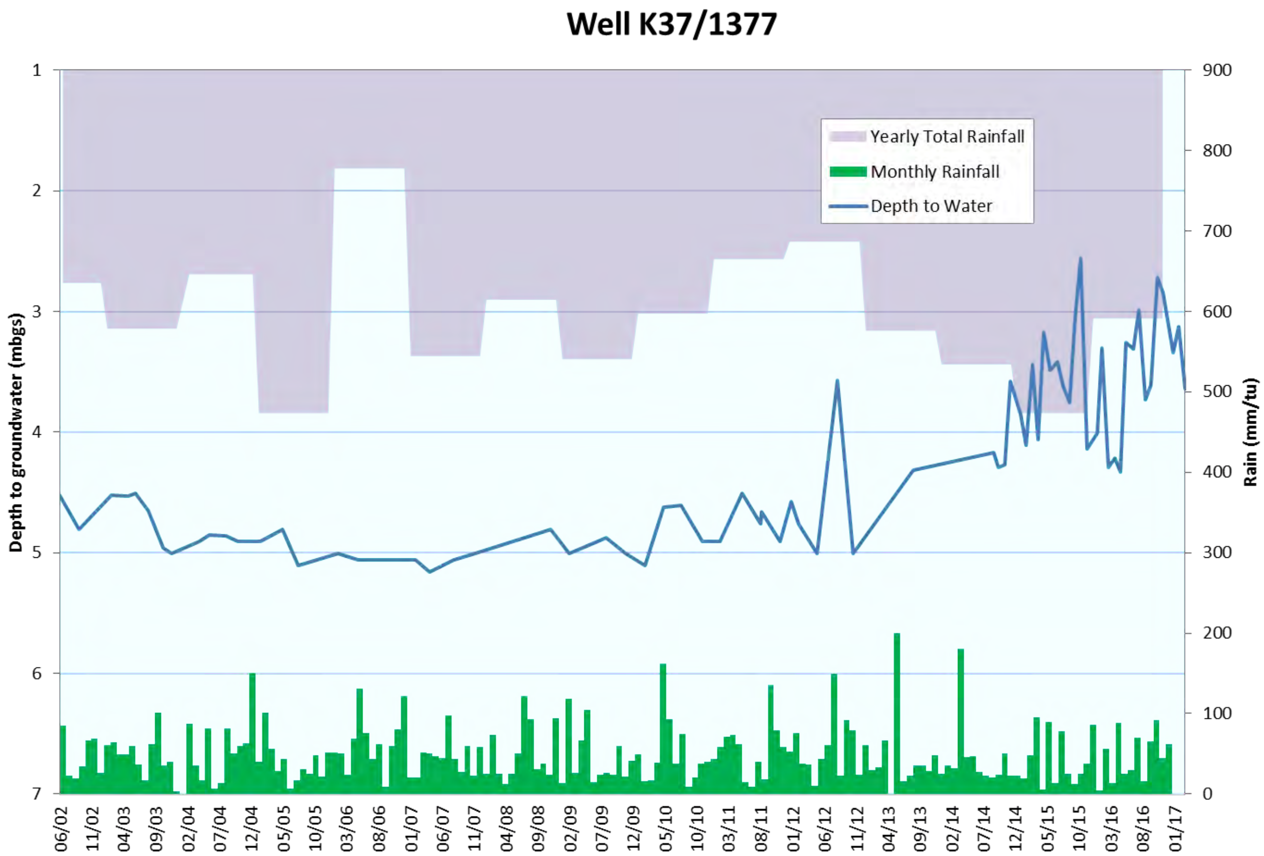
Well K37/1377
Depth to groundwater (mbgs)
Rain (mm/tu)
Yearly Total Rainfall
Monthly Rainfall
Depth to Water
1
2
3
4
5
6
7
900
800
700
600
500
400
300
200
100
0
06/02
11/02
04/03
09/03
02/04
07/04
12/04
05/05
10/05
03/06
08/06
01/07
06/07
11/07
04/08
09/08
02/09
07/09
12/09
05/10
10/10
03/11
08/11
01/12
06/12
11/12
04/13
09/13
02/14
07/14
12/14
05/15
10/15
03/16
08/16
01/17

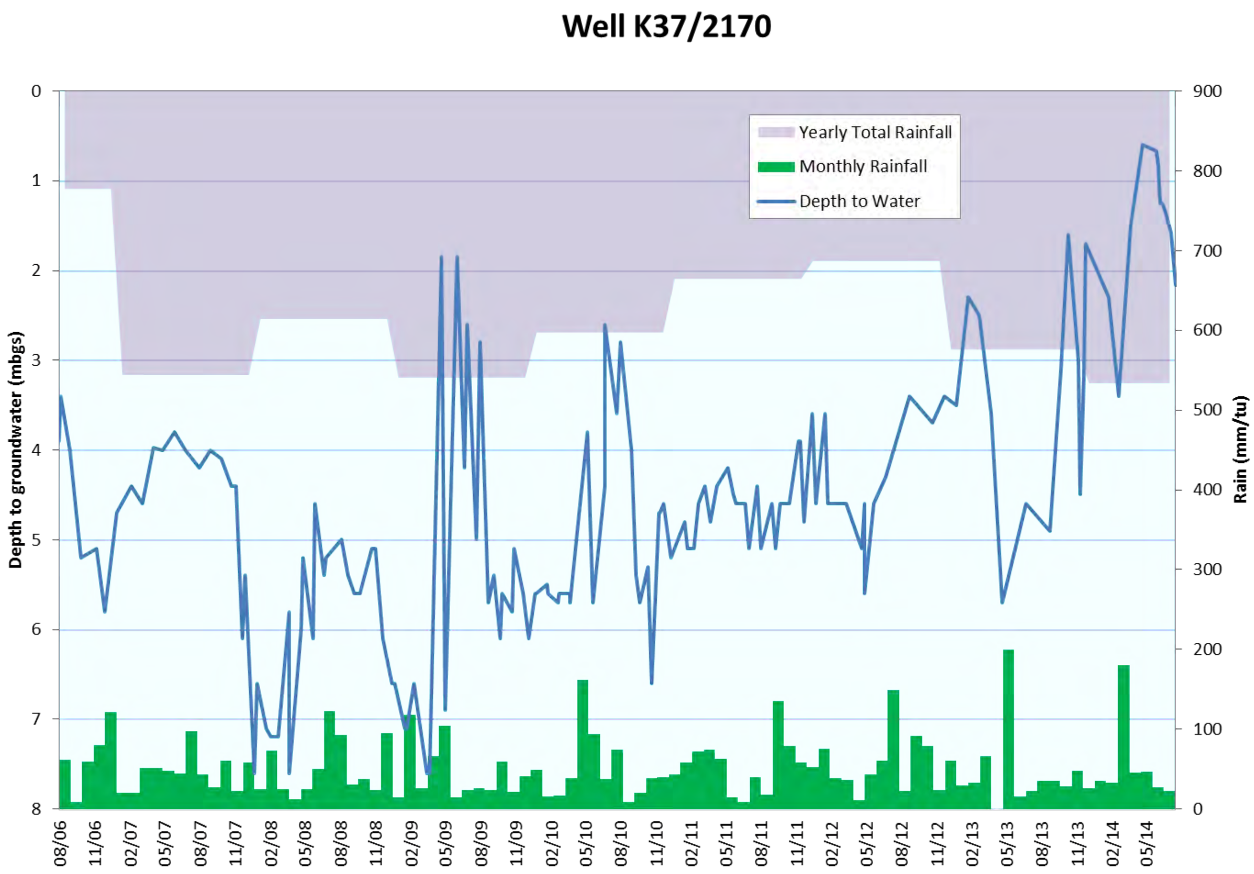
Well K37/2170
Yearly Total Rainfall
Monthly Rainfall
Depth to Water
Depth to groundwater (mbgs)
Rain (mm/tu)

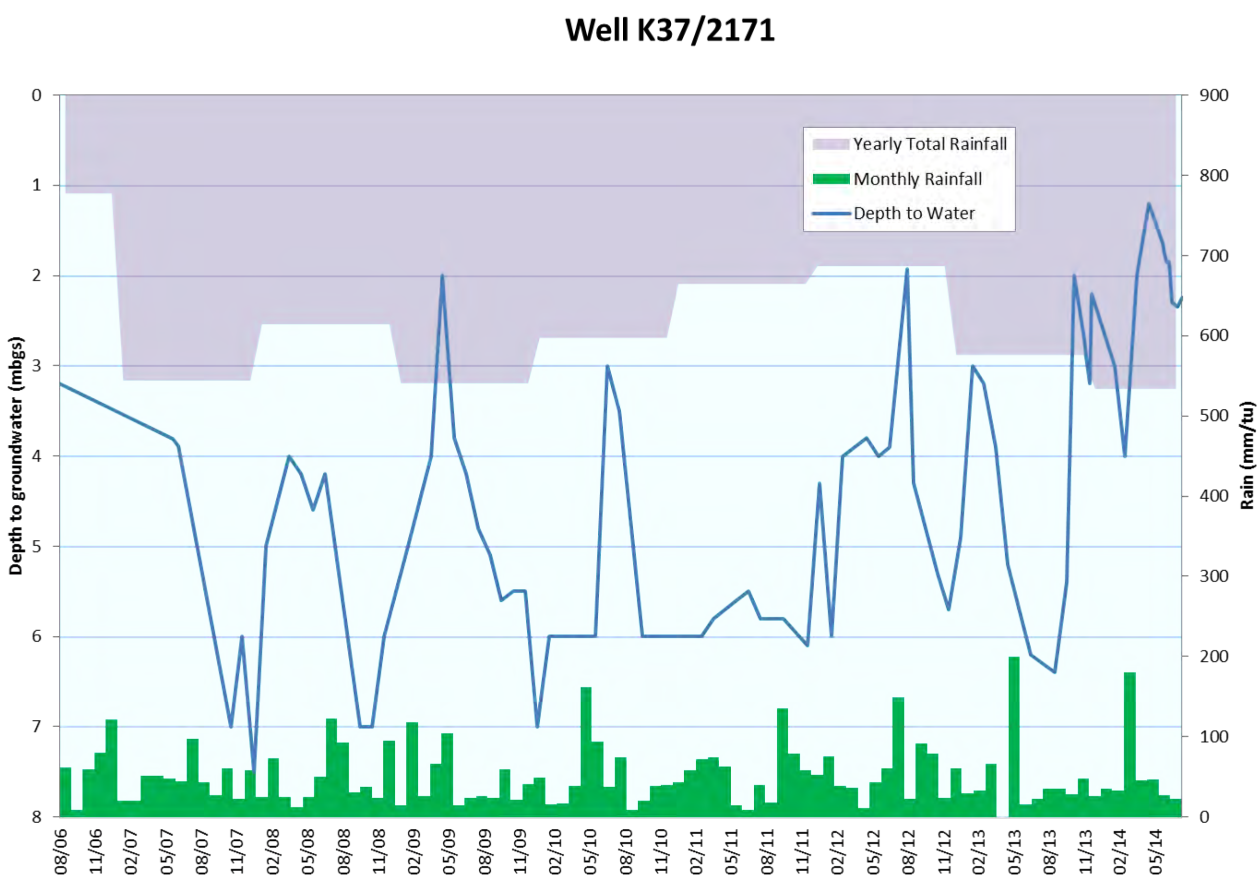
Well K37/2171
Yearly Total Rainfall
Monthly Rainfall
Depth to Water
Depth to groundwater (mbgs)
Rain (mm/tu)

Well K37/2896

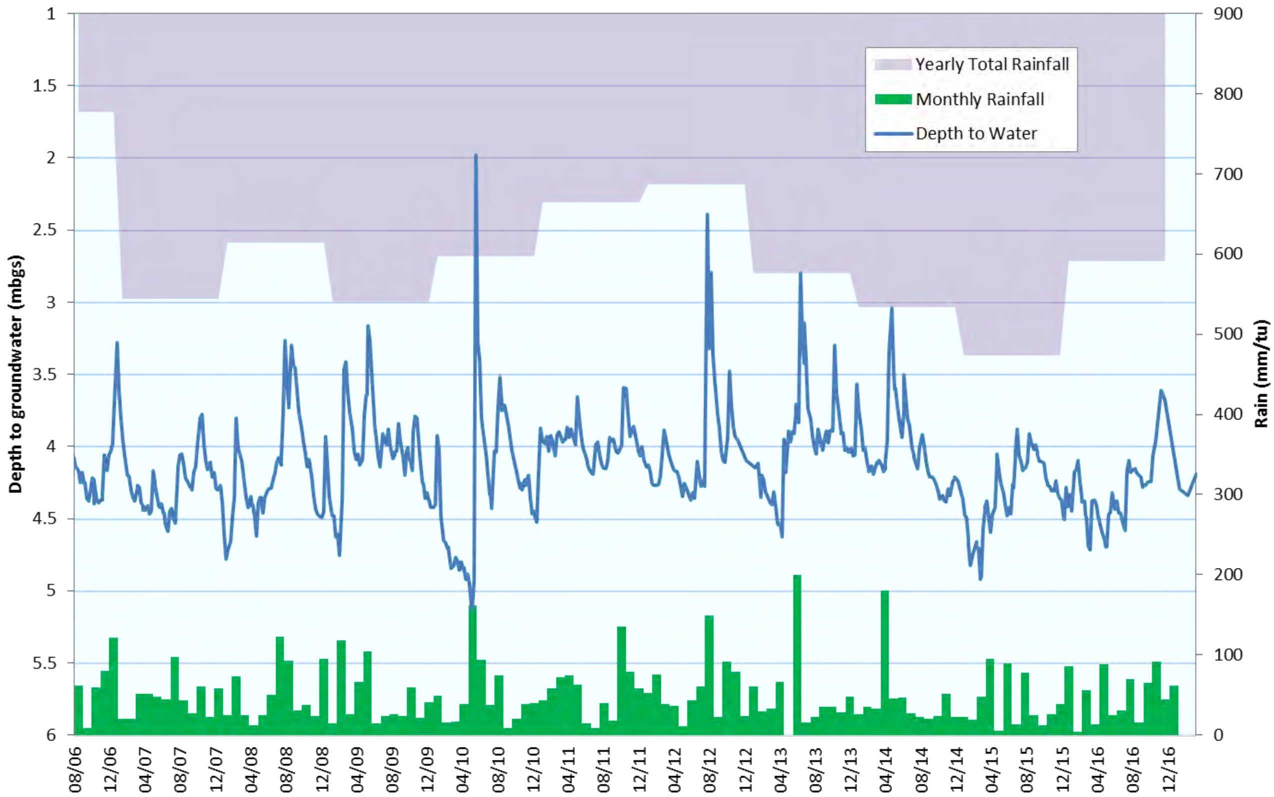

Well K37/2923

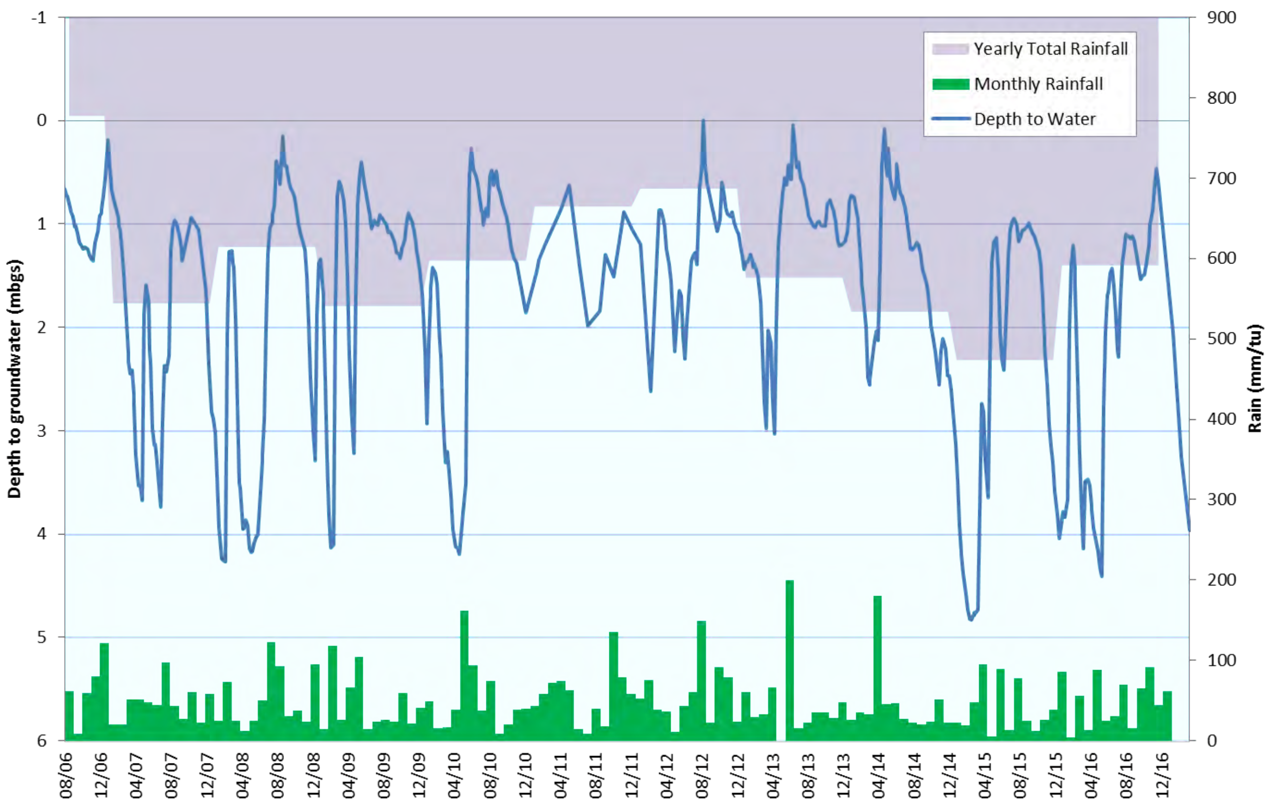

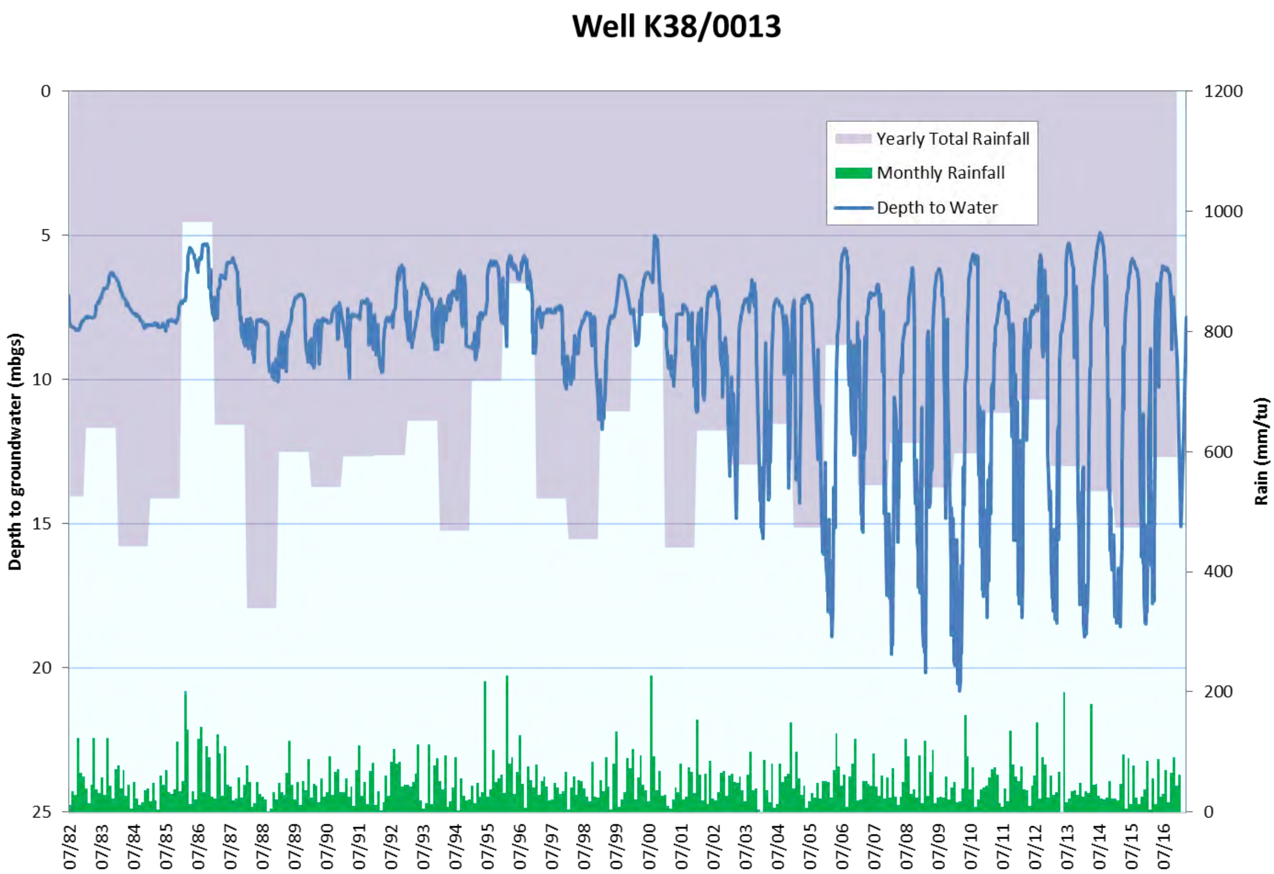
Well K38/0013
Yearly Total Rainfall
Monthly Rainfall
Depth to Water
Depth to groundwater (mbgs)
Rain (mm/tu)
0
5
10
15
20
25
1200
1000
800
600
400
200
0
07/82
07/83
07/84
07/85
07/86
07/87
07/88
07/89
07/90
07/91
07/92
07/93
07/94
07/95
07/96
07/97
07/98
07/99
07/00
07/01
07/02
07/03
07/04
07/05
07/06
07/07
07/08
07/09
07/10
07/11
07/12
07/13
07/14
07/15
07/16

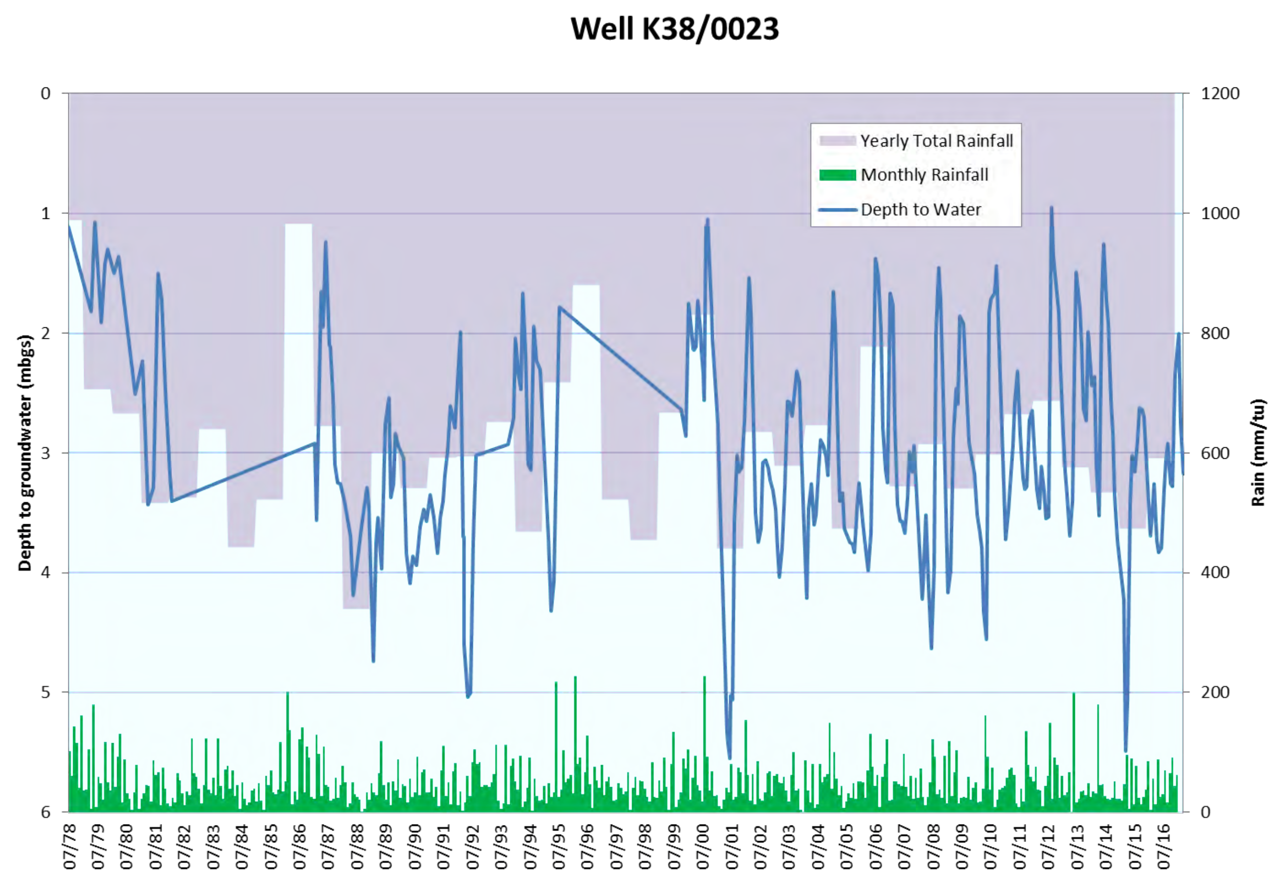
Well K38/0023
Yearly Total Rainfall
Monthly Rainfall
Depth to Water
Depth to groundwater (mbgs)
Rain (mm/tu)
0
1
2
3
4
5
6
1200
1000
800
600
400
200
0
07/78
07/79
07/80
07/81
07/82
07/83
07/84
07/85
07/86
07/87
07/88
07/89
07/90
07/91
07/92
07/93
07/94
07/95
07/96
07/97
07/98
07/99
07/00
07/01
07/02
07/03
07/04
07/05
07/06
07/07
07/08
07/09
07/10
07/11
07/12
07/13
07/14
07/15
07/16

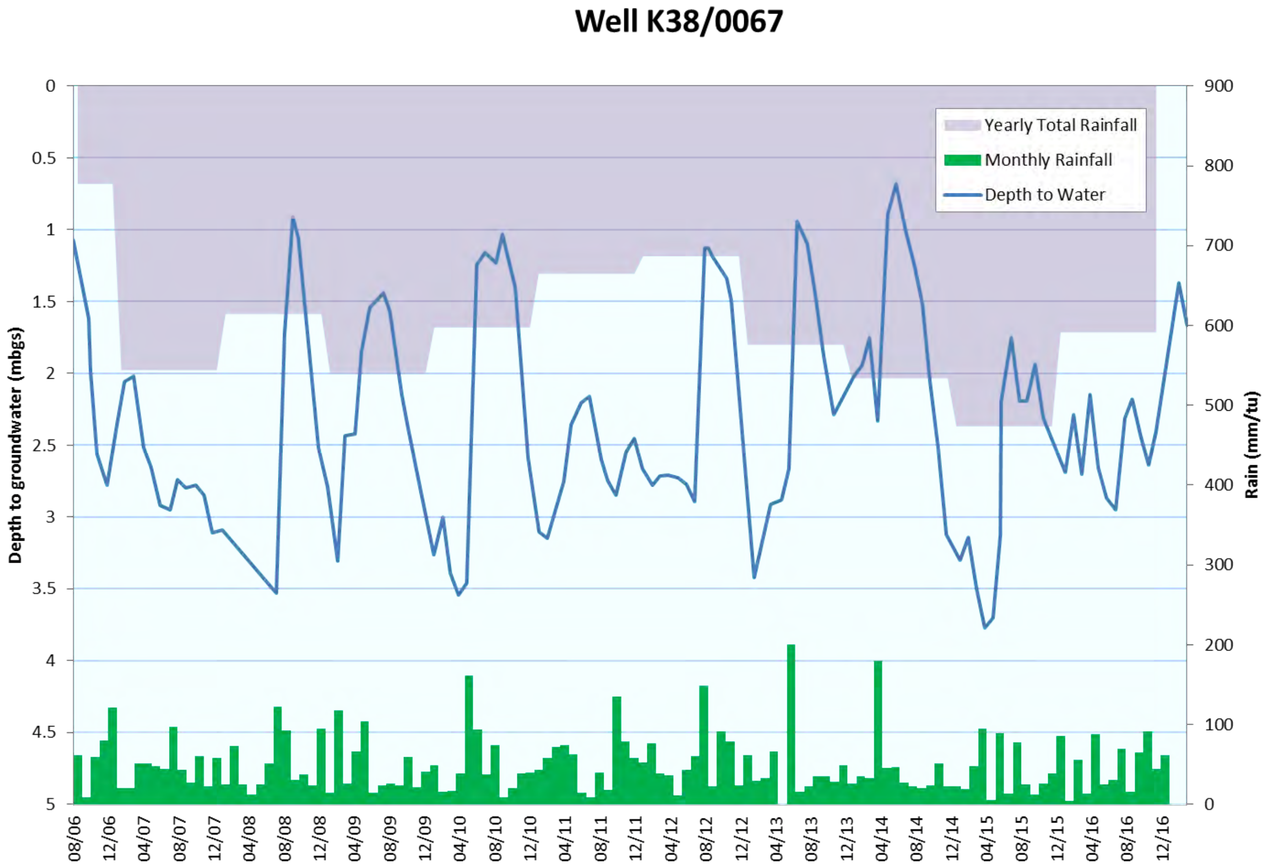
Well K38/0067
Yearly Total Rainfall
Monthly Rainfall
Depth to Water
Depth to groundwater (mbgs)
Rain (mm/tu)
0
0.5
1
1.5
2
2.5
3
3.5
4
4.5
5
900
800
700
600
500
400
300
200
100
0
08/06
12/06
04/07
08/07
12/07
04/08
08/08
12/08
04/09
08/09
12/09
04/10
08/10
12/10
04/11
08/11
12/11
04/12
08/12
12/12
04/13
08/13
12/13
04/14
08/14
12/14
04/15
08/15
12/15
04/16
08/16
12/16

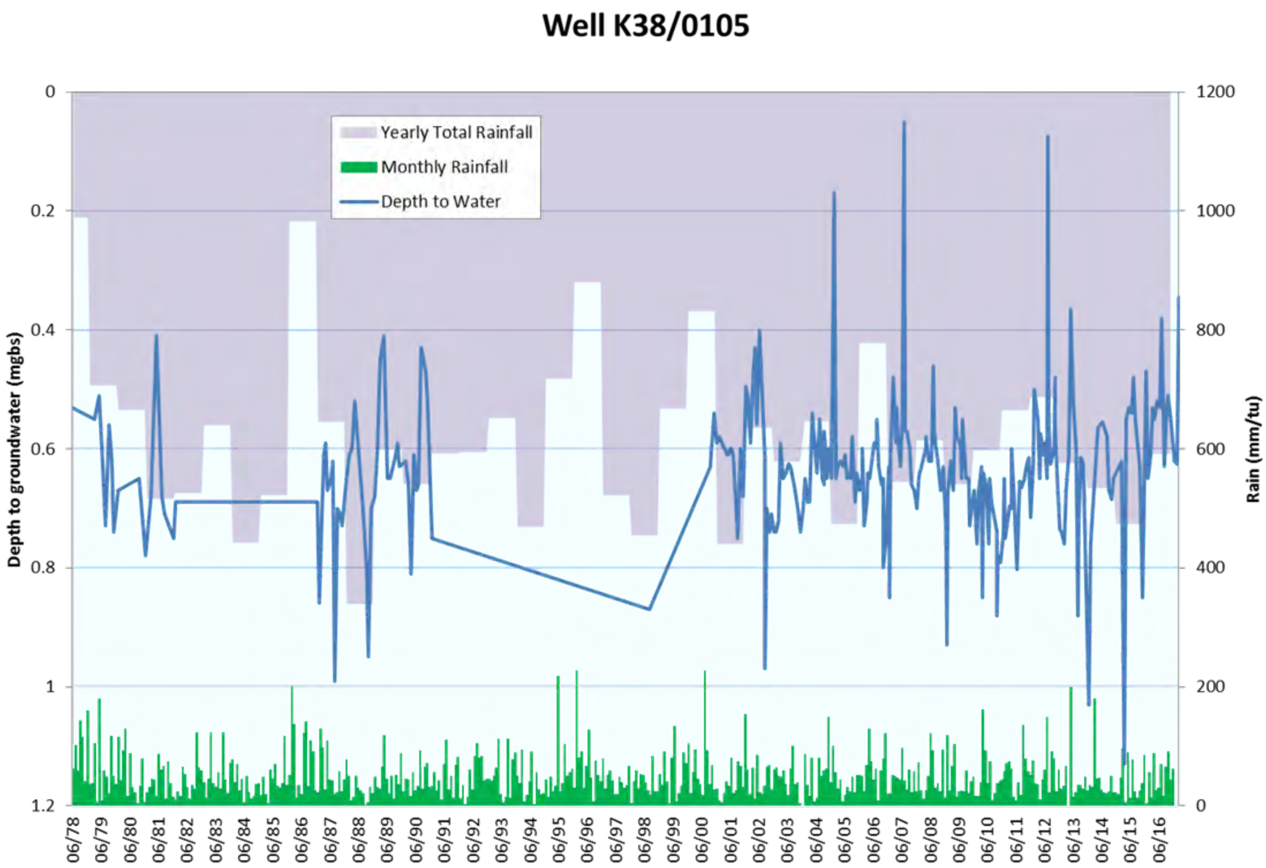
Well K38/0105
Yearly Total Rainfall
Monthly Rainfall
Depth to Water
Depth to groundwater (mgbs)
Rain (mm/tu)
0
0.2
0.4
0.6
0.8
1
1.2
1200
1000
800
600
400
200
0
06/78
06/79
06/80
06/81
06/82
06/83
06/84
06/85
06/86
06/87
06/88
06/89
06/90
06/91
06/92
06/93
06/94
06/95
06/96
06/97
06/98
06/99
06/00
06/01
06/02
06/03
06/04
06/05
06/06
06/07
06/08
06/09
06/10
06/11
06/12
06/13
06/14
06/15
06/16

Well K38/0117

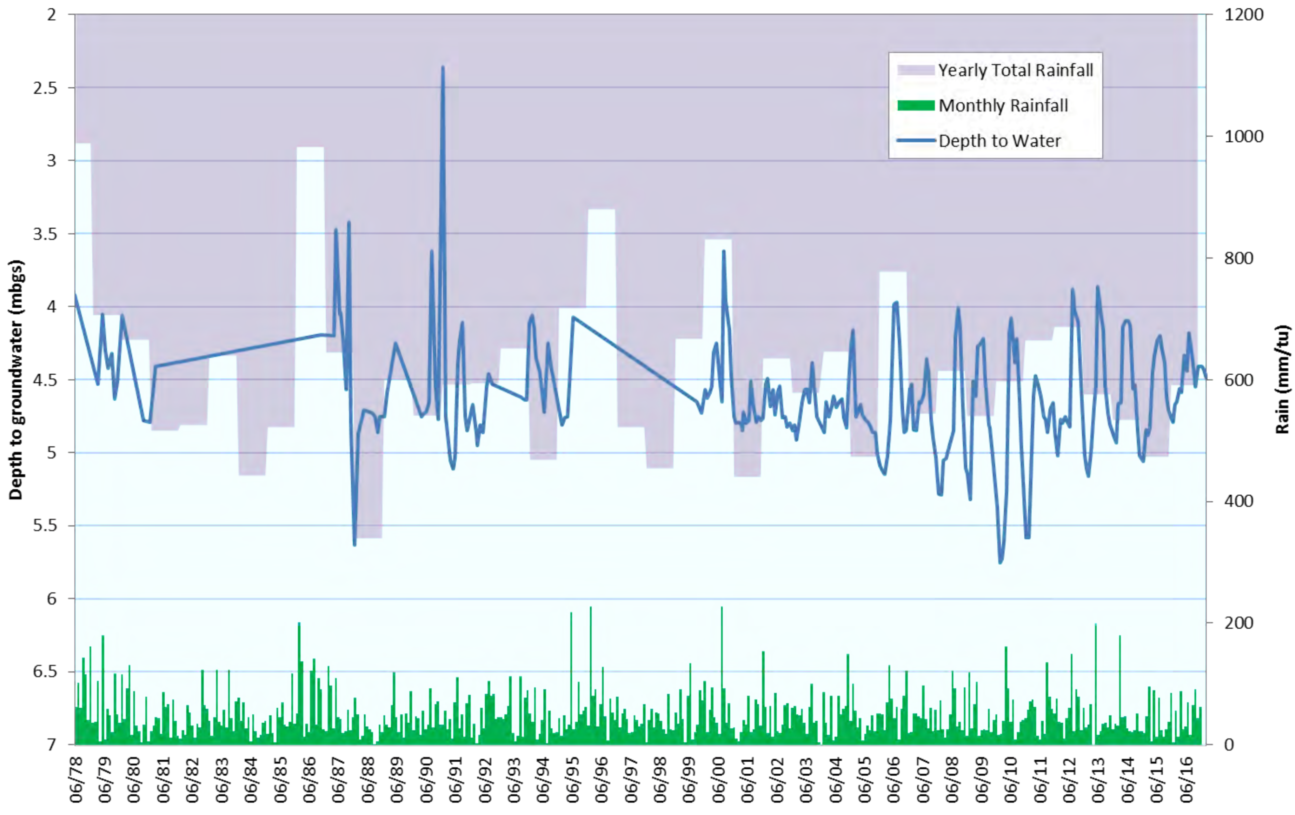

Well K38/0129

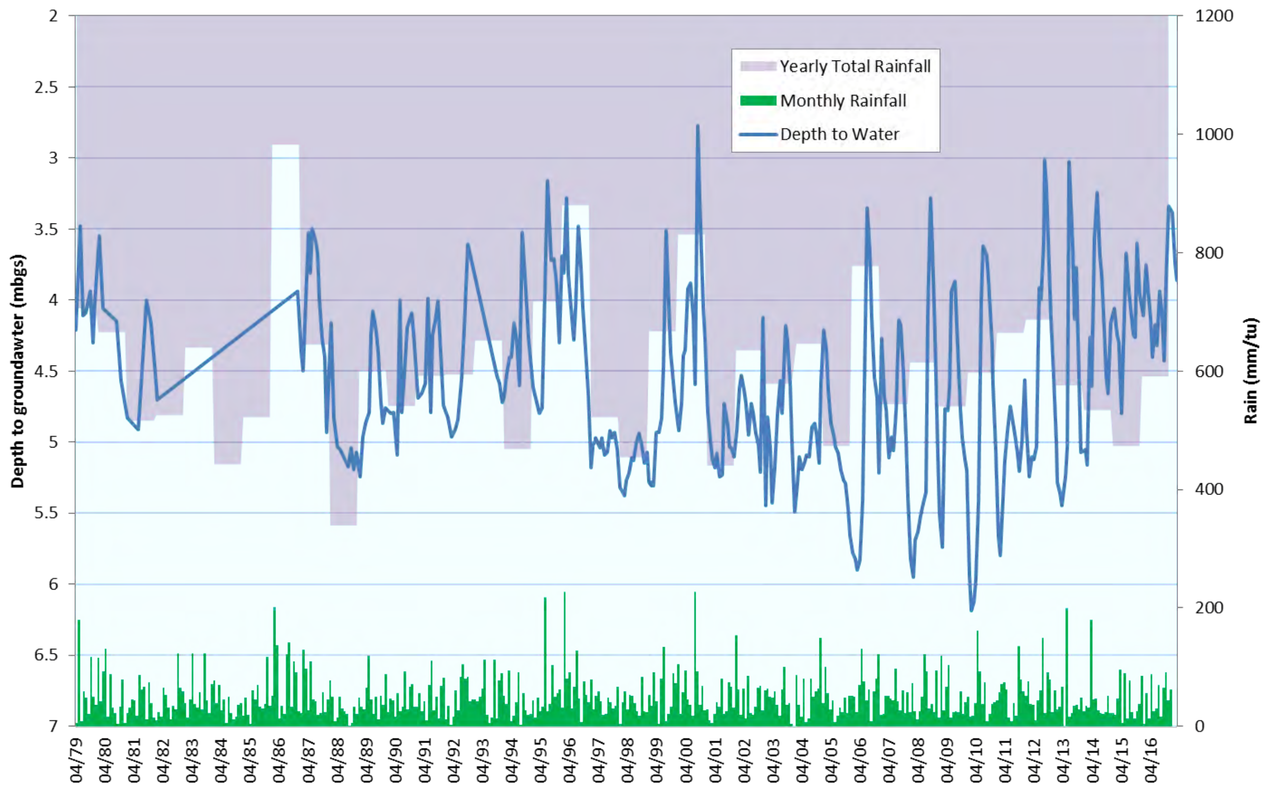

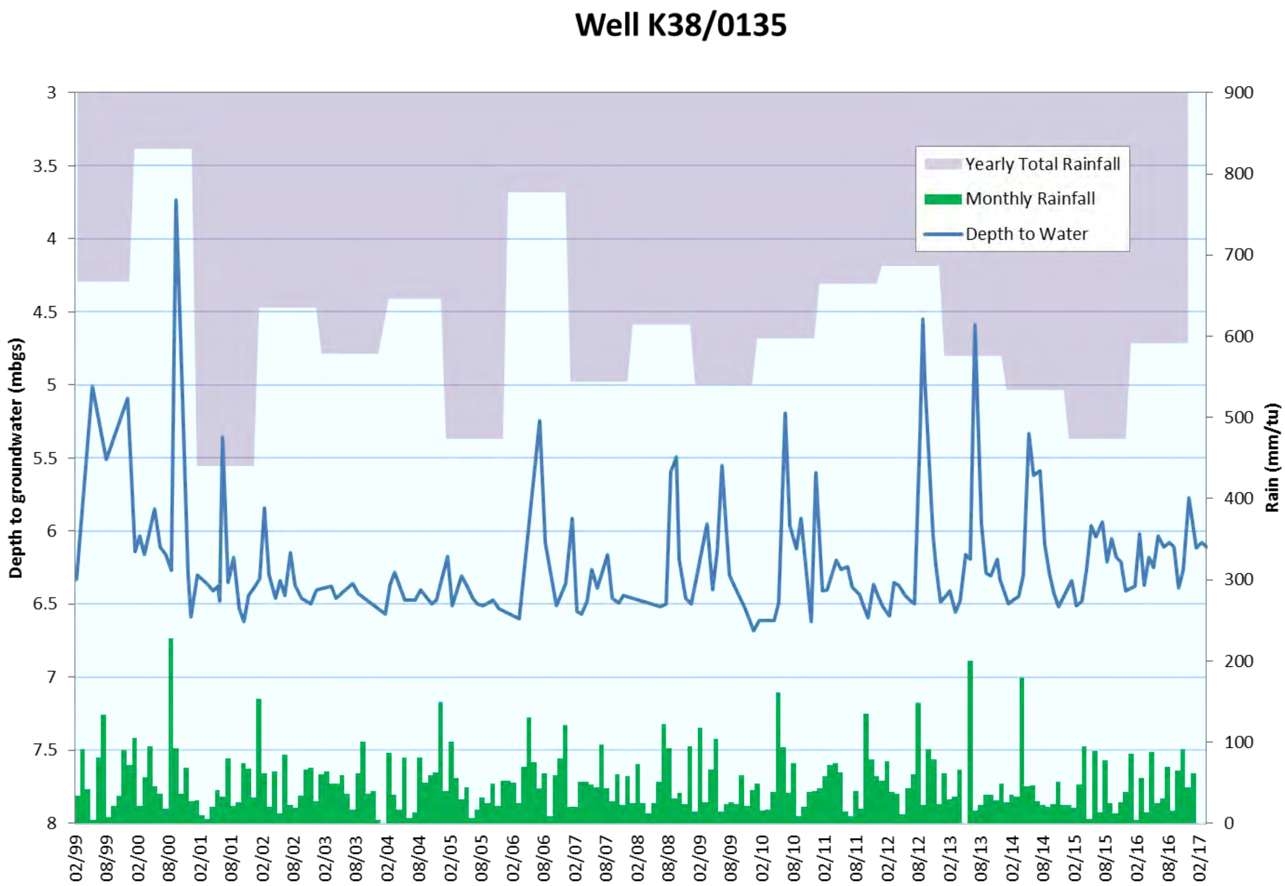

Well K38/0135
Yearly Total Rainfall
Monthly Rainfall
Depth to Water
Depth to groundwater (mbgs)
Rain (mm/tu)

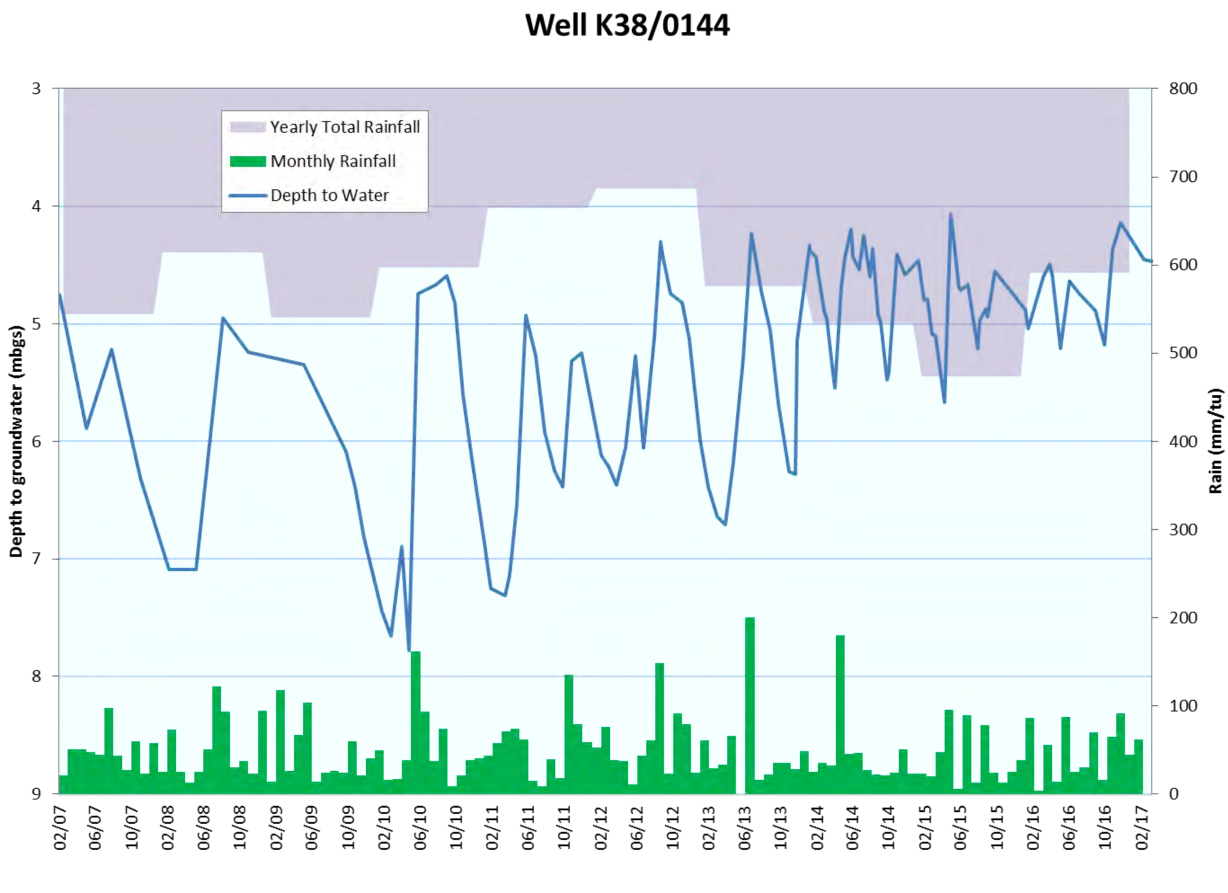

Well K38/0144
Yearly Total Rainfall
Monthly Rainfall
Depth to Water
Depth to groundwater (mbgs)
Rain (mm/tu)

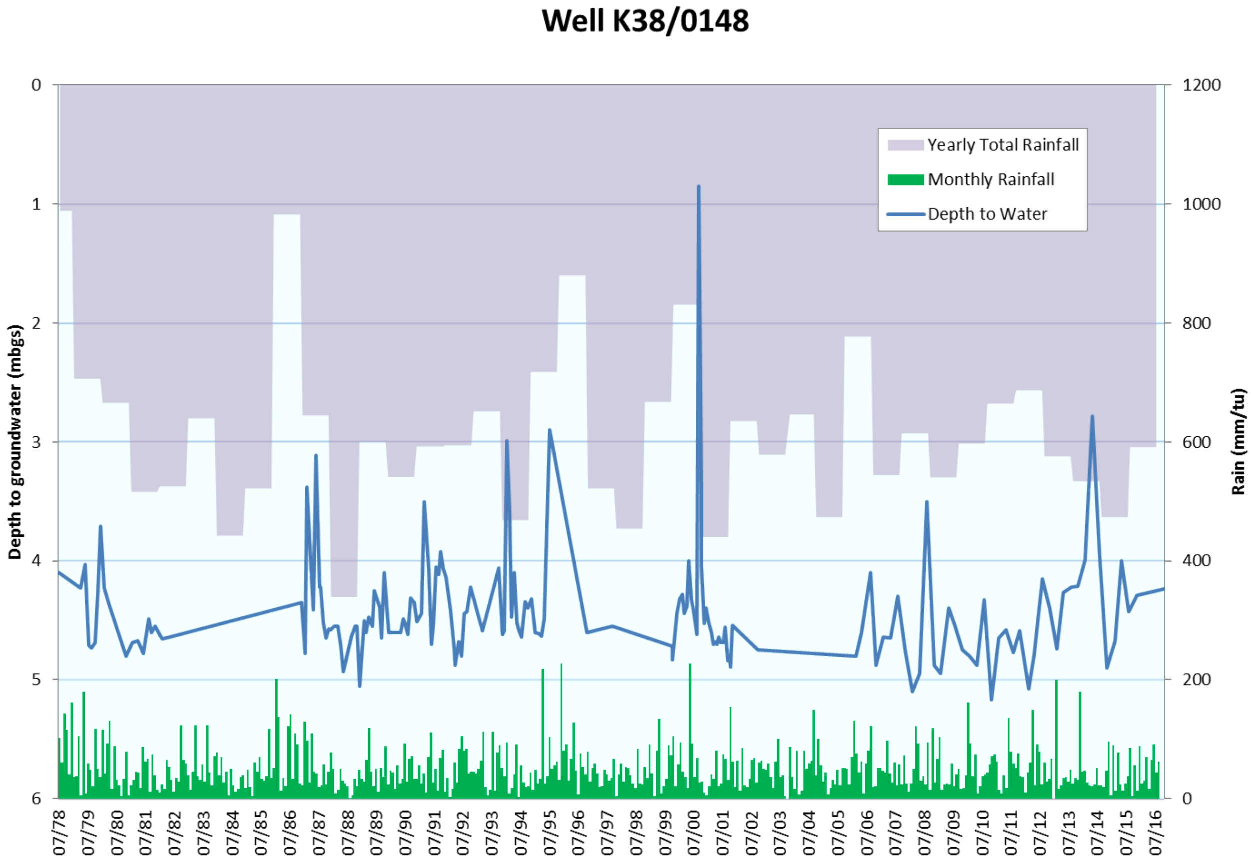
Well K38/0148
Yearly Total Rainfall
Monthly Rainfall
Depth to Water
Depth to groundwater (mbgs)
Rain (mm/tu)
0
1
2
3
4
5
6
1200
1000
800
600
400
200
0
07/78 07/79 07/80 07/81 07/82 07/83 07/84 07/85 07/86 07/87 07/88 07/89 07/90 07/91 07/92 07/93 07/94 07/95 07/96 07/97 07/98 07/99 07/00 07/01 07/02 07/03 07/04 07/05 07/06 07/07 07/08 07/09 07/10 07/11 07/12 07/13 07/14 07/15 07/16

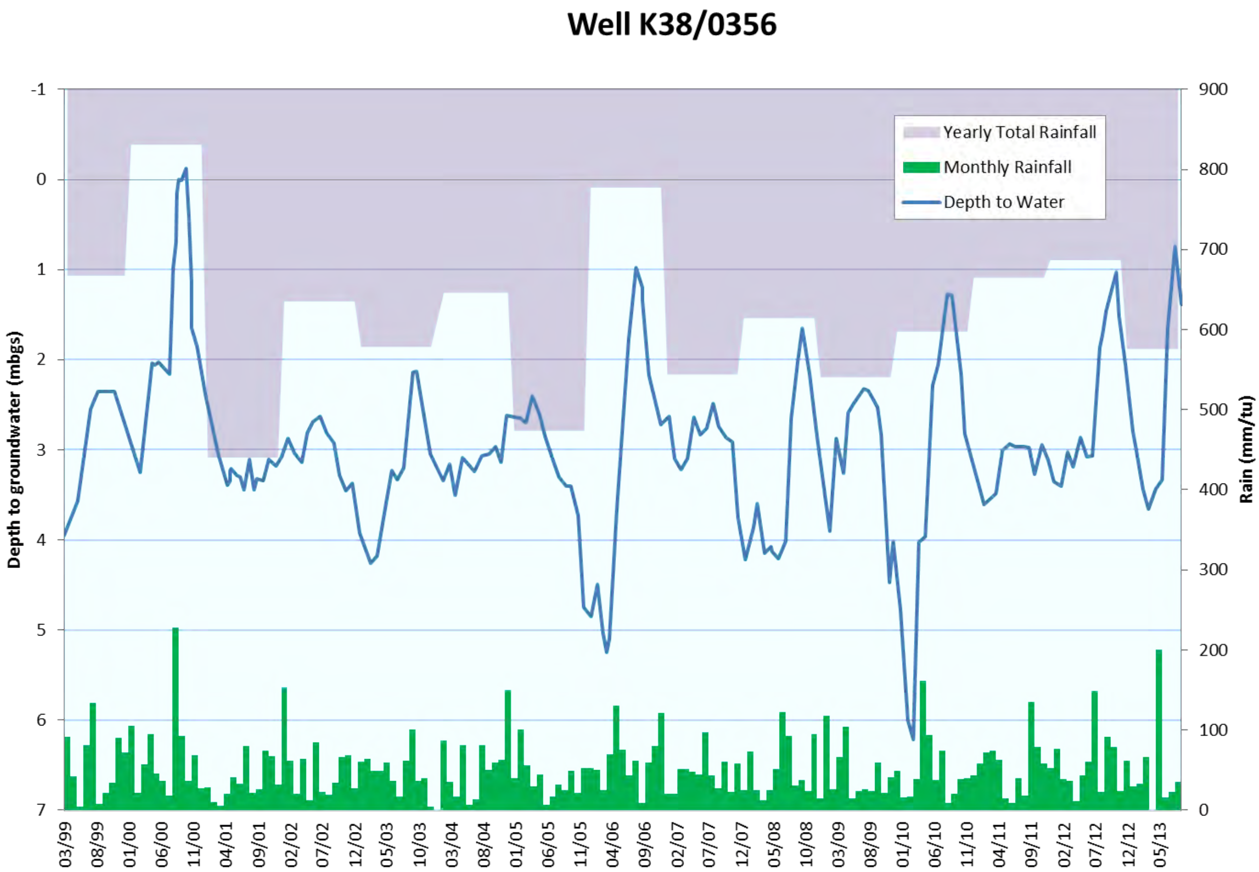
Well K38/0356
Yearly Total Rainfall
Monthly Rainfall
Depth to Water
Depth to groundwater (mbgs)
Rain (mm/tu)
-1
0
1
2
3
4
5
6
7
900
800
700
600
500
400
300
200
100
0
03/99 08/99 01/00 06/00 11/00 04/01 09/01 02/02 07/02 12/02 05/03 10/03 03/04 08/04 01/05 06/05 11/05 04/06 09/06 02/07 07/07 12/07 05/08 10/08 03/09 08/09 01/10 06/10 11/10 04/11 09/11 02/12 07/12 12/12 05/13

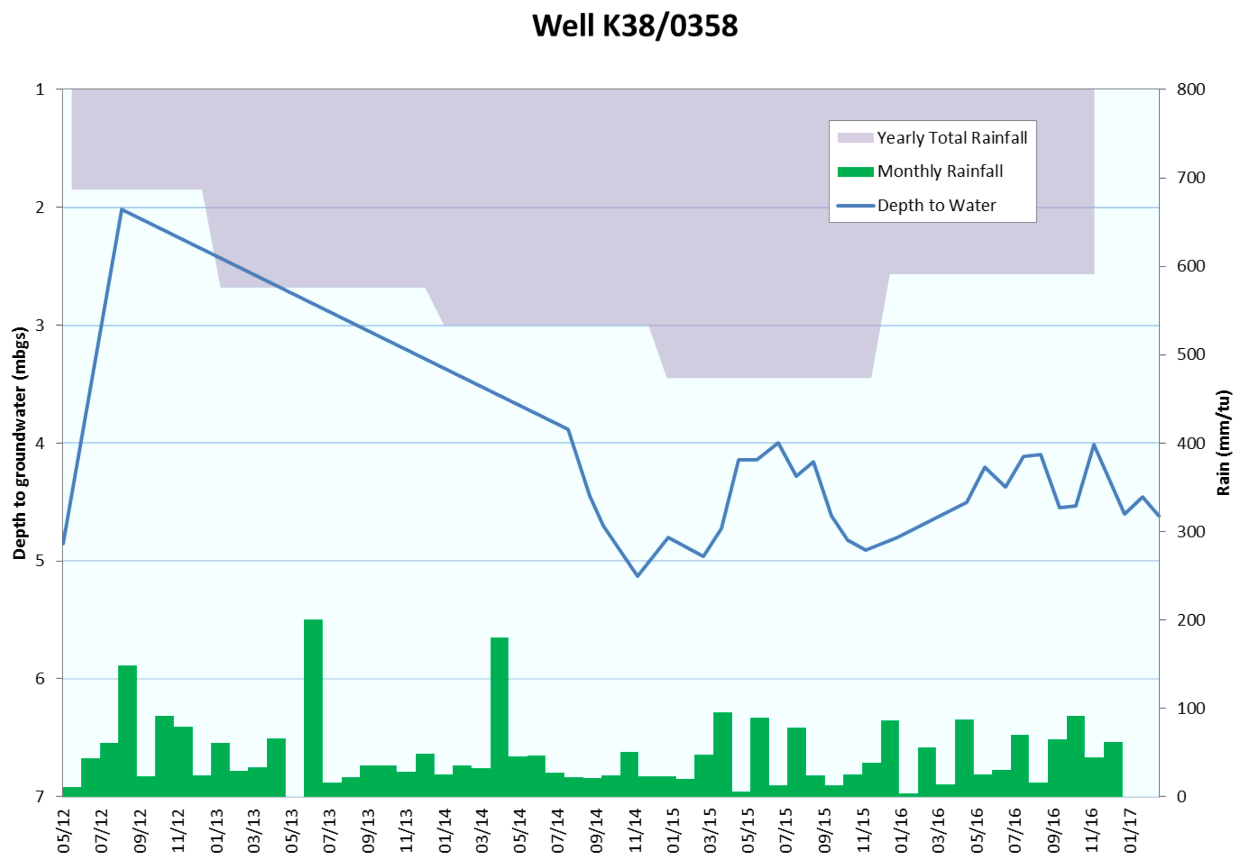
Well K38/0358
Yearly Total Rainfall
Monthly Rainfall
Depth to Water
Depth to groundwater (mbgs)
Rain (mm/tu)
1
2
3
4
5
6
7
800
700
600
500
400
300
200
100
0
05/12
07/12
09/12
11/12
01/13
03/13
05/13
07/13
09/13
11/13
01/14
03/14
05/14
07/14
09/14
11/14
01/15
03/15
05/15
07/15
09/15
11/15
01/16
03/16
05/16
07/16
09/16
11/16
01/17

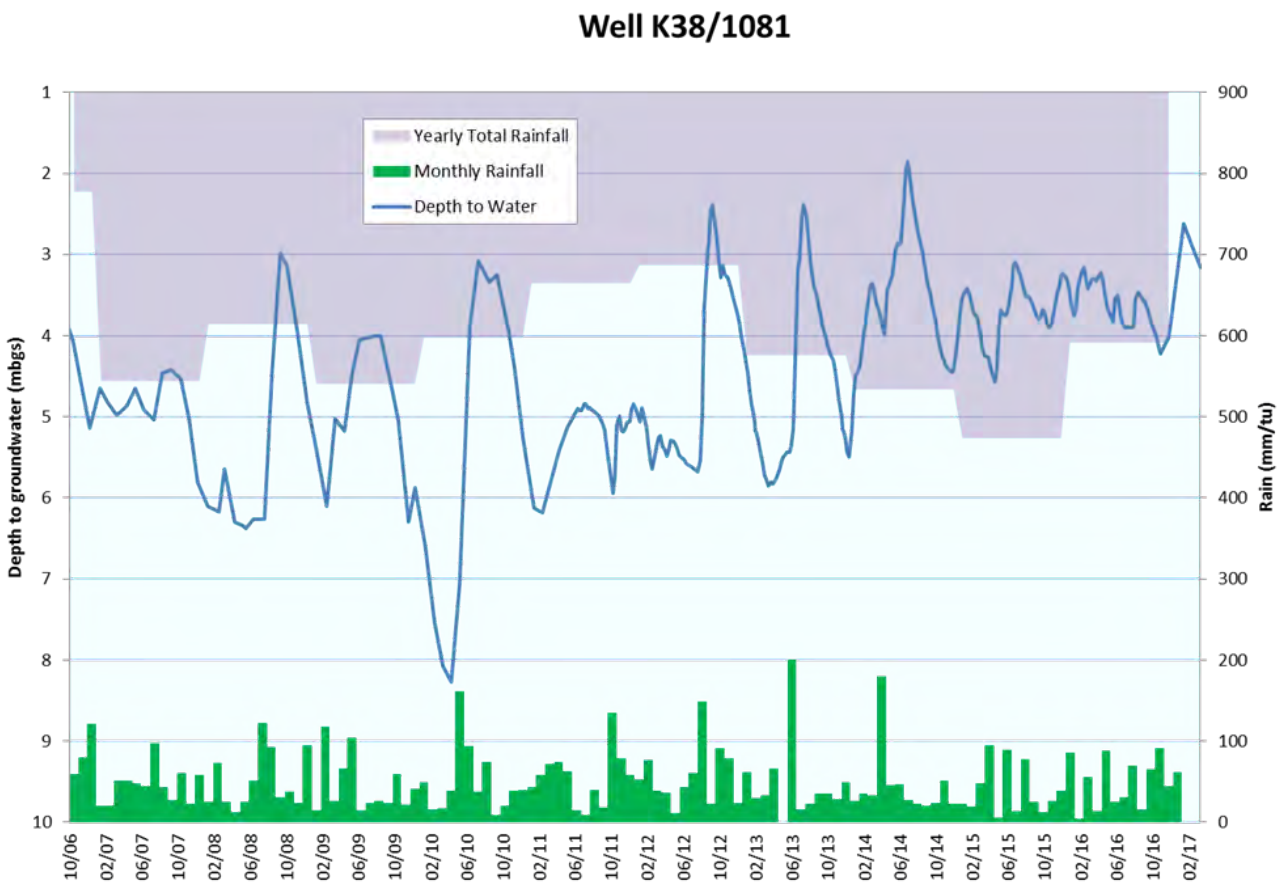
Well K38/1081
Yearly Total Rainfall
Monthly Rainfall
Depth to Water
Depth to groundwater (mbgs)
Rain (mm/tu)
1
2
3
4
5
6
7
8
9
10
900
800
700
600
500
400
300
200
100
0
10/06
02/07
06/07
10/07
02/08
06/08
10/08
02/09
06/09
10/09
02/10
06/10
10/10
02/11
06/11
10/11
02/12
06/12
10/12
02/13
06/13
10/13
02/14
06/14
10/14
02/15
06/15
10/15
02/16
06/16
10/16
02/17

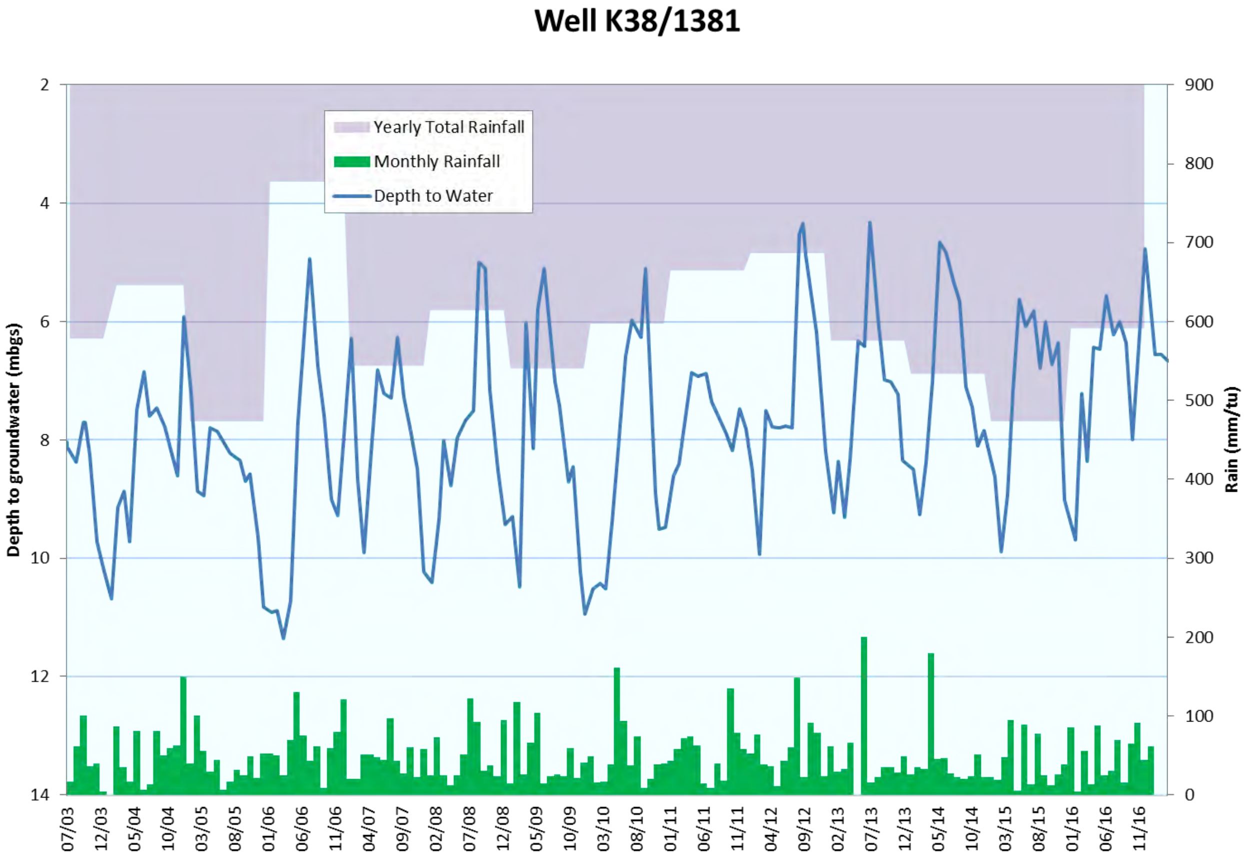
Well K38/1381
Yearly Total Rainfall
Monthly Rainfall
Depth to Water
Depth to groundwater (mbgs)
Rain (mm/tu)
2
4
6
8
10
12
14
900
800
700
600
500
400
300
200
100
0
07/03
12/03
05/04
10/04
03/05
08/05
01/06
06/06
11/06
04/07
09/07
02/08
07/08
12/08
05/09
10/09
03/10
08/10
01/11
06/11
11/11
04/12
09/12
02/13
07/13
12/13
05/14
10/14
03/15
08/15
01/16
06/16
11/16

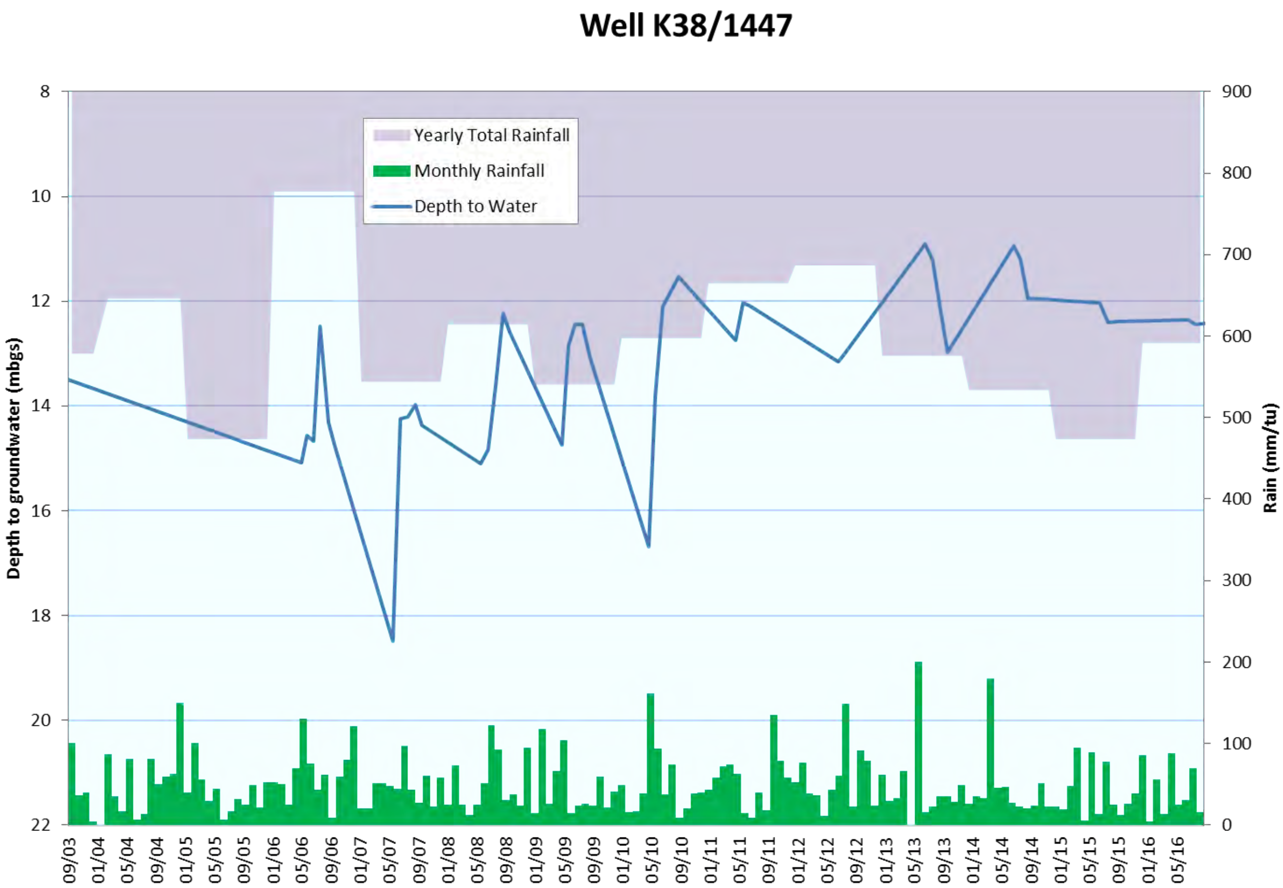
Well K38/1447
Yearly Total Rainfall
Monthly Rainfall
Depth to Water
Depth to groundwater (mbgs)
Rain (mm/tu)
8
10
12
14
16
18
20
22
900
800
700
600
500
400
300
200
100
0
09/03
01/04
05/04
09/04
01/05
05/05
09/05
01/06
05/06
09/06
01/07
05/07
09/07
01/08
05/08
09/08
01/09
05/09
09/09
01/10
05/10
09/10
01/11
05/11
09/11
01/12
05/12
09/12
01/13
05/13
09/13
01/14
05/14
09/14
01/15
05/15
09/15
01/16
05/16

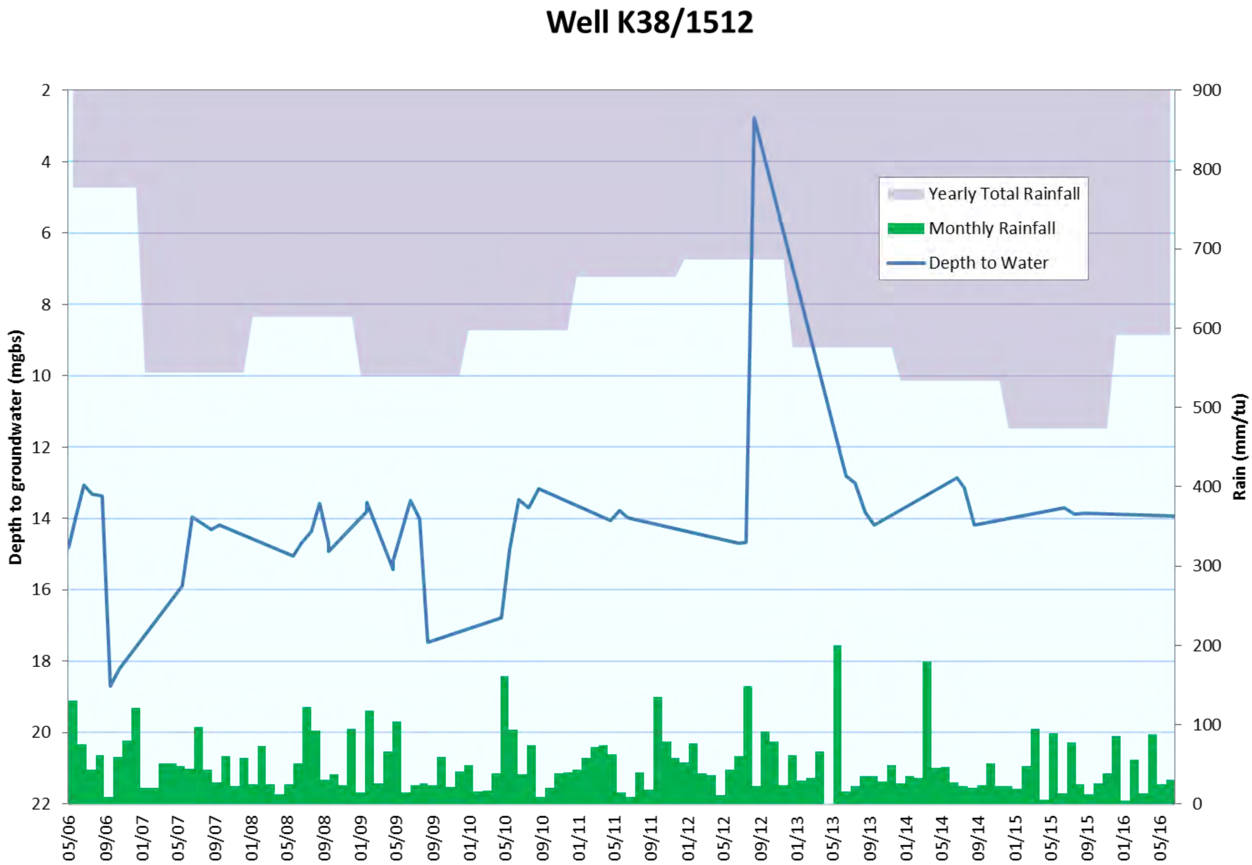

Well K38/1512
Yearly Total Rainfall
Monthly Rainfall
Depth to Water
Depth to groundwater (mgbs)
Rain (mm/tu)
2
4
6
8
10
12
14
16
18
20
22
900
800
700
600
500
400
300
200
100
0
05/06
09/06
01/07
05/07
09/07
01/08
05/08
09/08
01/09
05/09
09/09
01/10
05/10
09/10
01/11
05/11
09/11
01/12
05/12
09/12
01/13
05/13
09/13
01/14
05/14
09/14
01/15
05/15
09/15
01/16
05/16

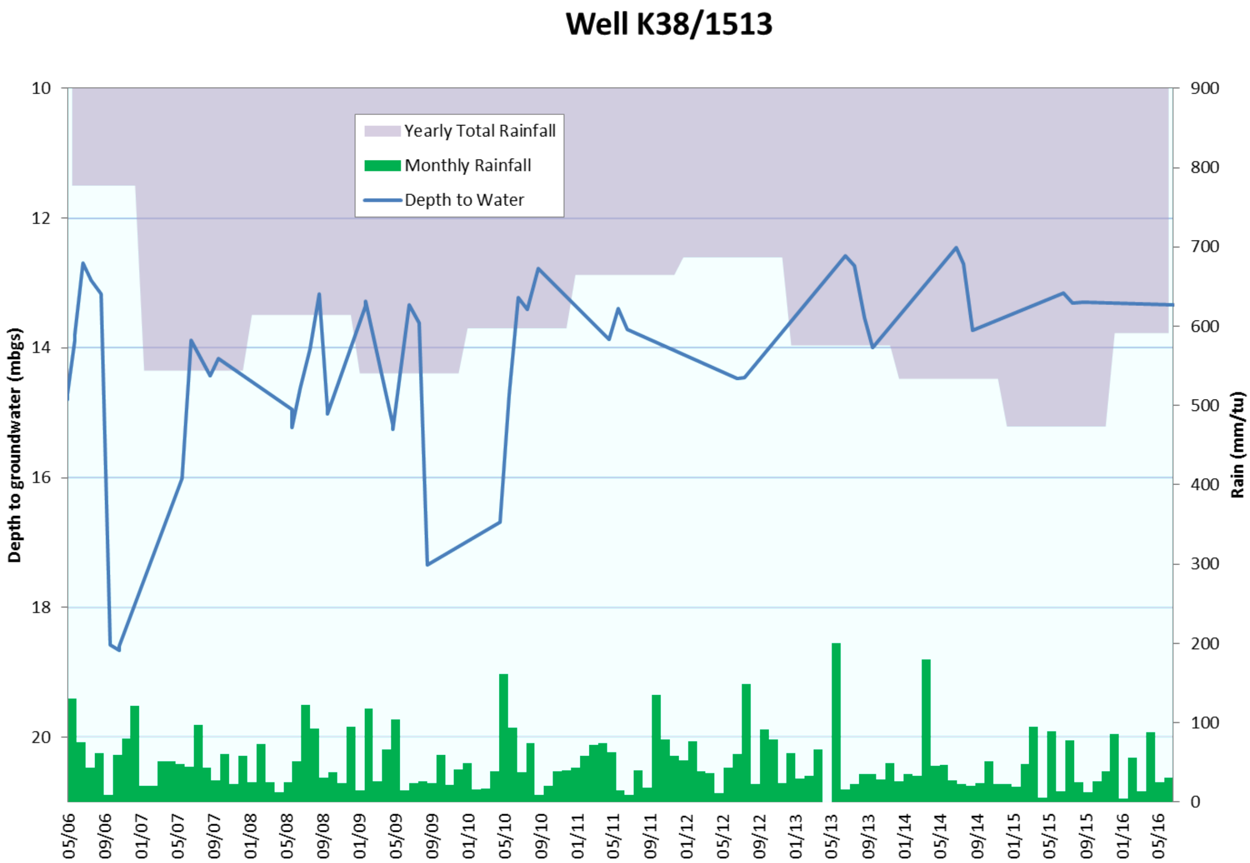

Well K38/1513
Yearly Total Rainfall
Monthly Rainfall
Depth to Water
Depth to groundwater (mbgs)
Rain (mm/tu)
10
12
14
16
18
20
900
800
700
600
500
400
300
200
100
0
05/06
09/06
01/07
05/07
09/07
01/08
05/08
09/08
01/09
05/09
09/09
01/10
05/10
09/10
01/11
05/11
09/11
01/12
05/12
09/12
01/13
05/13
09/13
01/14
05/14
09/14
01/15
05/15
09/15
01/16
05/16

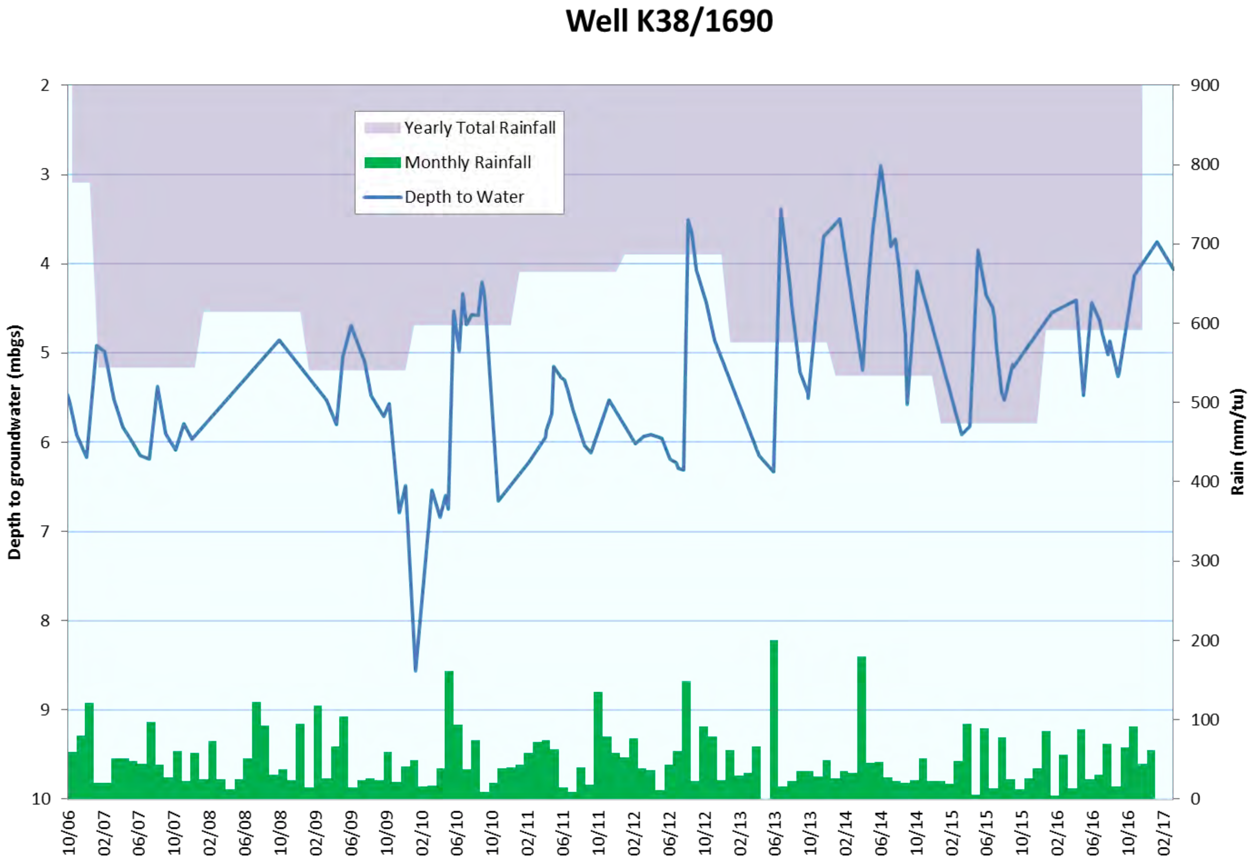
Well K38/1690
Yearly Total Rainfall
Monthly Rainfall
Depth to Water
Depth to groundwater (mbgs)
Rain (mm/tu)
2
3
4
5
6
7
8
9
10
900
800
700
600
500
400
300
200
100
0
10/06
02/07
06/07
10/07
02/08
06/08
10/08
02/09
06/09
10/09
02/10
06/10
10/10
02/11
06/11
10/11
02/12
06/12
10/12
02/13
06/13
10/13
02/14
06/14
10/14
02/15
06/15
10/15
02/16
06/16
10/16
02/17

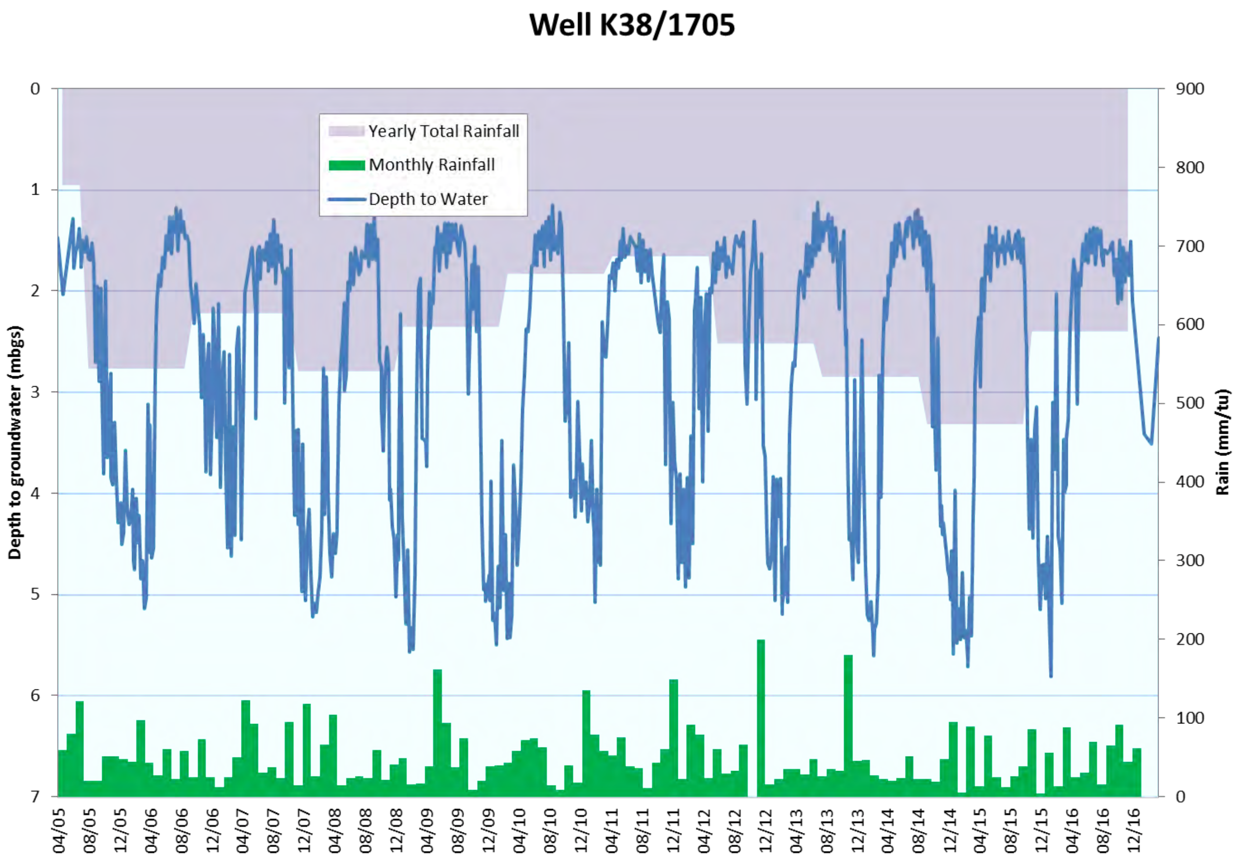
Well K38/1705
Yearly Total Rainfall
Monthly Rainfall
Depth to Water
Depth to groundwater (mbgs)
Rain (mm/tu)
0
1
2
3
4
5
6
7
900
800
700
600
500
400
300
200
100
0
04/05
08/05
12/05
04/06
08/06
12/06
04/07
08/07
12/07
04/08
08/08
12/08
04/09
08/09
12/09
04/10
08/10
12/10
04/11
08/11
12/11
04/12
08/12
12/12
04/13
08/13
12/13
04/14
08/14
12/14
04/15
08/15
12/15
04/16
08/16
12/16

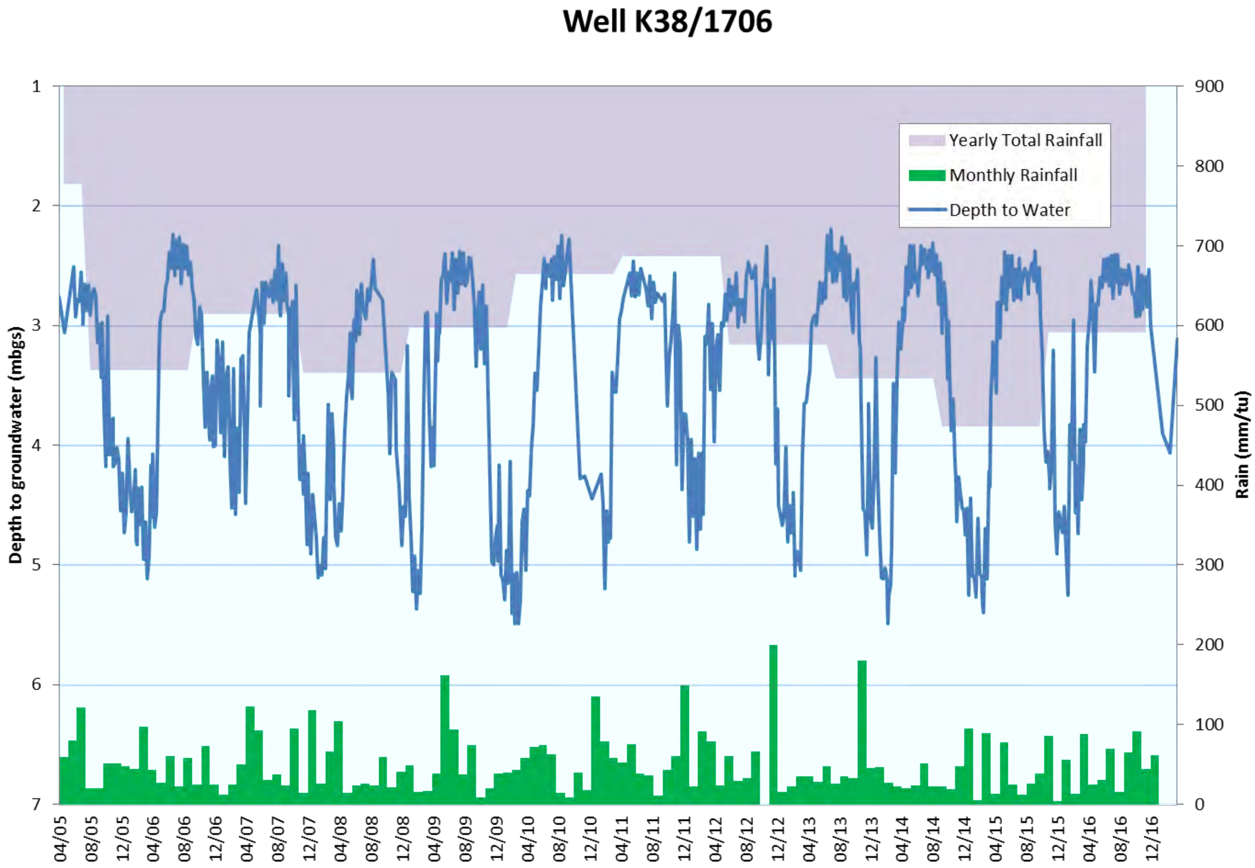
Well K38/1706
Yearly Total Rainfall
Monthly Rainfall
Depth to Water
Depth to groundwater (mbgs)
Rain (mm/tu)
1
2
3
4
5
6
7
900
800
700
600
500
400
300
200
100
0
04/05
08/05
12/05
04/06
08/06
12/06
04/07
08/07
12/07
04/08
08/08
12/08
04/09
08/09
12/09
04/10
08/10
12/10
04/11
08/11
12/11
04/12
08/12
12/12
04/13
08/13
12/13
04/14
08/14
12/14
04/15
08/15
12/15
04/16
08/16
12/16

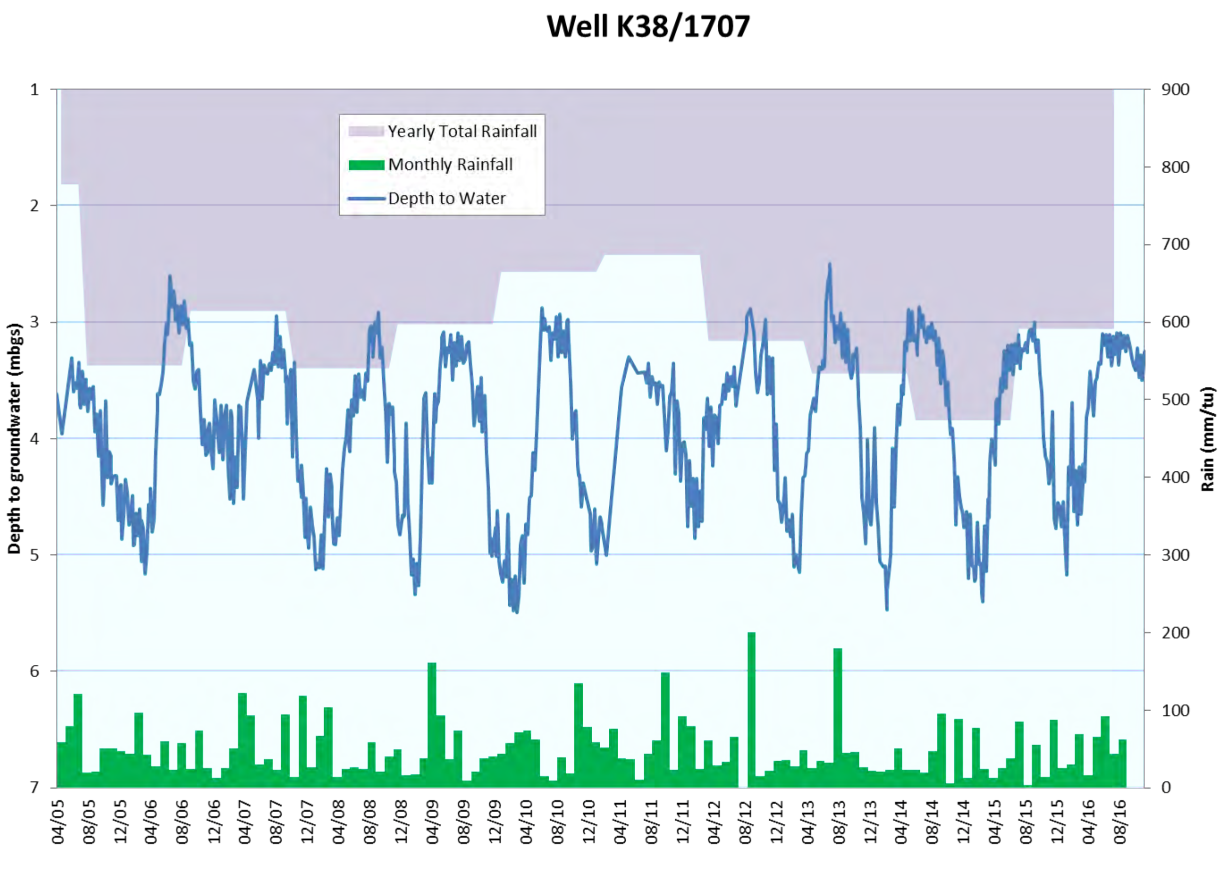
Well K38/1707
Yearly Total Rainfall
Monthly Rainfall
Depth to Water
Depth to groundwater (mbgs)
Rain (mm/tu)
1
2
3
4
5
6
7
900
800
700
600
500
400
300
200
100
0
04/05
08/05
12/05
04/06
08/06
12/06
04/07
08/07
12/07
04/08
08/08
12/08
04/09
08/09
12/09
04/10
08/10
12/10
04/11
08/11
12/11
04/12
08/12
12/12
04/13
08/13
12/13
04/14
08/14
12/14
04/15
08/15
12/15
04/16
08/16

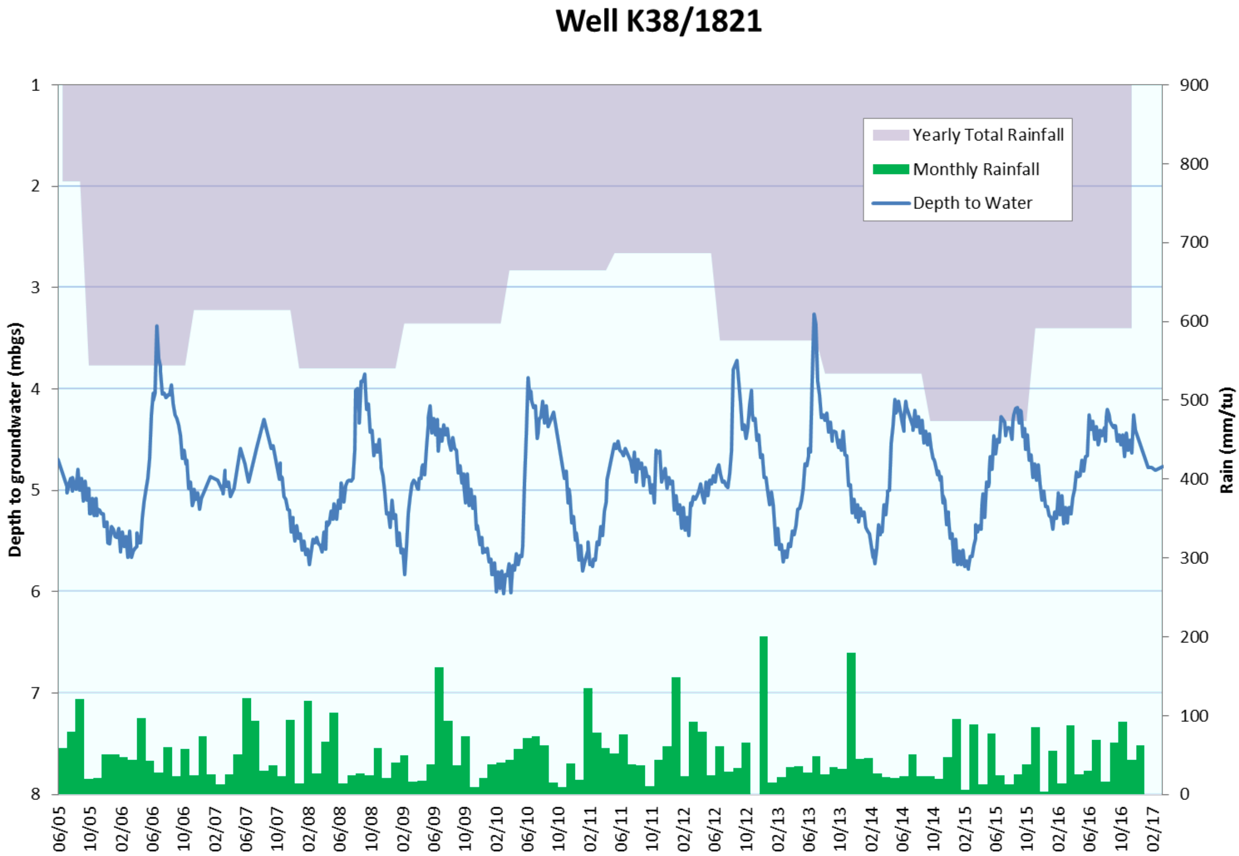
Well K38/1821
Yearly Total Rainfall
Monthly Rainfall
Depth to Water
Depth to groundwater (mbgs)
Rain (mm/tu)

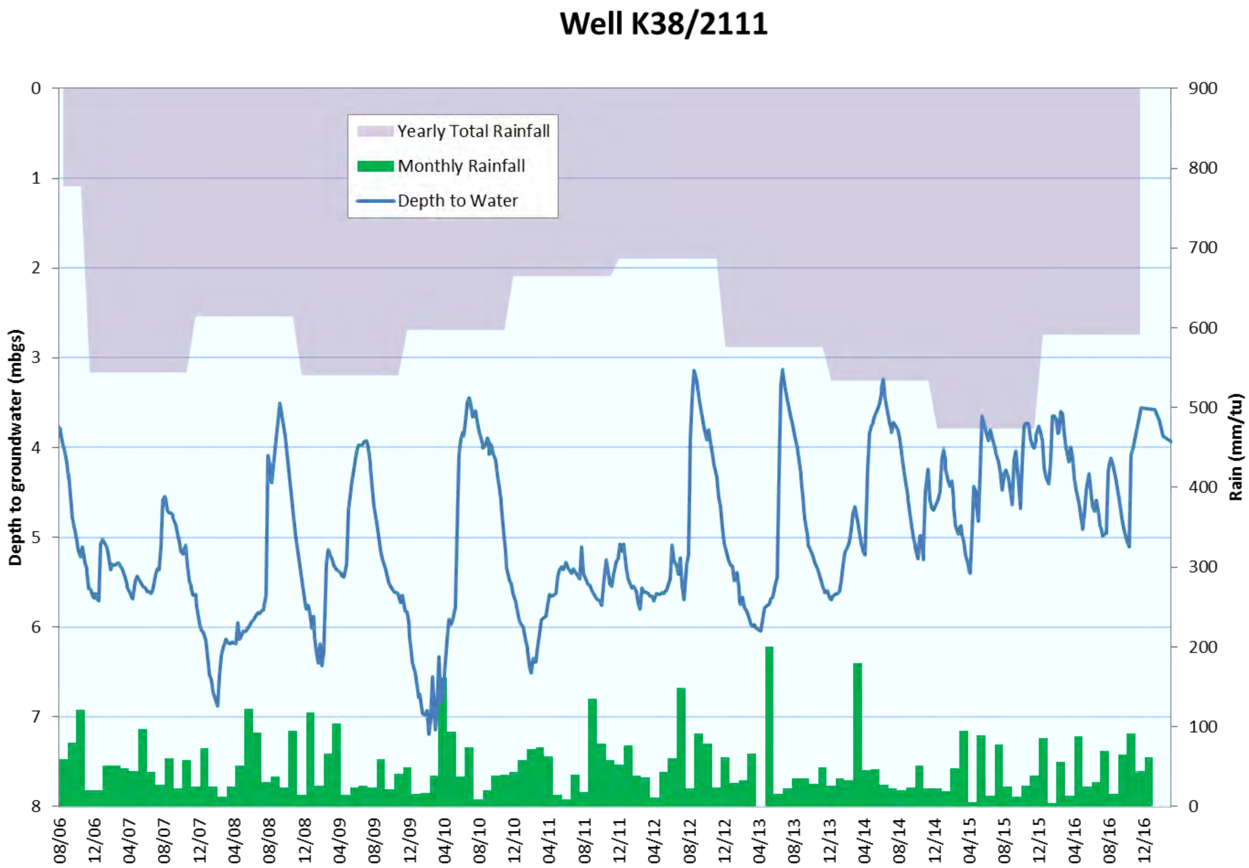
Well K38/2111
Yearly Total Rainfall
Monthly Rainfall
Depth to Water
Depth to groundwater (mbgs)
Rain (mm/tu)

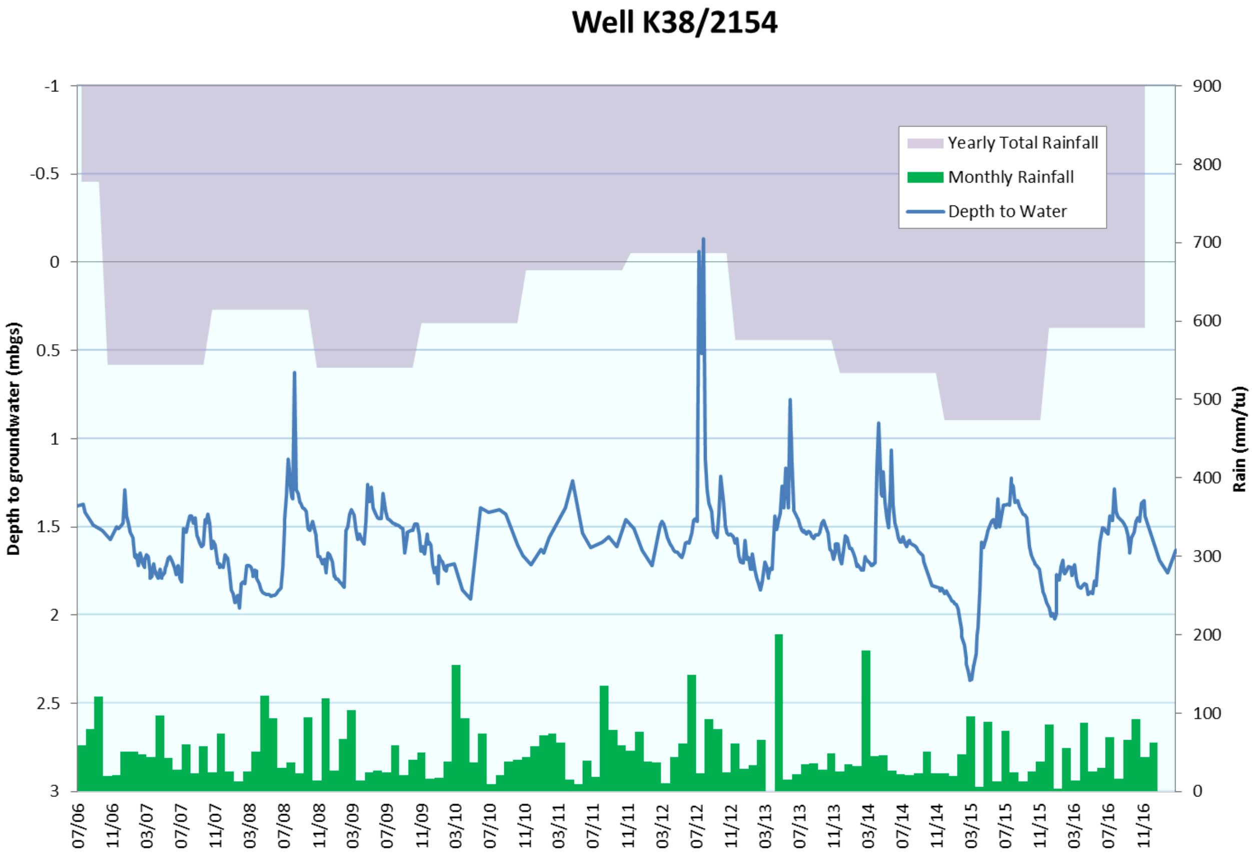
Well K38/2154
Yearly Total Rainfall
Monthly Rainfall
Depth to Water
Depth to groundwater (mbgs)
Rain (mm/tu)
-1
-0.5
0
0.5
1
1.5
2
2.5
3
900
800
700
600
500
400
300
200
100
0
07/06
11/06
03/07
07/07
11/07
03/08
07/08
11/08
03/09
07/09
11/09
03/10
07/10
11/10
03/11
07/11
11/11
03/12
07/12
11/12
03/13
07/13
11/13
03/14
07/14
11/14
03/15
07/15
11/15
03/16
07/16
11/16

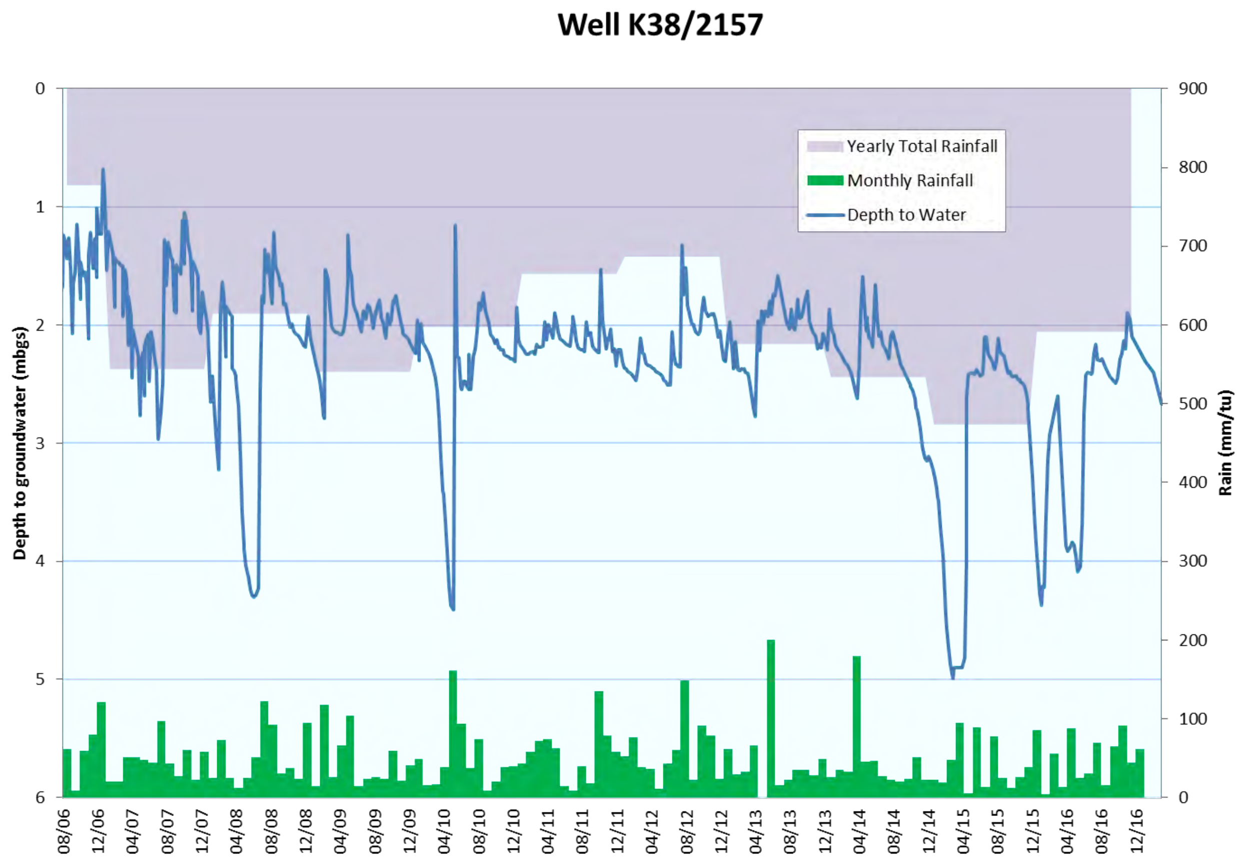
Well K38/2157
Yearly Total Rainfall
Monthly Rainfall
Depth to Water
Depth to groundwater (mbgs)
Rain (mm/tu)
0
1
2
3
4
5
6
900
800
700
600
500
400
300
200
100
0
08/06
12/06
04/07
08/07
12/07
04/08
08/08
12/08
04/09
08/09
12/09
04/10
08/10
12/10
04/11
08/11
12/11
04/12
08/12
12/12
04/13
08/13
12/13
04/14
08/14
12/14
04/15
08/15
12/15
04/16
08/16
12/16

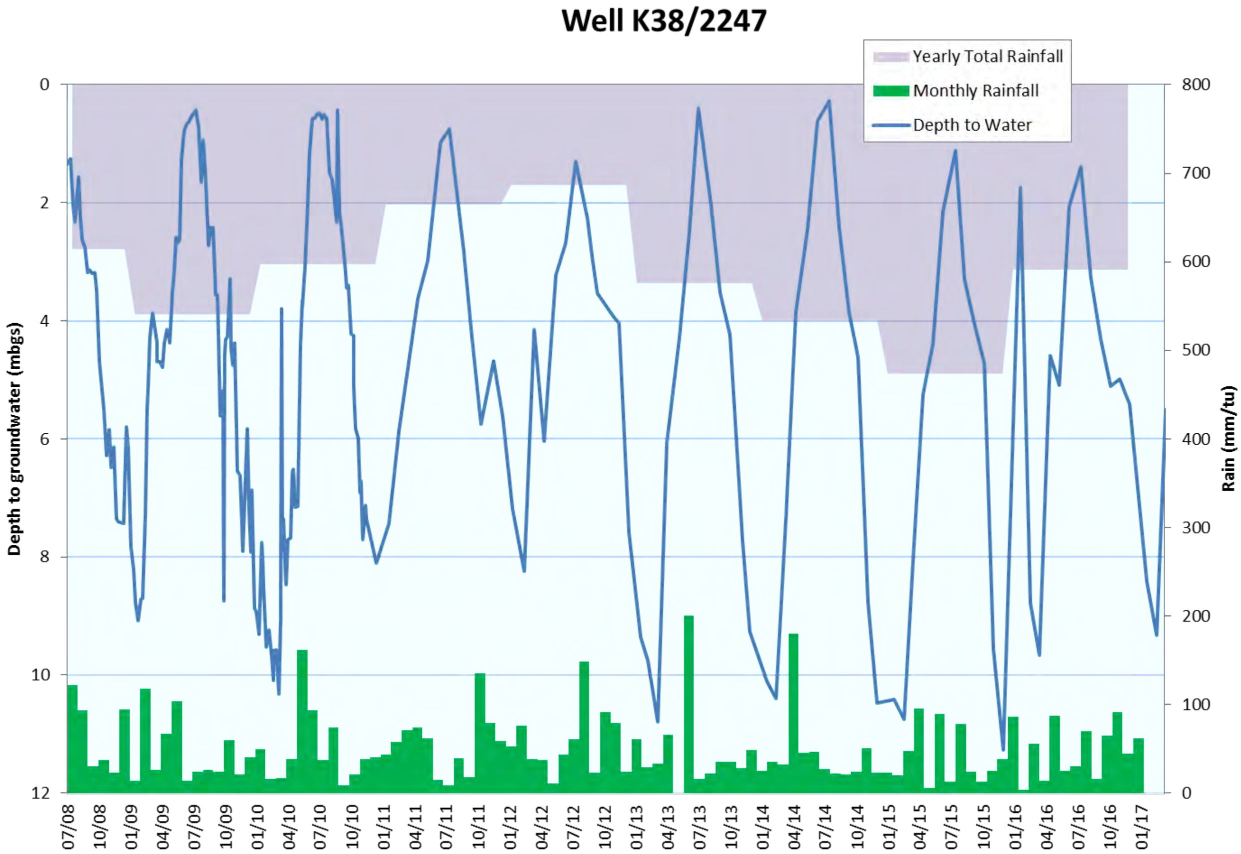
Well K38/2247
Yearly Total Rainfall
Monthly Rainfall
Depth to Water
Depth to groundwater (mbgs)
Rain (mm/tu)
0
2
4
6
8
10
12
800
700
600
500
400
300
200
100
0
07/08
10/08
01/09
04/09
07/09
10/09
01/10
04/10
07/10
10/10
01/11
04/11
07/11
10/11
01/12
04/12
07/12
10/12
01/13
04/13
07/13
10/13
01/14
04/14
07/14
10/14
01/15
04/15
07/15
10/15
01/16
04/16
07/16
10/16
01/17

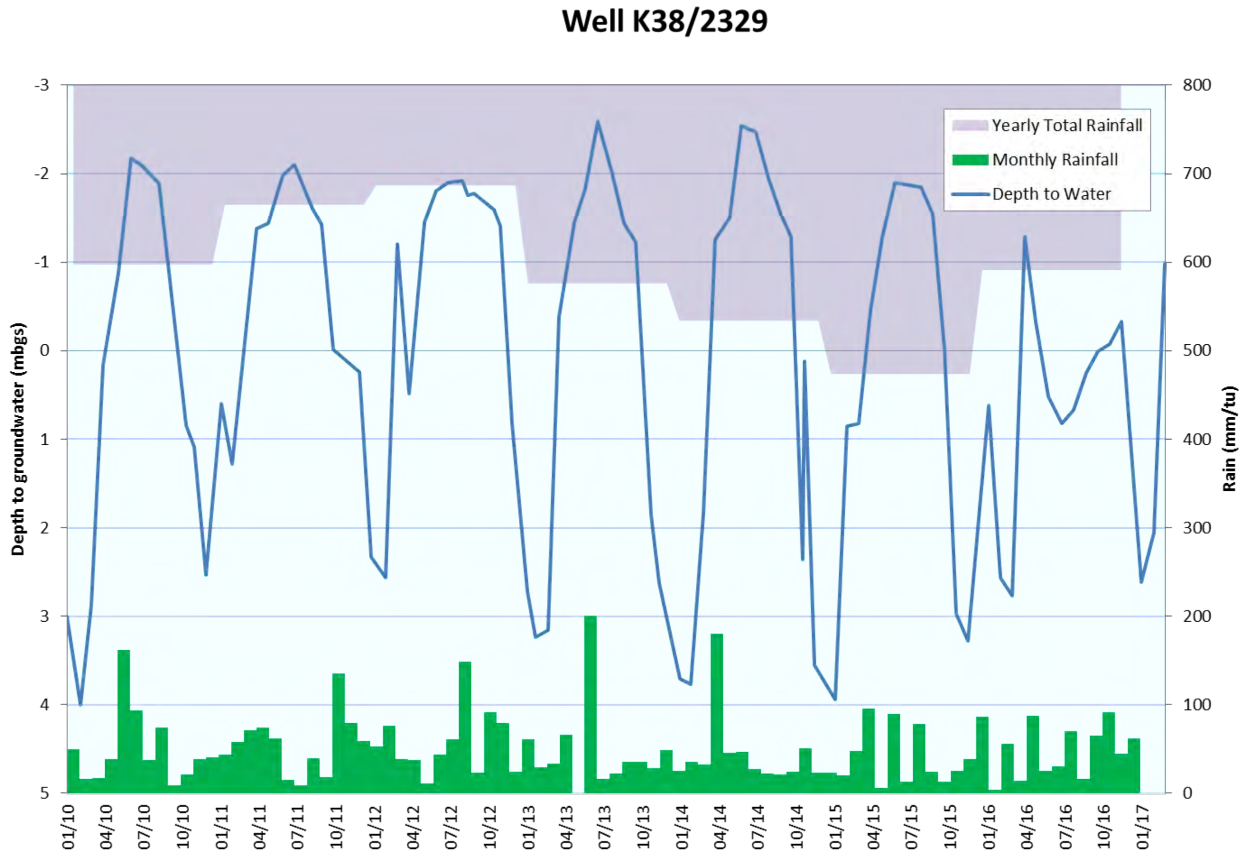
Well K38/2329
Yearly Total Rainfall
Monthly Rainfall
Depth to Water
Depth to groundwater (mbgs)
Rain (mm/tu)
-3
-2
-1
0
1
2
3
4
5
800
700
600
500
400
300
200
100
0
01/10
04/10
07/10
10/10
01/11
04/11
07/11
10/11
01/12
04/12
07/12
10/12
01/13
04/13
07/13
10/13
01/14
04/14
07/14
10/14
01/15
04/15
07/15
10/15
01/16
04/16
07/16
10/16
01/17

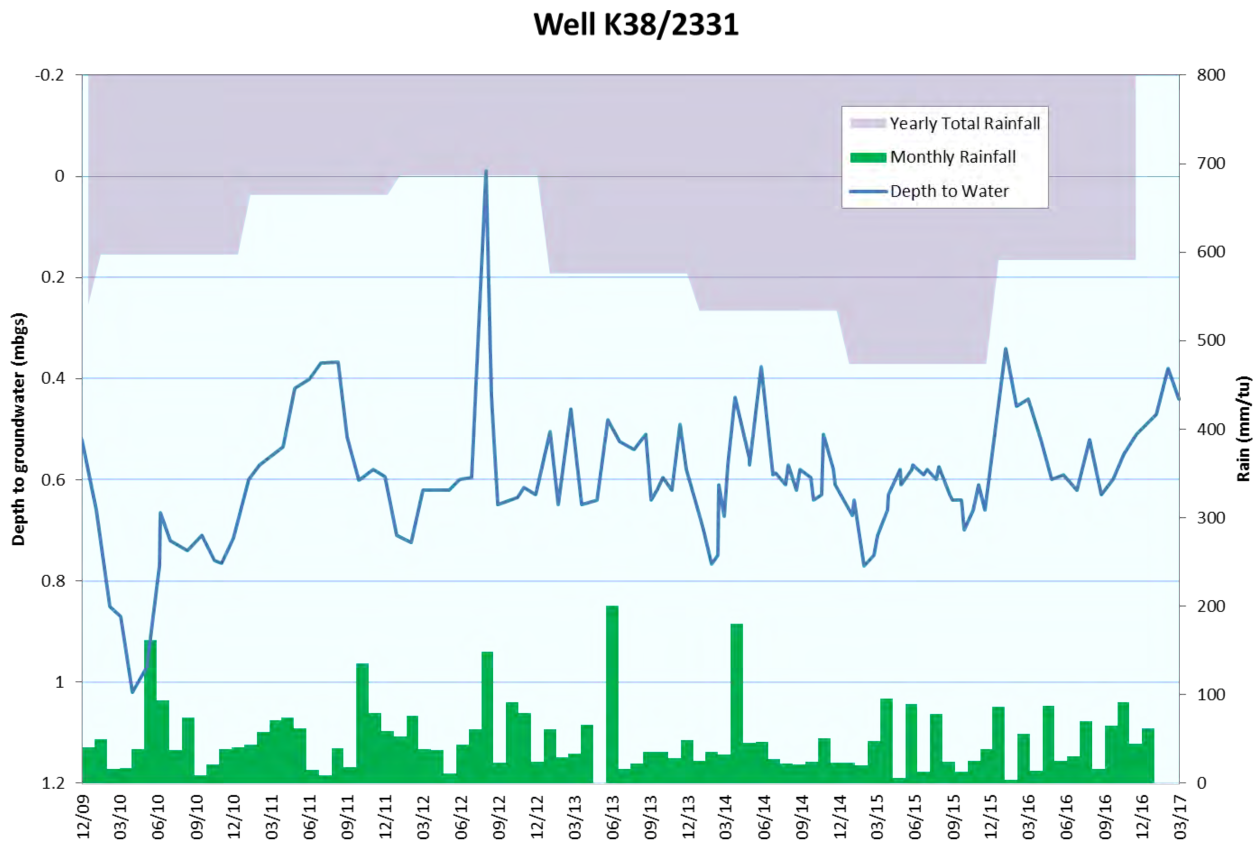
Well K38/2331
Yearly Total Rainfall
Monthly Rainfall
Depth to Water
Depth to groundwater (mbgs)
Rain (mm/tu)
-0.2
0
0.2
0.4
0.6
0.8
1
1.2
800
700
600
500
400
300
200
100
0
12/09
03/10
06/10
09/10
12/10
03/11
06/11
09/11
12/11
03/12
06/12
09/12
12/12
03/13
06/13
09/13
12/13
03/14
06/14
09/14
12/14
03/15
06/15
09/15
12/15
03/16
06/16
09/16
12/16
03/17

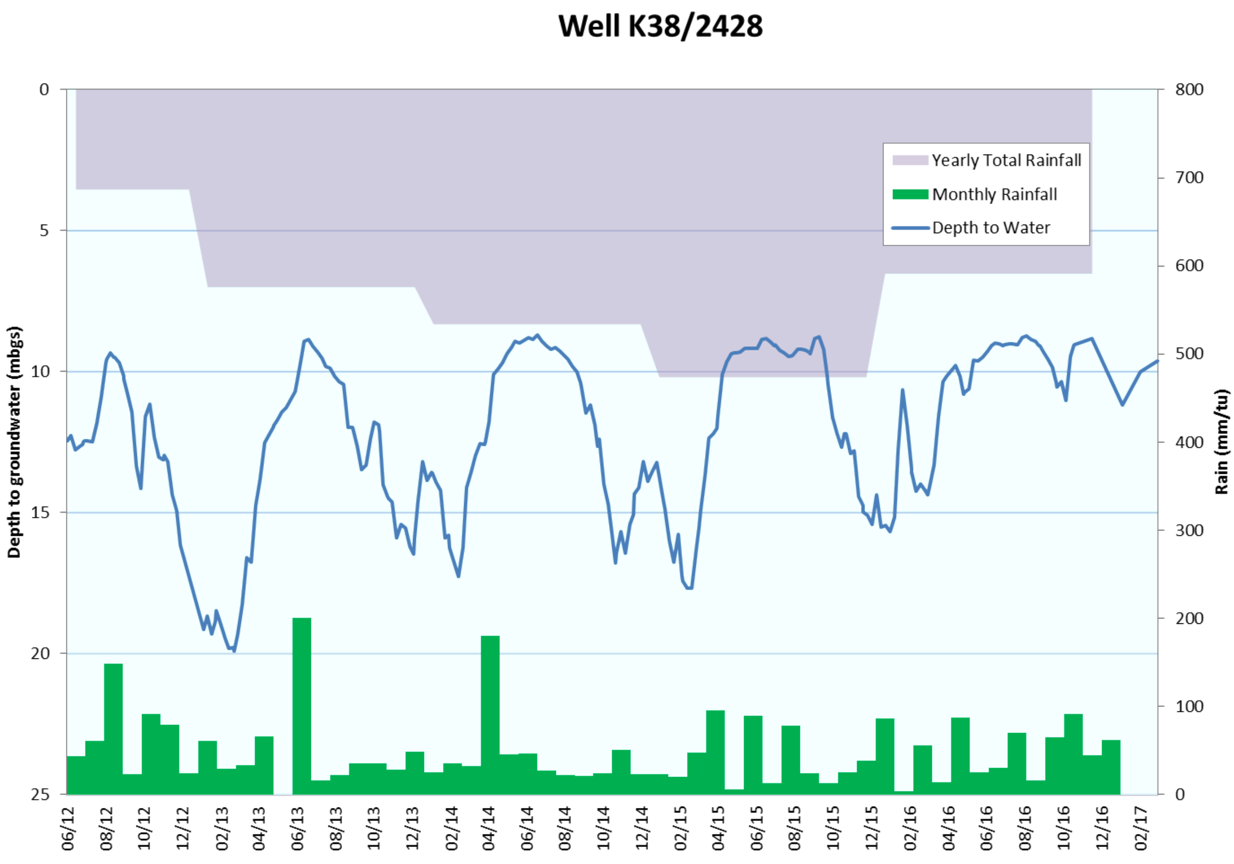
Well K38/2428
Yearly Total Rainfall
Monthly Rainfall
Depth to Water
Depth to groundwater (mbgs)
Rain (mm/tu)
0
5
10
15
20
25
800
700
600
500
400
300
200
100
0
06/12
08/12
10/12
12/12
02/13
04/13
06/13
08/13
10/13
12/13
02/14
04/14
06/14
08/14
10/14
12/14
02/15
04/15
06/15
08/15
10/15
12/15
02/16
04/16
06/16
08/16
10/16
12/16
02/17

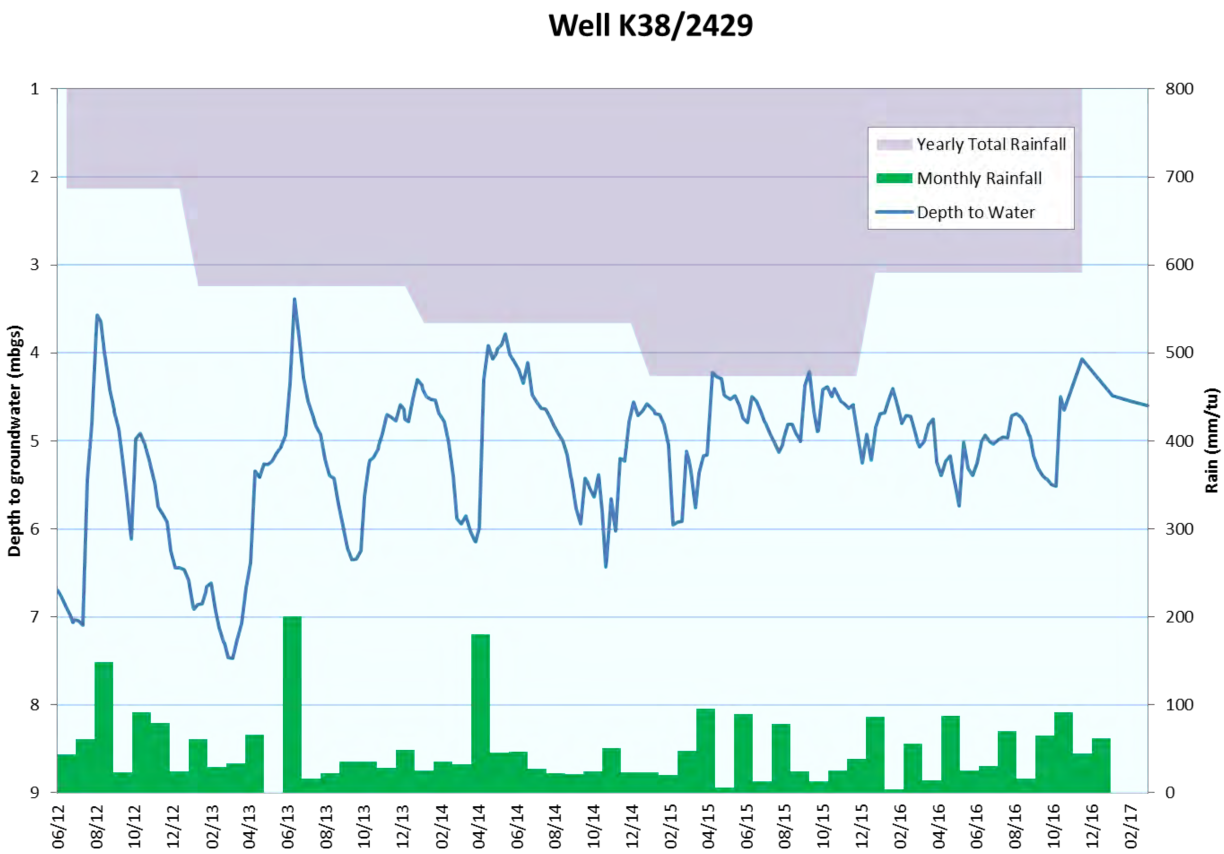
Well K38/2429
Yearly Total Rainfall
Monthly Rainfall
Depth to Water
Depth to groundwater (mbgs)
Rain (mm/tu)
1
2
3
4
5
6
7
8
9
800
700
600
500
400
300
200
100
0
06/12
08/12
10/12
12/12
02/13
04/13
06/13
08/13
10/13
12/13
02/14
04/14
06/14
08/14
10/14
12/14
02/15
04/15
06/15
08/15
10/15
12/15
02/16
04/16
06/16
08/16
10/16
12/16
02/17

Appendix B: Groundwater quality records for monitoring wells in the study area

Acronyms:

mg/l	=	milligrams per litre
mS/m	=	milliSiemens per metre
mg/l $CaCO_3$	=	mg/l of calcium carbonate

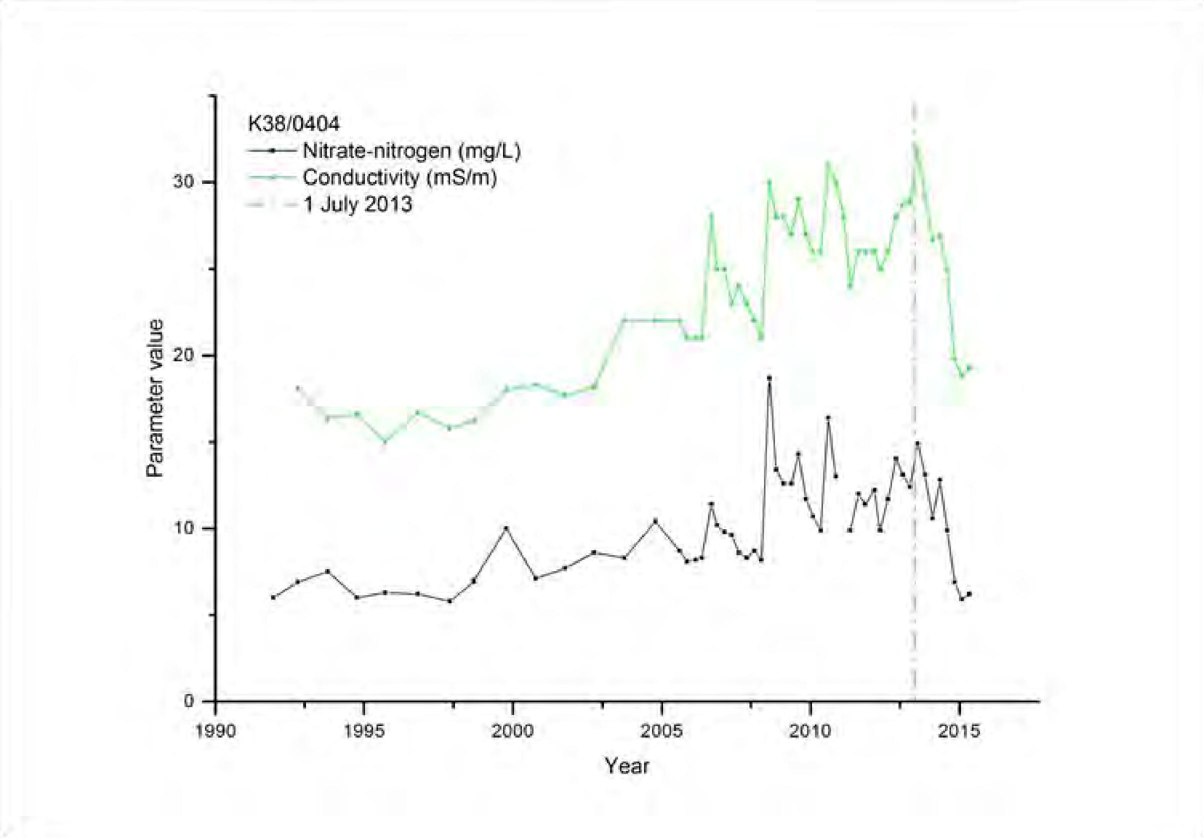
K38/0404
Nitrate-nitrogen (mg/L)
Conductivity (mS/m)
1 July 2013
Parameter value
0
10
20
30
1990
1995
2000
2005
2010
2015
Year

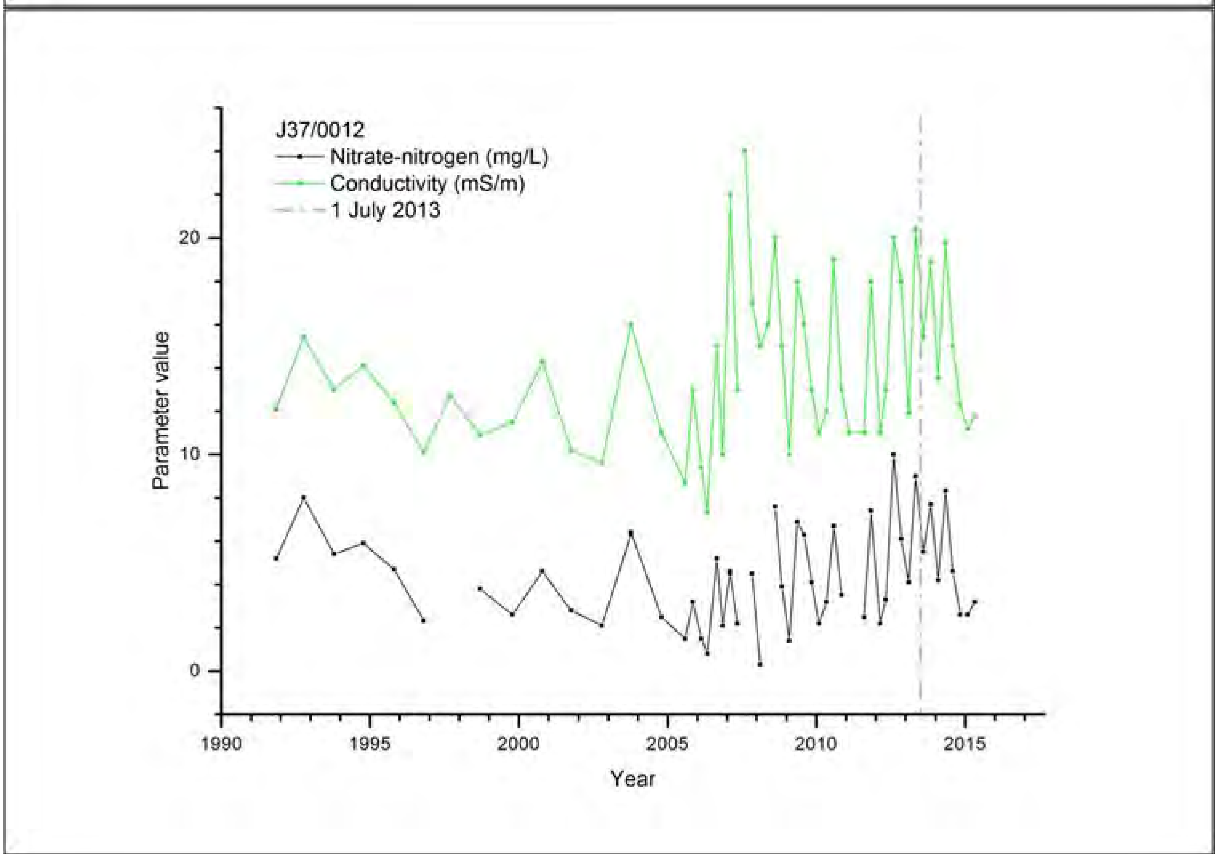
J37/0012
Nitrate-nitrogen (mg/L)
Conductivity (mS/m)
1 July 2013
Parameter value
0
10
20
1990
1995
2000
2005
2010
2015
Year

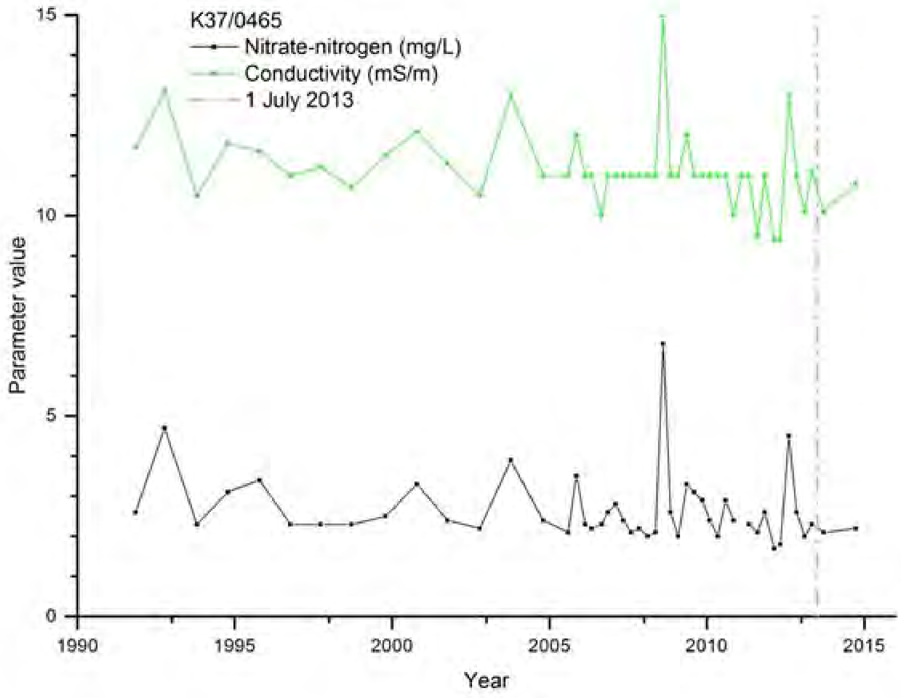
K37/0465
Nitrate-nitrogen (mg/L)
Conductivity (mS/m)
1 July 2013
Parameter value
Year
0
5
10
15
1990
1995
2000
2005
2010
2015

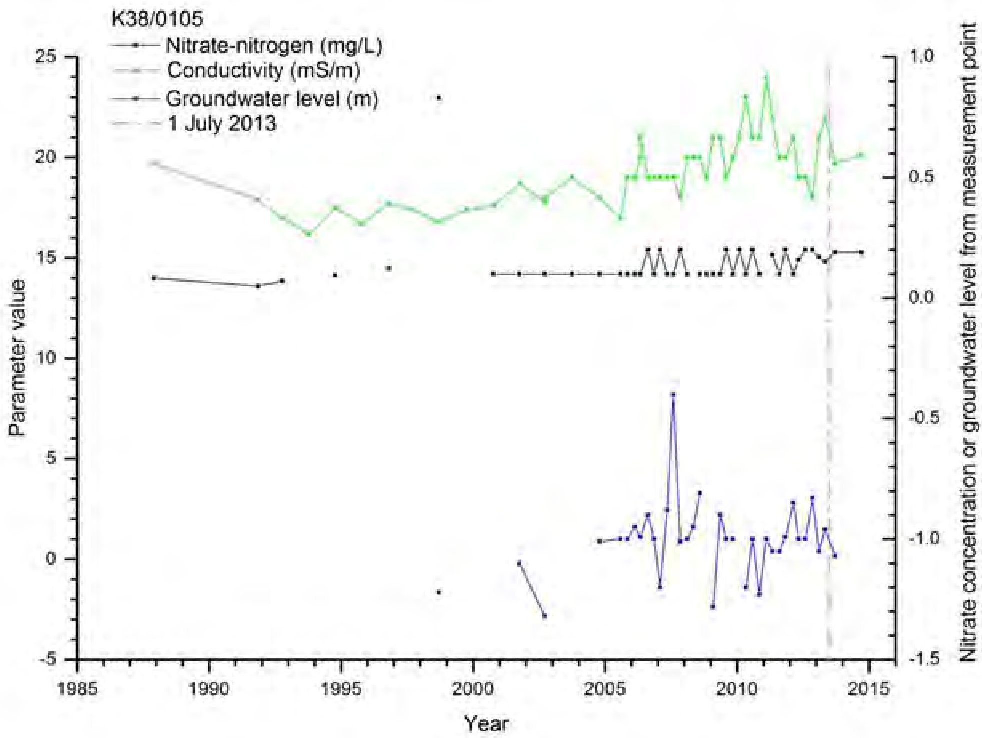
K38/0105
Nitrate-nitrogen (mg/L)
Conductivity (mS/m)
Groundwater level (m)
1 July 2013
Parameter value
Nitrate concentration or groundwater level from measurement point
Year
-5
0
5
10
15
20
25
1.0
0.5
0.0
-0.5
-1.0
-1.5
1985
1990
1995
2000
2005
2010
2015

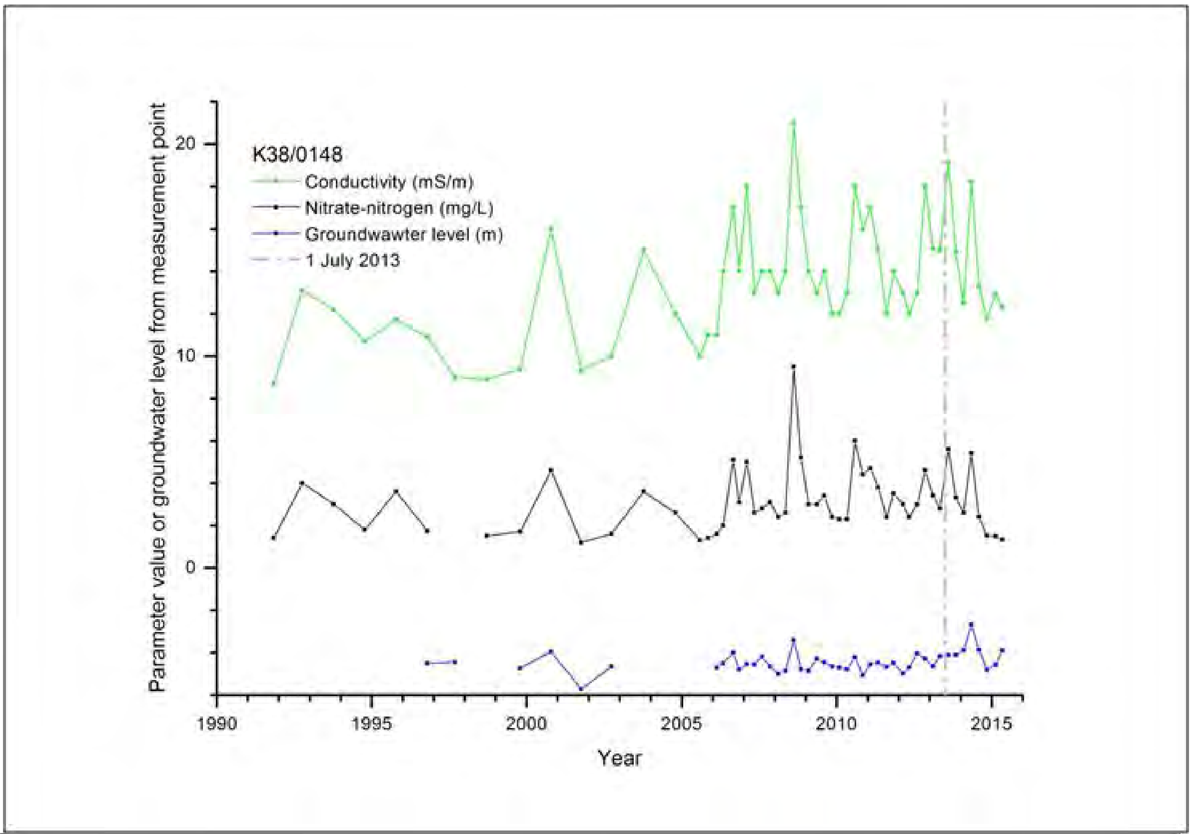
K38/0148
Conductivity (mS/m)
Nitrate-nitrogen (mg/L)
Groundwawter level (m)
1 July 2013
Parameter value or groundwater level from measurement point
Year
0
10
20
1990
1995
2000
2005
2010
2015

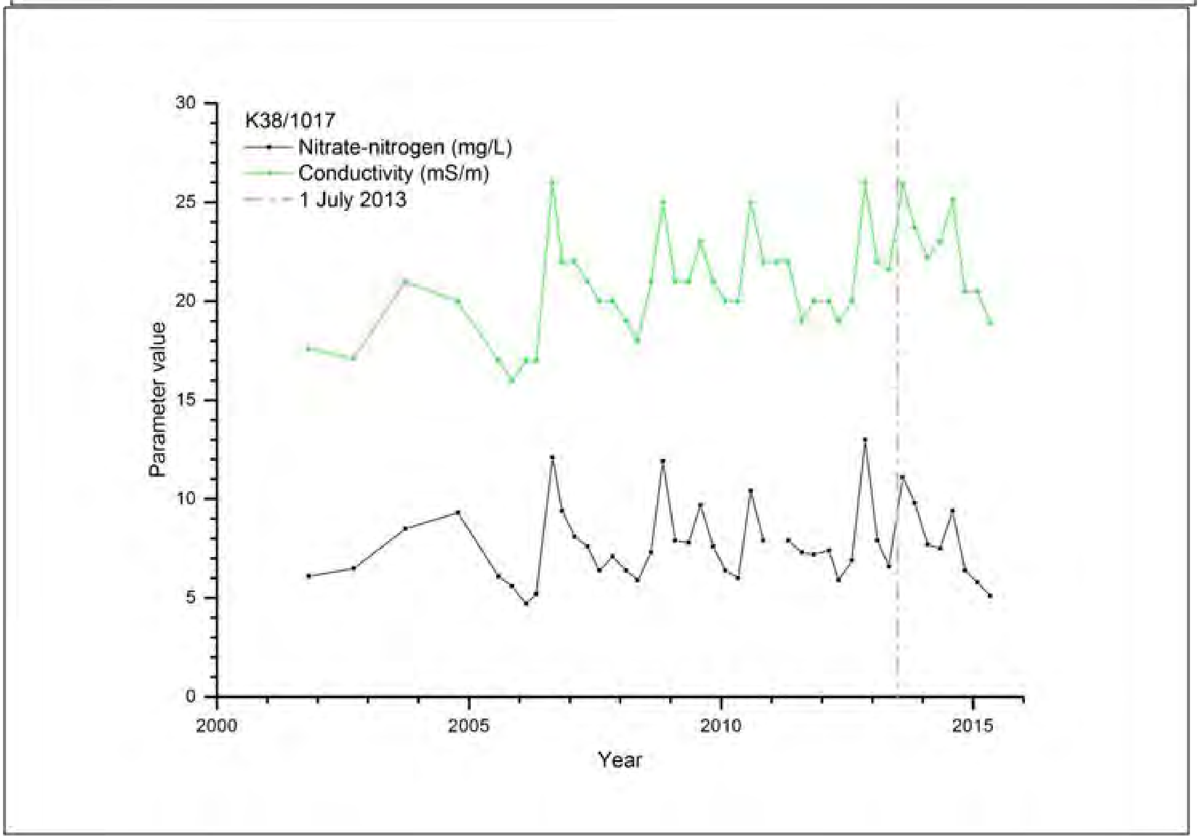
K38/1017
Nitrate-nitrogen (mg/L)
Conductivity (mS/m)
1 July 2013
Parameter value
Year
0
5
10
15
20
25
30
2000
2005
2010
2015

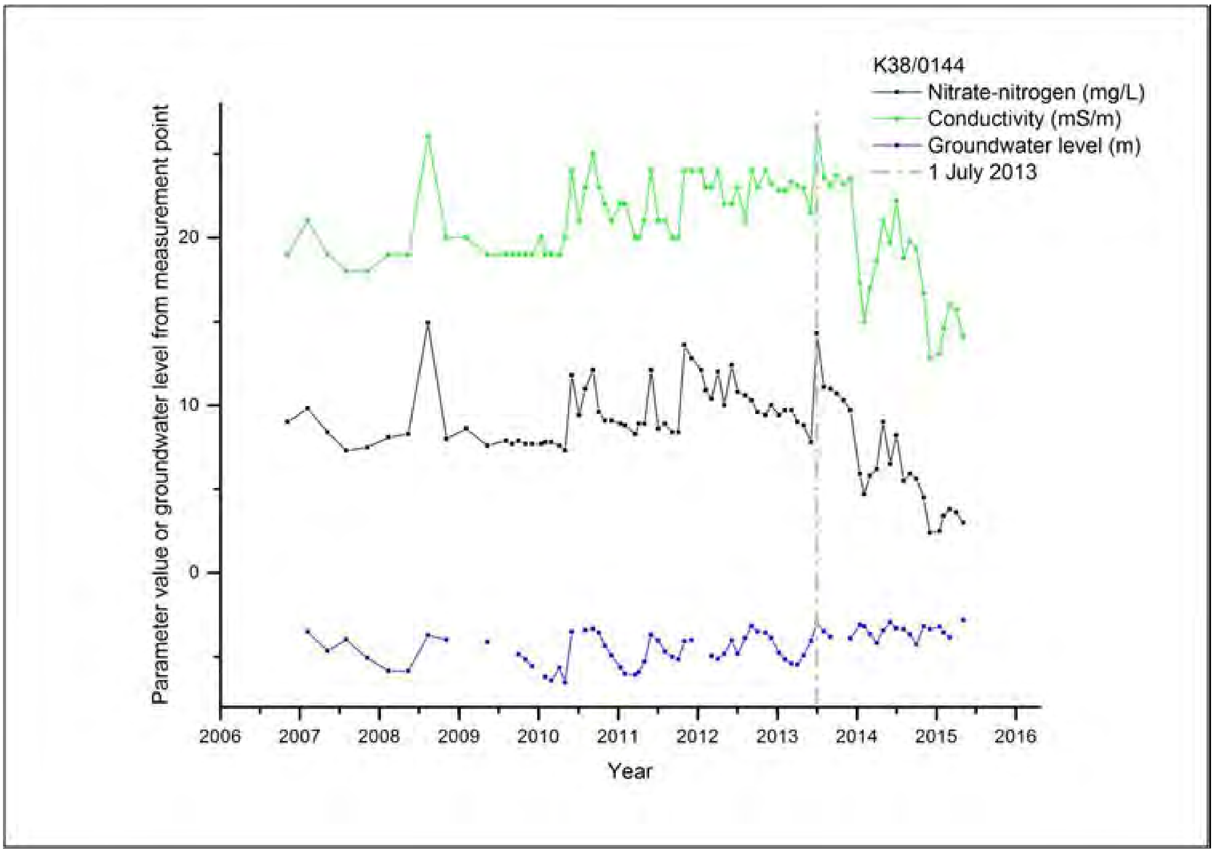
K38/0144
Nitrate-nitrogen (mg/L)
Conductivity (mS/m)
Groundwater level (m)
1 July 2013
Parameter value or groundwater level from measurement point
20
10
0
2006
2007
2008
2009
2010
2011
2012
2013
2014
2015
2016
Year

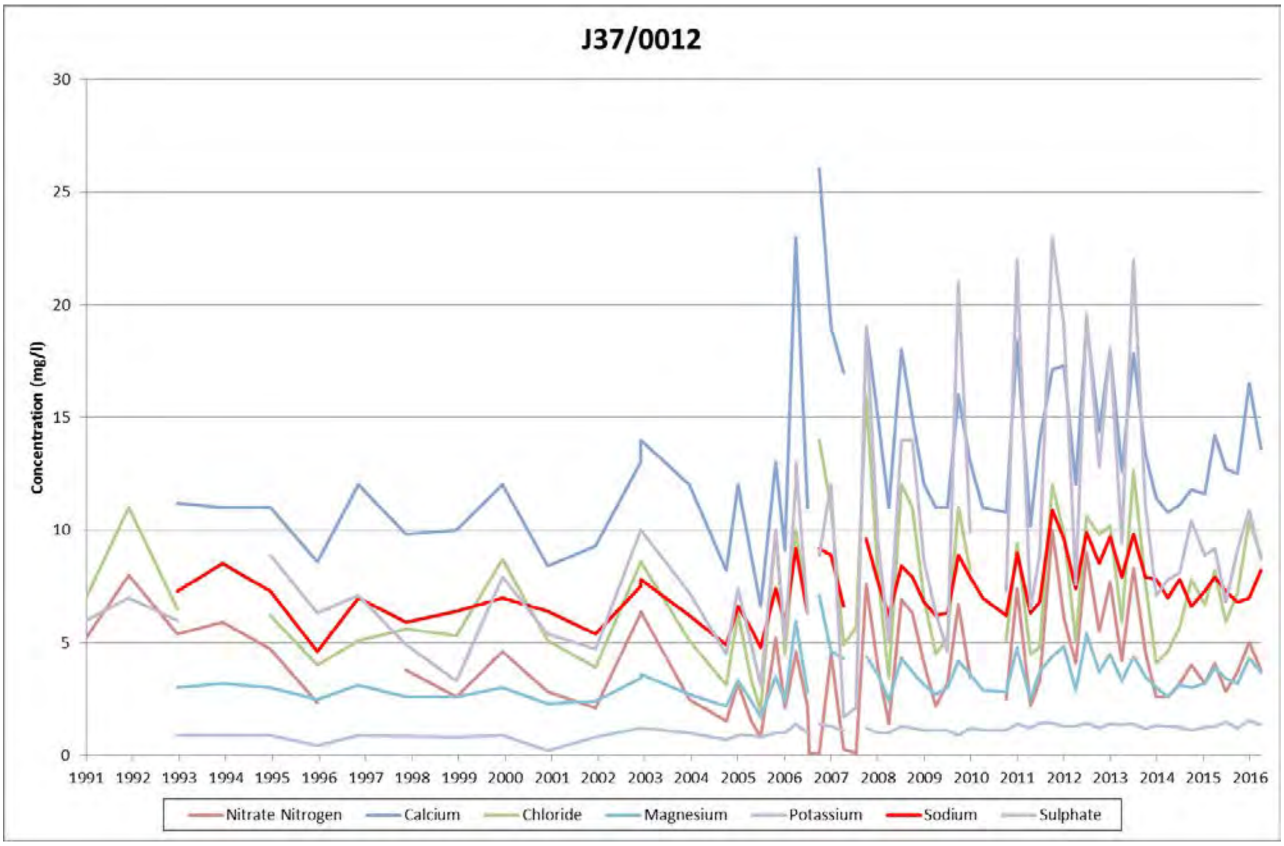
J37/0012
Concentration (mg/l)
30
25
20
15
10
5
0
1991 1992 1993 1994 1995 1996 1997 1998 1999 2000 2001 2002 2003 2004 2005 2006 2007 2008 2009 2010 2011 2012 2013 2014 2015 2016
Nitrate Nitrogen
Calcium
Chloride
Magnesium
Potassium
Sodium
Sulphate

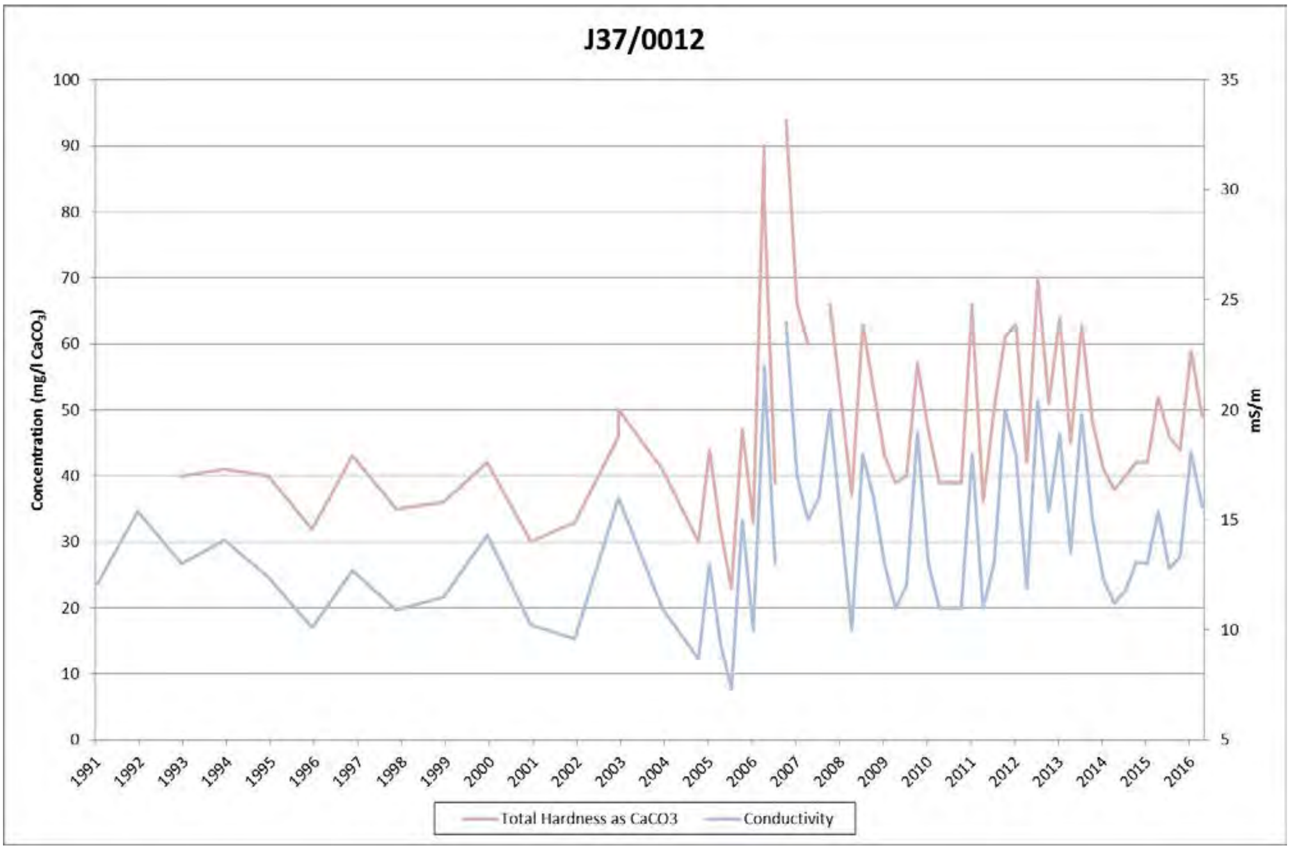
J37/0012
Concentration (mg/l CaCO3)
100
90
80
70
60
50
40
30
20
10
0
mS/m
35
30
25
20
15
10
5
1991 1992 1993 1994 1995 1996 1997 1998 1999 2000 2001 2002 2003 2004 2005 2006 2007 2008 2009 2010 2011 2012 2013 2014 2015 2016
Total Hardness as CaCO3
Conductivity

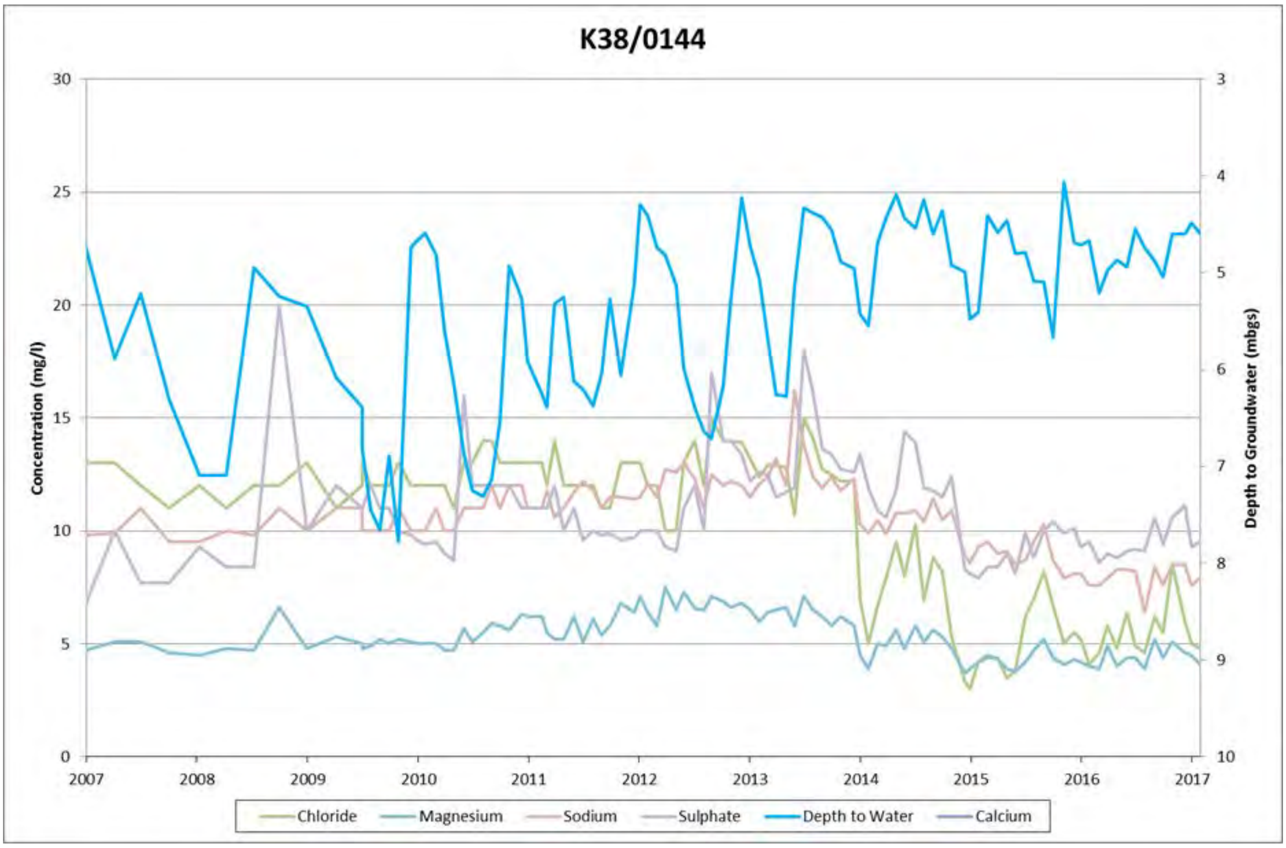
K38/0144
Concentration (mg/l)
Depth to Groundwater (mbgs)
30
25
20
15
10
5
0
3
4
5
6
7
8
9
10
2007
2008
2009
2010
2011
2012
2013
2014
2015
2016
2017
Chloride
Magnesium
Sodium
Sulphate
Depth to Water
Calcium

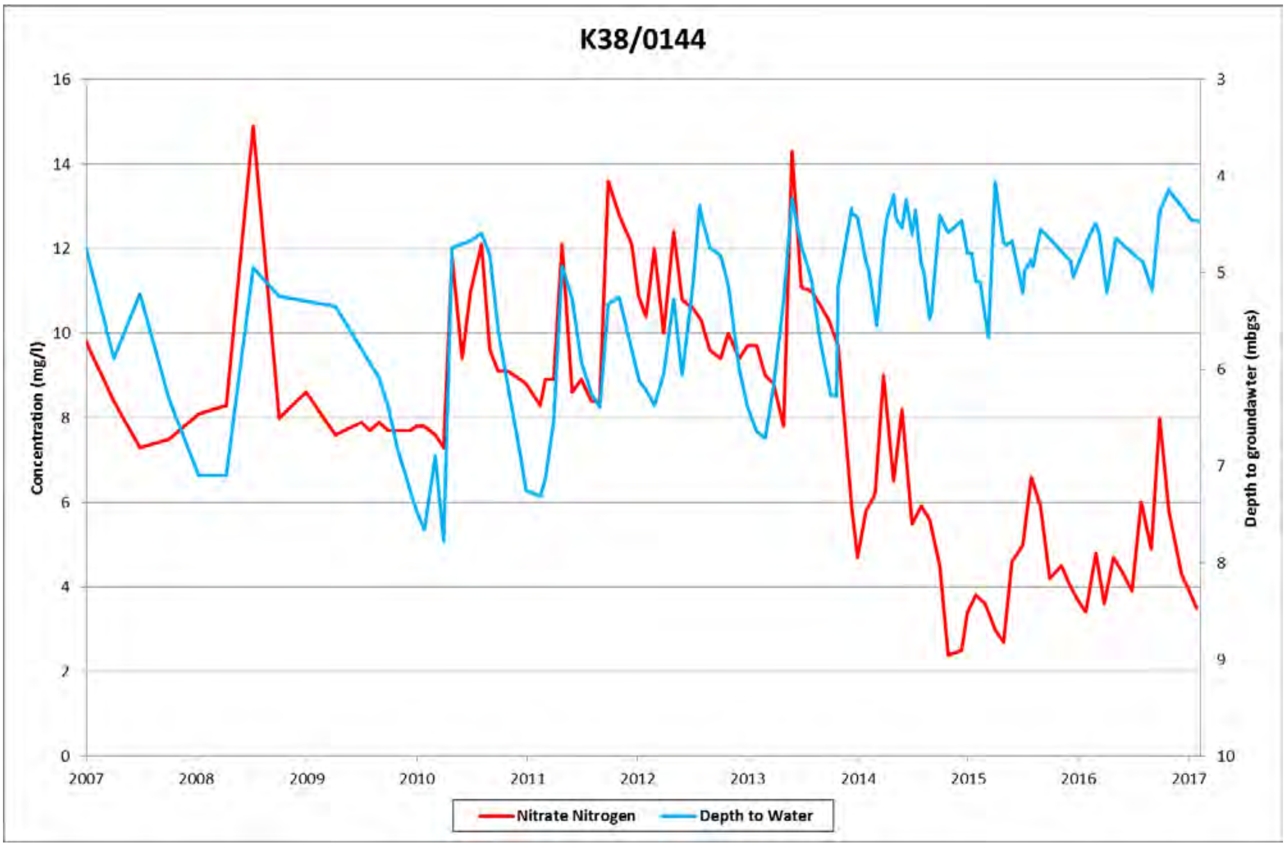
K38/0144
Concentration (mg/l)
Depth to groundawter (mbgs)
16
14
12
10
8
6
4
2
0
3
4
5
6
7
8
9
10
2007
2008
2009
2010
2011
2012
2013
2014
2015
2016
2017
Nitrate Nitrogen
Depth to Water

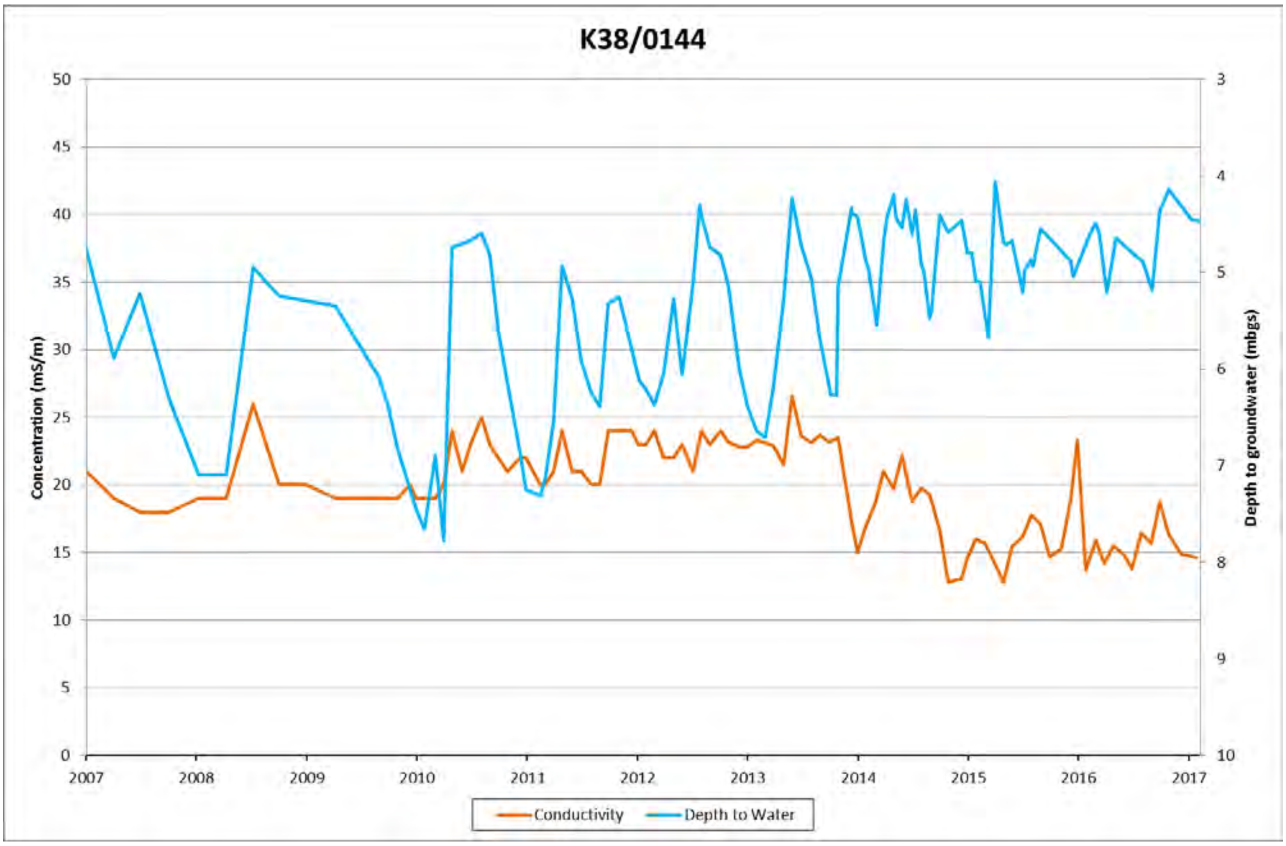
K38/0144
Concentration (mS/m)
Depth to groundwater (mbgs)
Conductivity
Depth to Water

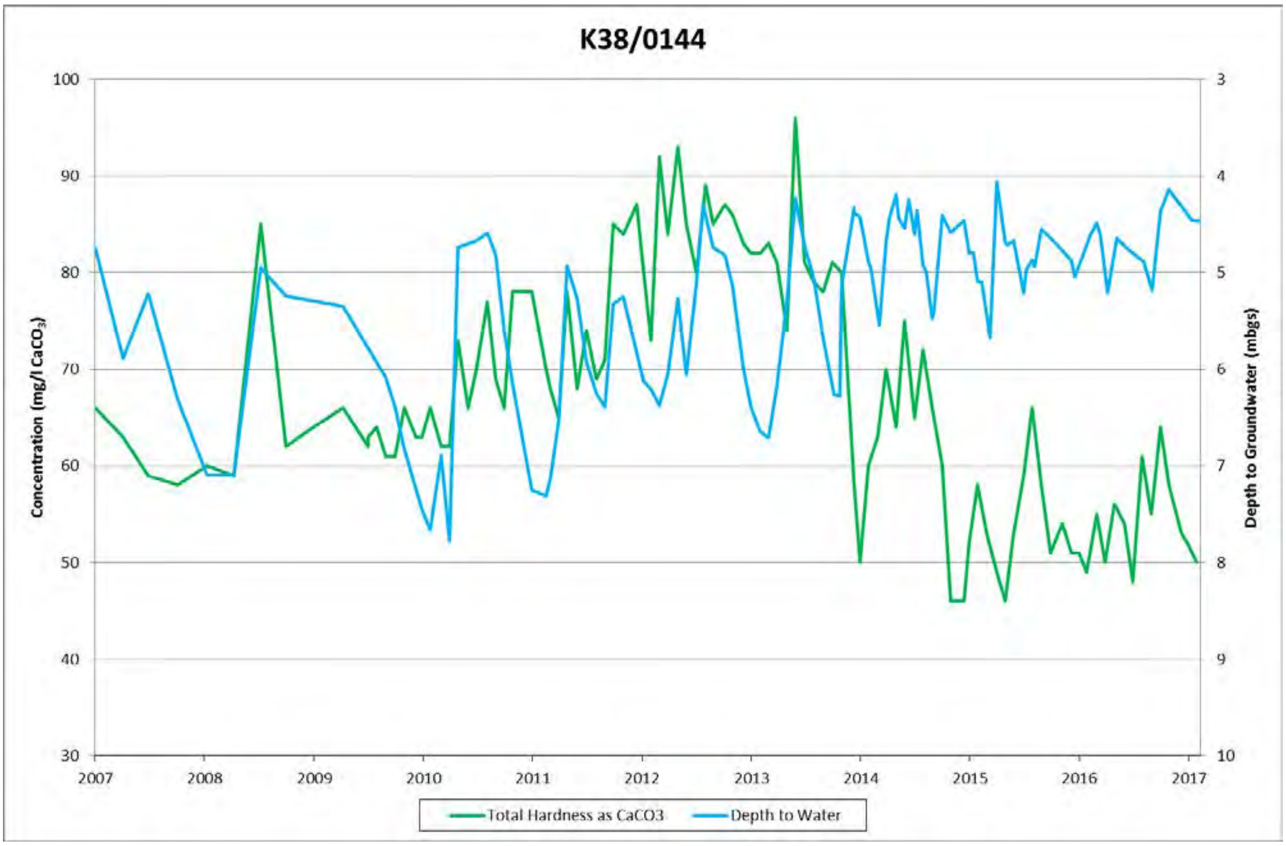
K38/0144
Concentration (mg/l CaCO3)
Depth to Groundwater (mbgs)
Total Hardness as CaCO3
Depth to Water

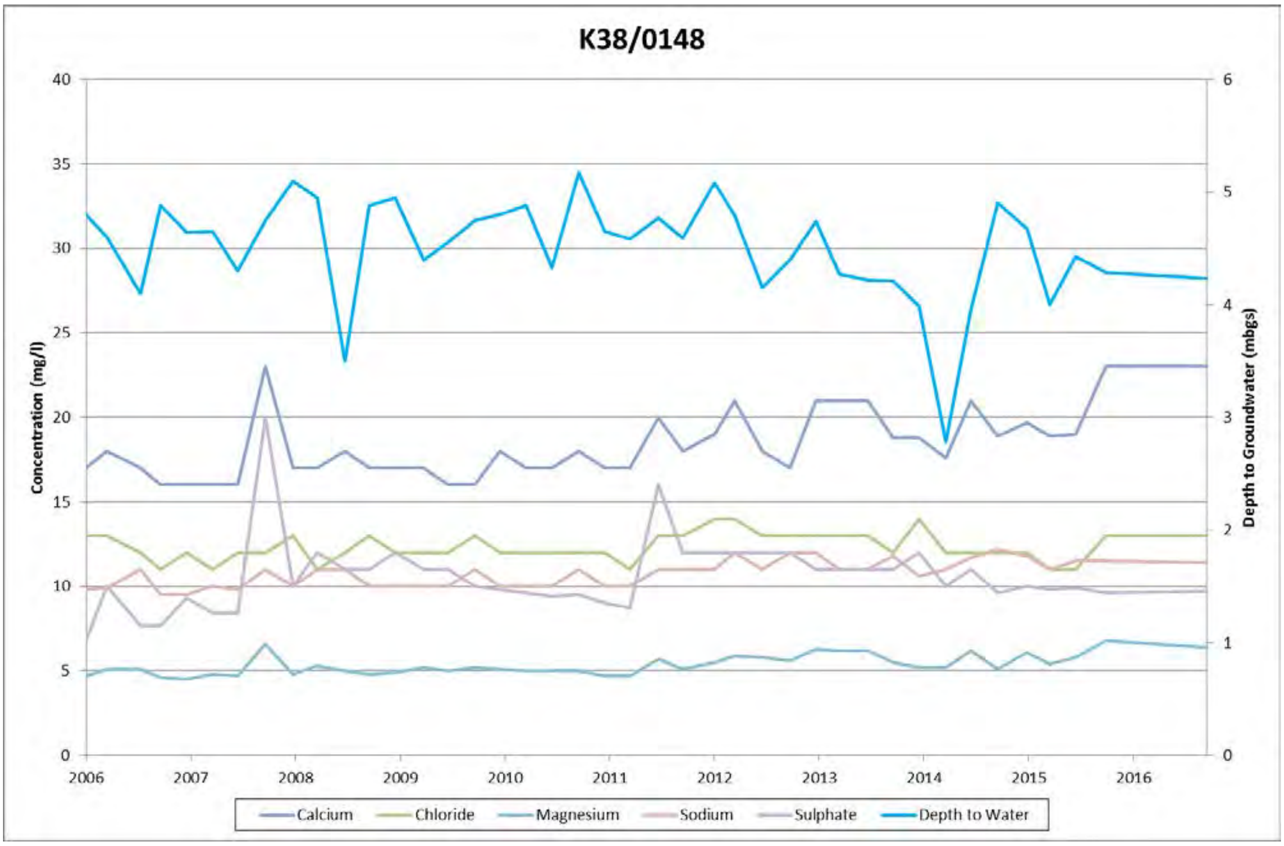
K38/0148
Concentration (mg/l)
Depth to Groundwater (mbgs)
0
5
10
15
20
25
30
35
40
0
1
2
3
4
5
6
2006
2007
2008
2009
2010
2011
2012
2013
2014
2015
2016
Calcium
Chloride
Magnesium
Sodium
Sulphate
Depth to Water

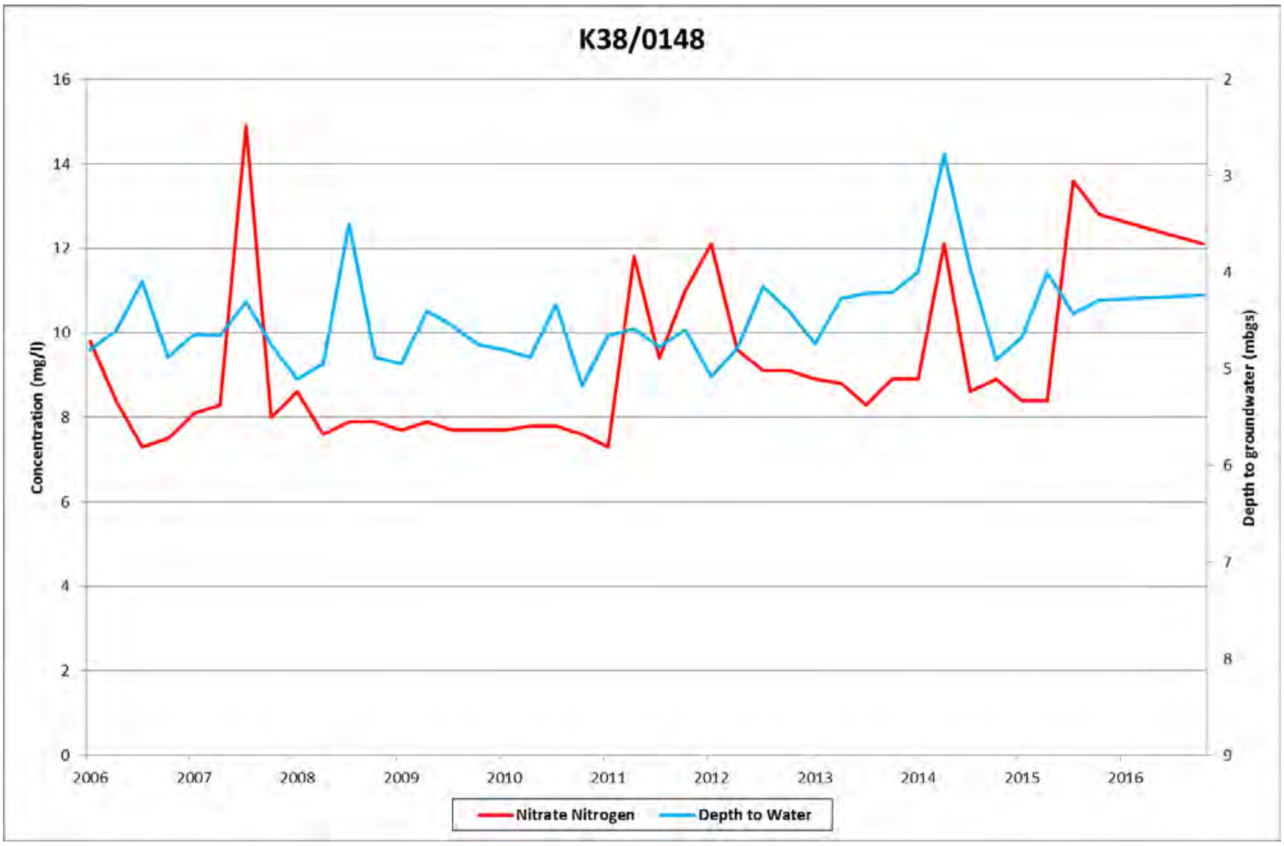
K38/0148
Concentration (mg/l)
Depth to groundwater (mbgs)
0
2
4
6
8
10
12
14
16
2
3
4
5
6
7
8
9
2006
2007
2008
2009
2010
2011
2012
2013
2014
2015
2016
Nitrate Nitrogen
Depth to Water

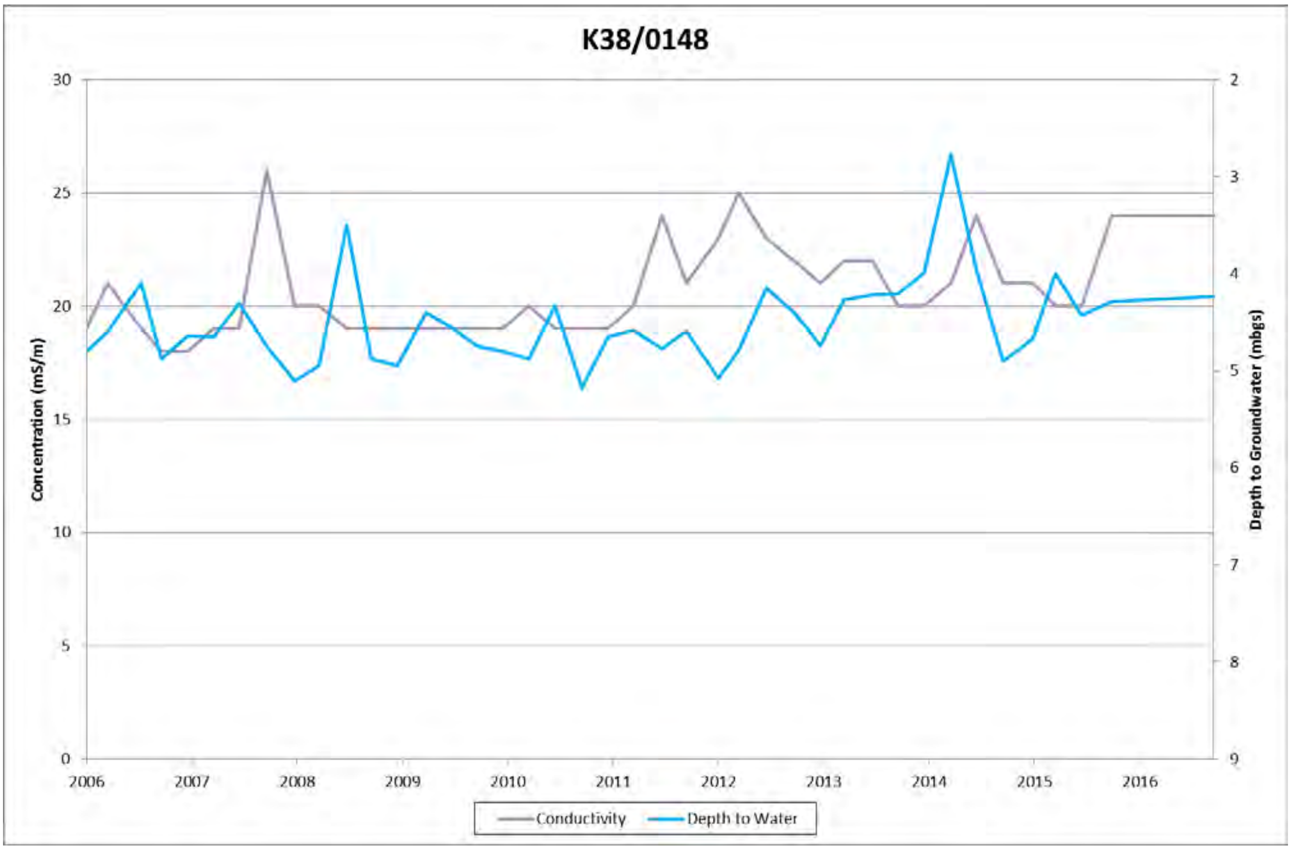
K38/0148
30
25
20
15
10
5
0
Concentration (mS/m)
2
3
4
5
6
7
8
9
Depth to Groundwater (mbgs)
2006
2007
2008
2009
2010
2011
2012
2013
2014
2015
2016
Conductivity
Depth to Water

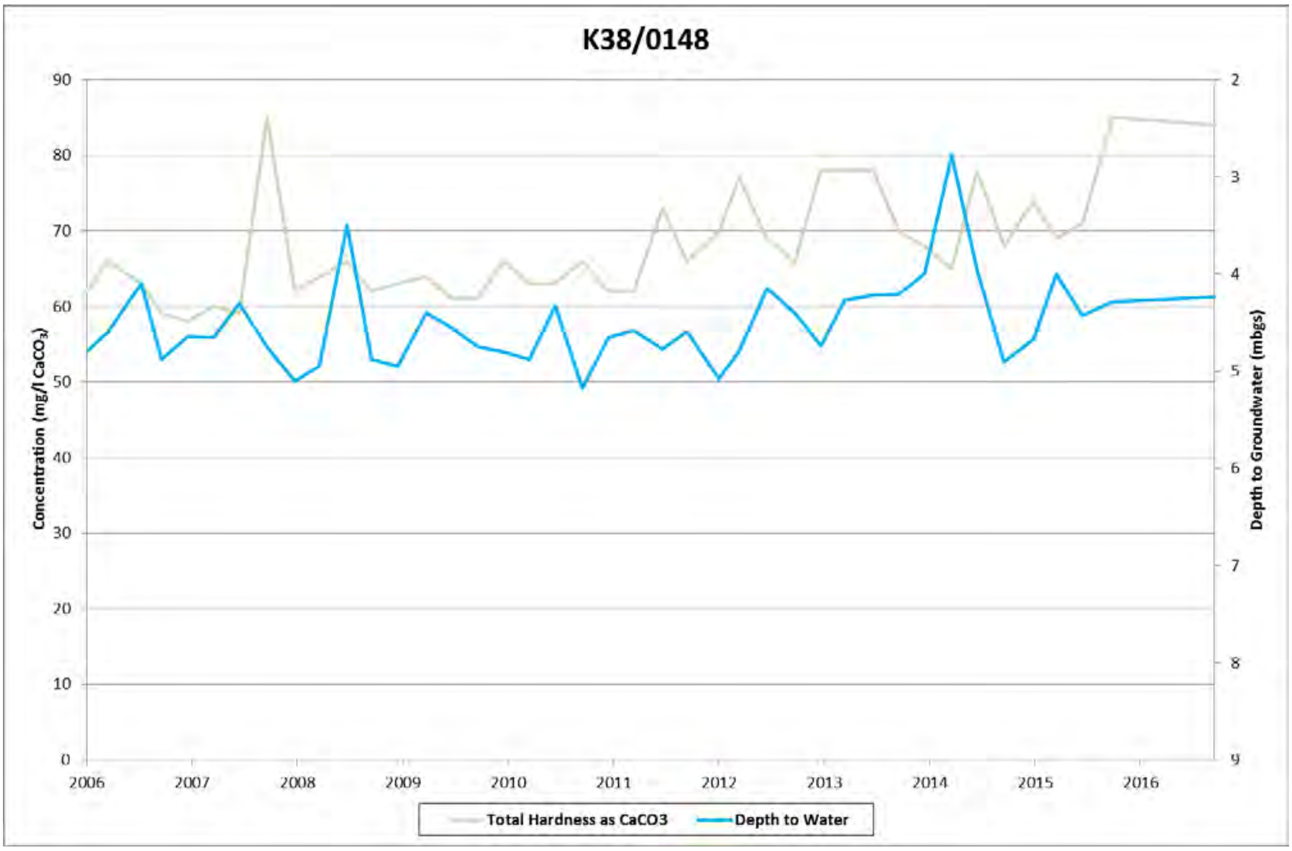
K38/0148
90
80
70
60
50
40
30
20
10
0
Concentration (mg/l $CaCO_3$)
2
3
4
5
6
7
8
9
Depth to Groundwater (mbgs)
2006
2007
2008
2009
2010
2011
2012
2013
2014
2015
2016
Total Hardness as CaCO3
Depth to Water

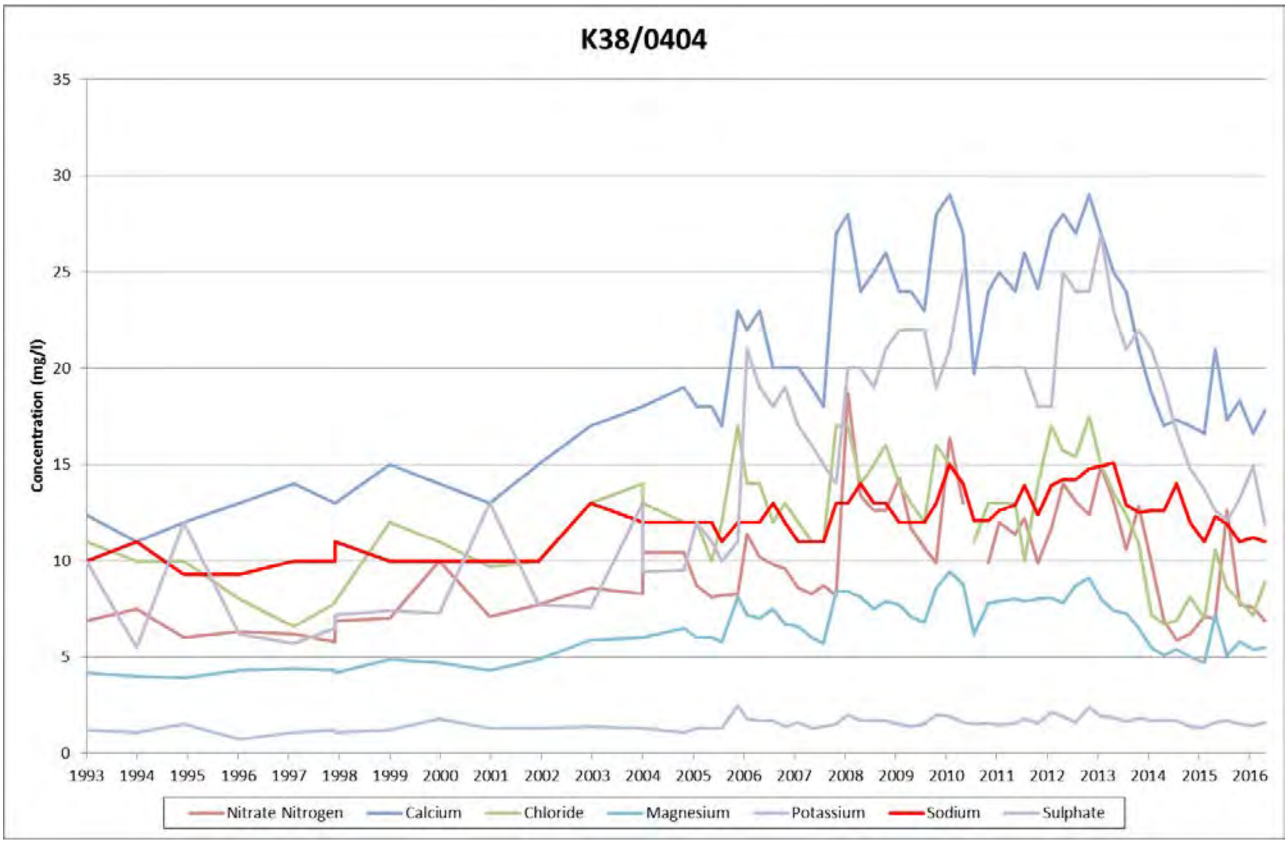
K38/0404
Concentration (mg/l)
35
30
25
20
15
10
5
0
1993 1994 1995 1996 1997 1998 1999 2000 2001 2002 2003 2004 2005 2006 2007 2008 2009 2010 2011 2012 2013 2014 2015 2016
Nitrate Nitrogen
Calcium
Chloride
Magnesium
Potassium
Sodium
Sulphate

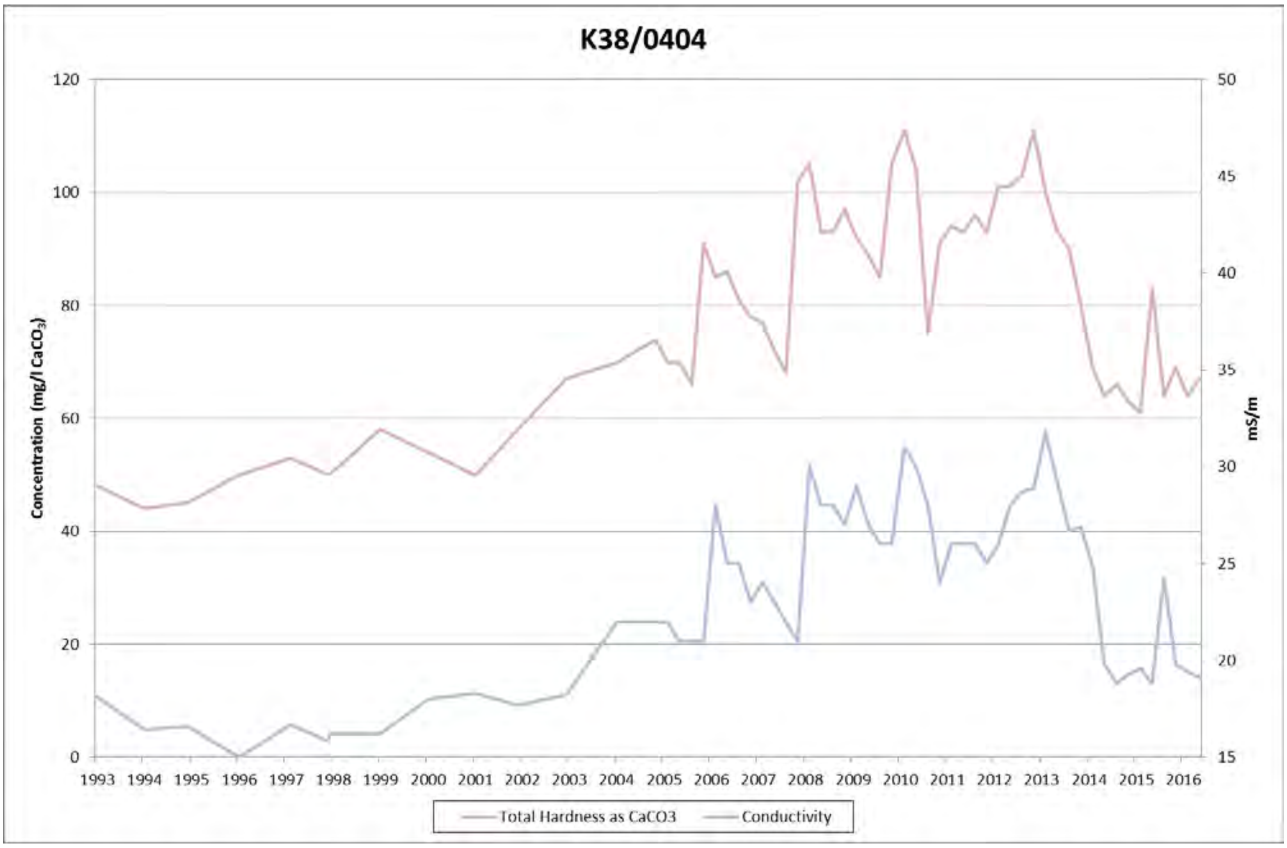
K38/0404
Concentration (mg/l CaCO3)
120
100
80
60
40
20
0
mS/m
50
45
40
35
30
25
20
15
1993 1994 1995 1996 1997 1998 1999 2000 2001 2002 2003 2004 2005 2006 2007 2008 2009 2010 2011 2012 2013 2014 2015 2016
Total Hardness as CaCO3
Conductivity

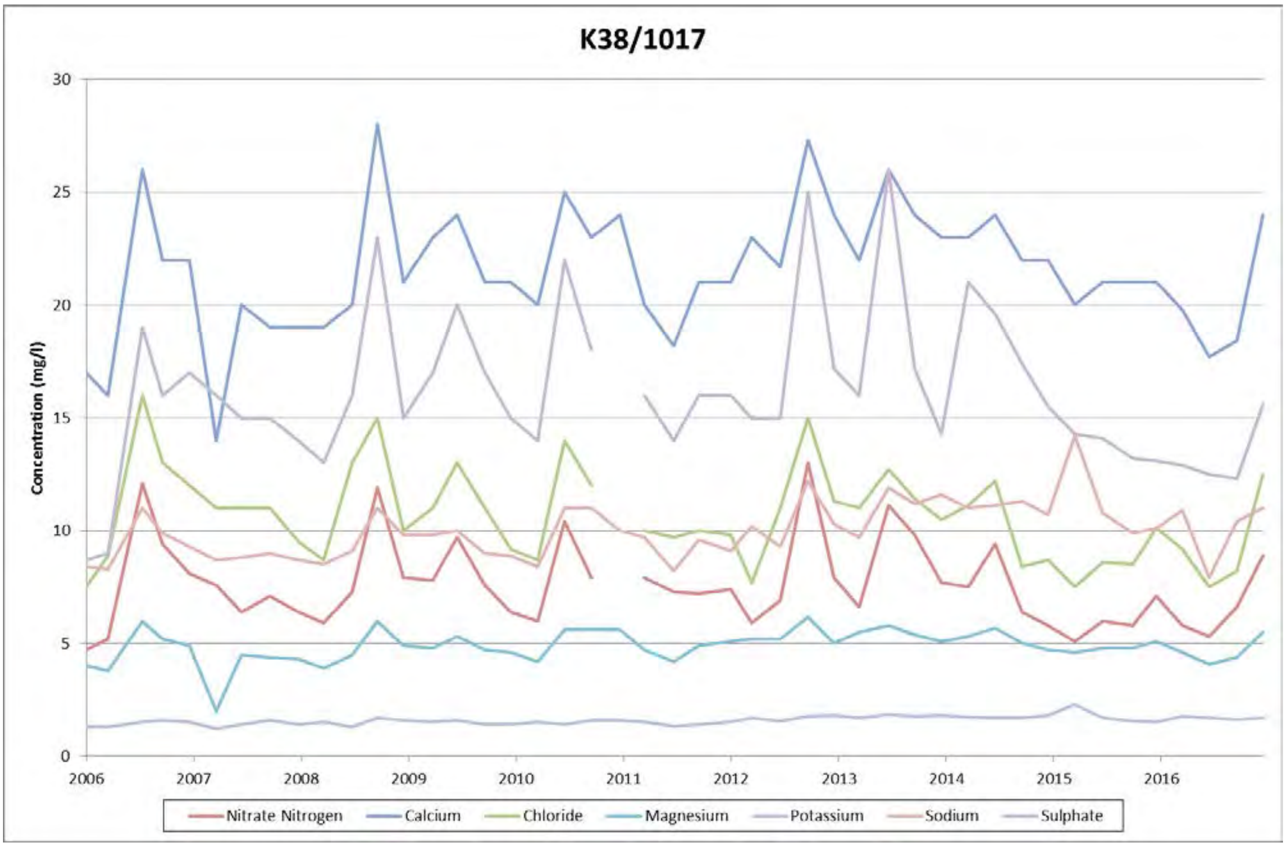
K38/1017
Concentration (mg/l)
30
25
20
15
10
5
0
2006
2007
2008
2009
2010
2011
2012
2013
2014
2015
2016
Nitrate Nitrogen
Calcium
Chloride
Magnesium
Potassium
Sodium
Sulphate

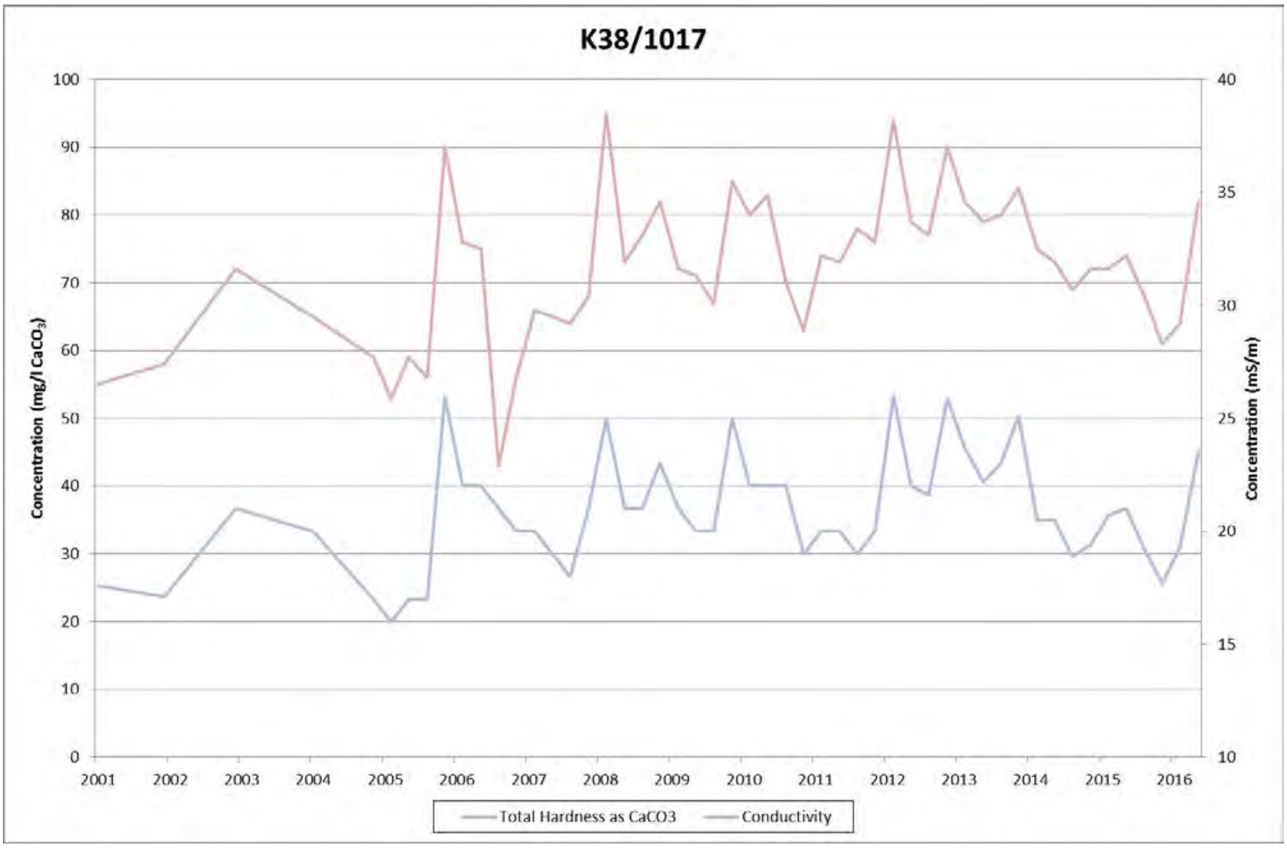
K38/1017
Concentration (mg/l CaCO3)
Concentration (mS/m)
100
90
80
70
60
50
40
30
20
10
0
40
35
30
25
20
15
10
2001
2002
2003
2004
2005
2006
2007
2008
2009
2010
2011
2012
2013
2014
2015
2016
Total Hardness as CaCO3
Conductivity

Appendix C: MIKE SHE recharge modelling

C.1 Introduction

We developed the Rangitata South model based on a partially completed MIKE SHE model of the Orari plains, which Environment Canterbury is constructing to support the coming sub-regional chapter of the Land and Water Regional Plan focusing on the Orari-Opihi and Pareora sub-region. We chose MIKE SHE to model groundwater recharge for this project because it provides us with a physically realistic representation of plant water uptake and unsaturated zone process. Environment Canterbury is currently preparing a report on the MIKE SHE model. However, components utilised in the construction of the model used in this investigation are detailed in this appendix. We utilised the MIKE SHE software to calculate a unified land surface recharge (LSR) input and evapotranspiration output from groundwater for use in the MODFLOW model described in Appendix C.

C.2 Construction of recharge layer for input into MODFLOW

Saturated zone (groundwater) recharge consists of both river infiltration and land surface recharge. Because for our MODFLOW model we were letting the model decide inputs to and from rivers, we are only concerned with calculating the water infiltrating through the unsaturated zone using MIKE SHE. MIKE SHE unsaturated flow and recharge output is saved in a file called ‘Model_Name_2DUZ_ALL cells.DFS2’. The required data is in a drop down menu and called ‘exchange between UZ and SZ (pos. up)’. In this file, if the water moves upward (from the SZ to UZ) the sign is positive. When the recharge occurs, the sign is negative. We multiplied the resulting grid file by negative one to convert recharge into positive values and then used MIKE SHE’s statistics tool to calculate average daily recharge in metres.

In MIKE SHE, ET from the saturated zone is included in the same file as a recharge. We have used the combined recharge and ET layer and therefore have not had to consider it in our MODFLOW model. This means our recharge layer contains some negative values in areas of very shallow groundwater, representative of evaporation from soil surface and transpiration from the root zone.

To enable our MODFLOW model to capture groundwater extraction without explicitly modelling it we extracted a layer of calculated groundwater abstraction from MIKE SHE, converted the gridded values into units of negative recharge depth in m/d and added these values to the recharge layer. Before determining that this would work successfully, several iterations of the MODFLOW model were constructed and assessed that did explicitly model groundwater extraction separately from recharge. Whilst results were not identical, they were all within one standard deviation of the target head, and added little value in terms of assessment of the RSIS pond losses.

We finally converted the completed gridded recharge layer into gridded 250 m polygons for input into MODFLOW (Figure C-1) to ensure consistency in recharge placement on the MODFLOW model grid.

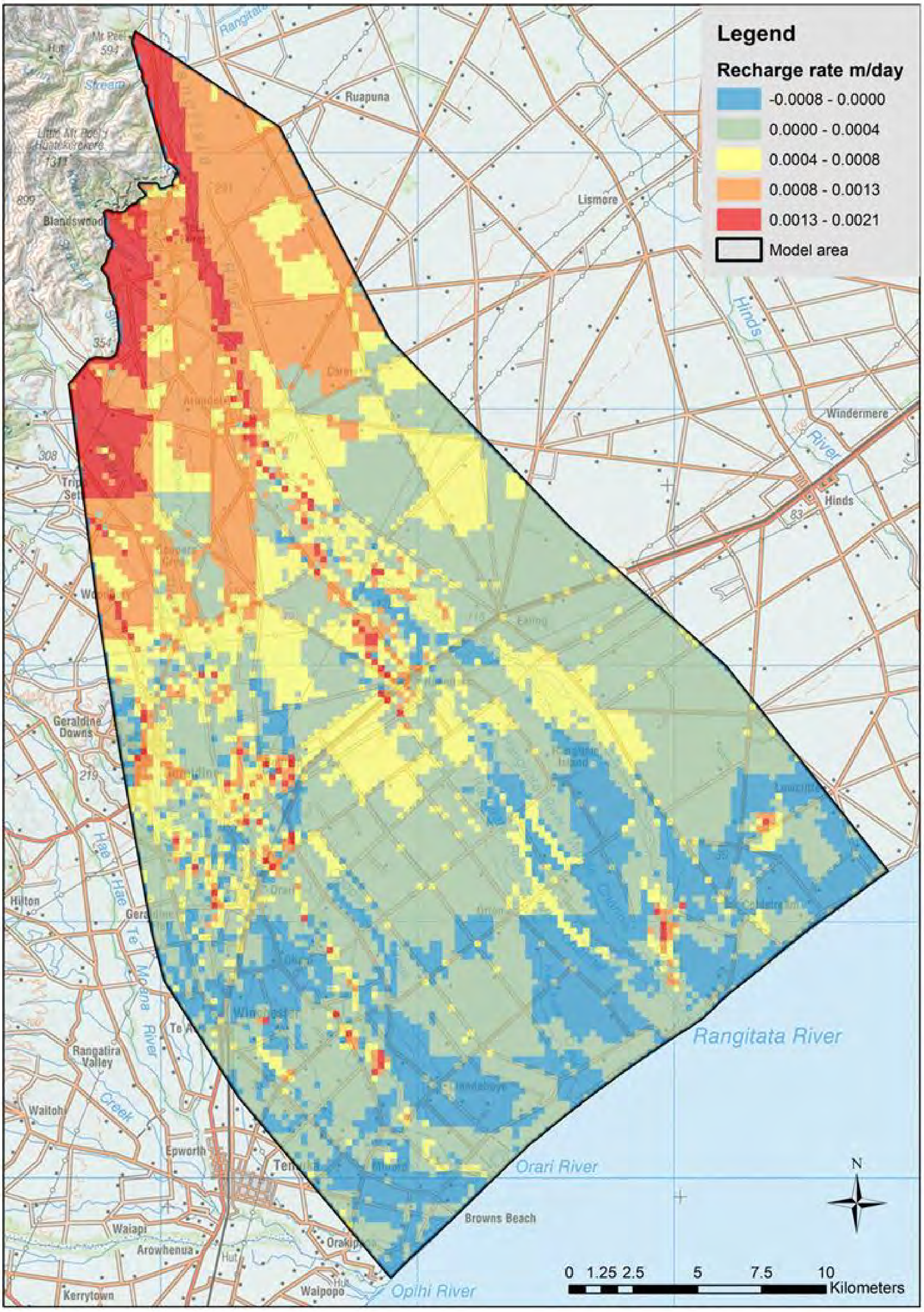

Figure C-1: Recharge map produced using MIKE SHE for input into MODFLOW

C.3 MIKE SHE

To model LSR to groundwater we utilised the following components of MIKE SHE (Figure C-2):

- **Climate (ET) model**: inputs to the model are NIWA's Virtual Climate Station (VCS) precipitation and evapotranspiration. The model links to the unsaturated zone model. The outputs are the quantity and timing of water that enters and exits from the unsaturated zone model, or the quantity of water delivered to the overland flow model.
- **Unsaturated zone (UZ) model**, which simulates the infiltration of water into the soil profile and is directly coupled to the evapotranspiration model. Infiltration is dependent on topography, land use and irrigation and is affected by the evapotranspiration model. Inputs to the UZ model are the outputs from the climate ET model and any ponding from the overland flow model. Outputs are water infiltrated into the saturated zone model and evapotranspiration into the climate model.
- **Overland flow (OL) model**, which models rainfall runoff and interaction with the surface water model. This is directly linked to the ET model and is affected by both topography and the ability of water to infiltrate and evaporate. Inputs are precipitation, evapotranspiration from the climate model, river flooding and irrigation returns, and upwelling from the saturated zone model when the water table is at the land surface accounting for groundwater within tha capillary fringe. Outputs are overland flow, which may infiltrate via the unsaturated model or transfer to the nearest river model. Alternatively, the water may directly infiltrate into the saturated zone model.
- **River model (surface-water model) created using the DHI model software MIKE 11**. This model was built to remove surface flow from the model and prevent it from infiltrating as LSR. MIKE 11 is a one-dimensional dynamic model which describes the flows and levels in rivers and floodplains through a series of interconnected channels.
- **Saturated zone (SZ) model** coupled with the unsaturated zone model and river model. Inputs are recharge from the river and unsaturated zone models and infiltration for the overland flow model that bypasses the unsaturated zone model. Outputs are flow that exits the model, discharge to the river and/or the overland flow model and evapotranspiration to the climate model.

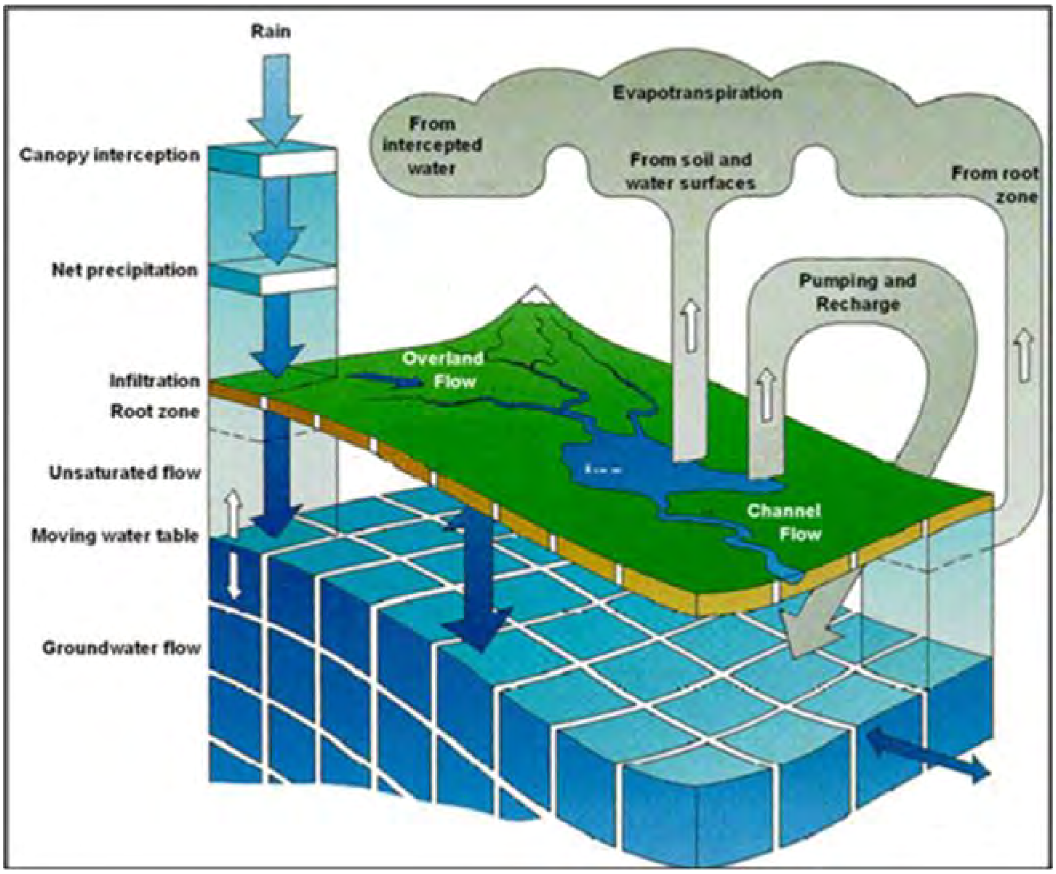

Figure C-2: Schematic of MIKE SHE model components and interactions

C.4 Model domain and spatial discretisation

Model domain is a term that describes the area the model covers, in which model calculations are performed on a model grid. Spatial discretisation refers to the mapping of the physiographic features in the model domain onto the model grid. MIKE SHE uses a conceptual model build approach where shape files and grids can be used to define the physical environment inside the modelling software. The software then uses a process called pre-processing to map these data to the model grid.

The model domain has been extended beyond the study area to capture the physical interactions that influence it and to limit the effects of model boundary conditions on the area of interest. In hydrological modelling studies, the flow system is usually enclosed by a boundary that corresponds to identifiable hydrological features at which some characteristic of surface or groundwater flow is easily described. Some examples of this are a body of surface water, an almost impermeable surface, a coastal boundary, a groundwater flow divide or a water table. At these boundaries the water level can be fixed at a certain elevation; the boundaries can provide a source of flux of water, they can be boundaries across which no water flows, or they can represent a combination of these. Each of these boundary types has an effect on the computation cells immediately adjacent to them and standard modelling practice places them as far as possible from key model areas.

There is considerable variability in the physiography and hydrology of the catchment, i.e. variable soils; topography; geology; climate; and land use. Another large source of heterogeneity in the study area is irrigation. Irrigation in the area varies by source (surface or groundwater), application type (pivot, rotorainer, gun) and demand. We assumed that 250 m grid resolution would capture sufficient variability within the study area without placing a detrimental burden on the available computing resources.

C.5 Model time-steps

MIKE SHE models use adaptive time-steps which are adjusted to reflect temporal or spatial hydrological changes such as high intensity rainfall or rapid changes in stream water levels and flows. Essentially in MIKE SHE every time step is considered a stress period. The time-steps are automatically reduced or increased to maintain numerical stability and computational efficiency without introducing water balance errors. In MIKE SHE, the automatic time-step control requires only the specification of a maximum allowed computational time-step for each hydrological process component.

Table C-1 presents the maximum time-step allowed for each model component that was able to produce stable model runs with the shortest simulation times. If any of these controls are exceeded then all the time-steps are adjusted in unison, except for MIKE 11. This means that if one time-step needs to be halved, then all the time-steps are halved. The MIKE 11 (river model), manages time steps separately.

Table C-1: Time-steps controls implemented in the MIKE SHE model

Maximum allowed time-step		Parameters for precipitation dependent time-step control	Value
Overland flow	2 Hours	Maximum precipitation per time-step	10 mm
Unsaturated zone model	2 Hours	Maximum infiltration per time-step	30 mm
MIKE 11 (river model) time-steps	2 Minutes		
Saturated zone model	2 Hours	Input precipitation rate requiring its own time-step	10 mm/hr

C.6 Climate model

NIWA provides a VCS dataset of synthetic daily rainfall and potential evaporation on an approximately 5 km grid covering all of New Zealand. The estimates are produced from the spatial interpolation of actual data observations made at climate stations and extend as far back as 1972 (NIWA, 2012).

In developing the Rangitata South model recharge layer, we extracted daily precipitation and potential evapotranspiration data from the NIWA VCS dataset (NIWA, 2012) for a period of 30 years (between 1984 and 2014)

C.6.1 MIKE SHE climate input

VCS network provides precipitation and potential evapotranspiration data at a fine resolution (5 km). A limitation of the data is that the values at each of the VCS stations are an extrapolation from a limited sample of input data (weather stations) that are not evenly distributed across the study area. MIKE SHE requires polygonal inputs with each polygon linked to a time series file of either precipitation or evapotranspiration. We drew Thiessen polygons around each VCS to define its area of influence and assigned the corresponding station to that polygon for input into MIKE SHE.

C.7 Unsaturated zone

The UZ model plays a central role in MIKE SHE simulations. It links the processes taking place at the land surface to those happening in the groundwater system. The model is essential for the calculation of:

- evaporation from land surface
- transpiration from plants
- overland runoff
- soil moisture distribution within the soil profile
- irrigation demand
- land surface recharge to the saturated zone.

C.7.1 Unsaturated zone model

In MIKE SHE, the UZ and SZ models are explicitly coupled (i.e. they run separately but in parallel to each other) rather than implicitly coupled (where the UZ and SZ differential equations would be combined and run together). Explicit coupling of the UZ and SZ models optimises the time-steps used and allows utilisation of time-steps that are representative of the UZ (minutes to hours) and the SZ (hours to days) regimes. MIKE SHE overcomes stability problems associated with the explicit coupling of the UZ and SZ models by employing an iterative procedure that conserves mass for the entire column by considering outflows and source/sink terms in the saturated zone.

Time-series data of precipitation and potential evapotranspiration feed into the UZ model that performs a series of calculations using:

- crop properties and demand
- soil properties
- varying depth to groundwater
- unsaturated flow through the soil profile using Richards' equation (Richards, 1931).

At each UZ time-step, the amount of water available for infiltration is calculated in the following manner:

1. the amount of ponded water is added to the net rainfall at the ground surface and then the evaporation is subtracted from it
2. if the water table is below the surface, water infiltrates through the unsaturated zone model
3. if the water table is at the surface, numerically, the ponded water directly recharges the SZ model bypassing the UZ model
4. if the water table rises, numerically, above the surface, the saturated zone (SZ) discharges to ponded water and then to OL
5. transpiration from the UZ, and in some cases even from the SZ (when the roots reach and abstract the groundwater), reduces the amount of recharge.

The resulting total recharge in MIKE SHE is modelled as a flux in a length per time unit (e.g. mm/d) rather than a flow.

Unsaturated flow is calculated as moving vertically in one-dimension, and the resulting total recharge is modelled in units of length per time. Except for some rare instances (like hilly terrain), a 1D model is generally suitable, as 2D and 3D UZ flow is unlikely to be greater than the computational grid size. 1D sufficiently describes the land surface recharge to the groundwater system in the Rangitata South Irrigation Scheme area as the hill slopes are less than 15 degrees, meaning water will generally infiltrate rather than flow across the surface.

C.7.2 Topography

The MIKE SHE model requires a reasonable representation of the surface elevation as an input to form the top layer of the model. A 250 m x 250 m digital elevation model was created by resampling from a high resolution LIDAR digital elevation model (DEM) of the study area. Resampling included first aggregating to the mean elevation, then hydrological flow correction using ESRI ARC GIS. Random elevation spot checks were performed manually across the plan area to confirm the resampling produced satisfactory results.

Figure C-2 shows the DEM generated in MIKE SHE. Elevation changes are subtle throughout the majority of the study area, with the highest change occurring at the north-eastern boundary in the vicinity of the foothills.

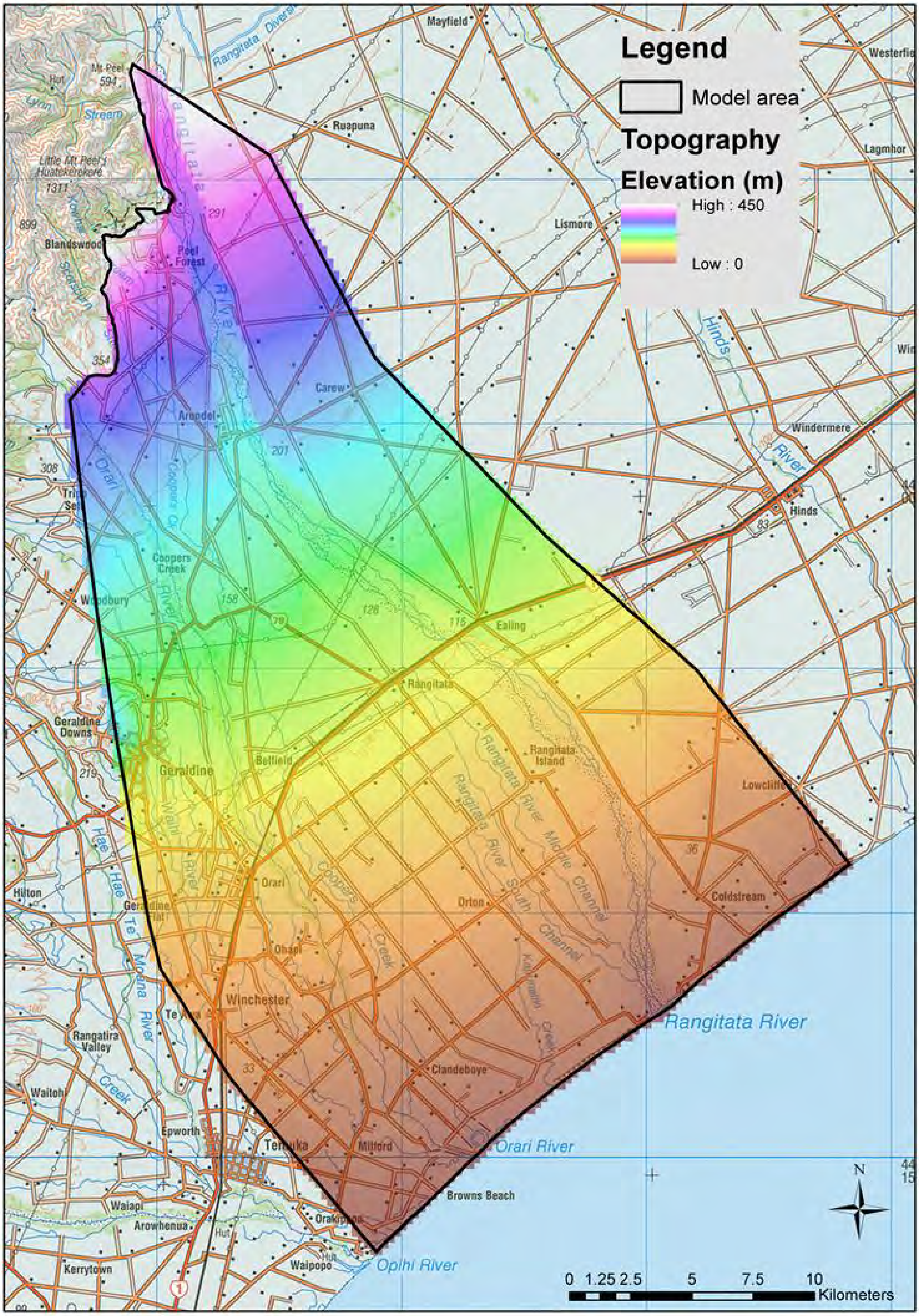

Figure C-3: **Digital elevation model used in MIKE SHE**

C.7.3 Soils

In MIKE SHE, the term 'soil' refers to the geological material that makes up the entire unsaturated zone. It includes the soil profile that soil scientists are generally concerned with (the weathered material at the ground surface where plant roots are active) as well as the vadose zone material beneath the soil, extending downward to the water table. Soil spatial distribution, vertical distribution and the soil physical characteristics are needed to accurately model the unsaturated zone.

In developing the soil profiles in the MIKE SHE model, the primary source of soil information was from Landcare Research. The data from Landcare Research was obtained by using S-map Online[4]. Soil physical parameters were supplied by AgResearch and are detailed in Lilburne *et al.* (2012). S-map Online is a web-based interactive map viewer with soil factsheets. Environment Canterbury holds a GIS copy of the latest S-maps, which we used in the spatial discretisation of the soils. The factsheets contain average physical properties for a specific soil and their vertical distributions to a depth of one metre; below one metre, we have modelled the soil as sandy gravel material. Relevant main physical properties of soils described in the factsheet are:

- soil horizons
- soil depths
- soil textures
- a qualitative description of its profile available water
- drainage class
- bulk density
- leaching vulnerability and drought vulnerability.

Details from the soil factsheets have been supplemented with information in Lilburne *et al.* (2012), Webb and Lilburne (2011) and inputs to IRAP FARM-SIM (Webb, T.H., 2003; Webb, T.H., *et al.*, 2000; Cichota, *et al*., 2013a; Cichota, *et al.,* 2013b).

Spatial distribution and discretisation
An ArcGIS shapefile map of S-map was extracted from Environment Canterbury's GIS databases as the input map into MIKE SHE (Figure C-3). We then simplified the map by grouping the soils into five categories based on soil drainage rates and profile available water (PAW) (Table C-2).

Table C-2: Soil types

Soil type and SMAP series	Environment Canterbury soil classification	Average PAW	Maximum drainage class[5]	Minimum drainage class
Heavy - Hatfield, Templeton, Wakanui; Deep Barrhill, Templeton, Wakanui; Poorly drained Flaxton	H (including Pd, Pdl and D)	165.2	w(100%)	p(100%)
Medium - Hatfield, Templeton, Wakanui moderately deep silt loam	M	123.6	w(100%)	i(70%), p(30%)
Light - Chertsey and Lismore shallow and stoney silty loam	L	97.1	w(100%)	i(60%), p(40%)
Very light - Longbeach, Waimakariri and Eyre stony silt loam, Lismore and Balmoral very stony silt loam	VL	69.2	w(100%)	w(75%), p(25%)
Extremely light - Waimakariri very stony sand	XL	47.7	w(100%)	i(100%)

[4] http://smap.landcareresearch.co.nz/
[5] w- well drained; p – poorly drained; I – imperfectly drained (details can be found in Webb and Lilburne, 2011)

Figure C-3 highlights that:

- light soils (L), with moderate to high recharge, cover the majority of the study area
- the coarsest soils (XL), with highest recharge rates, occur primarily along the braided rivers
- the finest soils (Pd, PdL, H), with the lowest recharge rates, occur near the coast.

The extent of the poorly-drained soils coincides with the extent of the historical Holocene swamp deposits located near the coast.

The lateral discretisation of the soil map (Figure C-4) has to follow the general discretisation of the model, which is 250 metres. This means every single 250 m grid cell is assigned a single type of soil based on the area weighted value.

To model recharge through these soils we used Richards' (1931) equation for UZ flow. The equation is a means of representing the movement of water in unsaturated soils. Put simply, it states: water movement in the unsaturated zone occurs due to the difference in what is called the hydraulic head, h, which is the sum of a gravitational component, z, and a pressure component, ψ, so:

$$h = z + \psi$$

The gravitational component at a point is the elevation of that point above a specified datum.

The pressure component represents the effect of the capillary forces and the adsorptive forces between the water molecules and the soil constituents. The pressure head, ψ, is always negative under unsaturated conditions.

In one dimension vertical flow, the driving force for the transport of water is the vertical gradient of the hydraulic head. If we consider Darcy's law in the unsaturated conditions:

$$q = -K(\theta)\frac{\partial h}{\partial z}$$

and the continuity equation:

$$\frac{\partial \theta}{\partial t} = \frac{\partial q}{\partial z} - S(z)$$

We obtain the governing equation for water transport in the unsaturated zone, the Richards Equation:

$$\frac{\partial \theta}{\partial t} = \frac{\partial}{\partial z}\left(K(\theta)\frac{\partial \psi}{\partial z}\right) + \frac{\partial K(\theta)}{\partial z} - S(z)$$

Where θ is the volumetric soil moisture, $K(\theta)$ is the unsaturated hydraulic conductivity and $S(z)$ is a sink term that accounts for the water that is extracted by roots in the upper part of the unsaturated zone (the root zone).

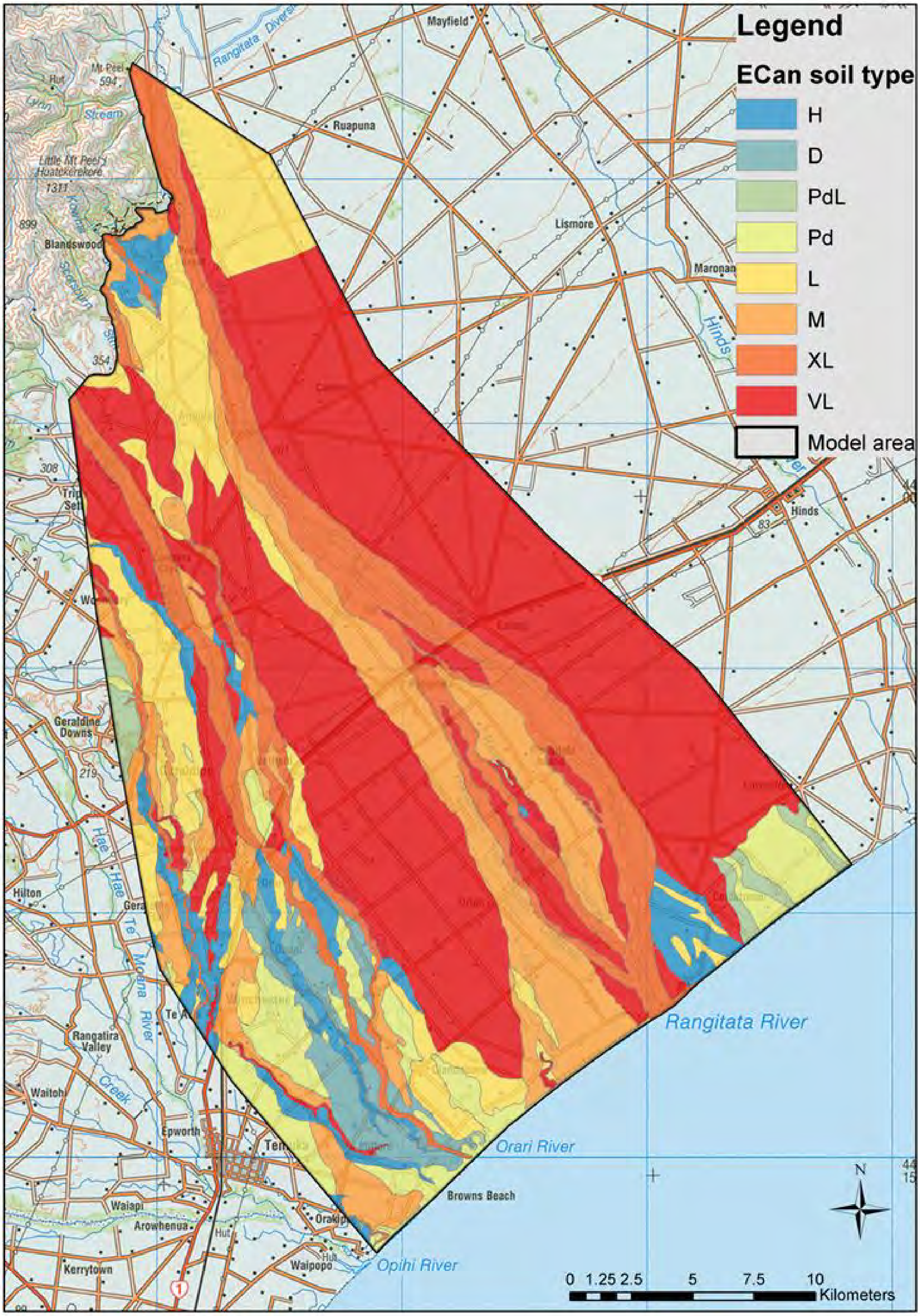

Figure C-4: S-Map soil coverage

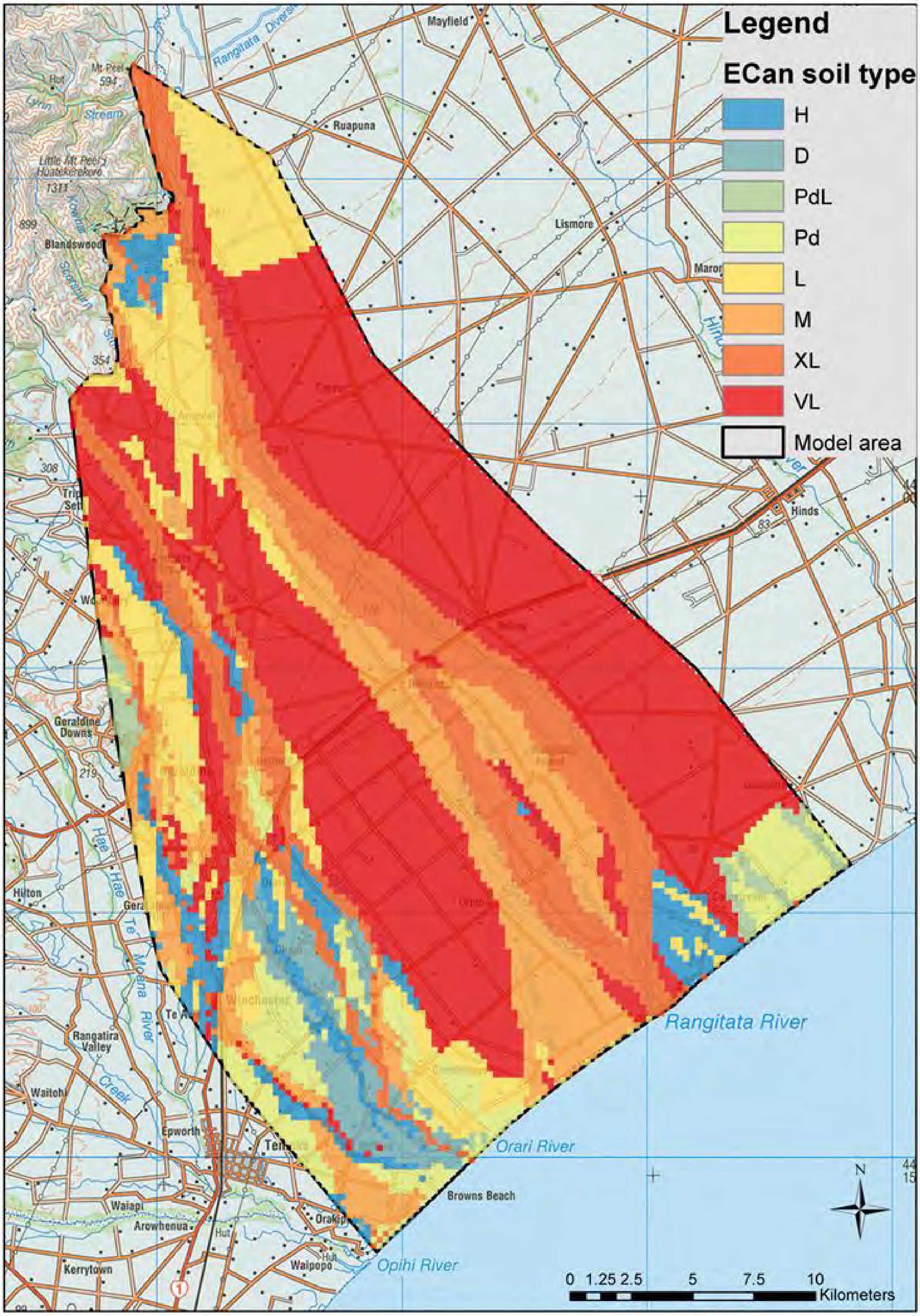

Figure C-5: Discretisation of soil data

Soil profiles and calibration of recharge

Saturated hydraulic conductivity is a fundamental parameter that controls the recharge through the soil profile. Unfortunately, this parameter is missing in the S-Map Online data, so we used it as a calibration parameter. We simplified the soils vertically to create a soil profile that allowed stable and faster model runs, whilst producing values of recharge calibrated to published values, and verified against lysimeter data.

To expedite calibration of the simplified soils we constructed a simple single cell (X and Y axis) model for each simplified soil. The saturated water content of each new soil profile was set as the average value of the different horizons that constituted the actual soil profile described in the parameters IRAP FARM-SIM (Webb, T.H., 2003; Webb, T.H., *et al.*, 2000; Cichota, Vogeler, Snow, Webb, 2013a; Cichota, Snow, Vogeler, 2013b).. In the soil profile we used the simplified soil type for the top metre and then used sandy gravel soil type (XA80 FARM-SIM soil class) for deeper soil in all models (parameters applied were from FARM-SIM and Lilburne *et al.*, 2012).

Use of the Richard's equation requires information about the relationship between the pressure head and moisture content (soil moisture retention curve) and information about the relationship between the pressure head and the unsaturated hydraulic conductivity (hydraulic conductivity curve). There are several methods of describing these relationships mathematically for use in numerical solvers. We chose to use Van Genuchten (1980) functions for both curves as they are the most widely used soil moisture-pressure-hydraulic conductivity relationships. To achieve calibration of recharge, we adjusted saturated hydraulic conductivity of each soil type so that the resultant recharge corresponded with the published recharge for each soil type based on:

- OVERSEER™ 6
- Look-up table recharge values (Lilburne *et al.,* 2010 and Lilburne *et al.,* 2014).

Finally we validated our results against Environment Canterbury held lysimeter data (Durney *et al.,* 2014).

Table C-3: Average hydraulic characteristics of the model soils

Soil class	Porosity %	Saturated hydraulic conductivity (m/sec)
Heavy/medium	35	8.00E-07
Light	28	3.00E-06
VERY Light	28	7.00E-06
Extra light	25	2.00E-05
New XA80	38	1.00E-04

We used the vertical discretisation described in Table C-4 in single cell models and ultimately in the actual Rangitata South model. We used fine cells at the top of the profile and introduced a smooth transition to coarser cells at the base. This enabled smoother and shorter runs of the unsaturated zone model.

Table C-4: Soil vertical discretisation

From depth (m)	To depth (m)	Cell height (m)	Number of cells
0	1	0.2	5
1	10	0.5	18
10	40	1	30
40	180	2	70

C.7.4 Evapotranspiration

We used the Kristensen and Jensen (1975) method for calculating actual evapotranspiration. The approach is based on:

- potential evaporation
- length of growth stage
- leaf area index
- root depth for each vegetation type
- a set of empirical parameters[6].

C.7.5 Growth stage

In MIKE SHE, the temporal variation in vegetation growth is described by a number of characteristic stages of specific duration (Table C-5).

C.7.6 Leaf area index

In broadleaf canopies, the leaf area index (LAI) is the one-sided, green leaf area per unit ground area; or the projected needle-leaf area per unit ground area in needle canopies. In the MIKE SHE model, we took leaf area index values from the global synthesis of leaf area observations published by Asner *et al.,* 2003. Further to the global synthesis we made minor changes to the leaf area index of dryland and irrigated grass, using values based on the work of Korte, 1981. For arable land parcels, we assigned higher leaf area index values than grassland parcels, and introduced more seasonal variability to simulate multiple crops grown in one season. Irrigated parcels, whether arable or grassland are assigned higher leaf area index values than their respective non-irrigated parcels.

C.7.7 Rooting depth

Rooting depth controls the amount of transpiration through root uptake in the soil profile. It is defined as the maximum depth of active roots in the unsaturated zone. A shallower root depth will lead to more transpiration from the upper unsaturated zone layers, but also may lead to decreased transpiration if the ability of the soil to move water upwards is limited. We assigned larger rooting depth values to grassland areas than to arable areas. We used this setup as grazing often only removes the green leaf area; in effect the plant remains in the ground year round, whereas with arable crops, harvesting often involves the removal of the plant and the root system. Rooting depth values were assigned in consultation with staff at Environment Canterbury based on professional opinion.

C.7.8 Crop coefficient

The crop coefficient (Kc) is a property of plants used in predicting evapotranspiration. A crop coefficient value of one sets the maximum evapotranspiration equal to the reference evapotranspiration.

In the early crop stages, where the LAI of a crop is lower than the LAI of the reference grass crop, the evapotranspiration of the crop is less than the calculated reference evapotranspiration. This is accounted for in the Kristensen & Jensen (1975) ET calculation, since a crop LAI is used as input. Therefore, for most field crops it is not necessary to specify Kc values below one in the early crop stages (DHI, 2012).

In the crop mid-season, the opposite situation may occur, where crop potential evapotranspiration is larger than the calculated reference evapotranspiration of the reference grass crop. This is not considered in the ET calculations, and Kc values above one may be relevant for some crops during the period where crop leaf area index is at its maximum (DHI, 2012). For irrigated grass, we utilised Kc values greater than one during the irrigation season.

[6] We adopted the default parameters for Kristensen and Jensen (1975) and interception storage (DHI, 2012).

Table C-5: Vegetation development

Vegetation	Day from 1 January	LAI	Rooting depth (mm)	Kc
Forest and bush	0-90	6.00	1,000	1.00
	90-180	6.00	1,000	1.00
	180-270	6.00	1000	1.00
	270-365	6.00	1000	1.00
	365	6.00	1000	1.00
Arable	0-30	2.50	500	0.90
	30-60	0.10	300	0.90
	60-180	2.50	500	0.90
	180-270	0.10	300	0.90
	270-365	1.70	300	0.90
	365	2.50	500	0.90
Irrigated arable	0-90	3.00	600	1.00
	90-180	2.50	350	1.00
	180-270	0.25	100	1.00
	270-365	2.50	350	1.00
	365	3.00	600	1.00
Grass	0-90	2.00	600	0.85
	90-180	1.50	600	0.85
	180-270	2.00	600	0.85
	270-365	1.50	600	0.85
	365	2.00	600	0.85
Irrigated grass	0-90	4.00	650	1.10
	90-180	4.00	650	1.10
	180-270	1.50	600	1.00
	270-365	1.50	600	1.00
	365	4.00	650	1.10

C.7.9 Irrigation

Irrigation systems are represented in MIKE SHE by establishing irrigation command areas and irrigation demand profiles. The water application method is set separately for each command area. This approach allows multiple schemes of varying irrigation source and type to be applied in a spatially explicit manner with associated irrigation rules that can represent the interconnectedness between surface and groundwater sources.

The Rangitata South model area is highly managed and irrigation is a major component of the local water balance. A combination of surface-water and groundwater resources are used to irrigate grass and arable land parcels with spray application methods (including pivot, rotorainers and gun). Each individual consented water abstraction can take water from either:

1. groundwater well source only
2. surface-water source only
3. surface-water and groundwater sources (when demand exceeds the surface-water supply, the farmer may take water from a groundwater source).

These irrigation abstractions are constrained by volume restrictions which differ for each consent. Licence conditions are applied in the model to limit volume used and the timing of irrigation to those permitted by consents.

C.7.10 Irrigation command areas

Irrigation in MIKE SHE is defined in the setup of irrigated command areas. Each command area:

- identifies an area with a unique irrigation source
- is assigned a water application type (e.g. spray)
- is assigned a rate and timing of irrigation application.

For simplicity, we modelled takes from the rivers and coastal streams as coming from shallow groundwater. We consider this appropriate because of the goals of the model.

For every groundwater source command area, the following inputs are required:

- the type of source (single well or well field)
- the well details (including: maximum depth to water, top of screen, bottom of screen and maximum pumping rate in m^3/s).

We selected the well field method for source type. The well field method means that irrigation is sourced from the computational grid cell immediately below the irrigated cell in which demand has been calculated. This enables us to effectively capture the spatial complexity of irrigation across the model area, whilst still maintaining an appropriately realistic spatial distribution of pumping for a regional scale model.

Since in MIKE SHE irrigation demand is determined by modelling the soil water deficit in the root zone, there may be a demand for irrigation any time throughout the year. In practice, even if a biophysical demand for irrigated water exists, irrigation is controlled by many externalities such as:

- indirect supply, such as irrigation scheme water on rotation periods
- farmer preference
- general farm management guidelines.

In MIKE SHE, licence limited irrigation can be used to limit the amount and timing of irrigation applied when a demand exists. In our Rangitata South MIKE SHE model, license limited irrigation was used to ensure the model only irrigated land parcels throughout the irrigation season (9 September – 9 May). Daily maximum volumes were assigned for each surface and groundwater source to ensure irrigated volumes did not exceed the total consented volumes. Figure C-6 shows the modelled irrigated areas.

Figure C-6: **Modelled irrigation command areas**

C.7.11 Irrigation demand

Irrigation demand varies spatially to account for differences in irrigation efficiencies across water application types. We used a few basic assumptions to model irrigation. We applied an irrigation demand of best practice deficit demand irrigation, where soil moisture is allowed to reach 40% of field capacity[7] before irrigation is applied bringing the soil moisture back to field capacity.

C.8 Overland flow

The surface-water flow components in the MIKE SHE model of Rangitata South area include the OL and the river hydrodynamics stream models (MIKE 11).

The OL model component simulates the two-dimensional movement of water over the land surface as sheet flow (flow across grid surface) until it discharges into a river, local depression, or out of the model. The OL model is dynamically coupled to the unsaturated zone model and becomes subject to infiltration to the unsaturated zone and to evapotranspiration. Ponded water on the surface may occur under high intensity rainfall when the soil infiltration capacity is exceeded, or when the soil profile becomes saturated.

If there is no unsaturated zone due to a high water table (wetlands and groundwater discharge areas), water may bypass infiltration into the unsaturated zone and will infiltrate directly into or out of the saturated zone.

For calculations, the overland flow model uses the finite difference method and depth-averaged Navier Stokes equations[8]. Flow direction is determined by the surface topographical gradients and the land surface resistance (Mannings roughness (n)) to flow. In the model, values for overland flow Mannings n have been assigned based on a pasture land use class and Chow's (1959) Mannings n (the inverse of Mannings M) values for floodplains.

The default values for detention storage have been used. Detention storage is the depth of ponded water that must be exceeded before water will flow as sheet flow to the adjacent model cell. This is equivalent to the trapping of surface water in small ponds or depressions within a grid cell (DHI, 2012).

C.9 River modelling

To ensure that overland flow and groundwater discharge was adequately removed from the model we built a detailed river network. Where weirs are specified in the model, structure hydraulics is included by forcing a flow computation at the location of the structure and replacing the momentum equation at this location (from the 1871[9] St Venant equation) with an equation representing the structure flow (e.g. the weir equation). The primary parameters adjusted during model calibration are the Manning's roughness and the structure head-loss coefficients. All modelled rivers need upstream and downstream chainages[10] and river cross-sections[11] to enable calculation of flow.

C.9.1 River network

Twelve stream reaches were created in MIKE 11 to represent the key surface-water features in the study area. The network consists of four main rivers: the Orari River, the Waihi River, the Rangitata River and the Opihi River. In addition to these, Coopers Creek and four tributaries are also included in the MIKE 11 network setup (Figure C-7).

[7] Field capacity is the amount of soil moisture or water content held in the soil after excess water has drained away.

[8] The 1840s Navier–Stokes equations describe the motion of fluid substances. These equations arise from applying Newton's second law to fluid motion, together with the assumption that the stress in the fluid is the sum of a diffusing viscous term (proportional to the gradient of velocity) and a pressure term - hence describing viscous flow. (http://en.wikipedia.org/wiki/Navier%E2%80%93Stokes_equations).

[9] A simplification of 2-dimensional flow equations and used to model transient 1-dimensional open channel flow.

[10] An imaginary point on a line used to measure distance along the length of a river and required by MIKE 11 to enable flow calculation. In MIKE11 the chainage units are in metres.

[11] River cross-sections are profiles of a river bed at a particular chainage, and are used in MIKE 11 to determine the virtual cross-sectional profile of the river.

Figure C-7: MIKE 11 river network setup

We manually digitised the branches using data from a DEM and aerial photos as existing shape files did not correctly represent the location of the rivers. In MIKE 11, flow is calculated either at each river cross-section or at the computational grid point spacing (dx). dx is the distance between two h (a water level computation point) or Q points (river flow calculation point). dx can be set at a different spacing for each river, and its spacing is dependent on how often flow or stage height needs to be calculated. The choice of dx spacing is generally based on how important it is for the model outcomes to calculate flow at a certain point on an individual river. In our Rangitata South model, dx has been set to 10,000 m. It is important to note that if there are river cross-sections closer together than the dx separation distance; calculations will take place at the cross-section as well as at the dx point.

The chainage values can be arbitrary numbers as long as the chainage value increases in the downstream direction. The upstream chainage value of each of the rivers was set to 0 m.

C.9.2 River cross-sections

As we chose to model the rivers as high order fully dynamic river features, cross-section data is only required to define the elevation of the riverbed at a given point. A uniform, relative resistance value was specified for the rivers with the Manning's M value set to 30 determined by professional opinion of Environment Canterbury's hydrologists based on riverbed type and literature (Chow, 1959). Manning's M roughness has its primary effects flow recession curves and timing of peak flows.

C.9.3 River boundary conditions

Every river branch in MIKE 11 requires an upstream and downstream boundary. If the upstream boundary is not connected to another branch, then it is usually defined as an open inflow boundary (e.g. gorge inflow). If the downstream boundary is not connected to another branch, then it is usually set to a water level or defined by a rating curve (sea level for offshore discharge).

In the Rangitata South model, all the open upstream boundaries were set to inflow boundaries and all the open downstream boundaries were set to either mean sea level or the elevation at which they exited the model area.

For the inflow boundaries where a flow time series was unavailable, a basic inflow rate of 10 L/s was used, except for Coopers Creek and the Waihi River, where the upstream inflow boundary was derived from NAM runoff calculations carried out for the two sub-catchments delineated upstream of these two branches (Table C-6).

Table C-6: MIKE 11 river boundary file setup

Boundary Description	Boundary Type	Branch Name
Open	Inflow	Rangitata
Open	Inflow	Orari
Open	Water Level	Orari
Open	Inflow	Coopers
Open	Water Level	Rangitata
Open	Inflow	Station Stm
Open	Inflow	Waihi
Open	Water Level	Waihi
Open	Inflow	Rangitata south
Open	Inflow	Ohapi 3
Open	Inflow	Ohapi 4
Open	Inflow	Ohapi 2
Open	Inflow	Ohapi main
Open	Water Level	Station Stm old
Open	Inflow	Station Stm old

C.10 Saturated zone

In parameterising the saturated zone component of the MIKE SHE model, we converted the hydrogeological conceptualisation described in Section 2 of this report into four numerical layers in the saturated zone model setup.

The top surface of the saturated zone numerical layer, corresponding to the shallow aquifer, coincides with the land surface. We derived the bottom surface elevation of the top numerical layer from the analysis of the screen depths. We created the surface by interpolation from selected bores followed by smoothing the created surface. The lower numerical layer in the model extends from the bottom of the third layer to a depth of approximately 150 mbgl, as this adequately captures the depths to which bores are drilled in the region (which are all screened at depths of less than 150 mbgl).

C.10.1 Aquifer parameters

For the purposes of developing the unified land surface recharge and evapotranspiration layer, we decided to adopt a uniform hydraulic conductivity across the model area. Other than maintaining groundwater levels below the surface and deep enough to avoid the effects of ET, it was unnecessary to accurately capture the spatial distribution of groundwater heads at this stage. However, near the coast we ensured that heads were close enough to ground surface to feed the spring-fed coastal waterbodies. Following several initial model runs, we adopted a uniform hydraulic conductivity of 30 m/d as this meet these criteria, for the purposes of modelling LSR and ET from the saturated zone.

C.10.2 Boundary conditions

In hydrological modelling involving groundwater and surface water interactions, the flow system is usually enclosed by boundaries that correspond to identifiable hydrological features at which some characteristic of surface or ground-water flow is easily described. Some examples of this are a body of surface water, an almost impermeable surface, a coastal boundary or a water table. At these boundaries the water level can be fixed at a certain elevation; the boundaries can provide a source of flux of water (Darcy flux, e.g. lateral inflow into the aquifer from a slope), they can be boundaries across which no water flows (no flux boundary; for example mountain ranges, flow divides), or they can represent a combination of these.

In the Rangitata South model, we assigned two types of external boundaries as follows:

1. No-flow boundary condition: Water cannot cross this boundary, nor is a water level or flux assigned to it. The model calculates the water level in the vicinity of the boundary.
2. Constant head or fixed-head boundary condition: The water level is set at a certain elevation decided beforehand and the model maintains that water level constantly.

North-eastern Boundary

The north-eastern model boundary has been set as a no-flow boundary, slightly north of the Rangitata River in the Mayfield-Hinds GAZ. A boundary of this type is justified in this case, as we know that:

- groundwater flows roughly parallel to the boundary location on either side under field conditions and, therefore, does not cross the boundary
- no hydrological feature of the model will change that parallel flow scheme (due to adequate distance of the boundary to the focus area where stresses are applied).

Placing the boundary location an adequate distance from the Rangitata River ensures accurate capture of groundwater flux beneath the river.

North-western model boundary

The north-western (inland) extent of the model terminates at the contact with basement. As we do not expect there to be significant inputs into the saturated zone from the very low permeability basement, we have set the boundary as a no-flow boundary. Modelling results indicate that this is a reasonable assumption.

South-western model boundary

The south-western boundary of the model was chosen at an approximate groundwater flow divide and far enough south of the study area to minimise effects of the boundary on the key model results.

Coastal model boundary

The upward hydraulic gradients observed along the coast demonstrate that groundwater must upwell where the fresh water/salt water interface exists. We set external boundary conditions following Motz's (2004) approach who assigned the lower layer with a fixed head appropriate to simulate the saline wedge. We calculated head at various depths zs using the Ghyben-Herzberg equation[12]:

$$Zs = \frac{\rho f}{\rho s - \rho f} Zw$$

where ρf is the density of fresh water, ρs is the density of saltwater and Zw is the head of freshwater above sea level. In the model, we have used the depth of the deep target calibration wells as Zs. Table C-7 details the coastal boundary conditions.

Table C-7: Coastal boundary conditions

Model computation layer	Boundary type	Head m msl
1	Fixed head	0.1
2	Fixed head	0.1
3	Fixed head	1.5 (based on depth 60 m below surface)
4	Fixed head	2.5 (based on depth 100 m below surface)

[12] *We analysed the coastal model boundary by adding additional layers to the model and setting the saltwater heads at a higher resolution in the vertical direction. The results were similar and we concluded that the 4-layer model adequately represents the situation in terms of the modelling objectives that do not include movement of the saltwater interface.*

Appendix D: Steady-state MODFLOW model

MODFLOW saturated zone model

We reproduced the model structure as detailed in Appendix C using MODFLOW. We adopted the recharge layer from MIKE SHE. We introduced the same layer structure as the MIKE SHE saturated zone model and utilised the MODFLOW River package to simulate surface water. Calibration aimed at matching observed head in Environment Canterbury monitoring wells, interpolated head elevations based on Wilson (2013) piezometric survey, and previous surveys conducted in the Mayfield-Hinds area. Secondary calibration targets were gauged losses and gains to local rivers inside the model area. Calibration criteria were head levels within two metres[13] and/or within one standard deviation of observed level where multiple readings were available.

We began initial manual calibration focusing on adjusting hydraulic conductivity uniformly across the model domain and applying default values for streambed conductance of 10 m^2/d. From poor calibration statistics from several model forward runs, it quickly became apparent that the default conductivity values used for the saturated zone in MIKE SHE are unsuccessful in producing adequate fits. To address this we began using pilot points in a uniform grid for calibration of the saturated zone hydraulic conductivity leaving river conductance values at the default value. Results of our initial runs highlighted that a one to one horizontal to vertical anisotropy would be sufficient to achieve calibration. This left us to focus on horizontal conductivity. We adopted an upper and lower bound for the conductivity of 100 m/d and 0.001 m/d respectively.

Following several PEST runs, we had achieved a reasonable fit to head by adjusting hydraulic conductivity. Calibration statistics at that point showed that without adjustment of the river bed conductance we would fail to meet our calibration criteria. So, we decided to begin calibrating streambed conductance. Our calibration criteria for streambed conductance were estimated losses and gains to the local rivers. We calibrated both saturated hydraulic conductivity and streambed conductance simultaneously. Figure D-1 provides a histogram of the variance between modelled and observed heads with our final calibration, overall 92% of the head elevation calibration targets were within the target range of less than two metres variance. Figure D-2 demonstrates the degree of fit between observed head and modelled head, whilst Figure D-3 and Figure D-4 show the spatial distribution of the calibration fit. Figure D-5 shows the final spatial pattern of conductivity, individual pilot point values are presented in Appendix F.

[13] We choose two metres variance as our criteria as this reflects the certainty of our data. The majority of calibration targets are based on inferred piezometric contours based on one off measurements; further grid spacing is 250 m and not necessarily specific observation point, having higher calibration criteria would lead to over fitting the data.

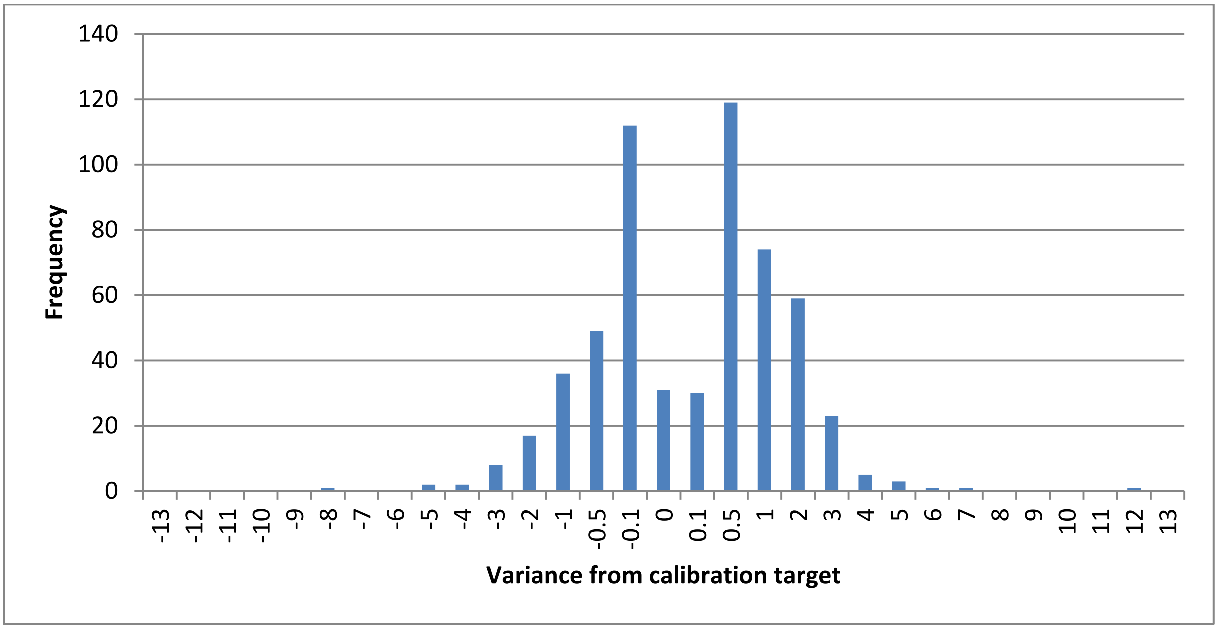

Figure D-1: **Histogram of variance in modelled head from observed head (sample size n=574)**

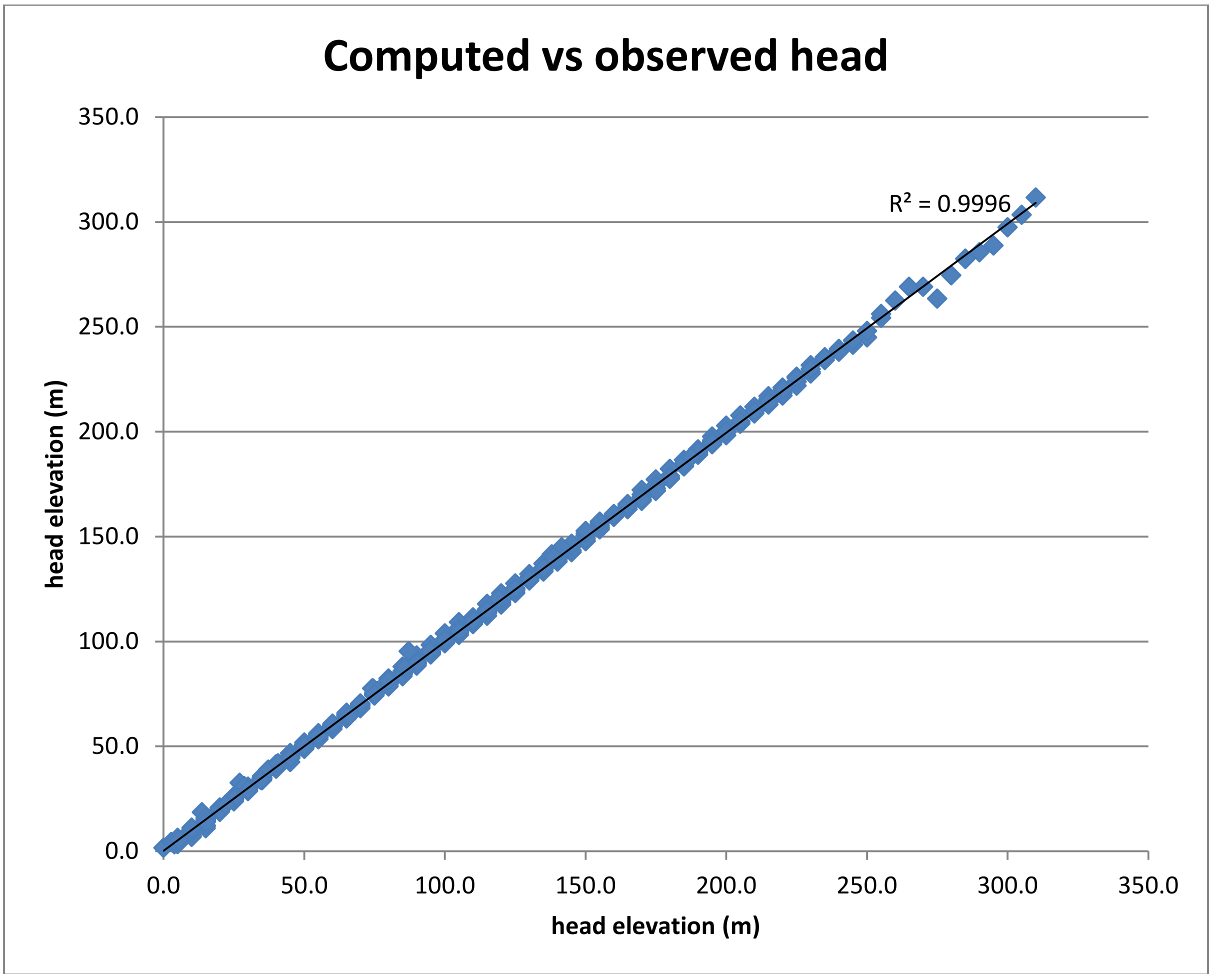

Figure D-2: **Simulated head vs piezometric survey and observation well head**

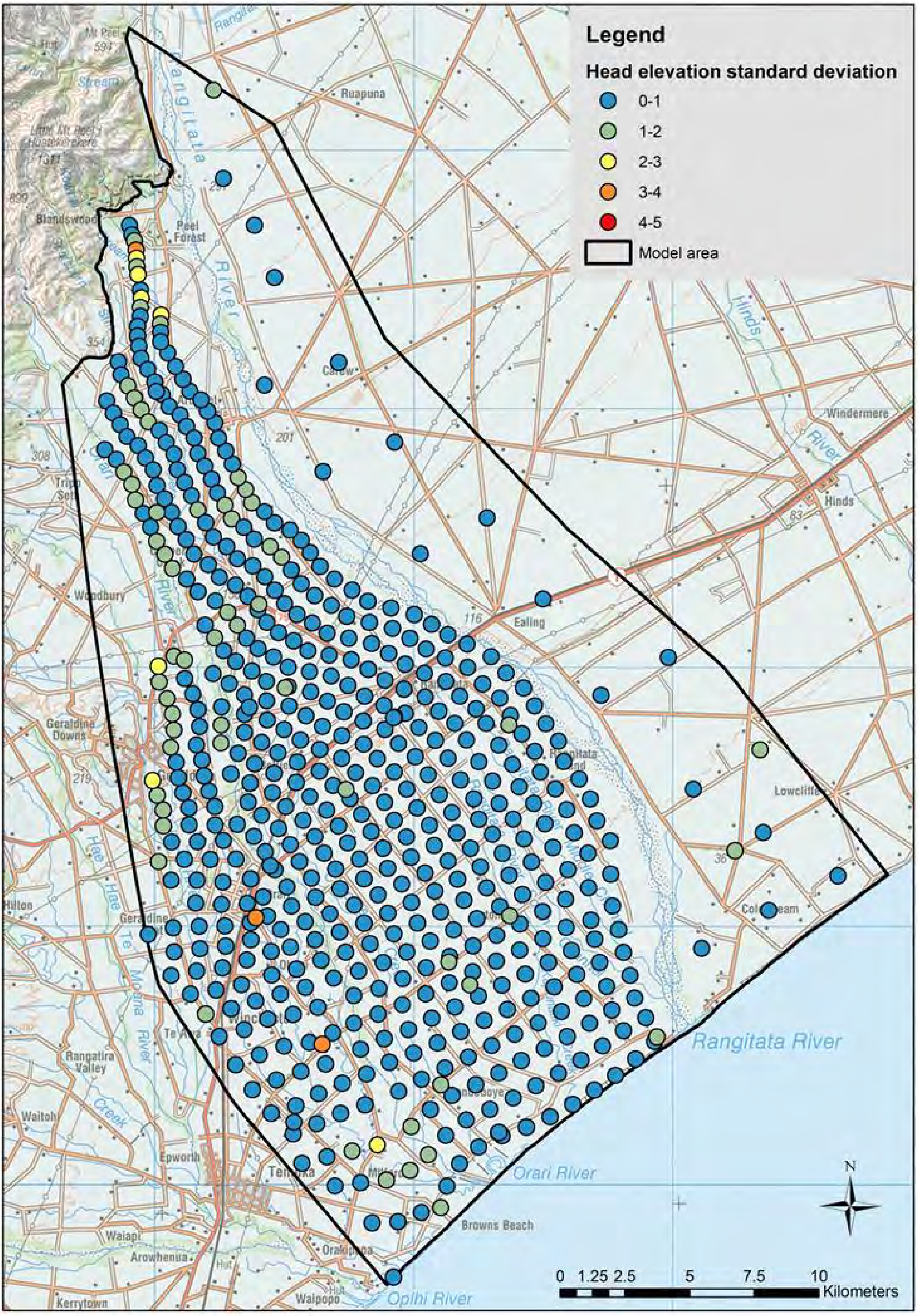

Figure D-3: Spatial distribution of calibration matches, as demonstrated calibration is with targets for majority of model area

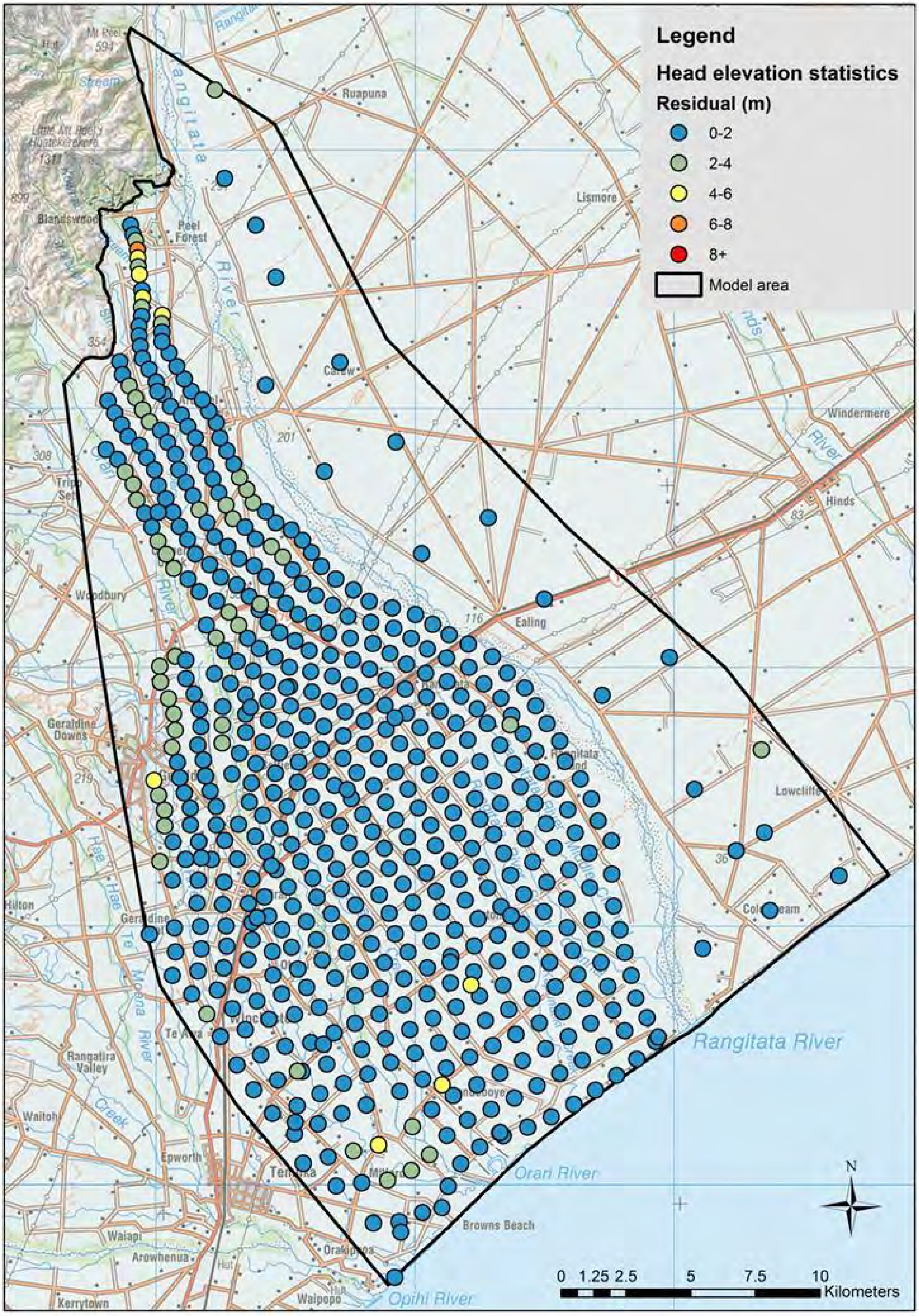

Figure D-4: **Spatial distribution of difference between modelled and observed head, as demonstrated calibration is with targets for majority of model area**

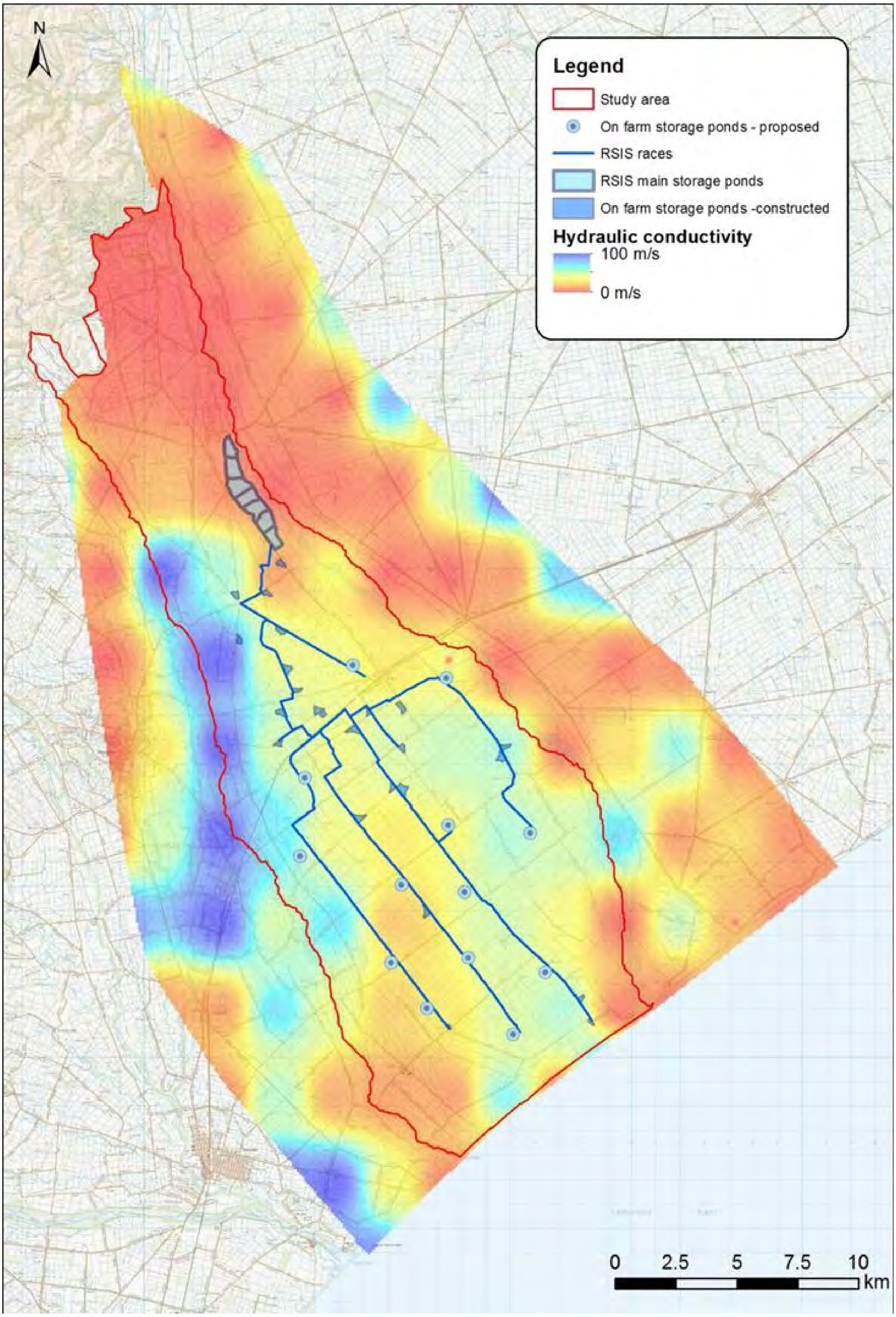

Figure D-5: Calibrated hydraulic conductivity

Stream bed conductance calibration focused on achieving both a good fit to groundwater heads and matching of gauged losses and gains. Table D-1 and Figure D-6 shows the modelled losses and gains for individual sections of rivers and drains. Segments of river are shown in Figure 5-1. Losses and gains across segments for the Orari River, Ohapi Creek and Coopers Creek are similar to measured gains and losses by Burbery and Ritson (2010) (Figure D-7). We did not achieve our desired level of calibration for the Waihi River and Station Stream Old (Dobies Stream), where the model failed to lose/gain as much as gauging data suggest; this is likely a factor of model design and/ or gauging error. We believe for the purposes of our model, these features are adequately represented, as they are outside our area of primary concern. There are no reliable gauging data to compare the losses and gains along the length of the Rangitata to (all gaugings of the Rangitata River are within the gauging error of each other). Appendix F details the streambed conductance values used in the final calibration.

Table D-1: Modelled losses/gains in rivers and drains. Negative numbers indicate groundwater is losing (i.e. surface water is gaining). Positive numbers indicate groundwater is gaining (i.e. surface water is losing)

Name	Type	Computed flow (m^3/d) over section of river/drain	Computed flow (l/sec) over section of river/drain
Coopers (11)	river	17,939	208
Coopers (23)	river	1,073	12
Coopers (26)	river	-44,174	-511
Ohapi 1	drain	-22,398	-259
Ohapi 2 (14)	drain	-3,344	-39
Ohapi 2 (16)	drain	-11,082	-128
Ohapi 2 (5)	drain	-4,602	-53
Ohapi 3	drain	-1,200	-14
Ohapi 4	drain	-4,727	-55
Ohapi main (18)	drain	-34,554	-400
Ohapi main (7)	drain	-11,138	-129
Opihi main (22)	drain	-2,013	-23
Orari (12)	river	308,362	3,569
Orari (15)	river	-2,280	-26
Orari (19)	river	783	9
Orari (20)	river	937	11
Orari (27)	river	-74,230	-859
Rangitata (17)	river	-55,379	-641
Rangitata (24)	river	-7,739	-90
Rangitata (25)	river	45,038	521
Rangitata (29)	river	53,235	616
Rangitata Sth	drain	-9	-0.11
Station Stm	drain	-43,227	-500
Station Stm old	drain	-554	-6
Waihi	river	5,791	67

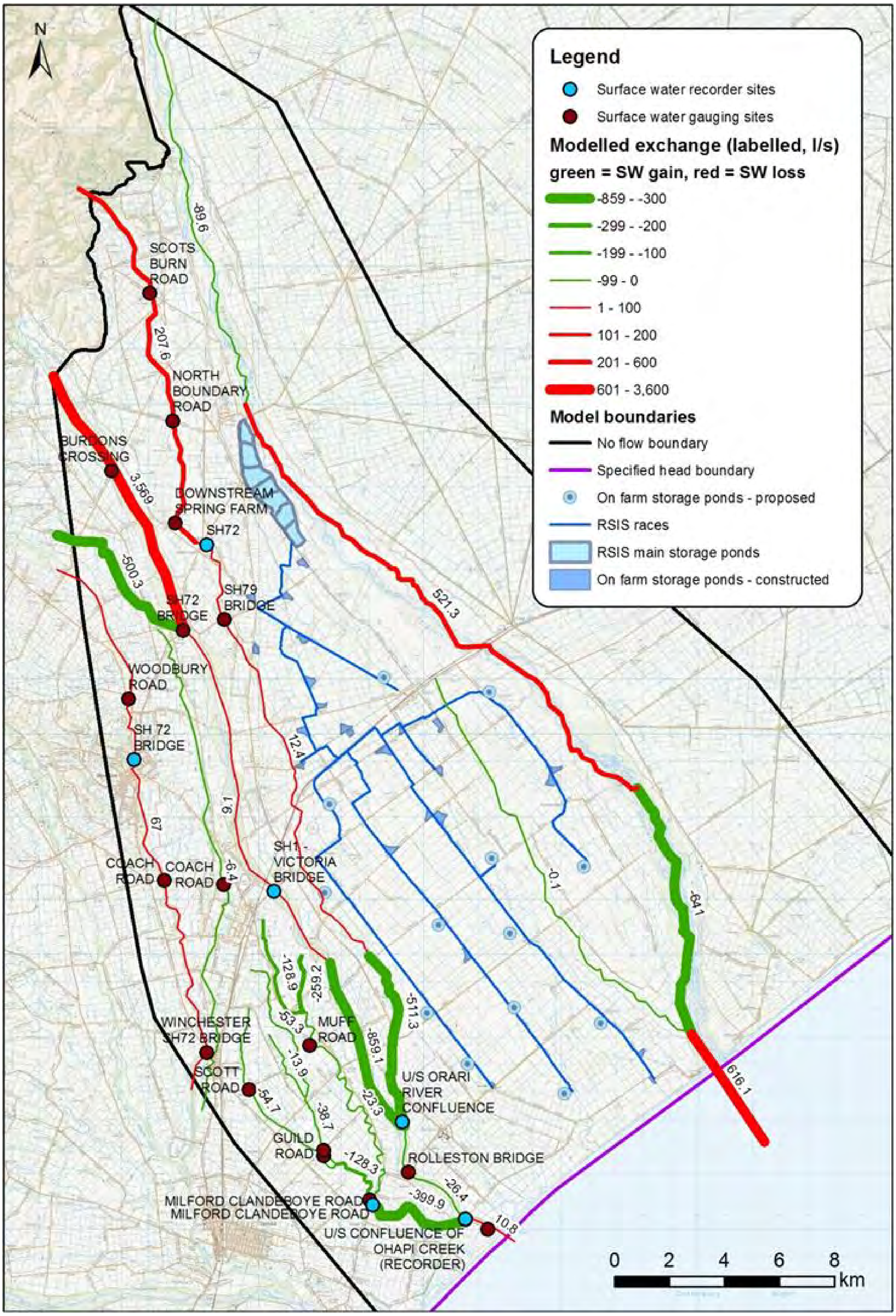

Figure D-6: Modelled surface waterways losses and gains

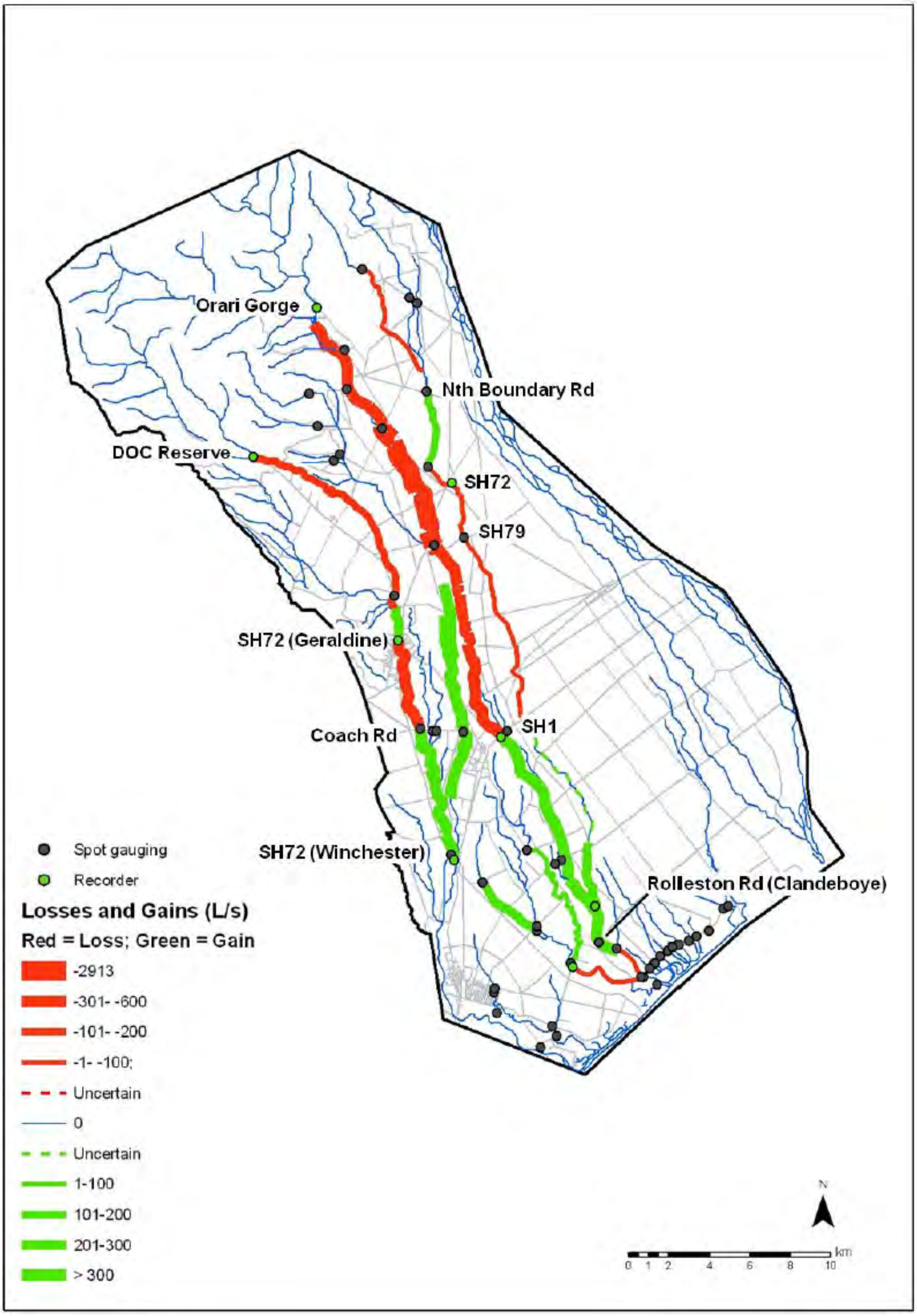

Figure D-7: **Average river flow losses and gains in the Orari catchment, measured from gauging runs conducted between September 2006 and September 2007 (calculated as L/s difference between consecutive gauging sites). Figure from Burbery and Ritson (2010)**

Appendix E: MODFLOW results

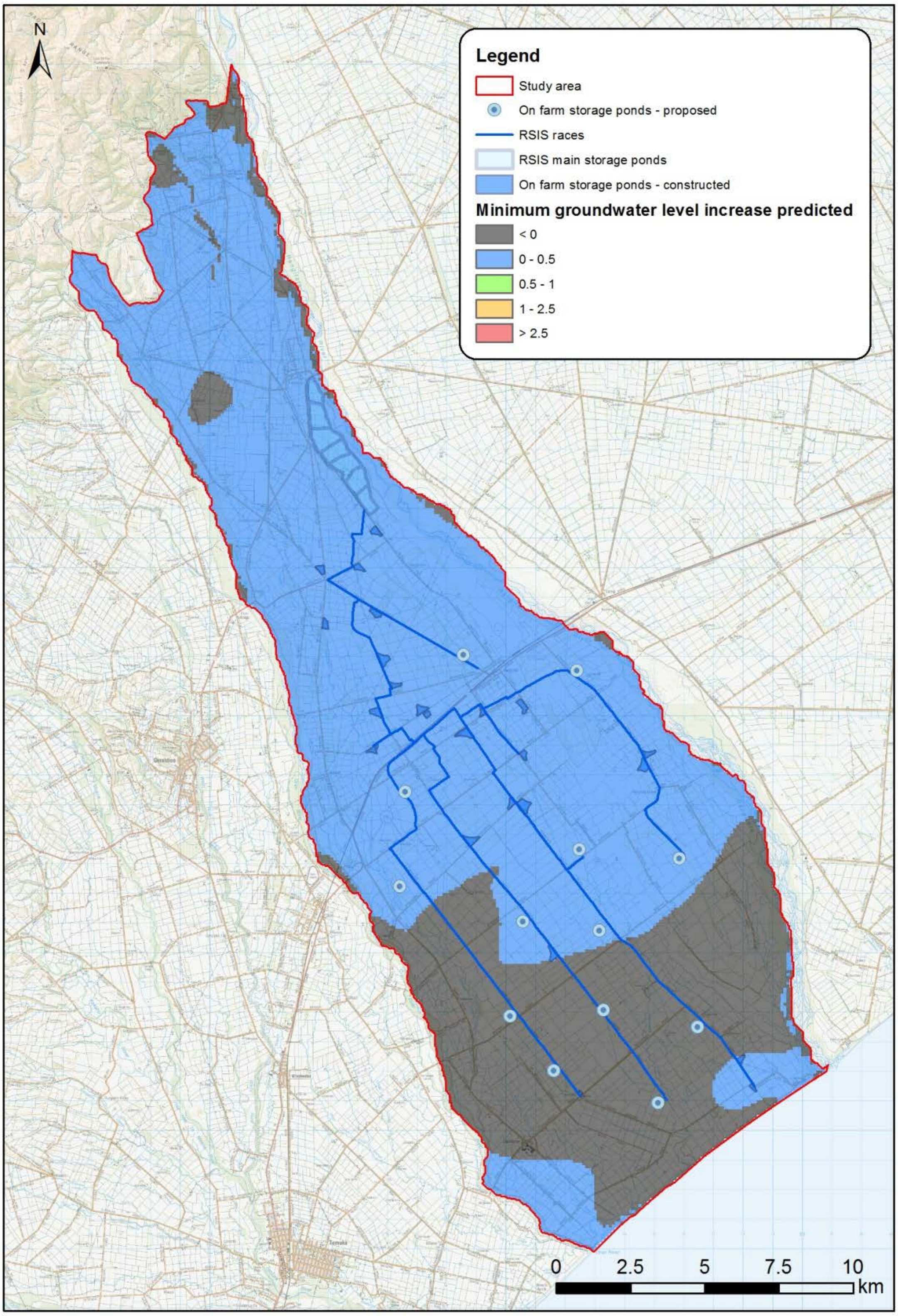

Figure E-1: Modelled minimum groundwater level (head) change resulting from all RSIS scheme infrastructure - simplified

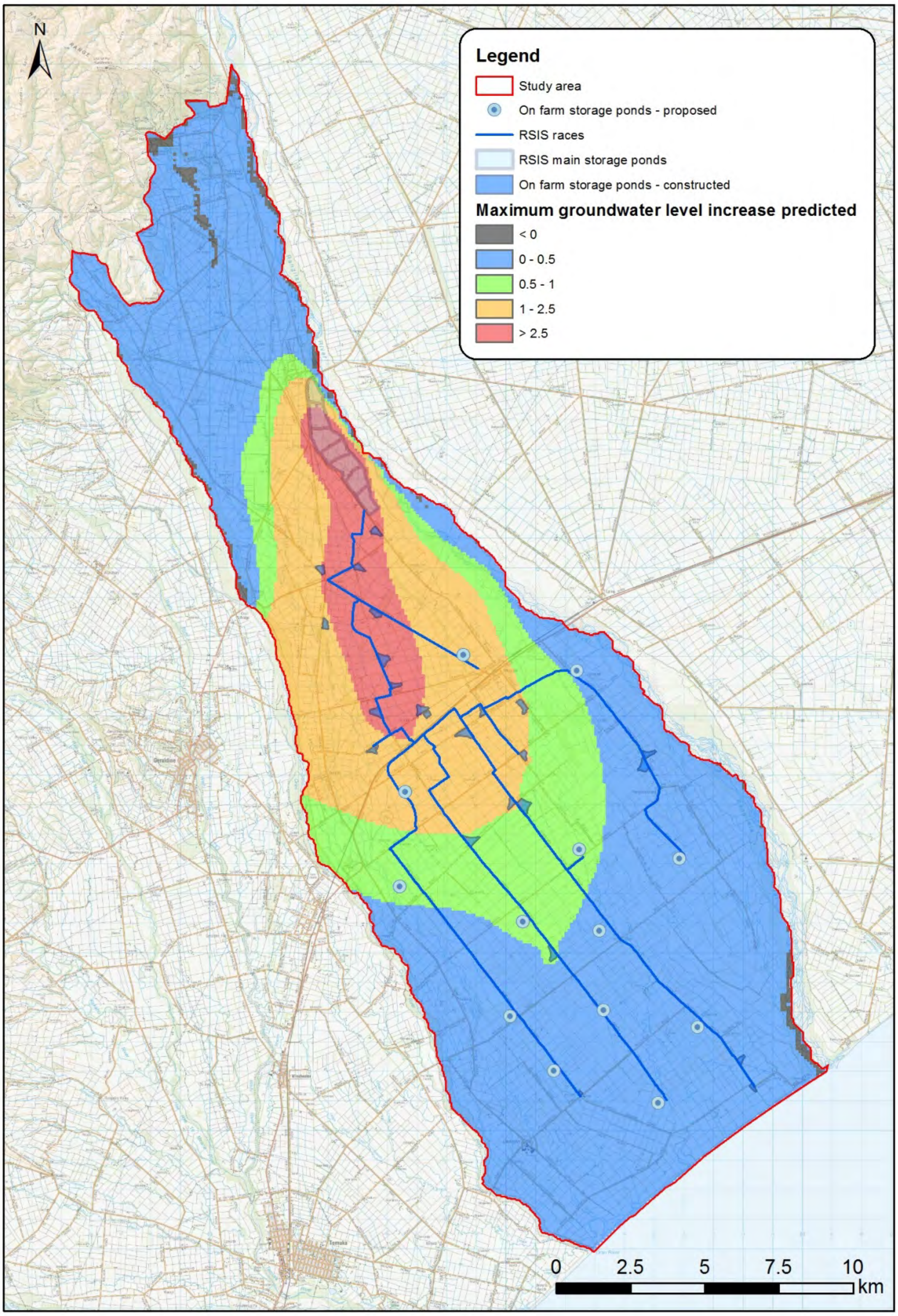

Figure E-2: Modelled maximum groundwater level (head) change resulting from all RSIS scheme infrastructure - simplified

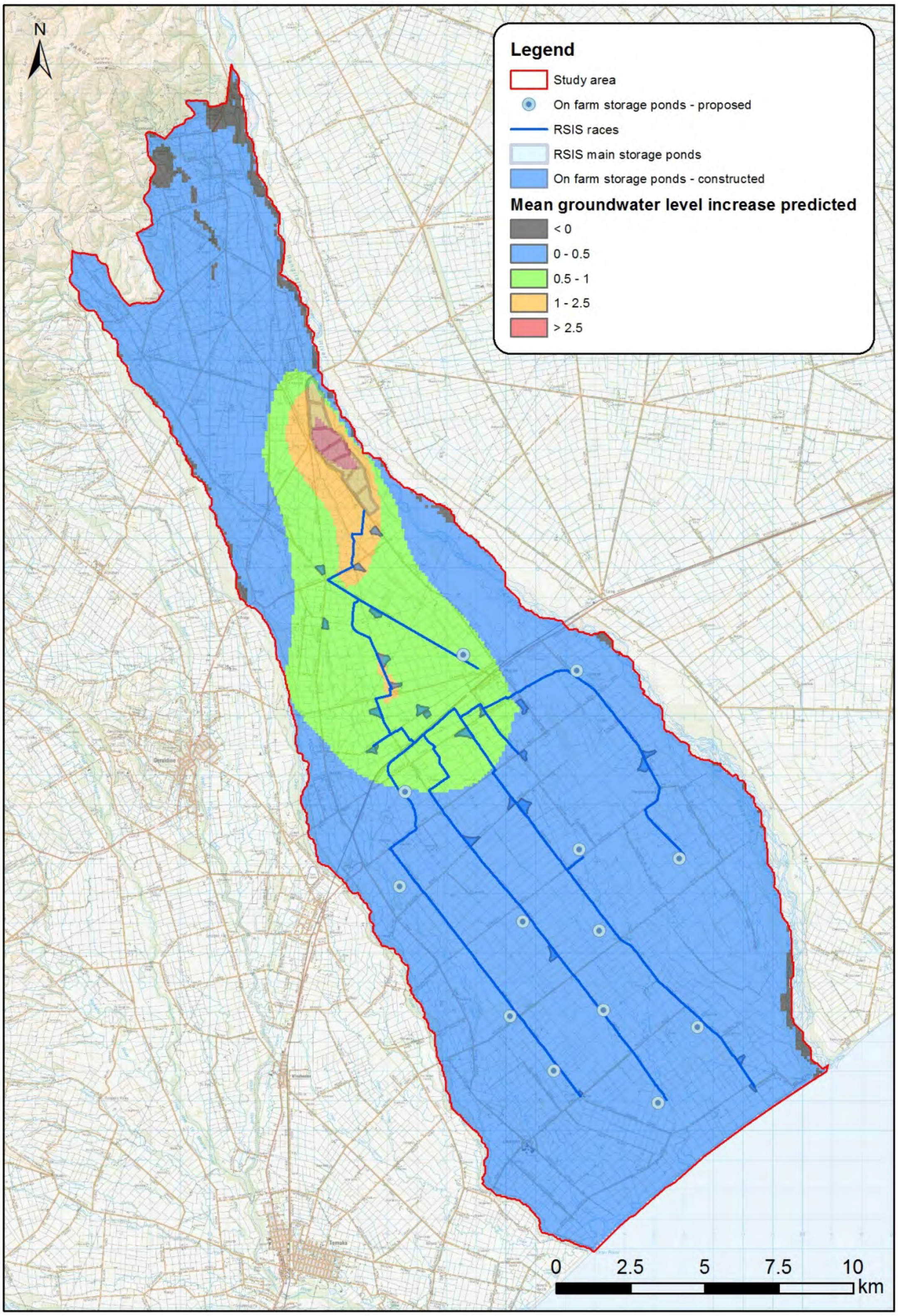

Figure E-3: Modelled mean groundwater level (head) change resulting from all RSIS scheme infrastructure - simplified

Appendix F: Calibration statistics

Table F-1: Pilot point calibrated hydraulic conductivity values for layers 1 to 4

NZTM[14] X	NZTM Y	K (m/d)
1458387	5134618	0.01
1458387	5138196	0.01
1460735	5134618	0.02
1463083	5134618	0.03
1460735	5138196	0.06
1458387	5120308	0.22
1463083	5131041	0.35
1465431	5134618	0.43
1472476	5123886	0.61
1463083	5141773	0.80
1458387	5116731	0.83
1486564	5109576	1.04
1472476	5131041	1.56
1458387	5131041	1.59
1465431	5127463	1.59
1470128	5123886	1.73
1479520	5109576	2.41
1458387	5113153	2.41
1458387	5145350	2.46
1477172	5120308	2.50
1458387	5127463	2.72
1479520	5120308	2.94
1467780	5127463	3.12
1463083	5138196	3.25
1481868	5113153	3.36
1479520	5116731	3.62
1486564	5113153	3.79
1477172	5102421	4.03
1481868	5109576	4.06
1479520	5105998	4.10
1484216	5116731	4.85
1481868	5105998	5.63
1460735	5145350	6.16
1467780	5131041	6.29
1477172	5116731	6.55
1460735	5141773	6.85
1484216	5109576	6.97
1474824	5120308	7.00

NZTM X	NZTM Y	K (m/d)
1477172	5123886	17.94
1474824	5127463	18.38
1478890	5103850	20.03
1479520	5113153	20.58
1460735	5116731	20.60
1458387	5123886	21.53
1460735	5105998	21.81
1470128	5131041	22.20
1456039	5127463	22.47
1465431	5123886	22.64
1474824	5116731	23.16
1477172	5113153	24.71
1456039	5123886	26.32
1472476	5102421	26.71
1474824	5109576	27.72
1474824	5113153	32.62
1472476	5113153	33.31
1474824	5105998	33.95
1470128	5109576	34.27
1465431	5109576	35.39
1460735	5113153	35.54
1470128	5120308	36.66
1479520	5123886	36.89
1472476	5098843	37.07
1472476	5116731	37.79
1470128	5113153	37.90
1467780	5102421	38.01
1470128	5105998	38.17
1467780	5123886	40.85
1467780	5134618	41.09
1465431	5120308	41.65
1467780	5116731	48.71
1467780	5105998	48.85
1467780	5113153	49.38
1472476	5105998	49.70
1465431	5116731	53.11
1467780	5120308	54.80
1470128	5116731	57.70

[14] NZGD 2000 Transverse Mercator

1481868	5120308	7.34
1465431	5131041	8.94
1470128	5102421	9.02
1465431	5141773	9.63
1463083	5127463	11.49
1470128	5127463	11.61
1460735	5127463	11.88
1465431	5138196	12.05
1484216	5113153	12.66
1456039	5131041	12.90
1474824	5123886	12.92
1477172	5105998	13.96
1481868	5116731	14.02
1472476	5127463	14.29
1463083	5102421	14.81
1472476	5120308	15.01
1463083	5105998	15.21
1477172	5109576	16.55
1463083	5123886	62.12
1465431	5113153	69.18
1465431	5102421	71.11
1474824	5102421	73.50
1467780	5109576	74.02
1474730	5100360	74.65
1460735	5123886	82.35
1465431	5105998	86.39
1470128	5098843	92.87
1463083	5109576	93.10
1463083	5120308	94.15
1463083	5116731	100.00
1463083	5113153	100.00
1458387	5109576	100.00
1465431	5098843	100.00
1467780	5098843	100.00
1467780	5095266	100.00
1470128	5095266	100.00

Table F- 2: Surface water features final calibrated conductance values

River	Surface water package	Stream bed conductance values
Waihi	river	25,000.00
Coopers	river	5.47
Orari	river	25,000.00
Orari	river	0.28
Orari	river	496.93
Rangitata	river	0.10
Rangitata	river	1.97
Orari	river	0.10
Coopers	river	2,456.13
Rangitata	river	81.81
Rangitata	river	3.08
Coopers	river	4.74
Orari	river	0.05
Station Stm old	drain	20,000.00
Ohapi 4	drain	0.21
Ohapi 3	drain	0.21
Ohapi 2	drain	0.37
Ohapi 1	drain	17.58
Ohapi main	drain	1.75
Station Stm	drain	36.67
Ohapi 2	drain	0.38
Ohapi 2	drain	10.21
Ohapi main	drain	6,219.27
Opihi main	drain	0.10
Rangitata Sth	drain	0.00

Table F- 3: Calibration statistics for calibration points

Observation point	X NZTM	Y NZTM	Z (masl)	Observed head	Observed head interval	Observed head confidence %	Observed head standard deviation	Modelled head	Residual head
J37/0008	1460097	5130653	217.2	220.3	2	95	1	220.2	0.1
K37/0130	1464058	5122433	135.4	141.6	4.8	95	2.4	144.9	-3.3
K37/0289	1463685	5118454	107	119.2	3.5	95	1.8	120.2	-1.1
K37/0987	1465078	5119200	114.6	119	1.7	95	0.9	120.3	-1.3
K37/1301	1460177	5120029	98.1	137.9	3	95	1.5	141.6	-3.7
K37/2896	1460117	5125976	184	187.5	0.7	95	0.4	187.9	-0.4
K37/2923	1461189	5120271	133.2	138.6	2	95	1	140.3	-1.7
K38/0013	1472202	5107715	-41.4	27	5.8	95	3	32.7	-5.7
K38/0060	1465413	5102409	19.7	22	0.5	95	0.3	22.3	-0.2
K38/1081	1471399	5108598	30.3	37.2	2.1	95	1.1	38.8	-1.7
K38/1377	1471085	5099101	-3.9	3.8	0.6	95	0.3	3.3	0.5
K38/1380	1473716	5117765	9.2	74.1	3	95	1.5	77.6	-3.5
K38/1381	1473716	5117765	61.7	74.5	3.1	95	1.6	77.6	-3.1
K38/1571	1483539	5113600	28.7	29.9	1	95	0.5	30.3	-0.4
K38/1673	1465503	5104381	-15.3	28.6	0.9	95	0.5	31.1	-2.4
K38/1690	1467420	5115265	81.4	85.8	1.9	95	1	87.4	-1.6
K38/1706	1479436	5105701	-61.7	5.3	1.8	95	0.9	4.7	0.6
K38/1707	1479436	5105701	-23.2	4.8	1.4	95	0.7	4.7	0.2
K38/1758	1466499	5105417	24.5	34.6	0.3	95	0.2	34	0.6
K38/1774	1482452	5112903	-31.5	30.1	1.4	95	0.7	29.3	0.8
K38/1776	1469494	5098159	-63.5	2.7	0.6	95	0.3	4.4	-1.6
K38/1821	1479435	5105702	-8.6	3.9	1	95	0.5	4.7	-0.8
K38/2111	1473752	5110391	38.5	40.7	1.6	95	0.8	42	-1.3
K38/2154	1461779	5112621	75.2	80	0.4	95	0.2	81.2	-1.3
K38/2155	1463944	5110316	60.6	65.9	0.8	95	0.4	64.6	1.3
K38/2157	1464498	5112327	72.5	76	1	95	0.5	76.5	-0.5
K38/2247	1471091	5103855	-45	13.6	5.7	95	2.9	18.6	-5

Observation point	X NZTM	Y NZTM	Z (masl)	Observed head	Observed head interval	Observed head confidence %	Observed head standard deviation	Modelled head	Residual head
K38/2329	1473308	5102001	-55.9	6.3	4.1	95	2.1	5.4	1
K38/2331	1473335	5102014	1.4	5.3	0.3	95	0.1	5.4	-0.1
K38/2428	1469301	5118068	5.2	87.1	6	95	3	95.3	-8.2
K38/2429	1469264	5118043	83.3	94.7	2	95	1	95.4	-0.7
point_1	1481156	5109129	1	15	1	95	2	14.4	0.6
point_2	1460667	5111758	65.7	75	2	70	2	75.9	-0.9
point_3	1479875	5120372	1	75	1	95	2	75	0
point_4	1462683	5113296	78.8	85	2	70	2	84.9	0.1
point_5	1476858	5114900	47.3	55	2	70	2	53.6	1.4
point_6	1476428	5115673	50.1	60	2	70	2	59.4	0.6
point_7	1475838	5116353	57.4	65	2	70	2	65.6	-0.6
point_8	1475632	5117139	60.2	70	2	70	2	69.7	0.3
point_9	1475139	5117809	65.1	75	2	70	2	74.3	0.7
point_10	1474710	5118504	69.5	80	2	70	2	78.5	1.5
point_11	1474280	5119191	73.7	85	2	70	2	83.5	1.5
point_12	1473606	5119772	80.6	90	2	70	2	90.4	-0.4
point_13	1473030	5120404	84.6	95	2	70	2	95.1	-0.1
point_14	1472103	5120884	91.2	100	2	70	2	100.9	-0.9
point_15	1460368	5113864	83.3	90	2	70	2	93.4	-3.4
point_16	1471358	5121247	96.9	105	2	70	2	106.5	-1.5
point_17	1470728	5121649	102	110	2	70	2	110.4	-0.4
point_18	1470059	5122032	105.7	115	2	70	2	113.9	1.1
point_19	1469158	5122282	109.7	120	2	70	2	119.4	0.6
point_20	1468269	5122539	116.5	125	2	70	2	125.3	-0.3
point_21	1467660	5122982	122.9	130	2	70	2	130.4	-0.4
point_22	1466980	5123402	129.2	135	2	70	2	135.1	-0.1
point_23	1466420	5123895	133.5	140	2	70	2	140	0
point_24	1466040	5124424	137	145	2	70	2	145.6	-0.6

Observation point	X NZTM	Y NZTM	Z (masl)	Observed head	Observed head interval	Observed head confidence %	Observed head standard deviation	Modelled head	Residual head
point_25	1465692	5124903	141.5	150	2	70	2	150.6	-0.6
point_26	1461367	5113903	84.5	90	2	70	2	91.3	-1.3
point_27	1475035	5122631	1	105	1	95	2	104.8	0.2
point_28	1465262	5125297	147.1	155	2	70	2	155.1	-0.1
point_29	1464658	5125575	152.2	160	2	70	2	159.5	0.5
point_30	1464272	5126011	158.9	165	2	70	2	163	2
point_31	1463788	5126354	167.1	170	2	70	2	167	3
point_32	1463545	5126860	170	175	2	70	2	171.8	3.2
point_33	1463257	5127330	170.9	180	2	70	2	177.8	2.2
point_34	1463039	5127853	172.1	185	2	70	2	183.9	1.1
point_35	1460279	5133605	233.4	250	2	70	2	245.1	4.9
point_36	1460253	5133270	231.5	245	2	70	2	241.6	3.4
point_37	1460266	5132942	228.7	240	2	70	2	238.9	1.1
point_38	1462367	5113893	84.2	90	2	70	2	89.4	0.6
point_39	1462778	5128352	181.2	190	2	70	2	189.3	0.7
point_40	1462502	5128849	185.3	195	2	70	2	194.1	0.9
point_41	1462363	5129444	193.2	200	2	70	2	198.3	1.7
point_42	1461397	5130666	206.3	215	2	70	2	215.6	-0.6
point_43	1461125	5131130	211.4	220	2	70	2	221	-1
point_44	1460836	5131618	216.6	225	2	70	2	226.3	-1.3
point_45	1460538	5132143	220.9	230	2	70	2	231.8	-1.8
point_46	1460265	5132579	224.8	235	2	70	2	235.5	-0.5
point_47	1462076	5129888	200	205	2	70	2	203.8	1.2
point_48	1461826	5130330	204.3	210	2	70	2	209.9	0.1
point_49	1460365	5114470	88.2	95	2	70	2	98.4	-3.4
point_50	1459058	5137080	302.6	310	2	70	2	311.6	-1.6
point_51	1459154	5136715	292.8	305	2	70	2	303.4	1.6
point_52	1459249	5136477	286.3	300	2	70	2	297.5	2.5

Observation point	X NZTM	Y NZTM	Z (masl)	Observed head	Observed head interval	Observed head confidence %	Observed head standard deviation	Modelled head	Residual head
point_53	1459312	5136128	277.6	295	2	70	2	288.8	6.2
point_54	1459328	5135810	269	290	2	70	2	285.6	4.4
point_55	1459344	5135477	261.8	285	2	70	2	282.4	2.6
point_56	1459392	5135175	255.2	280	2	70	2	274.7	5.3
point_57	1459471	5134905	249.9	275	2	70	2	263.5	11.5
point_58	1459487	5134572	251.2	270	2	70	2	269.1	0.9
point_59	1459519	5134270	248.7	265	2	70	2	269.1	-4.1
point_60	1461361	5114556	89.7	95	2	70	2	96	-1
point_61	1459482	5133905	240.7	260	2	70	2	262.5	-2.5
point_62	1459482	5133561	238.2	255	2	70	2	254.3	0.7
point_63	1459373	5133184	231.6	250	2	70	2	248.1	1.9
point_64	1459373	5132800	231.3	245	2	70	2	243.4	1.6
point_65	1458633	5131801	239.9	240	2	70	2	238.6	1.4
point_66	1459429	5132406	227.2	240	2	70	2	239.5	0.5
point_67	1458735	5131301	235.4	235	2	70	2	234.1	0.9
point_68	1459507	5131935	225.5	235	2	70	2	235.1	-0.1
point_69	1458182	5130291	231.5	230	2	70	2	228.6	1.4
point_70	1458997	5130871	229.2	230	2	70	2	227.8	2.2
point_71	1462360	5114604	90.7	95	2	70	2	94.5	0.5
point_72	1459766	5131510	222.3	230	2	70	2	229.9	0.1
point_73	1458437	5129821	226	225	2	70	2	223.8	1.2
point_74	1459249	5130404	224.4	225	2	70	2	222	3
point_75	1460034	5131023	216.8	225	2	70	2	223.9	1.1
point_76	1458697	5129370	221.3	220	2	70	2	219.6	0.4
point_77	1459517	5129943	217.7	220	2	70	2	217.2	2.8
point_78	1460318	5130541	209.2	220	2	70	2	218.5	1.5
point_79	1458103	5128404	205.9	215	2	70	2	216.9	-1.9
point_80	1458962	5128915	213.7	215	2	70	2	215.2	-0.2

Observation point	X NZTM	Y NZTM	Z (masl)	Observed head	Observed head interval	Observed head confidence %	Observed head standard deviation	Modelled head	Residual head
point_81	1459783	5129485	212.2	215	2	70	2	212.9	2.1
point_82	1460135	5115041	94.7	100	2	70	2	103.9	-3.9
point_83	1460591	5130075	204.5	215	2	70	2	214	1
point_84	1458556	5128030	201.6	210	2	70	2	211.9	-1.9
point_85	1459401	5128565	210.7	210	2	70	2	209.7	0.3
point_86	1460214	5129147	204.7	210	2	70	2	208.6	1.4
point_87	1461018	5129742	202.3	210	2	70	2	209.8	0.2
point_88	1458838	5127545	198.1	205	2	70	2	207.9	-2.9
point_89	1459676	5128090	199.9	205	2	70	2	204.6	0.4
point_90	1460481	5128684	197.9	205	2	70	2	204.5	0.5
point_91	1461271	5129297	198.1	205	2	70	2	205.1	-0.1
point_92	1459151	5127065	194.2	200	2	70	2	202.9	-2.9
point_93	1461130	5115136	94.3	100	2	70	2	100.8	-0.8
point_94	1470295	5124386	1	135	1	95	2	134.9	0.1
point_95	1459980	5127625	193.9	200	2	70	2	199.7	0.3
point_96	1460776	5128230	192	200	2	70	2	200.2	-0.2
point_97	1461559	5128852	191.8	200	2	70	2	200.5	-0.5
point_98	1459296	5126462	187.8	195	2	70	2	197.7	-2.7
point_99	1460126	5127020	187.5	195	2	70	2	194.8	0.2
point_100	1460914	5127634	187.1	195	2	70	2	195.3	-0.3
point_101	1461696	5128258	187.1	195	2	70	2	195.9	-0.9
point_102	1459593	5125939	181.9	190	2	70	2	191.7	-1.7
point_103	1460416	5126506	181.2	190	2	70	2	189	1
point_104	1461191	5127138	184	190	2	70	2	190	0
point_105	1462128	5115208	94.6	100	2	70	2	99.4	0.6
point_106	1472872	5125772	1	135	1	95	2	135	0
point_107	1461969	5127765	183.2	190	2	70	2	190.9	-0.9
point_108	1459873	5125416	177.1	185	2	70	2	186.6	-1.6

Observation point	X NZTM	Y NZTM	Z (masl)	Observed head	Observed head interval	Observed head confidence %	Observed head standard deviation	Modelled head	Residual head
point_109	1460692	5125987	176.2	185	2	70	2	183.5	1.5
point_110	1461459	5126628	179.2	185	2	70	2	183.6	1.4
point_111	1462230	5127266	178.9	185	2	70	2	184.8	0.2
point_112	1460110	5124869	172.3	180	2	70	2	182.3	-2.3
point_113	1460931	5125440	172.4	180	2	70	2	178.9	1.1
point_114	1461696	5126084	174.4	180	2	70	2	177.7	2.3
point_115	1462453	5126737	175.1	180	2	70	2	178	2
point_116	1460431	5124360	167.1	175	2	70	2	177.2	-2.2
point_117	1483760	5110596	1	15	1	95	2	15.9	-0.9
point_118	1461666	5111760	67.4	75	2	70	2	75.1	-0.1
point_119	1459954	5115614	100.1	105	2	70	2	109.3	-4.3
point_120	1466542	5127560	1	165	1	95	2	165.1	-0.1
point_121	1461251	5124931	169.3	175	2	70	2	174.5	0.5
point_122	1462007	5125585	169.7	175	2	70	2	173	2
point_123	1462746	5126258	171.6	175	2	70	2	172.1	2.9
point_124	1460720	5123809	162.2	170	2	70	2	172.2	-2.2
point_125	1461550	5124365	164.1	170	2	70	2	170.1	-0.1
point_126	1462300	5125025	164.7	170	2	70	2	168.8	1.2
point_127	1463004	5125735	167	170	2	70	2	167.9	2.1
point_128	1461274	5123401	158.7	165	2	70	2	165.5	-0.5
point_129	1462105	5123956	158.3	165	2	70	2	164.7	0.3
point_130	1462813	5124660	161.8	165	2	70	2	164.4	0.6
point_131	1460949	5115715	97.7	105	2	70	2	105.9	-0.9
point_132	1469302	5128697	1	165	1	95	2	164.9	0.1
point_133	1463476	5125407	163.2	165	2	70	2	164.2	0.8
point_134	1461709	5122910	153.4	160	2	70	2	159.7	0.3
point_135	1462531	5123477	153.1	160	2	70	2	159.4	0.6
point_136	1463230	5124189	155.9	160	2	70	2	160.1	-0.1

Observation point	X NZTM	Y NZTM	Z (masl)	Observed head	Observed head interval	Observed head confidence %	Observed head standard deviation	Modelled head	Residual head
point_137	1463884	5124945	157.4	160	2	70	2	160.8	-0.8
point_138	1462374	5122557	146.5	155	2	70	2	153.5	1.5
point_139	1463157	5123173	149.4	155	2	70	2	154.2	0.8
point_140	1463823	5123918	152.3	155	2	70	2	156.2	-1.2
point_141	1464492	5124661	150	155	2	70	2	157.2	-2.2
point_142	1461981	5121622	142.4	150	2	70	2	148	2
point_143	1461946	5115793	98.6	105	2	70	2	104.1	0.9
point_144	1462850	5122115	141.4	150	2	70	2	147.8	2.2
point_145	1463634	5122733	144.6	150	2	70	2	149	1
point_146	1464287	5123490	147.6	150	2	70	2	151.5	-1.5
point_147	1464939	5124247	146.4	150	2	70	2	152.7	-2.7
point_148	1462354	5121128	136.2	145	2	70	2	142.7	2.3
point_149	1463228	5121612	136.4	145	2	70	2	142.6	2.4
point_150	1464023	5122217	139.6	145	2	70	2	143.5	1.5
point_151	1464678	5122972	142.8	145	2	70	2	145.4	-0.4
point_152	1465308	5123748	140.3	145	2	70	2	146.6	-1.6
point_153	1462697	5120634	131.8	140	2	70	2	138.1	1.9
point_154	1460863	5116321	102.3	110	2	70	2	111.5	-1.5
point_155	1463574	5121113	132.6	140	2	70	2	138.3	1.7
point_156	1464362	5121728	135.4	140	2	70	2	139	1
point_157	1465052	5122451	138.5	140	2	70	2	139.5	0.5
point_158	1465692	5123218	136.9	140	2	70	2	139.9	0.1
point_159	1462286	5119742	125.6	135	2	70	2	133.4	1.6
point_160	1463167	5120215	128.8	135	2	70	2	134	1
point_161	1464032	5120715	128.6	135	2	70	2	134.4	0.6
point_162	1464820	5121330	132	135	2	70	2	134.8	0.2
point_163	1465529	5122034	130.8	135	2	70	2	134.5	0.5
point_164	1466216	5122762	128.4	135	2	70	2	134.4	0.6

Observation point	X NZTM	Y NZTM	Z (masl)	Observed head	Observed head interval	Observed head confidence %	Observed head standard deviation	Modelled head	Residual head
point_165	1461859	5116410	103.4	110	2	70	2	109	1
point_166	1462910	5119364	123.3	130	2	70	2	129	1
point_167	1463785	5119846	123.8	130	2	70	2	129.8	0.2
point_168	1464627	5120385	124.5	130	2	70	2	130.2	-0.2
point_169	1465405	5121013	125.9	130	2	70	2	130	0
point_170	1466127	5121704	124.9	130	2	70	2	129.7	0.3
point_171	1466858	5122386	123.8	130	2	70	2	129.8	0.2
point_172	1462610	5118469	117.2	125	2	70	2	123.2	1.8
point_173	1463500	5118924	118.8	125	2	70	2	124.3	0.7
point_174	1464352	5119448	120.7	125	2	70	2	125.2	-0.2
point_175	1465189	5119995	119.9	125	2	70	2	125	0
point_176	1460651	5116901	108.6	115	2	70	2	117.9	-2.9
point_177	1465956	5120635	119.1	125	2	70	2	125	0
point_178	1466696	5121307	120.6	125	2	70	2	125	0
point_179	1467454	5121960	116.7	125	2	70	2	125.2	-0.2
point_180	1462597	5117757	111.7	120	2	70	2	117.6	2.4
point_181	1463503	5118179	113.4	120	2	70	2	118.6	1.4
point_182	1464359	5118695	113.7	120	2	70	2	119.9	0.1
point_183	1465194	5119245	113.2	120	2	70	2	120.1	-0.1
point_184	1466010	5119821	115.8	120	2	70	2	119.9	0.1
point_185	1466774	5120466	113.7	120	2	70	2	120.1	-0.1
point_186	1467536	5121114	111.3	120	2	70	2	120.3	-0.3
point_187	1461647	5116988	108.2	115	2	70	2	114.2	0.8
point_188	1468327	5121726	111.5	120	2	70	2	120.2	-0.2
point_189	1462592	5117063	107.6	115	2	70	2	112.3	2.7
point_190	1463502	5117476	110	115	2	70	2	113.5	1.5
point_191	1464382	5117951	106.2	115	2	70	2	114.7	0.3
point_192	1465223	5118492	107.7	115	2	70	2	115.2	-0.2

Observation point	X NZTM	Y NZTM	Z (masl)	Observed head	Observed head interval	Observed head confidence %	Observed head standard deviation	Modelled head	Residual head
point_193	1466056	5119045	110.9	115	2	70	2	115	0
point_194	1466852	5119650	111.8	115	2	70	2	115.1	-0.1
point_195	1467626	5120283	107.3	115	2	70	2	115.3	-0.3
point_196	1468408	5120906	106.7	115	2	70	2	115.4	-0.4
point_197	1469217	5121493	106.3	115	2	70	2	114.8	0.2
point_198	1460777	5117570	113.5	120	2	70	2	122.9	-2.9
point_199	1463261	5116670	101.5	110	2	70	2	108.3	1.7
point_200	1464167	5117093	99.6	110	2	70	2	109.4	0.6
point_201	1465036	5117587	101.9	110	2	70	2	110.1	-0.1
point_202	1465882	5118120	105.1	110	2	70	2	110.2	-0.2
point_203	1466708	5118684	106.4	110	2	70	2	110.2	-0.2
point_204	1467506	5119286	105.1	110	2	70	2	110.2	-0.2
point_205	1468286	5119911	102.3	110	2	70	2	110.4	-0.4
point_206	1469075	5120526	102.9	110	2	70	2	110.4	-0.4
point_207	1469886	5121110	100.3	110	2	70	2	110	0
point_208	1462971	5115876	97	105	2	70	2	103.2	1.8
point_209	1461768	5117698	111.8	120	2	70	2	119.6	0.4
point_210	1464276	5130902	1	195	1	95	2	195	0
point_211	1463894	5116259	96.1	105	2	70	2	104.2	0.8
point_212	1464795	5116693	95.7	105	2	70	2	104.8	0.2
point_213	1465667	5117182	99.6	105	2	70	2	105.1	-0.1
point_214	1466516	5117710	100.5	105	2	70	2	105.3	-0.3
point_215	1467341	5118275	101.1	105	2	70	2	105.1	-0.1
point_216	1468141	5118876	99.9	105	2	70	2	105	0
point_217	1468921	5119500	97.9	105	2	70	2	105.2	-0.2
point_218	1469712	5120113	97.7	105	2	70	2	105.3	-0.3
point_219	1470520	5120702	98.5	105	2	70	2	105.5	-0.5
point_220	1463718	5115516	92.4	100	2	70	2	99.2	0.8

Observation point	X NZTM	Y NZTM	Z (masl)	Observed head	Observed head interval	Observed head confidence %	Observed head standard deviation	Modelled head	Residual head
point_221	1460721	5118189	118.8	125	2	70	2	127.6	-2.6
point_222	1467139	5131781	1	195	1	95	2	194.7	0.3
point_223	1464643	5115895	91.9	100	2	70	2	99.5	0.5
point_224	1465544	5116330	93.8	100	2	70	2	99.7	0.3
point_225	1466417	5116817	95.3	100	2	70	2	100.2	-0.2
point_226	1467264	5117347	95.2	100	2	70	2	100.2	-0.2
point_227	1468089	5117913	95.6	100	2	70	2	99.8	0.2
point_228	1468888	5118514	94.9	100	2	70	2	99.6	0.4
point_229	1469663	5119146	94.1	100	2	70	2	99.8	0.2
point_230	1470451	5119762	91.9	100	2	70	2	100.1	-0.1
point_231	1471258	5120352	94.4	100	2	70	2	100.8	-0.8
point_232	1463646	5114786	86.9	95	2	70	2	93.8	1.2
point_233	1486428	5111933	1	15	1	95	2	13.8	1.2
point_234	1462664	5111688	65.9	75	2	70	2	74.3	0.7
point_235	1461707	5118351	117.6	125	2	70	2	125	0
point_236	1464578	5115147	87	95	2	70	2	94.4	0.6
point_237	1465499	5115538	87.9	95	2	70	2	94.5	0.5
point_238	1466395	5115981	89.3	95	2	70	2	94.9	0.1
point_239	1467263	5116477	90.3	95	2	70	2	95	0
point_240	1468104	5117017	93	95	2	70	2	94.8	0.2
point_241	1468923	5117592	91.4	95	2	70	2	94.4	0.6
point_242	1469708	5118210	89.4	95	2	70	2	94.4	0.6
point_243	1470482	5118844	90.7	95	2	70	2	94.5	0.5
point_244	1471283	5119442	88.4	95	2	70	2	95	0
point_245	1472123	5119984	87.4	95	2	70	2	95.4	-0.4
point_246	1460521	5118788	123.9	130	2	70	2	132.2	-2.2
point_247	1463222	5113924	85.1	90	2	70	2	88.4	1.6
point_248	1464161	5114269	80.5	90	2	70	2	89.3	0.7

Observation point	X NZTM	Y NZTM	Z (masl)	Observed head	Observed head interval	Observed head confidence %	Observed head standard deviation	Modelled head	Residual head
point_249	1465102	5114608	81	90	2	70	2	89.5	0.5
point_250	1466027	5114988	83.7	90	2	70	2	89.5	0.5
point_251	1466926	5115425	84.4	90	2	70	2	89.8	0.2
point_252	1467795	5115919	84.7	90	2	70	2	89.8	0.2
point_253	1468637	5116458	88.8	90	2	70	2	89.7	0.3
point_254	1469452	5117037	86.8	90	2	70	2	89.5	0.5
point_255	1470235	5117660	85	90	2	70	2	89.5	0.5
point_256	1471006	5118296	85.8	90	2	70	2	89.6	0.4
point_257	1461506	5118964	122.6	130	2	70	2	130.2	-0.2
point_258	1471821	5118874	82.6	90	2	70	2	89.8	0.2
point_259	1472702	5119347	84.3	90	2	70	2	89.8	0.2
point_260	1463864	5113455	76.9	85	2	70	2	84.5	0.5
point_261	1464817	5113757	75.9	85	2	70	2	84.8	0.2
point_262	1465765	5114075	76	85	2	70	2	84.7	0.3
point_263	1466683	5114471	79.1	85	2	70	2	84.9	0.1
point_264	1467577	5114919	78.2	85	2	70	2	85	0
point_265	1468446	5115414	81.4	85	2	70	2	85	0
point_266	1469290	5115950	81.3	85	2	70	2	84.9	0.1
point_267	1470103	5116532	81.5	85	2	70	2	84.8	0.2
point_268	1460203	5119425	127.7	135	2	70	2	137.1	-2.1
point_269	1464661	5135057	1	225	1	95	2	225.6	-0.6
point_270	1470873	5117169	81.3	85	2	70	2	84.8	0.2
point_271	1471624	5117829	79.9	85	2	70	2	85.1	-0.1
point_272	1472450	5118387	79.5	85	2	70	2	84.9	0.1
point_273	1473360	5118800	78.7	85	2	70	2	84.2	0.8
point_274	1464307	5112857	69.9	80	2	70	2	80.1	-0.1
point_275	1465267	5113137	68.7	80	2	70	2	80	0
point_276	1466218	5113444	70.8	80	2	70	2	79.9	0.1

Observation point	X NZTM	Y NZTM	Z (masl)	Observed head	Observed head interval	Observed head confidence %	Observed head standard deviation	Modelled head	Residual head
point_277	1467130	5113855	74.1	80	2	70	2	80.2	-0.2
point_278	1468025	5114300	75.3	80	2	70	2	80.2	-0.2
point_279	1468905	5114776	76.9	80	2	70	2	80.3	-0.3
point_280	1461193	5119557	126.6	135	2	70	2	135.2	-0.2
point_281	1469766	5115284	76.4	80	2	70	2	80.1	-0.1
point_282	1470597	5115839	75.1	80	2	70	2	79.8	0.2
point_283	1471368	5116475	74	80	2	70	2	79.9	0.1
point_284	1472079	5117178	72.6	80	2	70	2	80.5	-0.5
point_285	1472837	5117816	72.7	80	2	70	2	80.8	-0.8
point_286	1473782	5118131	73.8	80	2	70	2	79.1	0.9
point_287	1463743	5111816	64.8	75	2	70	2	74.3	0.7
point_288	1464679	5112168	64.7	75	2	70	2	75.2	-0.2
point_289	1465630	5112478	64.5	75	2	70	2	75.3	-0.3
point_290	1466574	5112807	65.8	75	2	70	2	75.2	-0.2
point_291	1460775	5120418	133.4	140	2	70	2	142.8	-2.8
point_292	1467493	5113201	67.5	75	2	70	2	75.1	-0.1
point_293	1468396	5113630	70.3	75	2	70	2	75.2	-0.2
point_294	1469289	5114081	71.7	75	2	70	2	75.4	-0.4
point_295	1470172	5114550	71.4	75	2	70	2	75.2	-0.2
point_296	1471030	5115063	71.6	75	2	70	2	74.8	0.2
point_297	1471845	5115639	66.8	75	2	70	2	74.6	0.4
point_298	1472554	5116344	67.6	75	2	70	2	75.2	-0.2
point_299	1473323	5116978	68.8	75	2	70	2	75.4	-0.4
point_300	1474219	5117417	68.6	75	2	70	2	74.5	0.5
point_301	1464224	5111112	59	70	2	70	2	69.2	0.8
point_302	1461615	5110876	60.1	70	2	70	2	69.4	0.6
point_303	1463889	5137079	1	240	1	95	2	238.2	1.8
point_304	1465146	5111500	59.8	70	2	70	2	70.3	-0.3

Observation point	X NZTM	Y NZTM	Z (masl)	Observed head	Observed head interval	Observed head confidence %	Observed head standard deviation	Modelled head	Residual head
point_305	1466085	5111843	59.9	70	2	70	2	70.3	-0.3
point_306	1467023	5112189	61.2	70	2	70	2	69.9	0.1
point_307	1467945	5112577	63.4	70	2	70	2	69.8	0.2
point_308	1468853	5112996	64.4	70	2	70	2	70.2	-0.2
point_309	1469753	5113433	66	70	2	70	2	70.2	-0.2
point_310	1470644	5113886	64.5	70	2	70	2	69.9	0.1
point_311	1471515	5114377	64.6	70	2	70	2	69.6	0.4
point_312	1472358	5114912	60.1	70	2	70	2	69.3	0.7
point_313	1473088	5115594	61.8	70	2	70	2	70	0
point_314	1462613	5110823	60	70	2	70	2	68.5	1.5
point_315	1462687	5138887	1	255	1	95	2	256.1	-1.1
point_316	1473852	5116238	62.2	70	2	70	2	70.5	-0.5
point_317	1474714	5116743	64.1	70	2	70	2	70.3	-0.3
point_318	1464391	5110370	53.3	65	2	70	2	64.4	0.6
point_319	1465312	5110760	55.4	65	2	70	2	65.4	-0.4
point_320	1466252	5111101	56.5	65	2	70	2	65.1	-0.1
point_321	1467194	5111435	56.2	65	2	70	2	64.5	0.5
point_322	1468120	5111814	57.4	65	2	70	2	64.6	0.4
point_323	1469032	5112223	58.1	65	2	70	2	65	0
point_324	1469935	5112652	59	65	2	70	2	65.1	-0.1
point_325	1470828	5113103	57.1	65	2	70	2	64.8	0.2
point_326	1463606	5110861	60.2	70	2	70	2	68.2	1.8
point_327	1471704	5113586	61	65	2	70	2	64.6	0.4
point_328	1472551	5114116	55.8	65	2	70	2	64.5	0.5
point_329	1473342	5114727	56.4	65	2	70	2	64.8	0.2
point_330	1474111	5115367	57.5	65	2	70	2	65.5	-0.5
point_331	1474930	5115939	58.5	65	2	70	2	66	-1
point_332	1464901	5109850	50.9	60	2	70	2	60.2	-0.2

Observation point	X NZTM	Y NZTM	Z (masl)	Observed head	Observed head interval	Observed head confidence %	Observed head standard deviation	Modelled head	Residual head
point_333	1465851	5110161	50	60	2	70	2	60.1	-0.1
point_334	1466804	5110465	51.7	60	2	70	2	59.6	0.4
point_335	1467743	5110807	51.3	60	2	70	2	59.4	0.6
point_336	1468665	5111196	52.7	60	2	70	2	59.9	0.1
point_337	1459784	5109671	57.2	65	2	70	2	64.5	0.5
point_338	1469575	5111609	53.5	60	2	70	2	60.4	-0.4
point_339	1470476	5112043	53.6	60	2	70	2	60.1	-0.1
point_340	1471364	5112502	52.9	60	2	70	2	59.7	0.3
point_341	1472234	5112995	54.1	60	2	70	2	59.4	0.6
point_342	1473078	5113532	52	60	2	70	2	59.3	0.7
point_343	1473886	5114120	53.1	60	2	70	2	59.7	0.3
point_344	1474676	5114733	53.3	60	2	70	2	60.4	-0.4
point_345	1475505	5115290	52.6	60	2	70	2	60.8	-0.8
point_346	1465267	5109171	45	55	2	70	2	54.7	0.3
point_347	1466225	5109456	44.3	55	2	70	2	54.5	0.5
point_348	1460186	5112483	74.9	80	2	70	2	82.4	-2.4
point_349	1460751	5109919	55.6	65	2	70	2	63.9	1.1
point_350	1467179	5109756	46.4	55	2	70	2	54.6	0.4
point_351	1468118	5110100	44.2	55	2	70	2	54.9	0.1
point_352	1469040	5110486	46.1	55	2	70	2	55.7	-0.7
point_353	1469950	5110901	48.9	55	2	70	2	55.9	-0.9
point_354	1470851	5111336	48.6	55	2	70	2	55.4	-0.4
point_355	1471739	5111795	48.5	55	2	70	2	54.7	0.3
point_356	1472612	5112283	50.1	55	2	70	2	54.3	0.7
point_357	1473466	5112803	49.3	55	2	70	2	54.2	0.8
point_358	1474296	5113361	48.7	55	2	70	2	54.7	0.3
point_359	1475109	5113943	48.7	55	2	70	2	55.2	-0.2
point_360	1461748	5109978	53.5	65	2	70	2	63.3	1.7

Observation point	X NZTM	Y NZTM	Z (masl)	Observed head	Observed head interval	Observed head confidence %	Observed head standard deviation	Modelled head	Residual head
point_361	1462307	5142309	1	285	1	95	2	282.6	2.4
point_362	1475949	5114484	48.9	55	2	70	2	55.1	-0.1
point_363	1464549	5108092	39.8	50	2	70	2	50.8	-0.8
point_364	1465518	5108321	39.2	50	2	70	2	48.8	1.2
point_365	1466455	5108669	40.4	50	2	70	2	49.4	0.6
point_366	1467407	5108976	39.3	50	2	70	2	50	0
point_367	1468351	5109305	39.3	50	2	70	2	50.4	-0.4
point_368	1469273	5109690	41.4	50	2	70	2	51	-1
point_369	1470183	5110105	44.8	50	2	70	2	50.9	-0.9
point_370	1471085	5110537	44.5	50	2	70	2	50.3	-0.3
point_371	1471979	5110986	45.2	50	2	70	2	49.7	0.3
point_372	1462748	5109992	55.8	65	2	70	2	63.5	1.5
point_373	1472858	5111463	46.5	50	2	70	2	49.4	0.6
point_374	1473727	5111957	45.2	50	2	70	2	49.5	0.5
point_375	1474587	5112468	45.9	50	2	70	2	49.9	0.1
point_376	1475420	5113020	44.3	50	2	70	2	50.3	-0.3
point_377	1476239	5113593	45.3	50	2	70	2	50.3	-0.3
point_378	1466951	5107972	32.8	45	2	70	2	44.9	0.1
point_379	1467913	5108246	34.6	45	2	70	2	45.4	-0.4
point_380	1468855	5108577	33.3	45	2	70	2	45.4	-0.4
point_381	1469769	5108984	37.3	45	2	70	2	45.5	-0.5
point_382	1470674	5109409	39.2	45	2	70	2	45.2	-0.2
point_383	1463738	5110119	54.2	65	2	70	2	63.6	1.4
point_384	1471579	5109836	39.8	45	2	70	2	44.8	0.2
point_385	1472480	5110269	40.6	45	2	70	2	44.5	0.5
point_386	1473360	5110743	41.9	45	2	70	2	44.6	0.4
point_387	1474242	5111213	41.8	45	2	70	2	44.9	0.1
point_388	1475127	5111680	41.7	45	2	70	2	45.2	-0.2

Observation point	X NZTM	Y NZTM	Z (masl)	Observed head	Observed head interval	Observed head confidence %	Observed head standard deviation	Modelled head	Residual head
point_389	1475997	5112170	39.5	45	2	70	2	45.1	-0.1
point_390	1476768	5112807	40.4	45	2	70	2	45.5	-0.5
point_391	1467729	5107298	27.1	40	2	70	2	40.1	-0.1
point_392	1468690	5107575	28.5	40	2	70	2	40.2	-0.2
point_393	1469615	5107954	30.5	40	2	70	2	40.4	-0.4
point_394	1460789	5108994	48.5	60	2	70	2	59.4	0.6
point_395	1470521	5108377	31.8	40	2	70	2	40.1	-0.1
point_396	1471422	5108810	34.3	40	2	70	2	39.8	0.2
point_397	1472334	5109220	33.7	40	2	70	2	39.6	0.4
point_398	1473247	5109628	35.5	40	2	70	2	39.4	0.6
point_399	1474146	5110065	34.5	40	2	70	2	39.6	0.4
point_400	1475018	5110554	37.4	40	2	70	2	40.1	-0.1
point_401	1475901	5111024	35.2	40	2	70	2	40.4	-0.4
point_402	1476794	5111472	33	40	2	70	2	40.1	-0.1
point_403	1467731	5106233	20.8	35	2	70	2	33.9	1.1
point_404	1468665	5106589	21.7	35	2	70	2	34.3	0.7
point_405	1461781	5109113	48.2	60	2	70	2	58.3	1.7
point_406	1469597	5106951	24.9	35	2	70	2	35.2	-0.2
point_407	1470507	5107366	26.2	35	2	70	2	35.3	-0.3
point_408	1471408	5107800	27.8	35	2	70	2	35	0
point_409	1472315	5108221	29	35	2	70	2	34.8	0.2
point_410	1473226	5108632	27.7	35	2	70	2	34.7	0.3
point_411	1474132	5109055	30.7	35	2	70	2	34.7	0.3
point_412	1475025	5109506	30.8	35	2	70	2	35	0
point_413	1475926	5109938	29.4	35	2	70	2	35.2	-0.2
point_414	1476883	5110216	27.8	35	2	70	2	34.2	0.8
point_415	1467984	5105231	16.8	30	2	70	2	28.7	1.3
point_416	1462776	5109214	50.1	60	2	70	2	59.4	0.6

Observation point	X NZTM	Y NZTM	Z (masl)	Observed head	Observed head interval	Observed head confidence %	Observed head standard deviation	Modelled head	Residual head
point_417	1468899	5105635	16	30	2	70	2	28.8	1.2
point_418	1469834	5105987	18.4	30	2	70	2	29.6	0.4
point_419	1470735	5106420	21	30	2	70	2	30.1	-0.1
point_420	1471634	5106858	21.2	30	2	70	2	30	0
point_421	1472538	5107286	23.8	30	2	70	2	29.9	0.1
point_422	1473445	5107707	22.4	30	2	70	2	29.8	0.2
point_423	1474350	5108133	25.6	30	2	70	2	29.8	0.2
point_424	1475244	5108582	25.9	30	2	70	2	30	0
point_425	1476132	5109041	25.6	30	2	70	2	30.2	-0.2
point_426	1477027	5109483	23.5	30	2	70	2	30.3	-0.3
point_427	1463745	5109456	49.7	60	2	70	2	59.9	0.1
point_428	1464533	5102745	14.5	25	2	70	2	24.9	0.1
point_429	1465484	5103045	12.4	25	2	70	2	24.7	0.3
point_430	1466369	5103510	14	25	2	70	2	25.8	-0.8
point_431	1467280	5103912	15.8	25	2	70	2	26.2	-1.2
point_432	1468214	5104268	12.4	25	2	70	2	24.6	0.4
point_433	1469103	5104724	10	25	2	70	2	23.7	1.3
point_434	1470038	5105078	12.8	25	2	70	2	25	0
point_435	1470955	5105475	15.8	25	2	70	2	25.3	-0.3
point_436	1471857	5105908	16.4	25	2	70	2	25.2	-0.2
point_437	1472759	5106340	17.9	25	2	70	2	25	0
point_438	1460669	5108077	44.5	55	2	70	2	56	-1
point_439	1473663	5106767	19	25	2	70	2	24.8	0.2
point_440	1474568	5107192	19.6	25	2	70	2	24.7	0.3
point_441	1475463	5107639	20	25	2	70	2	24.7	0.3
point_442	1476340	5108118	19.5	25	2	70	2	24.9	0.1
point_443	1477226	5108583	18.4	25	2	70	2	25.1	-0.1
point_444	1469461	5103598	4.6	20	2	70	2	19	1

Observation point	X NZTM	Y NZTM	Z (masl)	Observed head	Observed head interval	Observed head confidence %	Observed head standard deviation	Modelled head	Residual head
point_445	1470342	5104070	7.8	20	2	70	2	20.6	-0.6
point_446	1471245	5104498	9	20	2	70	2	20.9	-0.9
point_447	1472150	5104925	12.1	20	2	70	2	20.5	-0.5
point_448	1473048	5105366	12.6	20	2	70	2	20	0
point_449	1461655	5108246	42.7	55	2	70	2	53.4	1.6
point_450	1473943	5105810	13.5	20	2	70	2	19.8	0.2
point_451	1474845	5106242	14	20	2	70	2	19.8	0.2
point_452	1475744	5106680	14.6	20	2	70	2	19.6	0.4
point_453	1476610	5107180	14	20	2	70	2	19.7	0.3
point_454	1477490	5107654	13.7	20	2	70	2	19.7	0.3
point_455	1469938	5102233	0.3	15	2	70	2	12.4	2.6
point_456	1470686	5102894	2.3	15	2	70	2	14.7	0.3
point_457	1471524	5103437	4.2	15	2	70	2	16	-1
point_458	1472432	5103856	5.8	15	2	70	2	15.7	-0.7
point_459	1473324	5104306	7.3	15	2	70	2	14.9	0.1
point_460	1461182	5112569	71.5	80	2	70	2	81.5	-1.5
point_461	1462646	5108376	45.3	55	2	70	2	55.5	-0.5
point_462	1474198	5104792	7.9	15	2	70	2	14.9	0.1
point_463	1475087	5105249	8.9	15	2	70	2	15	0
point_464	1475970	5105719	9.9	15	2	70	2	15.1	-0.1
point_465	1476830	5106229	9.3	15	2	70	2	15.2	-0.2
point_466	1477690	5106739	8.4	15	2	70	2	15.4	-0.4
point_467	1470602	5101155	-2.4	10	2	70	2	7.2	2.8
point_468	1471274	5101895	-1.4	10	2	70	2	9.1	0.9
point_469	1472072	5102493	-0.2	10	2	70	2	10.4	-0.4
point_470	1472982	5102905	0.1	10	2	70	2	9.8	0.2
point_471	1473882	5103339	1.2	10	2	70	2	9.3	0.7
point_472	1463592	5108681	45.6	55	2	70	2	56.3	-1.3

Observation point	X NZTM	Y NZTM	Z (masl)	Observed head	Observed head interval	Observed head confidence %	Observed head standard deviation	Modelled head	Residual head
point_473	1474759	5103820	2.5	10	2	70	2	9.6	0.4
point_474	1475638	5104296	2.9	10	2	70	2	10.2	-0.2
point_475	1476500	5104803	5.6	10	2	70	2	10.4	-0.4
point_476	1477332	5105357	5.7	10	2	70	2	10.4	-0.4
point_477	1478143	5105943	5.8	10	2	70	2	11.1	-1.1
point_478	1471320	5099928	-7	5	2	70	2	3.4	1.6
point_479	1471810	5100800	-5.1	5	2	70	2	4.4	0.6
point_480	1472548	5101449	-2	5	2	70	2	5.2	-0.2
point_481	1473451	5101877	-3.8	5	2	70	2	4.8	0.2
point_482	1474392	5102216	-4.4	5	2	70	2	4.3	0.7
point_483	1464531	5109004	44.2	55	2	70	2	55.8	-0.8
point_484	1475307	5102617	-5	5	2	70	2	4	1
point_485	1476182	5103096	-4.2	5	2	70	2	4.3	0.7
point_486	1477017	5103645	-1.4	5	2	70	2	4.1	0.9
point_487	1477835	5104219	0.7	5	2	70	2	3.5	1.5
point_488	1478610	5104851	0.4	5	2	70	2	3.6	1.4
point_489	1469256	5096412	-8.6	0	2	70	2	1.7	-1.7
point_490	1461419	5107356	38.5	50	2	70	2	49.9	0.1
point_491	1462406	5107515	39.3	50	2	70	2	50.6	-0.6
point_492	1463383	5107719	38.9	50	2	70	2	51.9	-1.9
point_493	1462002	5106589	32.3	45	2	70	2	42.6	2.4
point_494	1462981	5106794	33.8	45	2	70	2	46.7	-1.7
point_495	1463933	5107094	33.3	45	2	70	2	46.9	-1.9
point_496	1464895	5107358	34.9	45	2	70	2	45.7	-0.7
point_497	1462179	5112566	71.7	80	2	70	2	80.6	-0.6
point_498	1465858	5107616	34.9	45	2	70	2	44.9	0.1
point_499	1462524	5105718	31.2	40	2	70	2	39.8	0.2
point_500	1463486	5105988	28.4	40	2	70	2	40.6	-0.6

Observation point	X NZTM	Y NZTM	Z (masl)	Observed head	Observed head interval	Observed head confidence %	Observed head standard deviation	Modelled head	Residual head
point_501	1464403	5106386	30	40	2	70	2	41.4	-1.4
point_502	1465381	5106568	29.9	40	2	70	2	40.7	-0.7
point_503	1466340	5106843	29.2	40	2	70	2	40.5	-0.5
point_504	1463159	5104626	26.3	35	2	70	2	34.9	0.1
point_505	1464081	5105014	24	35	2	70	2	35.2	-0.2
point_506	1465023	5105343	25.3	35	2	70	2	35.9	-0.9
point_507	1466012	5105485	25.9	35	2	70	2	35.2	-0.2
point_508	1480841	5115282	1	45	1	95	2	44.6	0.4
point_509	1463178	5112581	74	80	2	70	2	79.8	0.2
point_510	1466909	5105857	22.2	35	2	70	2	34.9	0.1
point_511	1463808	5103659	21.6	30	2	70	2	30.3	-0.3
point_512	1464734	5104036	19.6	30	2	70	2	30.3	-0.3
point_513	1465678	5104364	19.4	30	2	70	2	30.8	-0.8
point_514	1466635	5104656	20.8	30	2	70	2	30.6	-0.6
point_515	1465379	5101953	9.8	20	2	70	2	20.6	-0.6
point_516	1466297	5102345	7.3	20	2	70	2	20.3	-0.3
point_517	1467213	5102747	9	20	2	70	2	20.4	-0.4
point_518	1468158	5103072	9.4	20	2	70	2	19.9	0.1
point_519	1465720	5100817	1.9	15	2	70	2	15.5	-0.5
point_520	1483424	5116803	1	45	1	95	2	44.8	0.2
point_521	1460686	5113241	79.7	85	2	70	2	88	-3
point_522	1466688	5101067	2.2	15	2	70	2	14	1
point_523	1467661	5101295	2.8	15	2	70	2	11.9	3.1
point_524	1468633	5101533	0.5	15	2	70	2	10.9	4.1
point_525	1467000	5099942	-0.7	10	2	70	2	10.5	-0.5
point_526	1467989	5100066	-0.6	10	2	70	2	8.9	1.1
point_527	1468982	5100161	-2.2	10	2	70	2	7.6	2.4
point_528	1469897	5100543	-0.4	10	2	70	2	6.9	3.1

Observation point	X NZTM	Y NZTM	Z (masl)	Observed head	Observed head interval	Observed head confidence %	Observed head standard deviation	Modelled head	Residual head
point_529	1468433	5098507	-3.8	5	2	70	2	6.5	-1.5
point_530	1469426	5098557	-5.1	5	2	70	2	5.1	-0.1
point_531	1470335	5098919	-5.5	5	2	70	2	4.2	0.8
point_532	1477272	5118914	1	75	1	95	2	74.7	0.3
point_533	1461686	5113243	77.4	85	2	70	2	85.9	-0.9
point_534	1479340	5105535	0.5	5	2	70	2	4	1
point_535	1479007	5106442	1.6	10	2	70	2	11.3	-1.3
point_536	1478577	5107199	7.9	15	2	70	2	15	0
point_537	1478394	5108081	8.3	20	2	70	2	18.8	1.2
point_538	1478147	5108970	14.3	25	2	70	2	24.8	0.2
point_539	1477960	5109843	19.4	30	2	70	2	30	0
point_540	1477718	5110764	26.2	35	2	70	2	34.7	0.3
point_541	1477645	5111996	33.4	40	2	70	2	39.6	0.4
point_542	1477635	5113282	37.6	45	2	70	2	44.7	0.3
point_543	1477123	5114056	43.2	50	2	70	2	49.4	0.6

Environment Canterbury Regional Council
Kaunihera Taiao ki Waitaha

Facilitating sustainable development in the Canterbury region

ecan.govt.nz